USGS
science for a changing world

U.S. Geological Survey National Water Census and
Water Availability and Use Science Program

Simulations of Hydrologic Response in the Apalachicola-Chattahoochee-Flint River Basin, Southeastern United States

Scientific Investigations Report 2017–5133

U.S. Department of the Interior
U.S. Geological Survey

Cover. Roswell Mill dam on Big Creek in the Chattahoochee National Recreation Area, Fulton County, Georgia, July 27, 2008. Photograph by Alan M. Cressler, U.S. Geological Survey.

Simulations of Hydrologic Response in the Apalachicola-Chattahoochee-Flint River Basin, Southeastern United States

By Jacob H. LaFontaine, L. Elliott Jones, and Jaime A. Painter

U.S. Geological Survey National Water Census and
Water Availability and Use Science Program

Scientific Investigations Report 2017–5133

U.S. Department of the Interior
U.S. Geological Survey

U.S. Department of the Interior
RYAN K. ZINKE, Secretary

U.S. Geological Survey
William H. Werkheiser, Deputy Director,
exercising the authority of the Director

U.S. Geological Survey, Reston, Virginia: 2017

Suggested citation:
LaFontaine, J.H., Jones, L.E., and Painter, J.A., 2017, Simulations of hydrologic response in the Apalachicola-Chattahoochee-Flint River Basin, Southeastern United States: U.S. Geological Survey Scientific Investigations Report 2017–5133, 112 p., https://doi.org/10.3133/sir20175133.

ISSN 2328-0328 (online)

Contents

Figures

Tables

Appendix 1 and 2 tables:

Conversion Factors

International System of Units to U.S. customary units

Multiply	By	To obtain
	Length	
centimeter (cm)	0.3937	inch (in.)
millimeter (mm)	0.03937	inch (in.)
meter (m)	3.281	foot (ft)
kilometer (km)	0.6214	mile (mi)
	Area	
square kilometer (km^2)	247.1	acre

Temperature in degrees Celsius (°C) may be converted to degrees Fahrenheit (°F) as follows:

$$°F = (1.8 \times °C) + 32.$$

Datum

Vertical coordinate information in this report is referenced to the North American Vertical Datum of 1988 (NAVD 88).

Altitude, as used in this report, refers to distance above the vertical datum.

Abbreviations

ACFB	Apalachicola-Chattahoochee-Flint River Basin
DEM	digital elevation model
FAST	Fourier Amplitude Sensitivity Test
FDEP	Florida Department of Environmental Protection
GaEPD	Georgia Environmental Protection Division
GDP	GeoData Portal
GHCN	Global Hydro-Climatic Network
HRU	hydrologic response unit
HSPF	Hydrologic simulation program fortran
MODFE	MODular Finite-Element
NCDC	National Climatic Data Center
NLCD	National Land Cover Database
NOAA	National Oceanic and Atmospheric Administration
NSE	Nash-Sutcliffe Index
NWFWMD	Northwest Florida Water Management District
NWIS	National Water Information System
P_{bias}	Percent bias
PRMS	Precipitation-Runoff Modeling System
RSR	Ratio of the root mean square error to the standard deviation of the measured streamflow
SNOTEL	SNOwpack and TELemetry network
SWUDS	Site-specific Water Use Data System
USACE	U.S. Army Corps of Engineers
USGS	U.S. Geological Survey

Simulations of Hydrologic Response in the Apalachicola-Chattahoochee-Flint River Basin, Southeastern United States

By Jacob H. LaFontaine, L. Elliott Jones, and Jaime A. Painter

Abstract

A suite of hydrologic models has been developed for the Apalachicola-Chattahoochee-Flint River Basin (ACFB) as part of the National Water Census, a U.S. Geological Survey research program that focuses on developing new water accounting tools and assessing water availability and use at the regional and national scales. Seven hydrologic models were developed using the Precipitation-Runoff Modeling System (PRMS), a deterministic, distributed-parameter, process-based system that simulates the effects of precipitation, temperature, land cover, and water use on basin hydrology. A coarse-resolution PRMS model was developed for the entire ACFB, and six fine-resolution PRMS models were developed for six subbasins of the ACFB. The coarse-resolution model was loosely coupled with a groundwater model to better assess the effects of water use on streamflow in the lower ACFB, a complex geologic setting with karst features. The PRMS coarse-resolution model was used to provide inputs of recharge to the groundwater model, which in turn provide simulations of groundwater flow that were aggregated with PRMS-based simulations of surface runoff and shallow-subsurface flow. Simulations without the effects of water use were developed for each model for at least the calendar years 1982–2012 with longer periods for the Potato Creek subbasin (1942–2012) and the Spring Creek subbasin (1952–2012). Water-use-affected flows were simulated for 2008–12. Water budget simulations showed heterogeneous distributions of precipitation, actual evapotranspiration, recharge, runoff, and storage change across the ACFB. Streamflow volume differences between no-water-use and water-use simulations were largest along the main stem of the Apalachicola and Chattahoochee River Basins, with streamflow percentage differences largest in the upper Chattahoochee and Flint River Basins and Spring Creek in the lower Flint River Basin. Water-use information at a shorter time step and a fully coupled simulation in the lower ACFB may further improve water availability estimates and hydrologic simulations in the basin.

Introduction

The U.S. Geological Survey (USGS) National Water Census is a research program that focuses on developing new water accounting tools and assessing water availability and use at regional and national scales. The National Water Census, one of six major science directions identified by the USGS in its 2007 Science Plan (U.S. Geological Survey, 2007), consists of various topical (streamflow, groundwater, evaporation loss, water use, ecological water, and water quality) and geographically selected large river basin studies to assess the overall state of water resources in the United States. As part of the National Water Census, the USGS quantifies and reports the inputs, outputs, and changes in the amount of water by evaluating the water cycle by component.

As part of the first round of geographic focus area studies, three basins in the United States—each involved in long-term competition and conflict of water resources—were selected for study: (1) the Apalachicola-Chattahoochee-Flint River Basin (ACFB), (2) the Colorado River Basin (Bruce and others, 2015), and (3) the Delaware River Basin (fig. 1). For more than two decades, there has been conflict between Alabama, Florida, and Georgia and other stakeholders over water resources in the ACFB. As population, industry, and agriculture have increased in the ACFB over the last several decades, competition over the basin's water resources has become more pronounced, particularly during droughts. Much of the conflict between the various entities that have an interest in the allocation of water throughout the ACFB is focused on how the U.S. Army Corps of Engineers (USACE) manages four large main-stem reservoirs in the basin: Lake Seminole, Lake Sidney Lanier, Lake Walter F. George, and West Point Lake (fig. 2). Much work has been done by the USACE in optimizing flows in response to water use and reservoir management rules, but there are uncertainties about water availability in the tributary streams of the ACFB where there are concerns over the effects of reduced streamflows (Golladay and others, 2007; Singh and others, 2015; Singh and others, 2016).

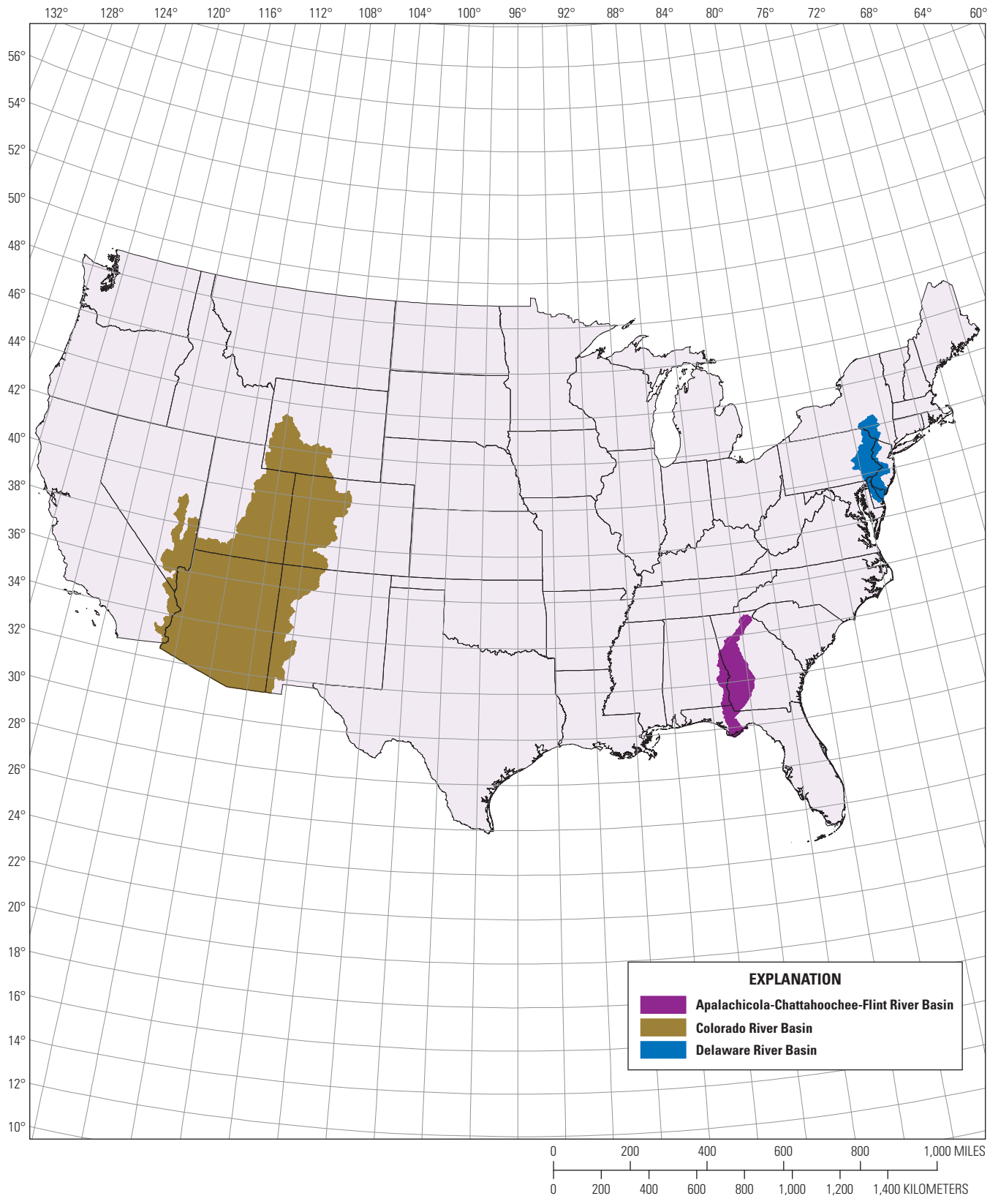

Figure 1. Locations of the first three U.S. Geological Survey National Water Census focus area studies: (1) the Apalachicola-Chattahoochee-Flint River Basin, (2) the Colorado River Basin, and (3) the Delaware River Basin.

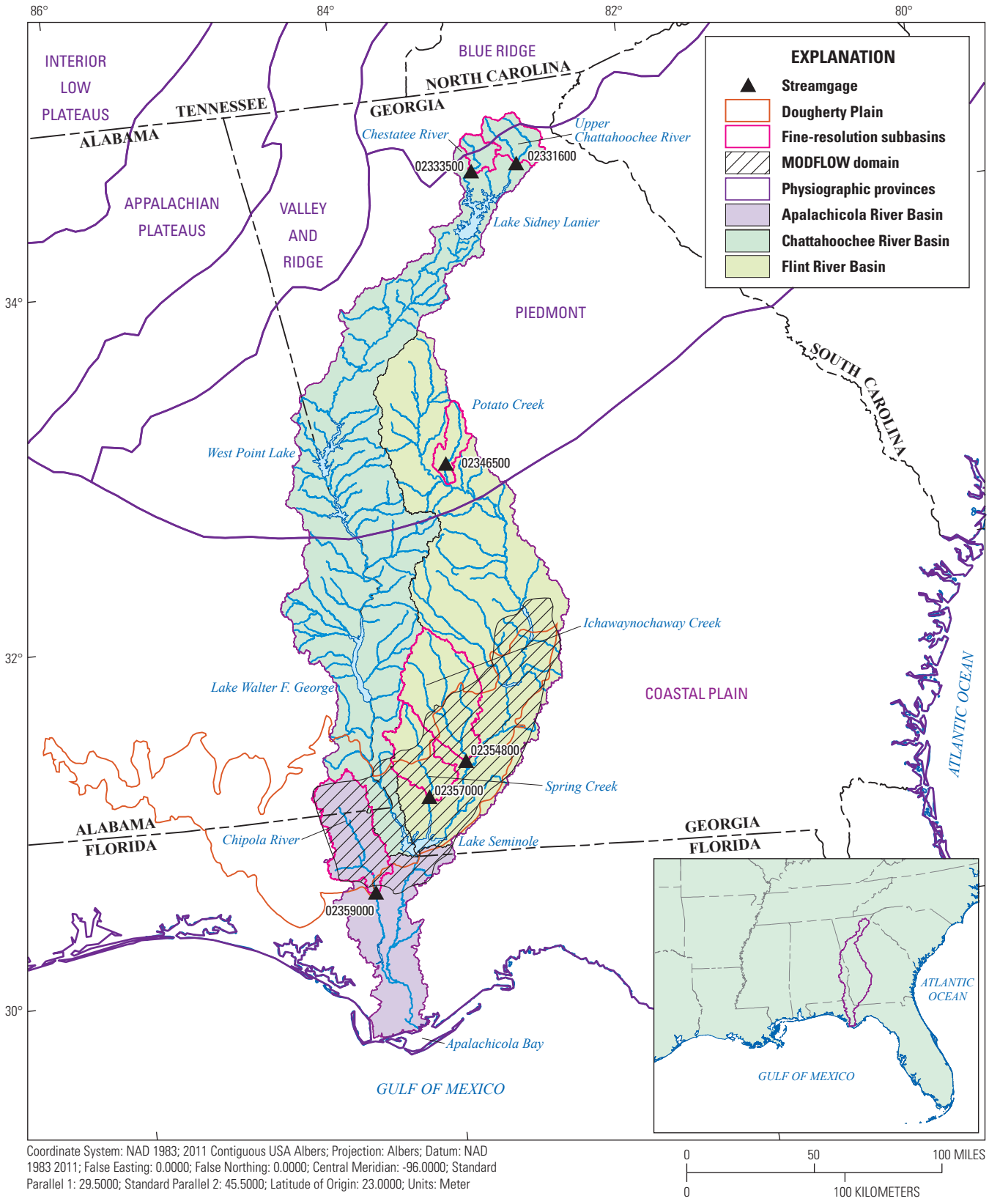

Figure 2. Location, hydrography, and physiography of the Apalachicola-Chattahoochee-Flint River Basin (ACFB).

The USGS ACFB focus area provides insight into some of the most critical uncertainties, such as the influence of surface-water withdrawals and returns on instream flows and the effects of groundwater pumping (primarily for agricultural irrigation) on surface-water availability and flow. The focus area study addresses these uncertainties and gaps in water-resources information with three major areas: (1) improving estimates of water use, (2) modeling surface-water and groundwater flow, and (3) improving the understanding of the ecological effects of hydrologic alterations. The various components of the ACFB focus area study and the relations between these components are shown in figure 3.

Previous Hydrologic Investigations in the Apalachicola-Chattahoochee-Flint River Basin (ACFB)

Several studies have been conducted to simulate either surface water or groundwater flux and storage in the ACFB individually, but none have directly coupled hydrologic simulations of surface water and groundwater to assess the effects of climate, land cover, and water use on basin hydrology. Groundwater resources of the ACFB were discussed in a series of USGS reports in the mid-1990s (Torak and McDowell, 1996; Chapman and Peck, 1997a, 1997b; Mayer, 1997). Additional groundwater studies were completed in parts of the lower ACFB, mainly where the Floridan aquifer system crops out (fig. 2), to simulate stream-aquifer relations and the effects of groundwater pumping on streamflow (Albertson and Torak, 2002; Mosner, 2002; Jones and Torak, 2006). In the past, surface-water hydrologic models have been developed for parts of the ACFB, using a variety of software packages. The Precipitation-Runoff Modeling System (PRMS) was used in the upper Flint River Basin (Viger and others, 2010; Hay and others, 2011; Viger and others, 2011; Walker and others, 2011) and for the entire ACFB (LaFontaine and others, 2013; Hay and others, 2014; LaFontaine and others, 2015) to study the effects of climate and land-use change on hydrology. The PRMS was also used to model many headwater watersheds in the Southeastern United States as part of two model intercomparison studies (Caldwell and others, 2015; Farmer and others, 2015).

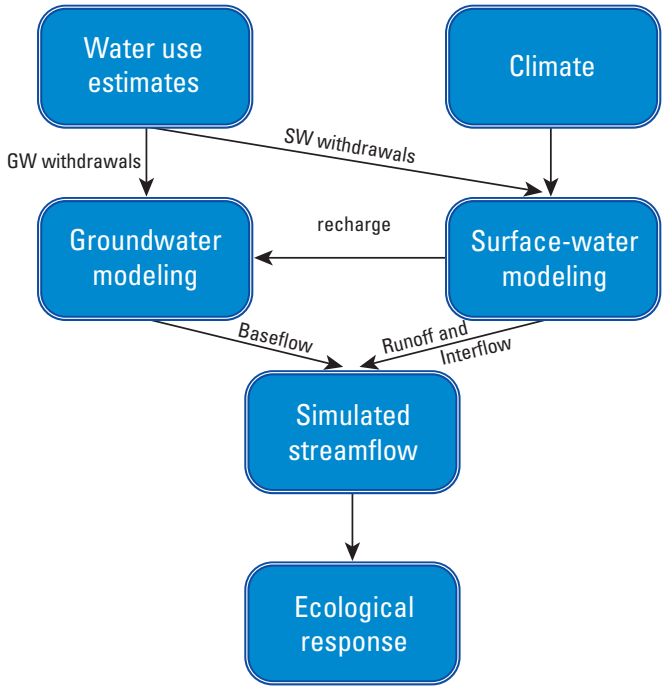

Figure 3. Components of the National Water Census Apalachicola-Chattahoochee-Flint River Basin focus area study showing relations of climate, landscape, streamflow components, and water use with the coupled hydrologic models.

Hydrologic models have been developed using the Hydrologic Simulation Program Fortran (HSPF) software for the headwaters of the Chattahoochee and Flint Rivers (Hummel and others, 2003), the Flint River Basin (Zhang and others, 2005), the main stem part of the lower Flint River Basin (Wen and others, 2007; Wen and Zhang, 2009), Ichawaynochaway Creek (Zeng and Wen, 2005), and Spring Creek (Zhang and Wen, 2005). The models of the lower Flint River, Ichawaynochaway Creek, and Spring Creek used estimates and effects of agricultural irrigation on streamflow from groundwater models developed using the MODular Finite-Element (MODFE) software (Jones and Torak, 2006). Wen and Zhang (2009) also computed monthly estimates of agricultural water-use effects on streamflow for the lower Flint River Basin for both drought and non-drought years.

Previous surface-water models have simulated streamflow in the ACFB without the incorporation of water-use information (Viger and others, 2011; LaFontaine and others, 2013). Recent enhancements to the PRMS include the capability of including water-use information in hydrologic simulations (Regan and LaFontaine, 2017). By including estimates of water withdrawals and returns, hydrologic simulations can better represent actual streamflows and water budgets, which can better inform management decisions that are based on these types of information.

The PRMS has been used in previous applications to estimate recharge (Bauer and Mastin, 1997; Lee and Risley, 2002; Allander and others, 2014). Previous estimates of calculating recharge for input to groundwater models in this region have been climate-fraction based (Jones and Torak, 2006). The PRMS hydrologic model provided estimates of recharge that incorporate landscape processes, such as canopy interception, evapotranspiration, and infiltration. Simulations of flow components from both the groundwater and surface-water models then were combined to provide coupled estimates of water-use-affected streamflows. This study combines groundwater and surface-water modeling simulations, as well as estimates of water use, using a loosely coupled methodology for the Upper Floridan aquifer in the Dougherty Plain (fig. 2).

This methodology accounts for estimated exchanges of recharge and groundwater flow between the surface-water and groundwater models.

Purpose and Scope

This report documents the construction, calibration, evaluation, and use of seven hydrologic models to simulate the effects of climate, land cover, and water use on water availability in the ACFB. The hydrologic models (one coarse resolution for the entire ACFB and six fine resolution for subbasins) were developed using the USGS PRMS (Leavesley and others, 1983; Markstrom and others, 2015), a deterministic, distributed-parameter, process-based model used to simulate the effects of precipitation, temperature, land use, and water use on basin hydrology. Monthly estimates of water use for 2008–12 were incorporated into the simulations through new enhancements to the PRMS. The coarse-resolution ACFB PRMS model provides hydrologic simulations with and without water-use effects for the calendar years 2008–12 and 1982–2012, respectively. The PRMS coarse-resolution simulations were coupled with simulations of groundwater flow from a transient modular hydrologic model (MODFLOW) to estimate water-use-affected streamflows in the lower ACFB region for 2008–12. The six fine-resolution PRMS models provide hydrologic simulations without water-use effects for the Upper Chattahoochee River (1982–2012), Chestatee River (1982–2012), Chipola River (1982–2012), Ichawaynochaway Creek (1982–2012), Potato Creek (1942–2012), and Spring Creek (1952–2012) subbasins (fig. 2). All six fine-resolution PRMS models provide hydrologic simulations with water-use effects for 2008–12. Daily maximum and minimum temperature and precipitation data, pre-processed and interpolated from measured data to an approximately 1-kilometer (km) grid, for 1980–2012 were used as climatic forcings for the coarse-resolution ACFB PRMS model. Measured daily maximum and minimum temperature and precipitation data from the National Climatic Data Center (NCDC) weather station network were used as climatic forcings for the six fine-resolution subbasin PRMS models. Water budgets for the coarse-resolution ACFB PRMS model and biologically relevant hydrologic statistics for the six fine-resolution PRMS models are presented for the ACFB that quantify the amount and timing of water movement throughout the basin.

Hydrologic Description of the ACFB

The ACFB includes three major rivers—the Apalachicola, Chattahoochee, and Flint Rivers (fig. 2). The Chattahoochee River begins in the mountains of northeastern Georgia and flows southwest to the Alabama-Georgia border, where the river flows southward to Lake Seminole on the Florida-Georgia border. The Flint River begins in north-central Georgia, just south of Atlanta, and flows south to Lake Seminole. The Apalachicola River begins at Lake Seminole, which is the confluence of the Chattahoochee and Flint Rivers, and flows southward through Florida to the Gulf of Mexico. The Chattahoochee River is regulated by four USACE reservoir dams (Buford, West Point, Walter F. George, and George W. Andrews) and has several non-USACE run-of-the-river dams (not operated to regulate flow), while the Flint River is relatively unregulated with two non-USACE run-of-the-river dams (U.S. Army Corps of Engineers, 1997). The Apalachicola River has one USACE reservoir (Lake Seminole-James Woodruff Dam) at its headwaters and one other impoundment, Dead Lakes, on the Chipola River (fig. 2). The dam at Dead Lakes was removed in 1987; however, water flowing from the Apalachicola River through the Chipola Cutoff to the Chipola River at the outlet of Dead Lakes effectively acts as a backwater dam to maintain water levels in Dead Lakes.

The Chattahoochee and Flint River Basins are approximately the same size, covering 22,600 and 21,900 square kilometers (km^2), respectively; the Apalachicola River Basin, not including the Chattahoochee and Flint River Basins, covers approximately 6,200 km^2. Historically (early 1700s to early 1900s), land cover in the ACFB was dominated by agriculture that greatly increased sediment supply and produced thick, fine overbank sediment deposits (Jacobson and Coleman, 1986). Since the 1930s, farm abandonment and introduction of soil conservation techniques have decreased sediment loads and allowed forest regrowth across the region (Jacobson and Coleman, 1986). In recent decades, the northern part of the ACFB has undergone substantial urban development. Current land-cover types and percentages in the ACFB, based on the 2001, 2006, and 2011 National Land Cover Database (NLCD; Homer and others, 2007; Fry and others, 2011; Homer and others, 2015), are provided in table 1. The ACFB is nearly half covered with forest, with about a tenth of the basin being developed (high-, medium-, or low-density) land and just over a tenth being cultivated crops. The majority of the developed land is in the Chattahoochee River Basin, with most attributed to metropolitan Atlanta. Nearly two-thirds of the cultivated cropland is located in the Flint River Basin, almost all of which is located in the lower Flint River Basin. This substantial amount of cropland in the lower Flint River Basin is irrigated by groundwater and surface-water withdrawals; the amount of these withdrawals varies depending on local precipitation and crop type. Irrigation withdrawals can account for more than 95 percent of total water use in some counties in southwestern Georgia (Fanning and Trent, 2009).

The ACFB includes the Blue Ridge, Coastal Plain, and Piedmont physiographic provinces (fig. 2). In the ACFB, the Blue Ridge and Piedmont physiographic provinces are present in the northern half of the basin and are underlain by crystalline rock. The Coastal Plain physiographic province is present in the southern half of the basin and is underlain by sedimentary rocks and unconsolidated sediments (Couch

Table 1. Land-cover percentages by river basin in the Apalachicola-Chattahoochee-Flint River Basin (ACFB).

[km², square kilometer; NLCD, National Land Cover Database]

Land-cover type	Land-cover percentage			
	Apalachicola River Basin[1]	Chattahoochee River Basin[2]	Flint River Basin[3]	ACFB[4]
2001 NLCD				
Developed	4.6	12.8	6.9	9.3
Forest	33.5	55.7	43.4	47.6
Cultivated crops	9.4	5.1	20.6	12.3
Hay/Pasture	5.0	8.9	8.7	8.3
Water	1.6	2.8	1.0	1.9
Barren	0.1	0.5	0.2	0.3
Shrub/Scrub/Herb	12.8	10.0	8.9	9.9
Wetlands	33.0	4.2	10.3	10.4
2006 NLCD				
Developed	4.6	13.8	7.3	9.9
Forest	33.8	55.0	43.6	47.5
Cultivated crops	9.6	4.9	20.5	12.2
Hay/Pasture	4.7	8.4	8.5	8.0
Water	1.7	2.9	1.0	1.9
Barren	0.1	0.3	0.2	0.2
Shrub/Scrub/Herb	12.7	10.6	8.8	10.1
Wetlands	32.8	4.1	10.1	10.2
2011 NLCD				
Developed	4.7	14.6	7.5	10.3
Forest	29.5	52.8	41.8	45.2
Cultivated crops	9.2	4.7	20.0	11.9
Hay/Pasture	4.6	8.1	8.3	7.8
Water	1.7	2.9	1.0	1.9
Barren	0.1	0.2	0.2	0.2
Shrub/Scrub/Herb	15.7	12.6	11.0	12.3
Wetlands	34.3	4.1	10.2	10.4

[1]Drainage area = 6,200 km².

[2]Drainage area = 22,600 km².

[3]Drainage area = 21,900 km².

[4]Drainage area = 50,700 km².

and others, 2010). Piedmont soils were developed from highly metamorphosed schist, gneiss, and granite and are typically less than 1 meter thick with low infiltration rates of 6 to 15 centimeters per hour (Costa, 1975; Markewich and others, 1990). The soil/saprolite, soil/rock, and saprolite/rock boundaries of the Piedmont are distinct (within 10 centimeters) with water movement through the soil into the saprolite, and from the saprolite into the rock located along joints, foliation, and bedding planes and faults (Markewich and others, 1990). The Blue Ridge is similar to the Piedmont with greater relief being the most substantial difference. Coastal Plain soils are derived from siliceous sedimentary parent material that is texturally coarser grained and more mature than that of the Piedmont with infiltration rates of 13–28 centimeters per hour (Markewich and others, 1990).

The ACFB is characterized by a warm and humid temperate climate. Because the basin is predominantly oriented north-south, substantial differences in temperature and precipitation are evident due to variations both in latitude and altitude, with the highest altitudes occurring at the most

northern latitudes. According to the Daymet gridded climate data product for 1980–2013 (Thornton and others, 1997; Thornton and Running, 1999; Thornton and others, 2000), average annual precipitation in the ACFB is 1,360 millimeters (53.5 inches), average maximum daily temperature is 24.4 degrees Celsius (°C; 75.9 degrees Fahrenheit [°F]), and average minimum daily temperature is 11.4 °C (52.5 °F). Precipitation accumulation is greater in the northernmost, mountainous part of the ACFB and the southernmost coastal part. Precipitation accumulations are closer to the average in the central part of the ACFB.

Water-use data in the ACFB used in this study consisted of surface-water withdrawals and returns, and groundwater withdrawals. Total mean monthly surface-water withdrawals for the ACFB range from 1,150 to 1,540 cubic feet per second (ft^3/s), mean monthly surface-water returns range from 720 to 937 ft^3/s, and mean monthly groundwater withdrawals range from 40.9 to 1,030 ft^3/s. Mean monthly surface-water and groundwater withdrawals are largest in the summer months of June, July, and August. Monthly surface-water withdrawals range from 1,040 to 1,710 ft^3/s, monthly surface-water returns range from 598 to 1,120 ft^3/s, and groundwater withdrawals range from 0 to 1,380 ft^3/s. Groundwater withdrawals have the largest seasonal variation due to water-supply uses in addition to agricultural. These data are available in LaFontaine and others (2017). Details on how the water-use data were compiled for the model inputs are provided in appendix 1 of this report.

Hydrologic Simulation Methods Used for Modeling the ACFB

Challenges exist in simulating the hydrology of the ACFB; for example, the karst setting of the Dougherty Plain in the southern part of the basin, where water use is substantial, is particularly challenging. To better simulate this complex region of the ACFB, models for simulating surface water, groundwater, and water use were integrated. PRMS models were developed to simulate the surface-water system for the entire ACFB at a coarse resolution and for six subbasin watersheds at a fine resolution. A MODFLOW groundwater model was developed by Jones and others (2017) for the lower part of the ACFB, an area that included the Dougherty Plain (fig. 2), a region of complex hydrology with substantial water use. Geostatistical methods were used by Painter and others (2015) to estimate irrigation uses in unmonitored areas of the ACFB, using point location monthly agricultural water-use information provided by the Georgia Soil and Water Conservation Commission. Daymet gridded climate data were used for the hydrologic model simulations for the period 1980 to 2013 (Thornton and others, 1997; Thornton and Running, 1999; Thornton and others, 2000). Estimates of surface-water and groundwater water-use information were incorporated into the PRMS and MODFLOW models.

The suite of computer codes used in this study simulates the full hydrologic cycle as determined by the energy and water budgets of the plant canopy, snowpack, and soil zone on the basis of distributed climate information (temperature, precipitation, and solar radiation). The hydrologic cycle, as conceptualized for this study, is shown in figure 4. Each arrow in figure 4 represents the various fluxes of water in, out, and across the landscape. Detailed documentation of the coarse-resolution simulation model for the ACFB and of the six fine-resolution simulation models for subbasins of the ACFB are provided in appendixes 1 and 2, respectively.

Precipitation-Runoff Modeling System (PRMS)

The PRMS (Leavesley and others, 1983; Markstrom and others, 2015) is a modular, deterministic, distributed-parameter, physical-process-based hydrologic simulation code. It was developed to evaluate the effects of various combinations of climate, physical characteristics, and simulation options on hydrologic response and water distribution at the watershed scale. The PRMS computes water flow and storage from and to the atmosphere, plant canopy, land surface, snowpack, surface depressions, shallow subsurface zone, deep aquifers, stream segments, and lakes. Physical characteristics, including topography, soils, vegetation, geology, and land use, are used to characterize and derive parameters required in simulation algorithms, spatial discretization, and topological connectivity. Computations of the hydrologic processes use historical, current, and (or) potential future climate data consisting of daily precipitation and minimum and maximum air temperature. Other datasets, such as potential evapotranspiration, solar radiation, streamflow, plant transpiration period, wind speed, and humidity, can be incorporated into PRMS simulations, but are optional. The PRMS operates on a daily time step with simulation periods from days to centuries. A schematic of the PRMS conceptualization is shown in figure 5. A more detailed schematic of just the soil zone part of the PRMS is shown in figure 6.

The PRMS simulates the hydrologic response of a geographic area, called the model domain. The model domain is typically discretized into spatial features called hydrologic response units (HRUs) on which PRMS computes water flux and storage in response to inputs of climate, air temperature, and precipitation. Stream segments are used to represent channelized flow in the model domain and connect the network of HRUs to simulate streamflow. The PRMS computes lateral flow components generated on each HRU for each time step. These flow components then are directed to stream segments for flow aggregation. In addition, two types of water bodies are simulated by PRMS, on-channel lakes and off-channel surface-depression storage. On-channel lakes can be used to simulate features such as reservoirs, while surface depressions are conceptualized as water bodies that are not directly connected to the stream network, such as farm ponds.

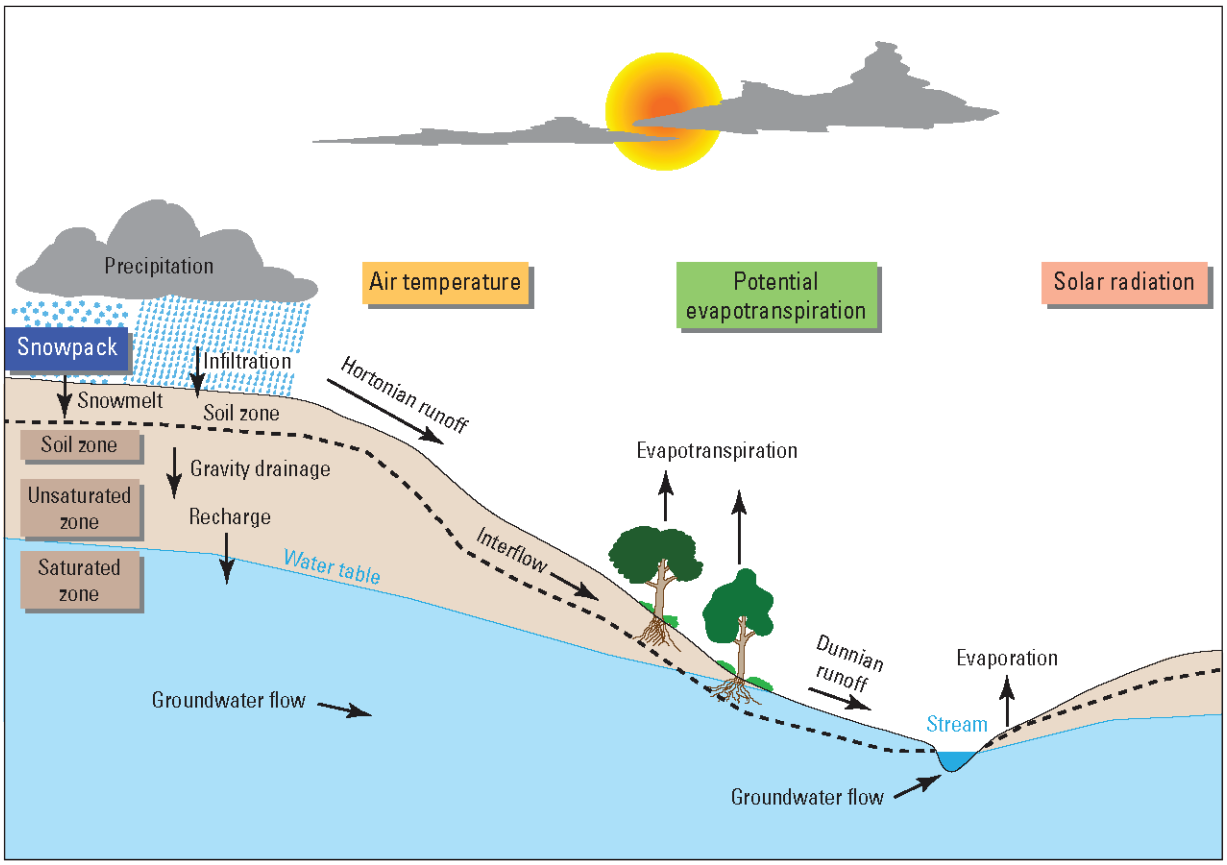

Figure 4. Conceptual flow model used to represent the hydrologic processes of the Apalachicola-Chattahoochee-Flint River Basin (ACFB; from Regan and LaFontaine, 2017). The dashed line represents the divide between the soil-zone capillary reservoir and the soil-zone gravity reservoir in the Precipitation-Runoff Modeling System structure.

Regan and LaFontaine (2017) describe recent enhancements to the PRMS, including the use of water-use data. This new capability allows for the simulation of surface-water and groundwater withdrawals and return flows throughout a PRMS modeling application. In the current version of PRMS (version 5), water can be withdrawn from or added to (as return flows) five conceptual storages (stream segments, groundwater reservoirs, surface-depression storage, external locations, and lakes). In addition, water can be added to two other storages—the capillary reservoir of the soil-zone and the plant canopy.

MODFLOW Groundwater Flow Model

The USGS MODular groundwater FLOW model version 2005 (MODFLOW-2005) is a finite difference model used to simulate groundwater flux and levels on the basis of hydrogeologic characteristics and inputs of climate and regional flow conditions. MODFLOW-2005 simulates groundwater flow using a block-centered, finite-difference approach and is described by Harbaugh (2005). MODFLOW-2005 can simulate layers as confined or unconfined and can incorporate external stresses, such as pumping from wells, recharge, evapotranspiration, rivers, and drains. MODFLOW-2005 is a modular program and is highly flexible, allowing users to develop new packages to improve or simulate new processes. Example packages include Drain, General-Head Boundary, Observation, Recharge, River, and Well (Harbaugh, 2005). Detailed guidelines of the input files required by these packages are described at the MODFLOW 6: USGS Modular Hydrologic Model website at https://water.usgs.gov/ogw/modflow/MODFLOW.html.

Because the ACFB region is a complex hydrogeologic setting that includes karst topography and substantial water use, the use of only a surface-water model to study the effects of groundwater use on streamflow was deemed insufficient. For this particular application, a groundwater model of the lower ACFB region has been developed and is documented in Jones and others (2017) (fig. 2). This application of MODFLOW-2005 was a transient simulation that received inputs of monthly areal recharge from a PRMS hydrologic model for the period 2008–12. Simulations of groundwater flow to streams in the model domain were used for coupling with surface runoff simulations from PRMS to provide monthly estimates of water-use-affected streamflow.

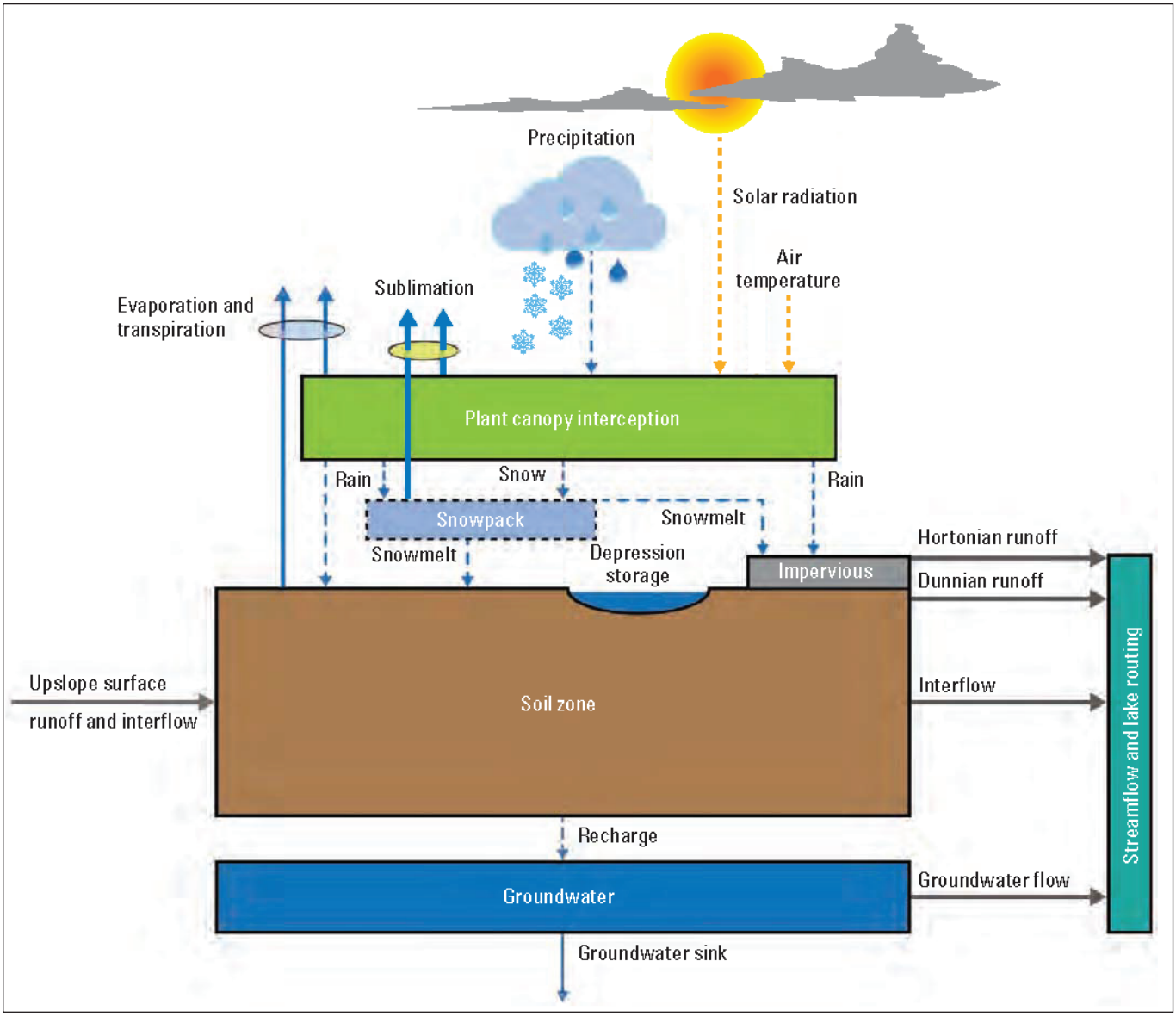

Figure 5. Schematic of the Precipitation-Runoff Modeling System (from Regan and LaFontaine, 2017).

PRMS-MODFLOW Coupling

The coupling method used in this study consists of two stages—recharge transfer and runoff assimilation. First, the coarse-resolution PRMS model simulates recharge (that is, flow to the water table from infiltration of precipitation). These recharge values are used as an input boundary condition for the MODFLOW groundwater simulations. The MODFLOW simulations then provide estimates of groundwater contribution of base flow to a network of rivers and drains. These MODFLOW estimates of base flow are then combined with PRMS estimates of surface runoff and interflow for the computation of total runoff, with the MODFLOW base-flow estimates incorporating the effects of groundwater water use. Further documentation of the coupling process is provided in appendix 1.

Applications of the Hydrologic Simulation Methods

Appendix 1 of this report describes the construction, calibration, and evaluation of the coarse-resolution hydrologic simulations using the PRMS and MODFLOW in the ACFB. A PRMS-only simulation was developed for the entire ACFB, and a coupled simulation was developed for subbasins in the lower ACFB where the PRMS and MODFLOW applications overlapped. Appendix 2 of this report describes the construction, calibration, and evaluation of the six subbasin hydrologic simulations using the PRMS in the ACFB. These simulations provide a finer discretization of spatial units and stream segments than the application described in appendix 1. Supporting datasets for model development are available in LaFontaine and others (2017).

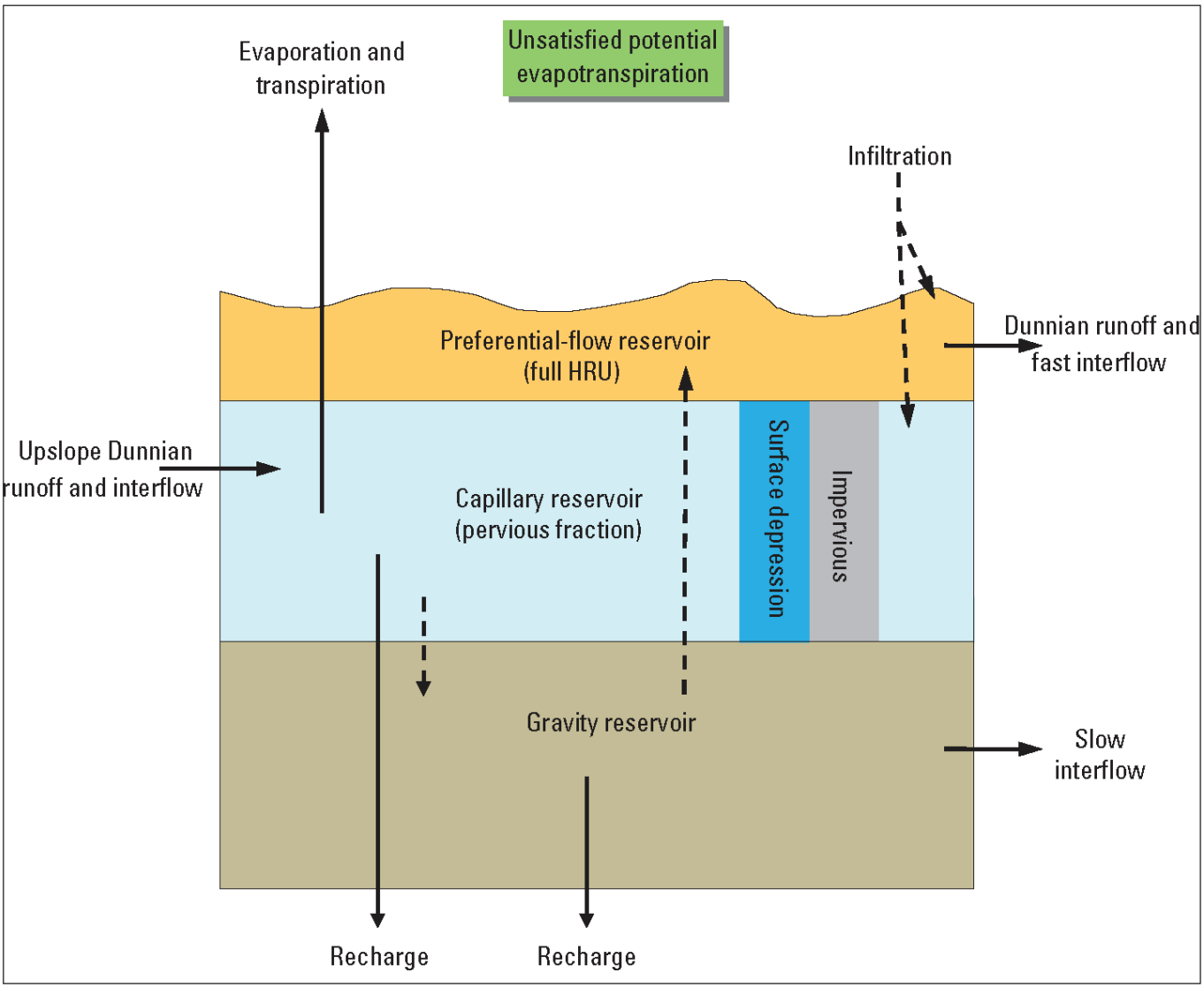

Figure 6. Schematic of the Precipitation-Runoff Modeling System showing the detail of the Soil Zone (from Regan and LaFontaine, 2017).

Hydrologic Simulations and Streamflow Statistics in the ACFB

The coarse- and fine-resolution PRMS hydrologic models (described in appendix 1 and appendix 2, respectively) were used to simulate no-water-use-affected and water-use-affected streamflow scenarios for the ACFB for the period 2008–12. Water budget components were simulated for the coarse- and fine-resolution model HRUs and stream segments to provide water availability estimates. The water budget components include estimates of the precipitation, actual evapotranspiration, recharge, runoff, and changes in storage. The six fine-resolution subbasin PRMS models were developed to provide various statistics of streamflow for use in ecological response models. These statistics provide hydrologic information for the spring and summer seasons when flow conditions affect biologic processes, such as recruitment, reproduction, growth, persistence, migration, dispersal, and colonization (Freeman and others, 2013). These statistics are computed for all stream segments in the subbasin models.

Hydrologic Simulations for the Coarse-Resolution ACFB PRMS Model

The spatial distribution of various water budget components at the HRU scale for the coarse-resolution ACFB PRMS model for the period 2008–12 is shown in figure 7. Long-term simulations of the water budget for the period 1982–2012 provide context for the study period and are shown in figure 8. Precipitation, actual evapotranspiration, recharge, and total runoff have similar spatial distributions across the ACFB for the background period 1982–2012 and the study period

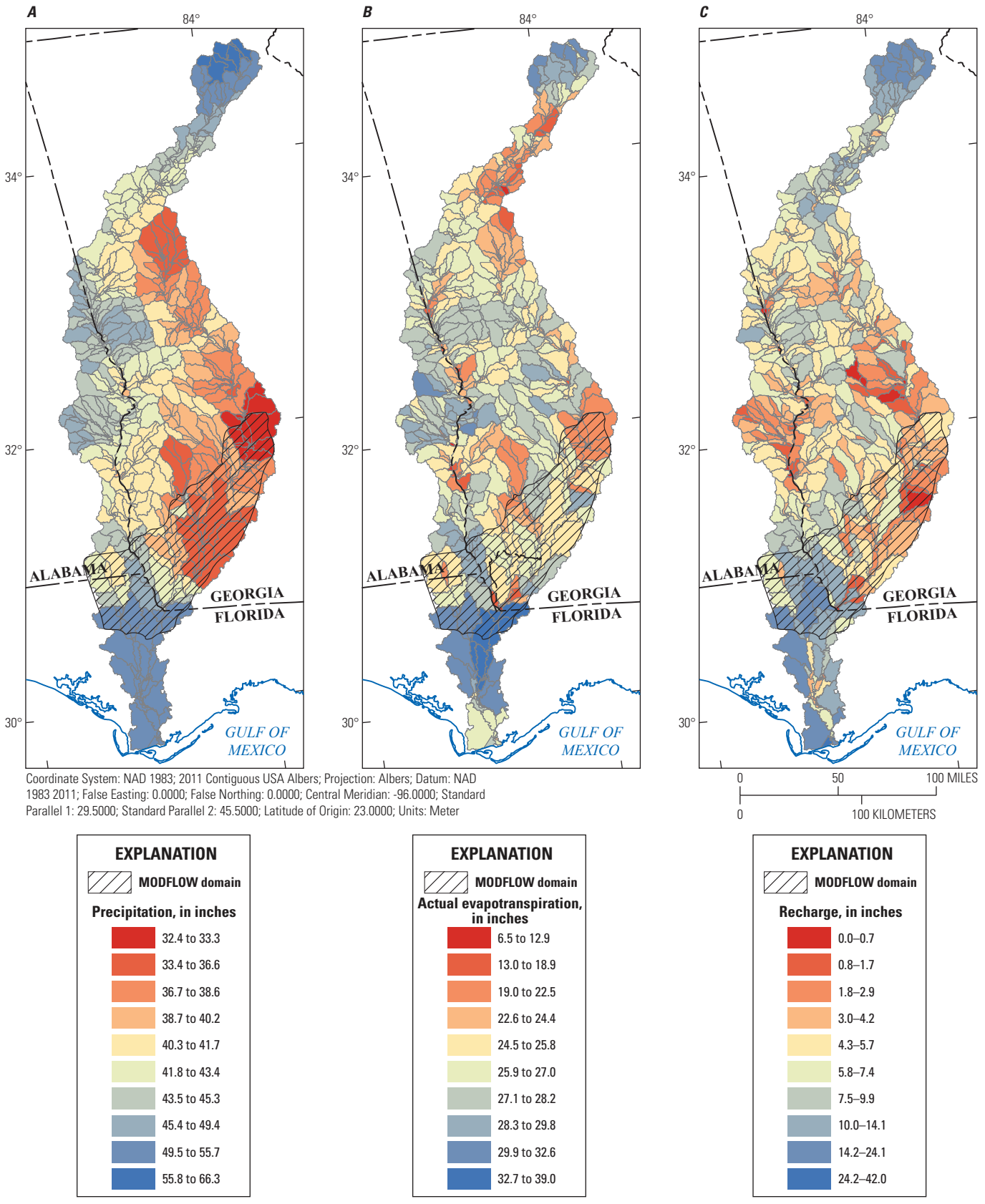

Figure 7. Water budget components, by hydrologic response unit, of the no-water-use simulation of the PRMS-only ACFB coarse-resolution model for the period 2008 to 2012. Components include (*A*) precipitation, (*B*) actual evapotranspiration, (*C*) recharge, (*D*) total runoff, and (*E*) storage change, in units of inches.

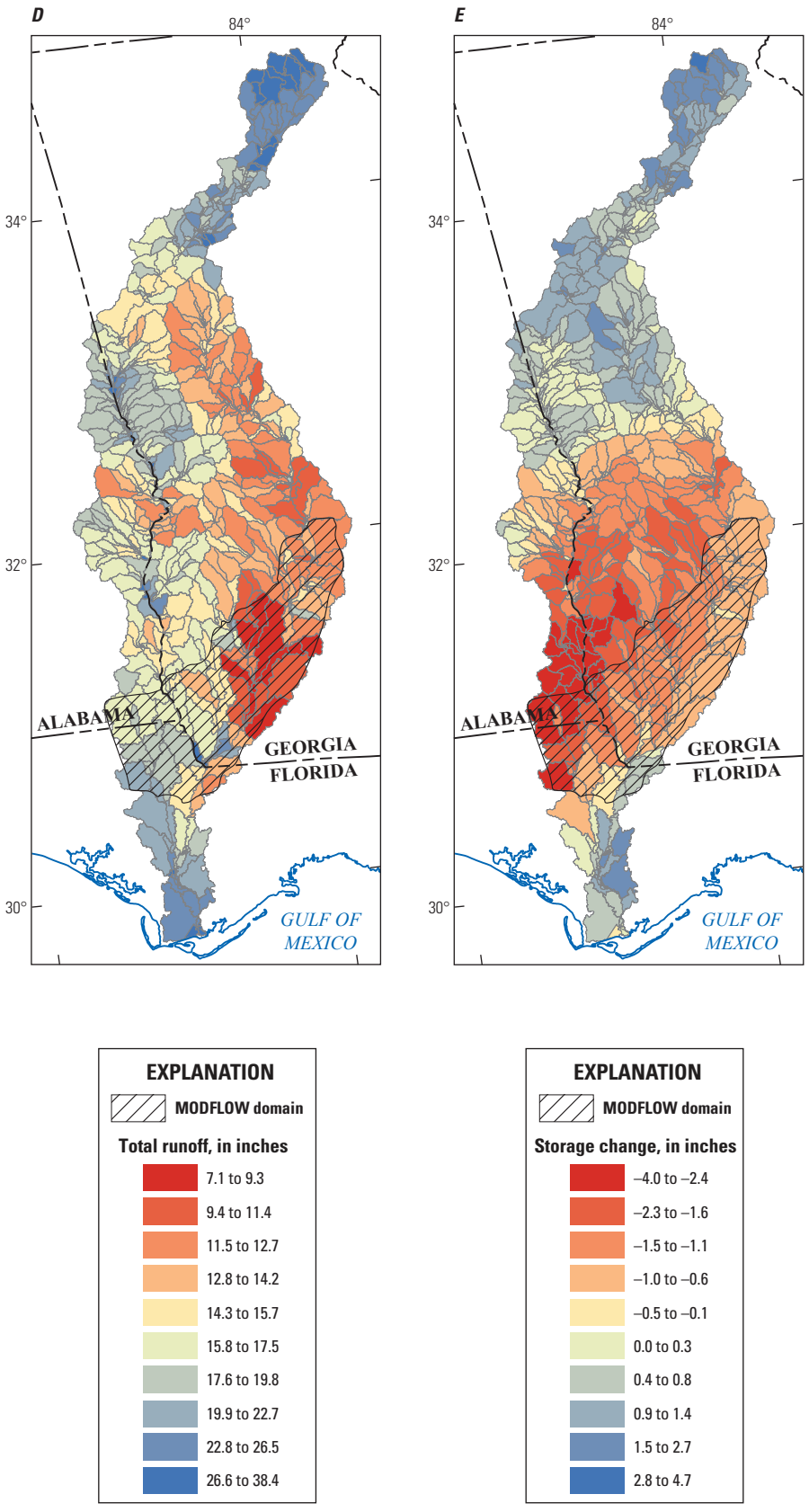

Figure 7.—Continued Water budget components, by hydrologic response unit, of the no-water-use simulation of the PRMS-only ACFB coarse-resolution model for the period 2008 to 2012. Components include (*A*) precipitation, (*B*) actual evapotranspiration, (*C*) recharge, (*D*) total runoff, and (*E*) storage change, in units of inches.

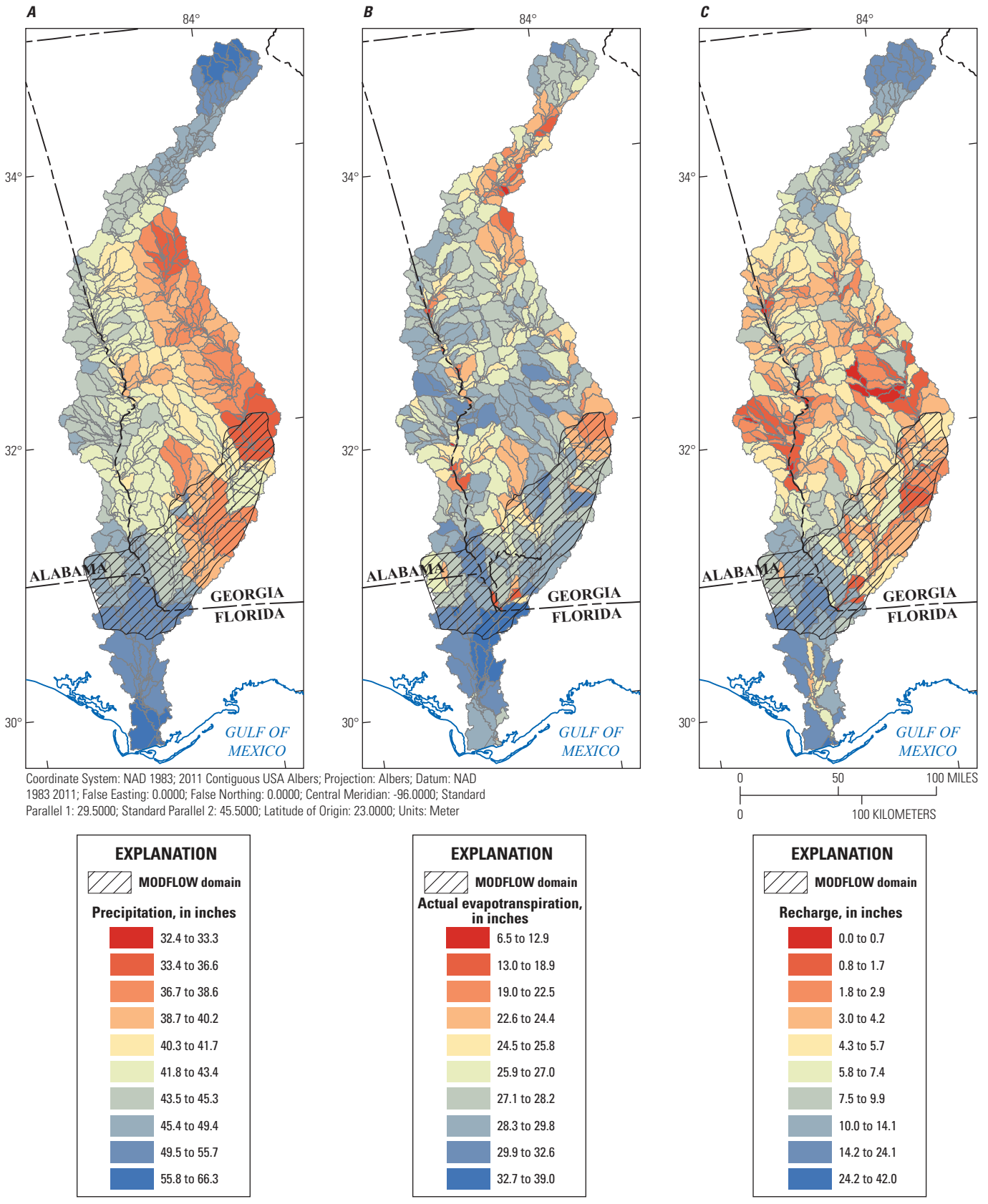

Figure 8. Water budget components, by hydrologic response unit, of the no-water-use simulation of the PRMS-only ACFB coarse-resolution model for the period 1982 to 2012. Components include (*A*) precipitation (hru_ppt), (*B*) actual evapotranspiration (hru_actet), (*C*) recharge, (*D*) total runoff (hru_outflow), and (*E*) storage change, in units of inches.

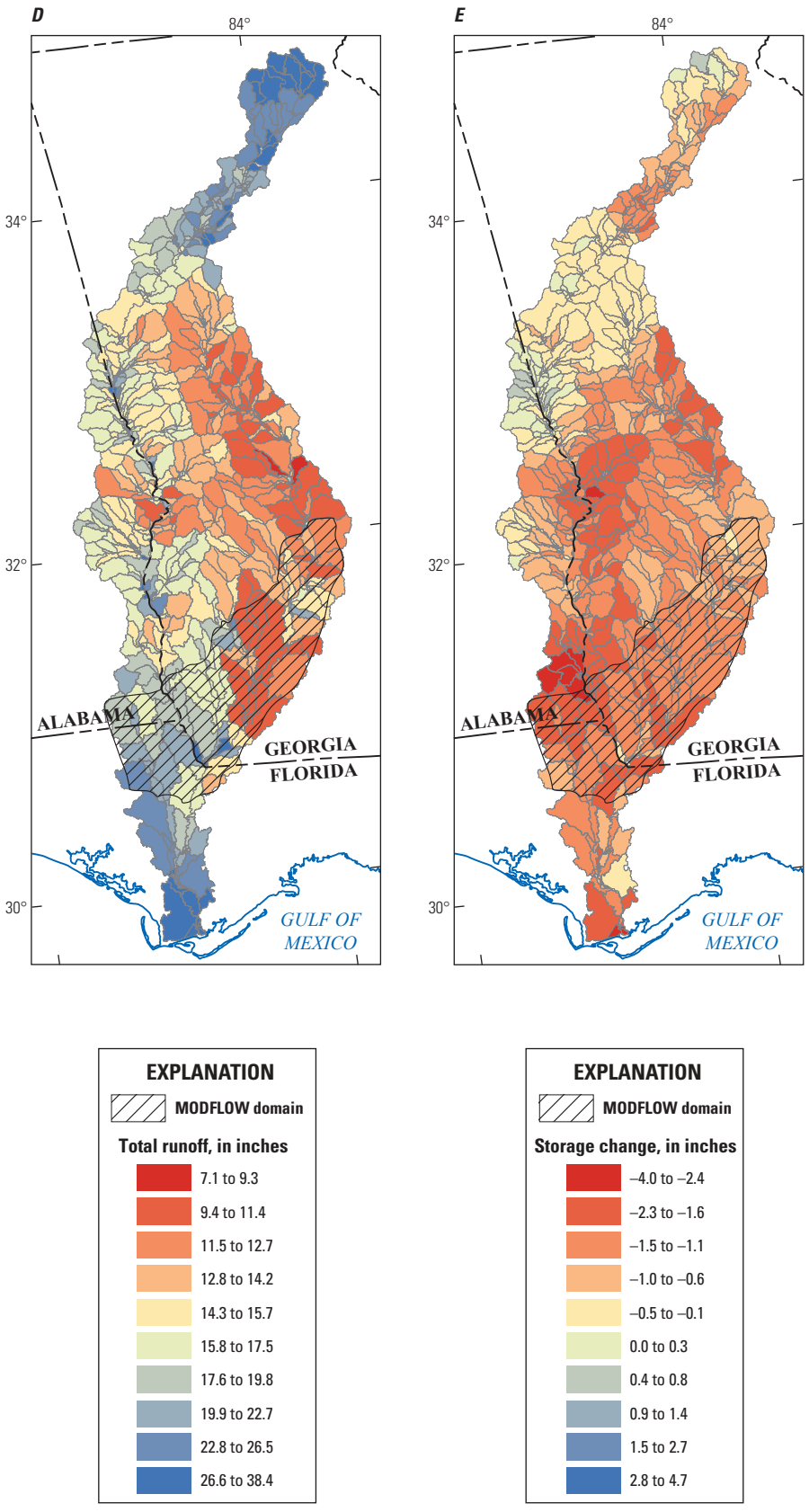

Figure 8.—Continued Water budget components, by hydrologic response unit, of the no-water-use simulation of the PRMS-only ACFB coarse-resolution model for the period 1982 to 2012. Components include (*A*) precipitation (hru_ppt), (*B*) actual evapotranspiration (hru_actet), (*C*) recharge, (*D*) total runoff (hru_outflow), and (*E*) storage change, in units of inches.

2008–12, but differing magnitudes of water. The 2008–12 period had lower precipitation accumulations and more evapotranspiration than the 1982–2012 period. Precipitation varies across the ACFB, with larger amounts in the northernmost and southernmost parts and lower amounts in the central part, with the lowest amounts in the Flint River Basin. Actual evapotranspiration is largest in the areas of largest precipitation and lowest in the urbanized areas around metropolitan Atlanta. This decreased amount of actual evapotranspiration in the urbanized areas is primarily due to less vegetation cover and more impervious areas. Recharge is largely precipitation driven, with larger amounts in the northernmost and southernmost parts of the basin and lower amounts in the central part of the basin. The distribution of total runoff follows the pattern of precipitation, with the largest amounts in the northernmost and southernmost parts of the basin and the smallest amounts in the central part of the basin. The central part of the Chattahoochee River Basin and the lower part of the Flint River Basin have the lowest total runoff. The total storage of the PRMS conceptual reservoirs (for example, soil-zone, groundwater reservoir, depression storage, plant canopy) in the ACFB predominantly decreased over the period 1982–2012, but showed a mix of increases in the northern part of the ACFB and decreases in the southern part of the ACFB for the period 2008–12. For 1982–2012, the lower part of the ACFB decreased more than the northern part of the ACFB, with a few spatial units showing a slight increase in storage. The largest decreases in storage for the period 2008–12 were in the southwestern part of the ACFB. This area generally is at the lower range of storage change for the period 1982–2012, but does not differ as much compared to the rest of the ACFB as during 2008–12. The difference in total storage for the two periods is largely contingent on the start and end dates of the simulation; thus, this comparison shows that the basin was generally wetter in 1982 than it was in 2012. The 2008–12 total storage, however, does show a divergence of wetting and drying across the basin, which is a different spatial distribution than the 1982–2012 period.

Water-use effects on streamflow for the period 2008–12, which were analyzed on the stream segments, are depicted in figure 9. Water use is predominantly for municipal and industrial uses in the northern part of the ACFB and predominantly for agricultural use in the southern part of the ACFB. Total streamflow decreases due to water use are larger in the Chattahoochee and Apalachicola Rivers than in the Flint River Basin (fig. 9). However, the percentage difference in total streamflow is largest in the upper and middle parts of the Chattahoochee River, the upper Flint River, and Spring Creek in the southern part of the basin. The pattern of these effects can vary seasonally, as well, because the agricultural water use occurs primarily during the warm, growing season when streamflows are generally lower due to increased evapotranspiration. Municipal and industrial water use has some seasonal variation, but much less than the agricultural water use. Further details about water use in the ACFB are provided in appendix 1.

Hydrologic Simulations for the Coarse-Resolution ACFB PRMS-MODFLOW Coupled Model

Coupled hydrologic simulations in the lower part of the ACFB were completed using a combination of streamflow components simulated by the coarse-resolution PRMS and MODFLOW models. Initially, simulations of recharge from the PRMS model were used as input to the groundwater model. Simulations from the groundwater model were then combined with PRMS flow components to simulate streamflow in the lower ACFB. The PRMS flow components of surface runoff (PRMS variable *sroff*) and subsurface flow (PRMS variable *ssres_flow*) and groundwater flows from a zone budget analysis of the MODFLOW simulation were combined for each HRU in the PRMS model and summarized at a monthly time step. Zones are groups of MODFLOW cells that are treated as subregions. The budget for a zone is the flow between each adjacent zone. For this application, the flow to the stream network from each zone was used. This coupling resulted in hydrologic simulations for the lower part of the ACFB that incorporated regional groundwater flow and water-use effects on streamflow.

Recharge was simulated by the PRMS as the water that moves vertically downward through the soil zone to the groundwater reservoir. Precipitation and recharge estimates from the PRMS simulation shown in figure 10 provide mean monthly averages of each variable. Precipitation does not have a strong seasonal signal, with the 2008–12 period showing some deviations from the long-term period 1982–2012 for the summer months. Recharge is greatest in the winter months and lowest in the summer months, a result primarily of lower evapotranspiration potential in the winter and higher evapotranspiration potential in the summer. The annual mean precipitation is 6.7 percent less and recharge is 8.8 percent less during the 2008–12 period than during the long-term period (fig. 10). Monthly precipitation and recharge simulations show that recharge is seasonal and precipitation driven (fig. 11). The highest recharge months occur when precipitation accumulations are greater and during the cool season months. On average, relatively little recharge occurs during the summer months in the lower ACFB (fig. 10), with evapotranspiration being a primary factor.

Coupled hydrologic simulations for three tributary watersheds in the lower ACFB that either fully or partially intersect the groundwater model active area are shown in figure 12. The simulations shown are for USGS streamgages at Ichawaynochaway Creek near Elmodel, GA (02354800), Spring Creek near Iron City, GA (02357000), and Chipola River near Altha, FL (02359000), for the period 2008–12 (fig. 2). The coupled simulations generally match measured streamflow volume better than the PRMS-only simulations throughout the simulation period and across the year at USGS streamgages 02354800 and 02357000. The coupled simulations at USGS streamgages 02354800 and 02357000 have

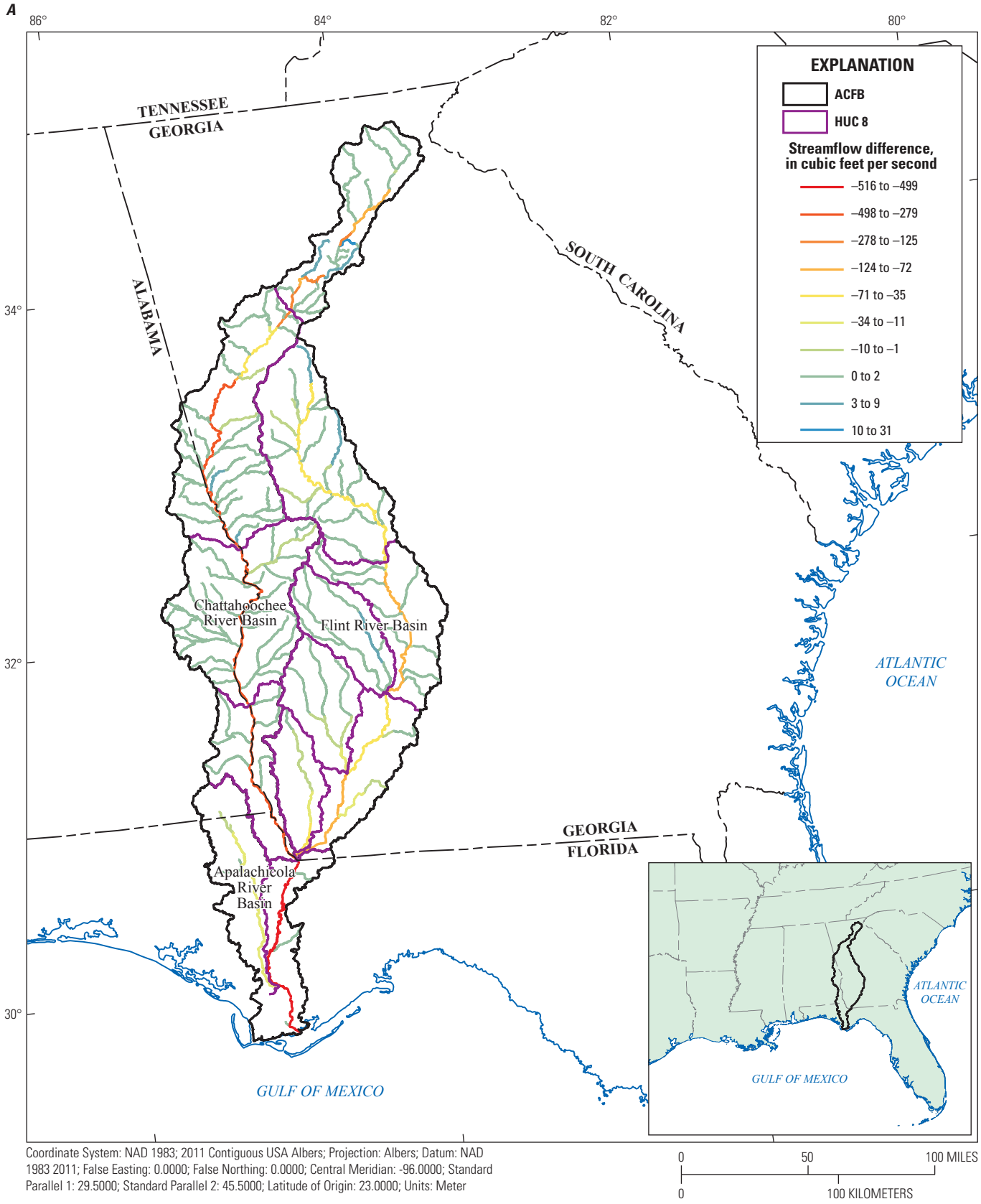

Figure 9. Water-use effects on streamflow in the ACFB for the period 2008–12. Effects are shown as (*A*) a difference in streamflow, in cubic feet per second, and (*B*) a percentage difference between no-water-use streamflows and water-use streamflows.

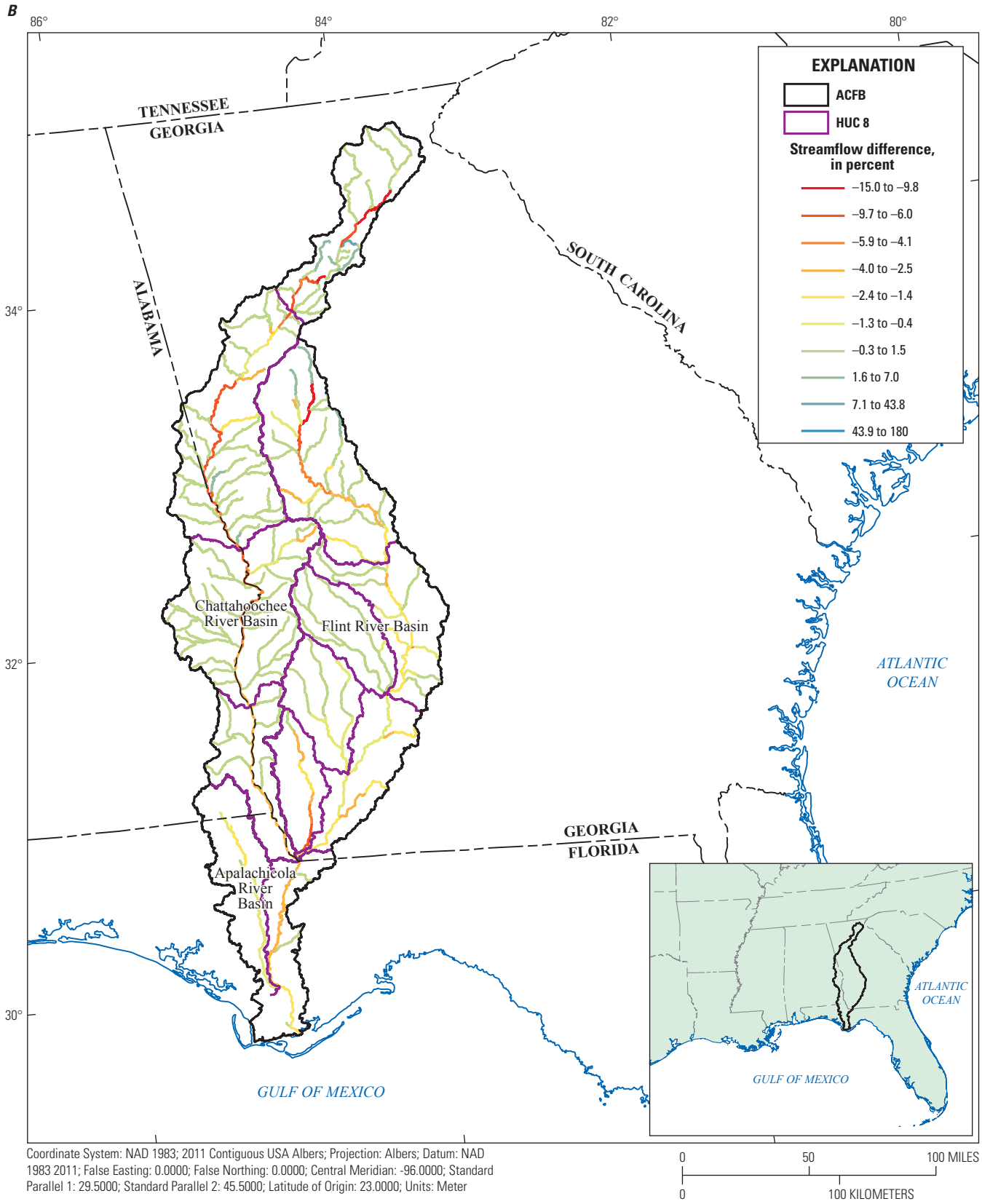

Figure 9.—Continued Water-use effects on streamflow in the ACFB for the period 2008–12. Effects are shown as (*A*) a difference in streamflow, in cubic feet per second, and (*B*) a percentage difference between no-water-use streamflows and water-use streamflows.

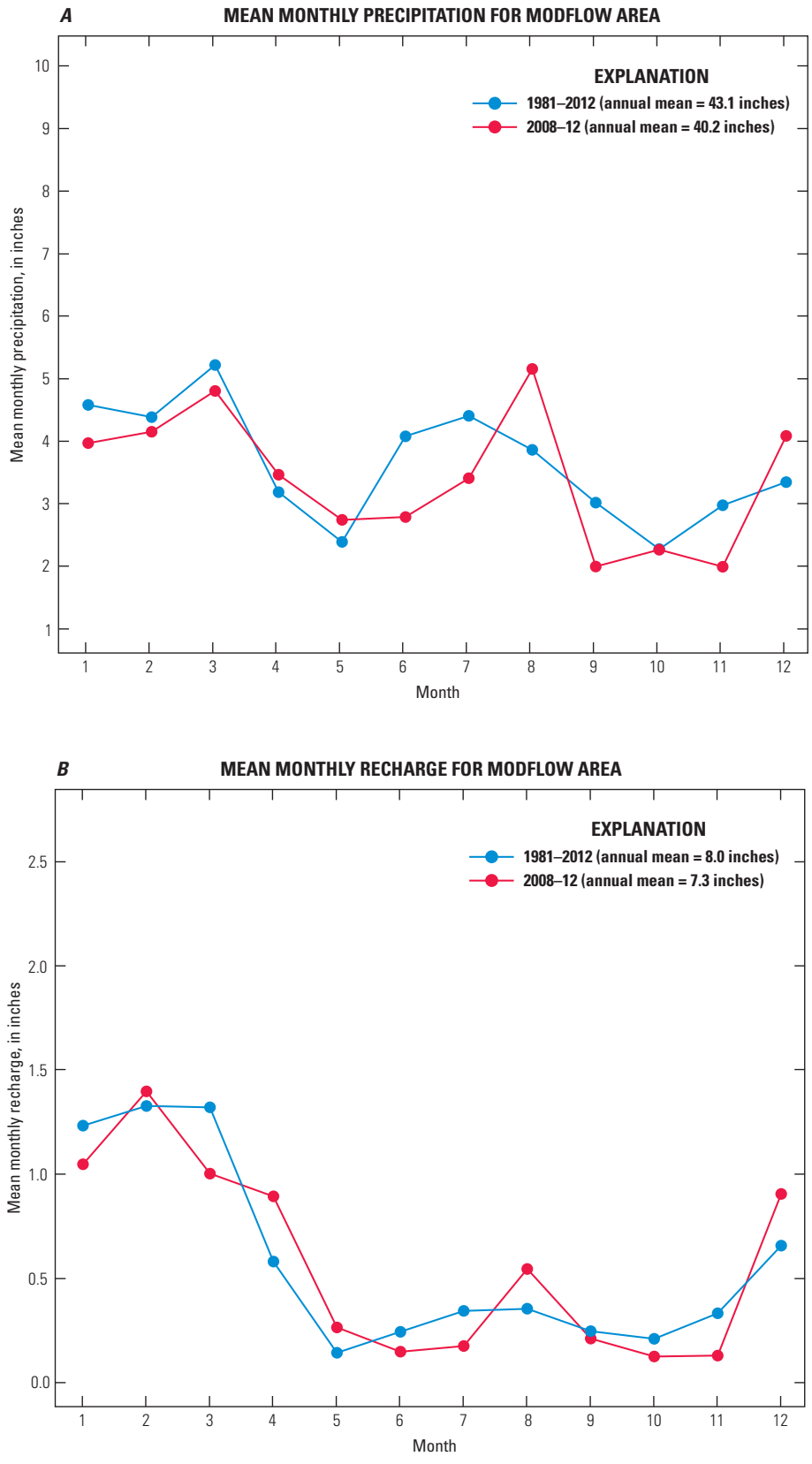

Figure 10. Plots of mean monthly (*A*) precipitation and (*B*) recharge, in inches, for the MODFLOW active area for the study period 2008–12 and the long-term period 1981–2012. Average annual mean values of precipitation and recharge, in inches, are provided for both periods.

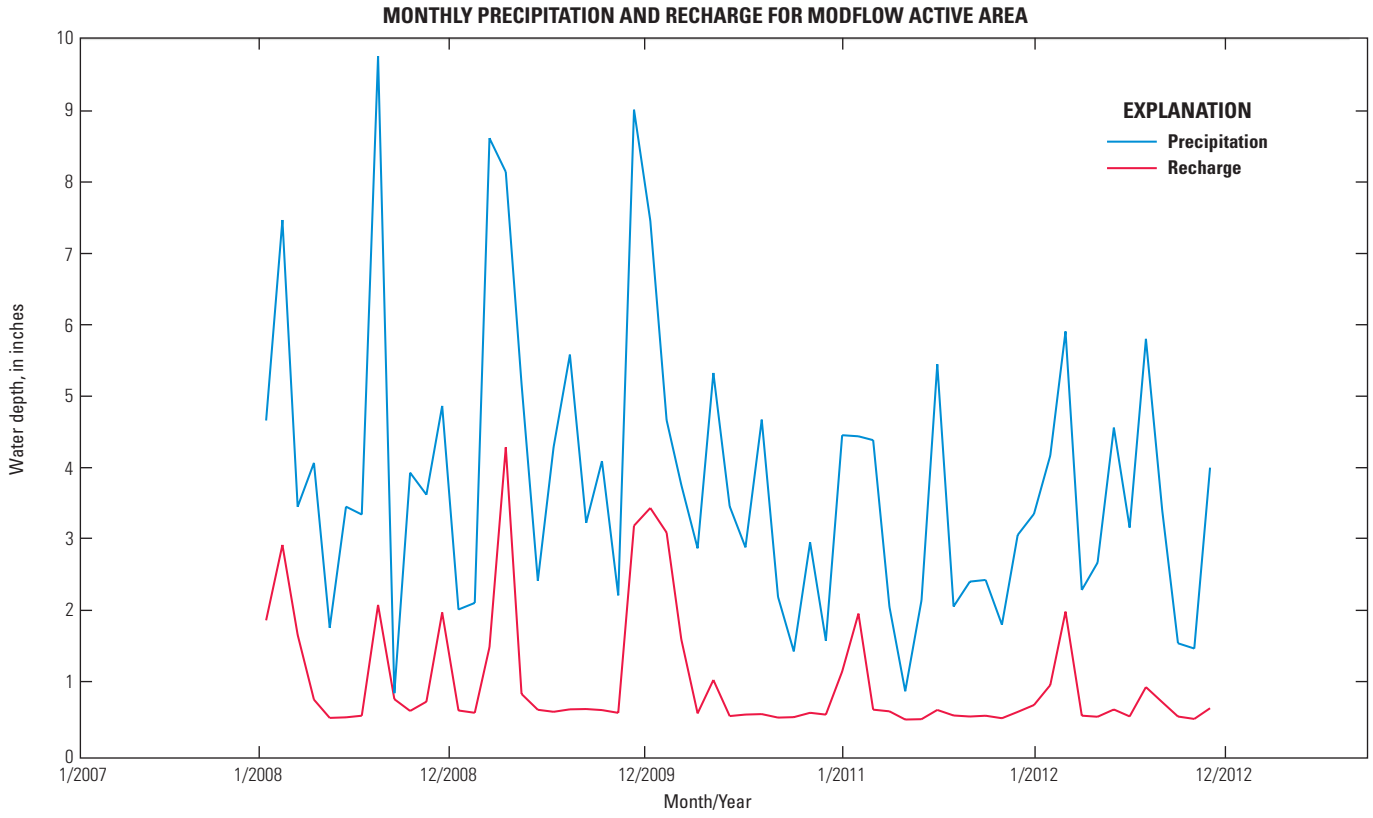

Figure 11. Plot of monthly precipitation and recharge for the MODFLOW active area for the study period 2008–12. The variables are shown in depth of water, in inches.

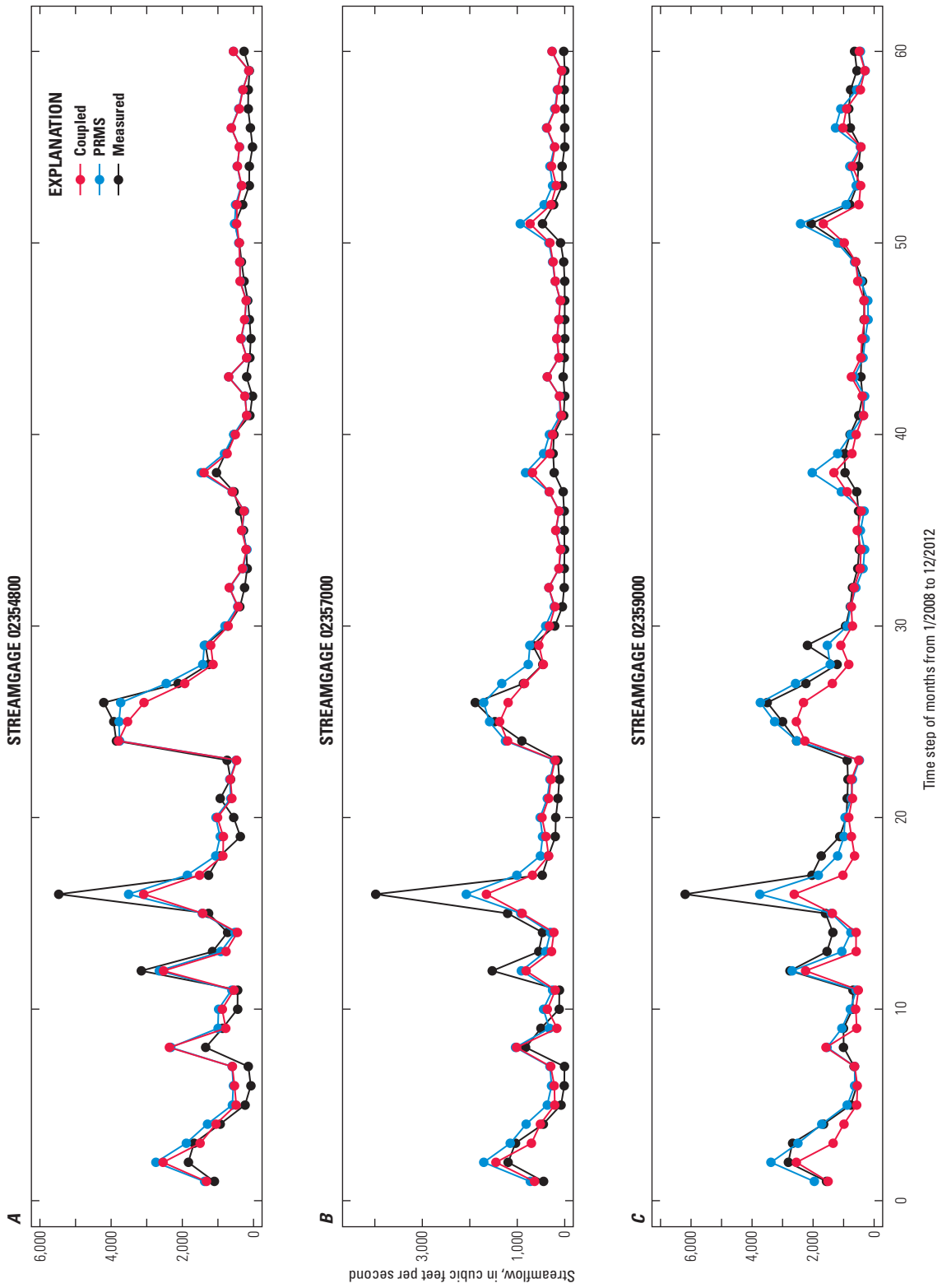

Figure 12. Comparison of PRMS-only simulations, coupled PRMS-MODFLOW streamflow simulations, and measured streamflow for three subbasins in the lower ACFB for 2008 to 2012. The subbasins have outlet streamgages (*A*) Ichawaynochaway Creek near Elmodel, GA (02354800), (*B*) Spring Creek near Iron City, GA (02357000), and (*C*) Chipola River near Altha, FL (02359000).

9.9 and 27.6 percent, respectively, less streamflow volume bias than the PRMS-only simulations during the months of April to September for the period 2008–12. The coupled simulation flow volume errors at USGS streamgage 02359000 are 11 percent greater and 2.3 percent less than the PRMS-only simulations for the April to September and July to September seasons, respectively, and have a 5.9-percent bias for the July to September season when compared to the measured streamflow volume. The improvement in streamflow volume bias for USGS streamgages 02354800 and 02357000 for the July to September season compared to the measured streamflow volumes are 7.5 and 23 percent, respectively. As the warm season months of April to September coincide with the time of most agricultural water use, these simulations seem to provide more accurate estimates of water availability than the PRMS-only simulations during low-flow months.

Streamflow Statistics for the Fine-Resolution Upper Chattahoochee River Subbasin PRMS Model

Streamflow statistics described in table 2 were computed for all 328 stream segments in the upper Chattahoochee River subbasin PRMS model for the period 1982 to 2012. These statistics were computed for the 31-year historical period without water-use effects to show the variation of each statistic and with water-use effects for the period 2008–12 to compare water-use and no-water-use simulations. The statistics were also computed for measured streamflow at USGS streamgage 02331600 (Chattahoochee River near Cornelia, GA) for the entire period. The long-term plots in figure 13 show reasonable agreement between statistics computed for measured and simulated streamflow values for the period 1982 to 2012. Water-use data for this subbasin show only a net use of 0.42 percent (2.42 ft^3/s) of mean annual streamflow (628 ft^3/s) at streamgage 02331600 for the study period (2008–12). Net water use was computed as the difference between mean annual surface-water withdrawals and mean annual surface-water return flows for the study period. Thus, the study period (2008–12) plots in figure 14 show virtually no difference between the water-use (red line) and no-water-use simulations (blue line); however, the simulation-based statistics are less variable from year to year than those based on measured streamflow. (The blue line in figure 14 is not visible where overlain by the red line.)

Streamflow Statistics for the Fine-Resolution Chestatee River Subbasin PRMS Model

Streamflow statistics described in table 2 were computed for all 168 stream segments in the Chestatee River subbasin PRMS model for the period 1982 to 2012. These statistics

Table 2. Seasonal statistics of streamflow computed for the ACFB subbasin models.

[Statistics were computed for each stream segment; 10-day statistics were computed on a moving window average of the daily streamflows for each stream segment]

Statistic	Season	Time step (days)	Description
March–June daily median	Spring	1	Median of daily streamflows during the months of March to June
July-September daily median	Summer	1	Median of daily streamflows during the months of July to September
March–June daily standard deviation	Spring	1	Standard deviation of daily streamflows during the months of March to June
July–September daily standard deviation	Summer	1	Standard deviation of daily streamflows during the months of July to September
March–June 10-day minimum	Spring	10	Minimum of 10-day moving average of streamflows during March to June
July–September 10-day minimum	Summer	10	Minimum of 10-day moving average of streamflows during July to September
March–June 10-day maximum	Spring	10	Maximum of 10-day moving average of streamflows during March to June
July–September 10-day maximum	Summer	10	Maximum of 10-day moving average of streamflows during July to September
March–June 10-day minimum standard deviation	Spring	10	Standard deviation of the 10-day moving average minimum streamflows during March to June
July–September 10-day minimum standard deviation	Summer	10	Standard deviation of the 10-day moving average minimum streamflows during July to September

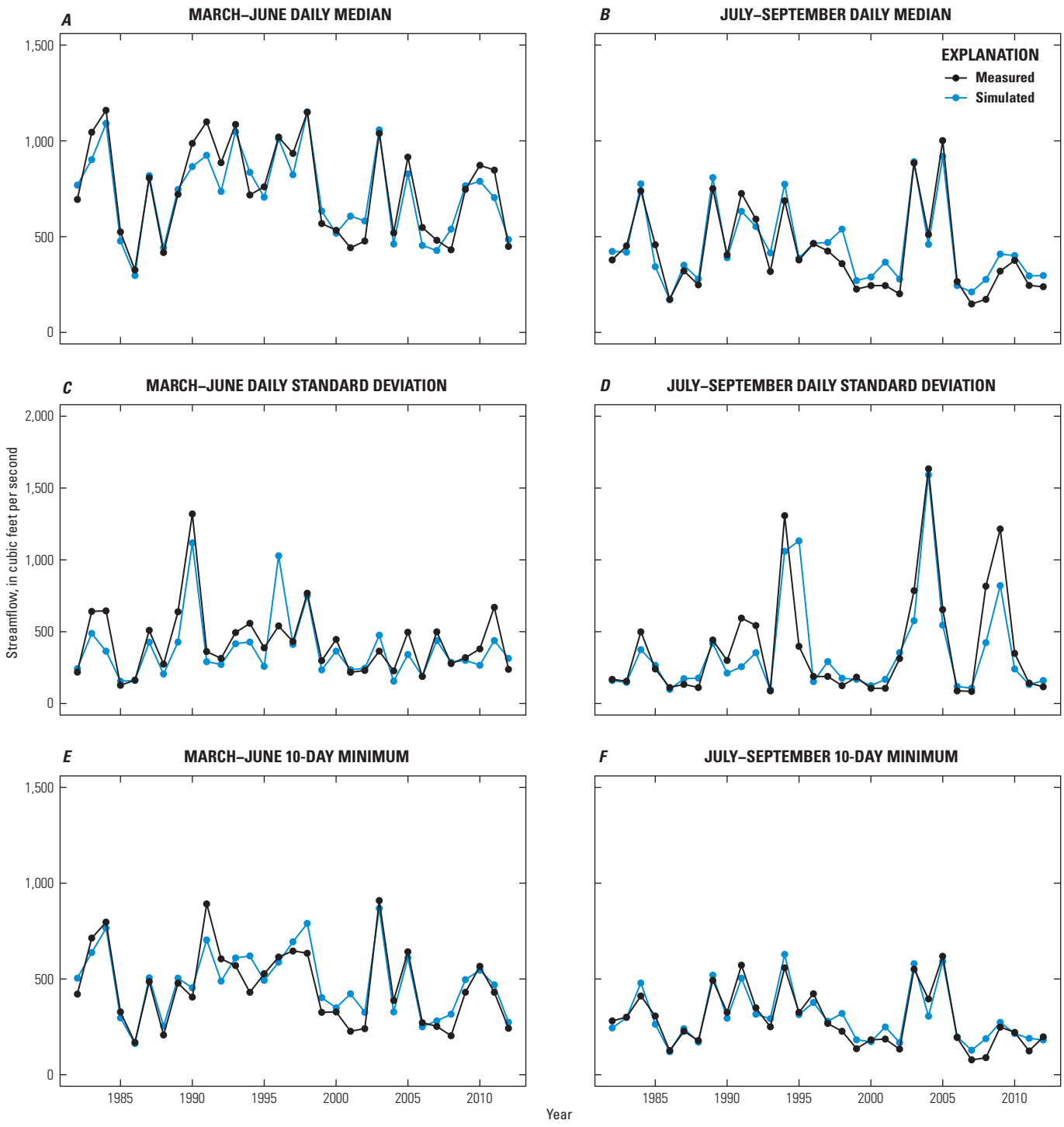

Figure 13. Plots of 10 biologically relevant hydrologic statistics for the upper Chattahoochee River subbasin for the period 1982 to 2012 at USGS streamgage 02331600 (Chattahoochee River near Cornelia, GA). These plots show the variation in these statistics for the recent climate period. The statistics shown in the plots are (*A*) March to June daily median streamflow, (*B*) July to September daily median streamflow, (*C*) March to June standard deviation of daily streamflow, (*D*) July to September standard deviation of daily streamflow, (*E*) March to June 10-day minimum moving average of daily streamflow, (*F*) July to September 10-day minimum moving average of daily streamflow, (*G*) March to June 10-day maximum moving average of daily streamflow, (*H*) July to September 10-day maximum moving average of daily streamflow, (*I*) March to June standard deviation of 10-day minimum moving average of daily streamflow, and (*J*) July to September standard deviation of 10-day minimum moving average of daily streamflow.

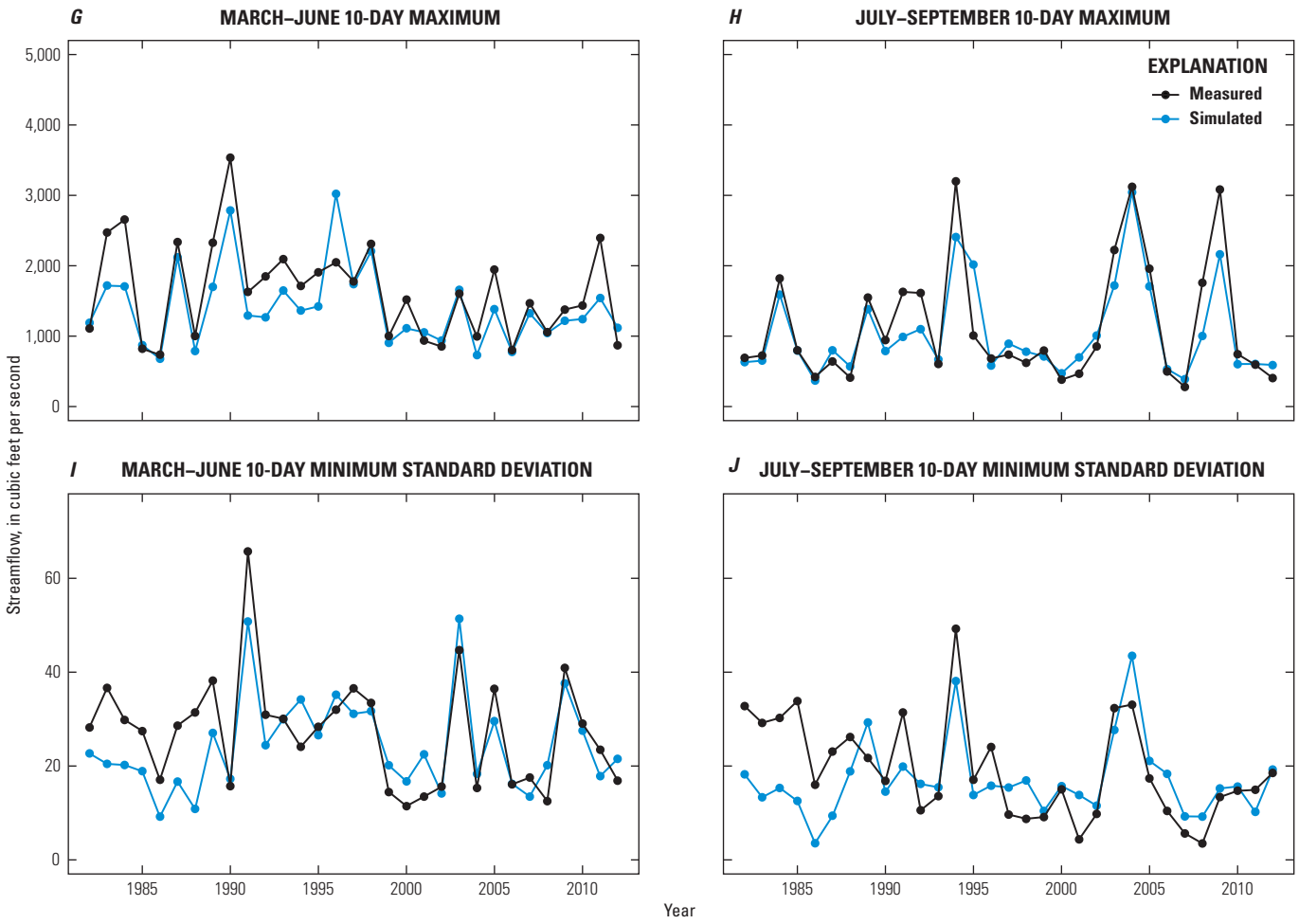

Figure 13.—Continued Plots of 10 biologically relevant hydrologic statistics for the upper Chattahoochee River subbasin for the period 1982 to 2012 at USGS streamgage 02331600 (Chattahoochee River near Cornelia, GA). These plots show the variation in these statistics for the recent climate period. The statistics shown in the plots are (*A*) March to June daily median streamflow, (*B*) July to September daily median streamflow, (*C*) March to June standard deviation of daily streamflow, (*D*) July to September standard deviation of daily streamflow, (*E*) March to June 10-day minimum moving average of daily streamflow, (*F*) July to September 10-day minimum moving average of daily streamflow, (*G*) March to June 10-day maximum moving average of daily streamflow, (*H*) July to September 10-day maximum moving average of daily streamflow, (*I*) March to June standard deviation of 10-day minimum moving average of daily streamflow, and (*J*) July to September standard deviation of 10-day minimum moving average of daily streamflow.

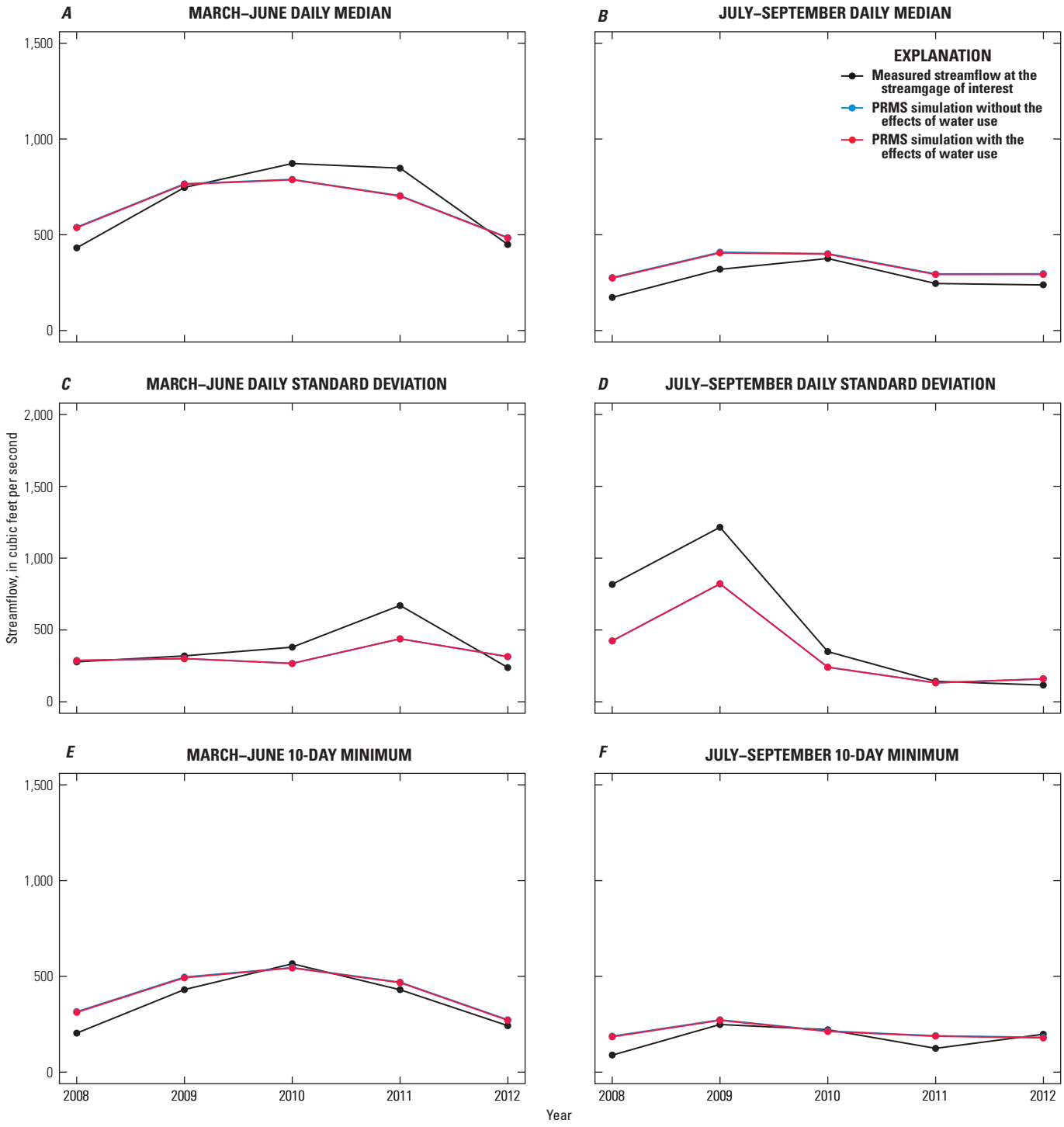

Figure 14. Plots of 10 biologically relevant hydrologic statistics for the upper Chattahoochee River subbasin for the period 2008 to 2012 at USGS streamgage 02331600 (Chattahoochee River at Cornelia, GA). These plots show the variation in the statistics for the study period with and without water-use effects. The statistics shown in the plots are (*A*) March to June daily median streamflow, (*B*) July to September daily median streamflow, (*C*) March to June standard deviation of daily streamflow, (*D*) July to September standard deviation of daily streamflow, (*E*) March to June 10-day minimum moving average of daily streamflow, (*F*) July to September 10-day minimum moving average of daily streamflow, (*G*) March to June 10-day maximum moving average of daily streamflow, (*H*) July to September 10-day maximum moving average of daily streamflow, (*I*) March to June standard deviation of 10-day minimum moving average of daily streamflow, and (*J*) July to September standard deviation of 10-day minimum moving average of daily streamflow. The blue line is not visible where overlain by the red line.

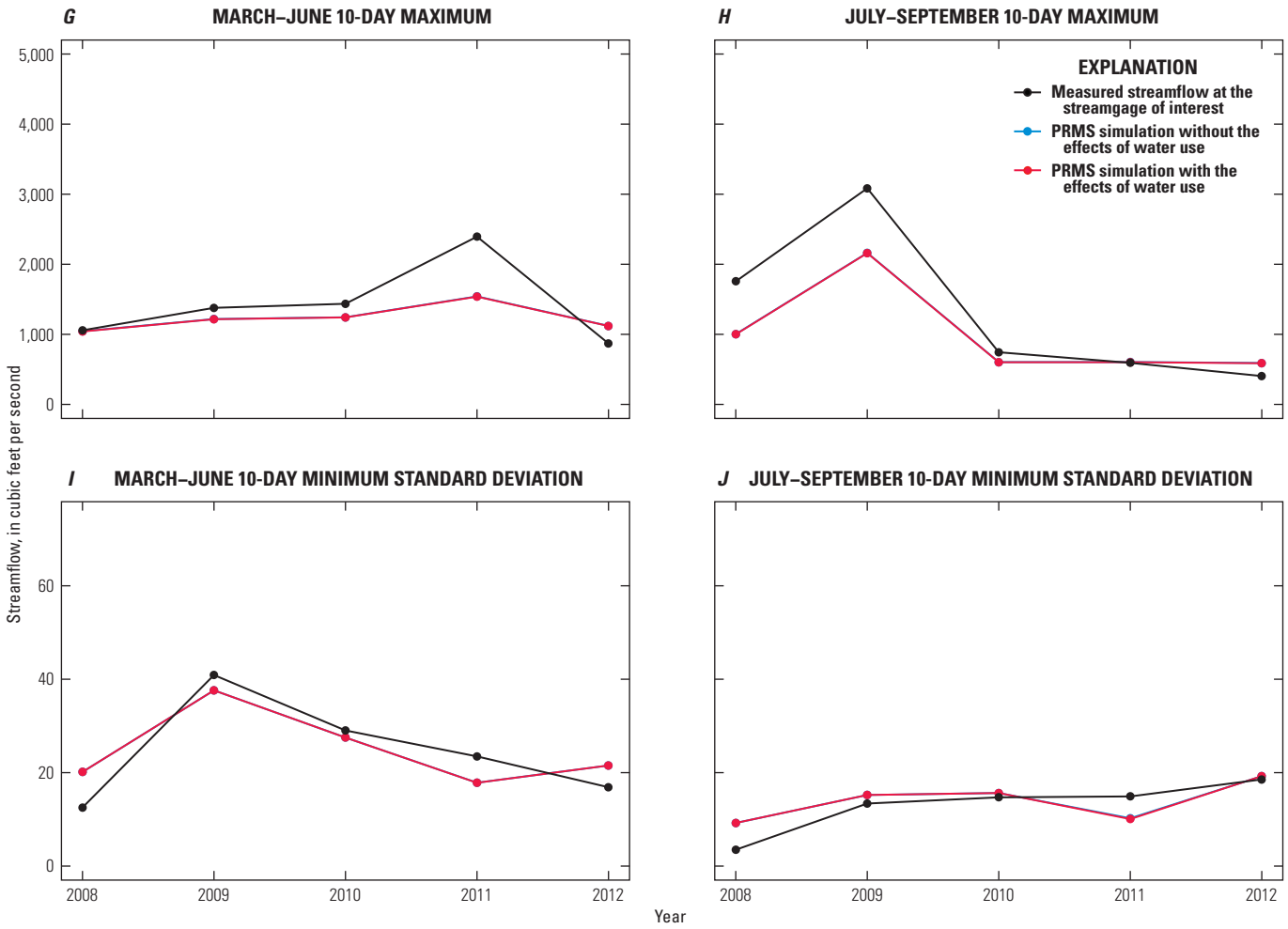

Figure 14.—Continued Plots of 10 biologically relevant hydrologic statistics for the upper Chattahoochee River subbasin for the period 2008 to 2012 at USGS streamgage 02331600 (Chattahoochee River at Cornelia, GA). These plots show the variation in the statistics for the study period with and without water-use effects. The statistics shown in the plots are (*A*) March to June daily median streamflow, (*B*) July to September daily median streamflow, (*C*) March to June standard deviation of daily streamflow, (*D*) July to September standard deviation of daily streamflow, (*E*) March to June 10-day minimum moving average of daily streamflow, (*F*) July to September 10-day minimum moving average of daily streamflow, (*G*) March to June 10-day maximum moving average of daily streamflow, (*H*) July to September 10-day maximum moving average of daily streamflow, (*I*) March to June standard deviation of 10-day minimum moving average of daily streamflow, and (*J*) July to September standard deviation of 10-day minimum moving average of daily streamflow. The blue line is not visible where overlain by the red line.

were computed for the 31-year historical period without water-use effects to show the variation of each statistic and with water-use effects for the period 2008–12 to compare water-use and no-water-use simulations. The statistics were also computed for measured streamflow at USGS streamgage 02333500 (Chestatee River near Dahlonega, GA) for the entire period. The long-term plots in figure 15 show good agreement between statistics computed for measured and simulated streamflow values for the period 1982 to 2012. The study period (2008–12) plots in figure 16 show virtually no difference between the water-use and no-water-use simulations. Water-use data for this subbasin show only a net use of 0.14 percent (0.42 ft^3/s) of mean annual streamflow (299 ft^3/s) at streamgage 02333500 for the study period (2008–12). Net water use was computed as the difference between mean annual surface-water withdrawals and mean annual surface-water return flows for the study period.

Streamflow Statistics for the Fine-Resolution Chipola River Subbasin PRMS Model

Streamflow statistics described in table 2 were computed for all 778 stream segments in the Chipola River subbasin PRMS model for the period 1982 to 2012. These statistics were computed for the 31-year historical period without water-use effects to show the variation of each statistic and with water-use effects for the period 2008–12 to compare water-use and no-water-use simulations. The statistics were also computed for measured streamflow at USGS streamgage 02359000 (Chipola River near Altha, FL) for the entire period. The long-term plots in figure 17 show good agreement between most statistics computed for measured and simulated streamflow values for the period 1982 to 2012; some larger differences occur for the standard deviations of the 10-day minimum streamflow for both spring (March to June) and summer (July to September) seasons (fig. 17*I* and 17*J*). The study period (2008–12) plots in figure 18 show virtually no difference between the water-use (red line) and no-water-use (blue line) simulations at streamgage 02359000, with water-use data for this subbasin consisting of groundwater withdrawals. In addition to the statistics that did not match well for the long-term period, there was some mismatch between measured and simulated statistics for the March–June 10-day minimum flow.

Streamflow Statistics for the Fine-Resolution Ichawaynochaway Creek Subbasin PRMS Model

Streamflow statistics described in table 2 were computed for all 824 stream segments in the Ichawaynochaway Creek subbasin PRMS model for the period 1982 to 2012. These statistics were computed for the 31-year historical period without water-use effects to show the variation of each statistic and with water-use effects for the period 2008–12 to compare water-use and no-water-use simulations. The statistics were also computed for measured streamflow at USGS streamgage 02354800 (Ichawaynochaway Creek near Elmodel, GA) when data were available (1995–2012). The long-term plots in figure 19 show good agreement between most statistics computed for measured and simulated streamflow values for the period 1995 to 2012. Some larger deviations occur for wetter years for the spring daily standard deviation and spring 10-day maximum, and for several years for the standard deviations of the 10-day minimum streamflow for both spring (March to June) and summer (July to September) seasons as shown in figure 19*I* and 19*J*, respectively. The study period (2008–12) plots in figure 20 show virtually no difference between the water-use (red line) and no-water-use (blue line) simulations at streamgage 02354800, with water-use data for this subbasin consisting primarily of groundwater withdrawals. This lack of a difference in the simulated streamflows points to either a more local effect of water use than at the full subbasin scale, or limitations in the model conceptualization or parameterization.

Streamflow Statistics for the Fine-Resolution Potato Creek Subbasin PRMS Model

Streamflow statistics described in table 2 were computed for all 221 stream segments in the Potato Creek subbasin PRMS model for the period 1942 to 2012. A longer historical period was simulated for this subbasin because measured streamflow at streamgage 02346500 (Potato Creek near Thomaston, GA) was discontinued in 1970. These statistics were computed for the 71-year historical period without water-use effects to show the long-term variation of each statistic and with water-use effects for the period 2008–12 to compare water-use and no-water-use simulations. The statistics were also computed for measured streamflow for the period of available data (1942–70). The long-term plots in figure 21 show good agreement between statistics computed for measured and simulated streamflow values for the period 1942 to 1970, with some mismatch occurring for the spring 10-day minimum flow during wetter years in the 1950s and 1960s. The study period (2008–12) plots in figure 22 show virtually no difference between the water-use and no-water-use simulations. Water-use data for this subbasin show a net gain of 0.22 ft^3/s for the study period (2008–12), and a minimal change from the mean annual streamgage flow of 235 ft^3/s. Net water use was computed as the difference between mean annual surface-water withdrawals and mean annual surface-water return flows for the study period. Figure 22 shows that streamflow statistics without water use generally are larger than streamflow statistics with water use for spring and summer seasonal median flows and 10-day minimum flows.

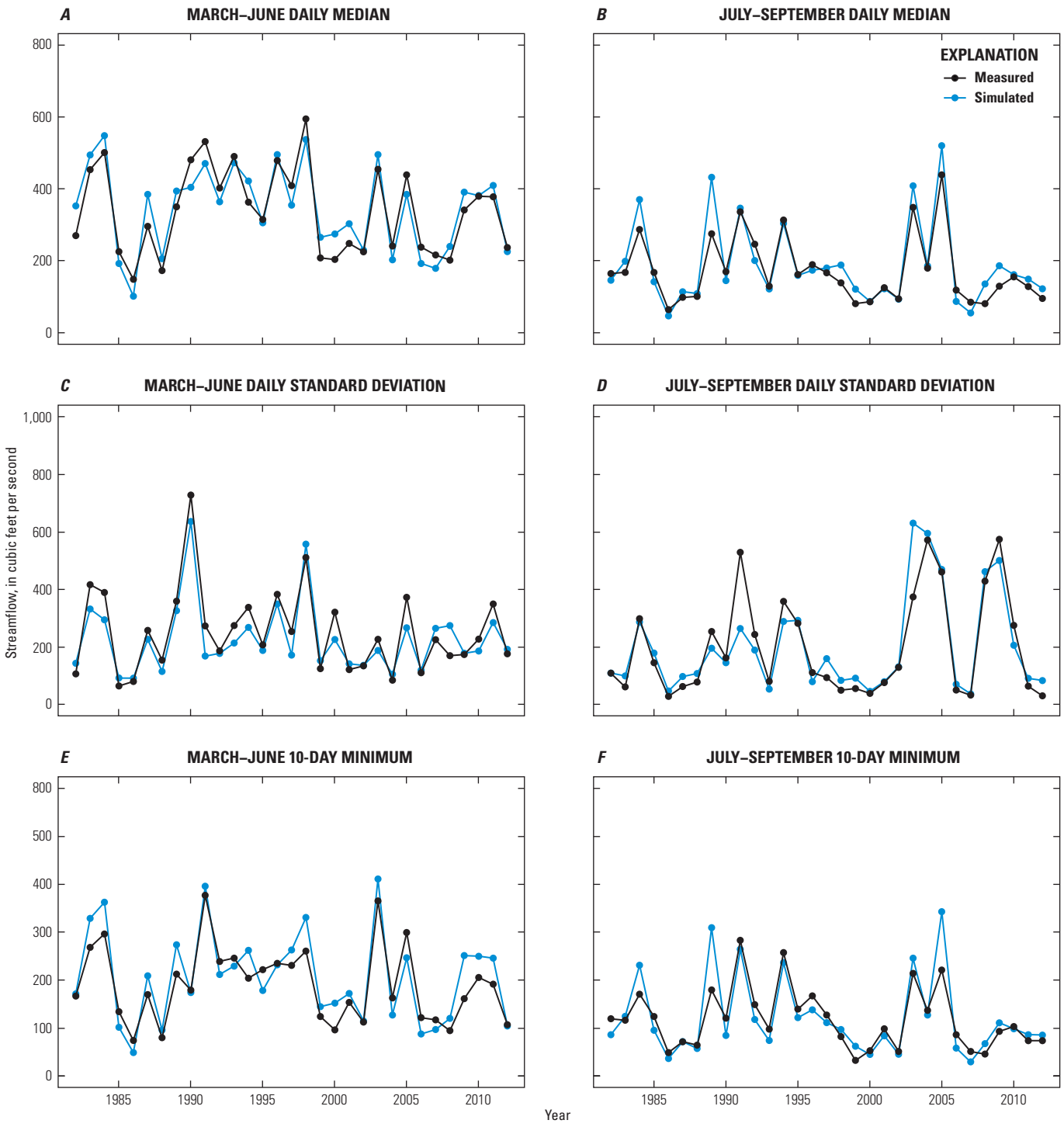

Figure 15. Plots of 10 biologically relevant hydrologic statistics for the Chestatee River subbasin for the period 1982 to 2012 at USGS streamgage 02333500 (Chestatee River near Dahlonega, GA). These plots show the variation in these statistics for the recent climate period. The statistics shown in the plots are (*A*) March to June daily median streamflow, (*B*) July to September daily median streamflow, (*C*) March to June standard deviation of daily streamflow, (*D*) July to September standard deviation of daily streamflow, (*E*) March to June 10-day minimum moving average of daily streamflow, (*F*) July to September 10-day minimum moving average of daily streamflow, (*G*) March to June 10-day maximum moving average of daily streamflow, (*H*) July to September 10-day maximum moving average of daily streamflow, (*I*) March to June standard deviation of 10-day minimum moving average of daily streamflow, and (*J*) July to September standard deviation of 10-day minimum moving average of daily streamflow.

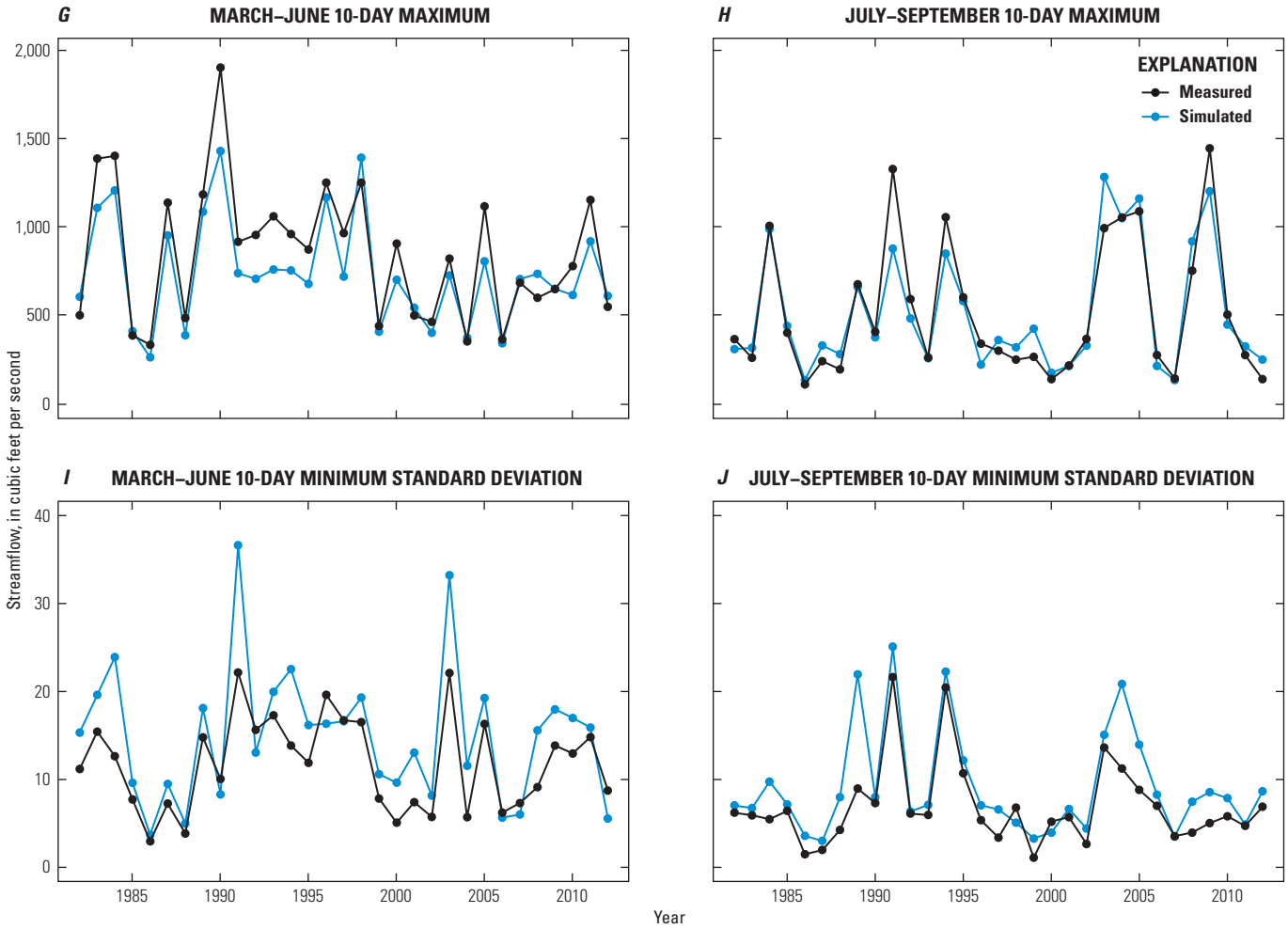

Figure 15.—Continued Plots of 10 biologically relevant hydrologic statistics for the Chestatee River subbasin for the period 1982 to 2012 at USGS streamgage 02333500 (Chestatee River near Dahlonega, GA). These plots show the variation in these statistics for the recent climate period. The statistics shown in the plots are (*A*) March to June daily median streamflow, (*B*) July to September daily median streamflow, (*C*) March to June standard deviation of daily streamflow, (*D*) July to September standard deviation of daily streamflow, (*E*) March to June 10-day minimum moving average of daily streamflow, (*F*) July to September 10-day minimum moving average of daily streamflow, (*G*) March to June 10-day maximum moving average of daily streamflow, (*H*) July to September 10-day maximum moving average of daily streamflow, (*I*) March to June standard deviation of 10-day minimum moving average of daily streamflow, and (*J*) July to September standard deviation of 10-day minimum moving average of daily streamflow.

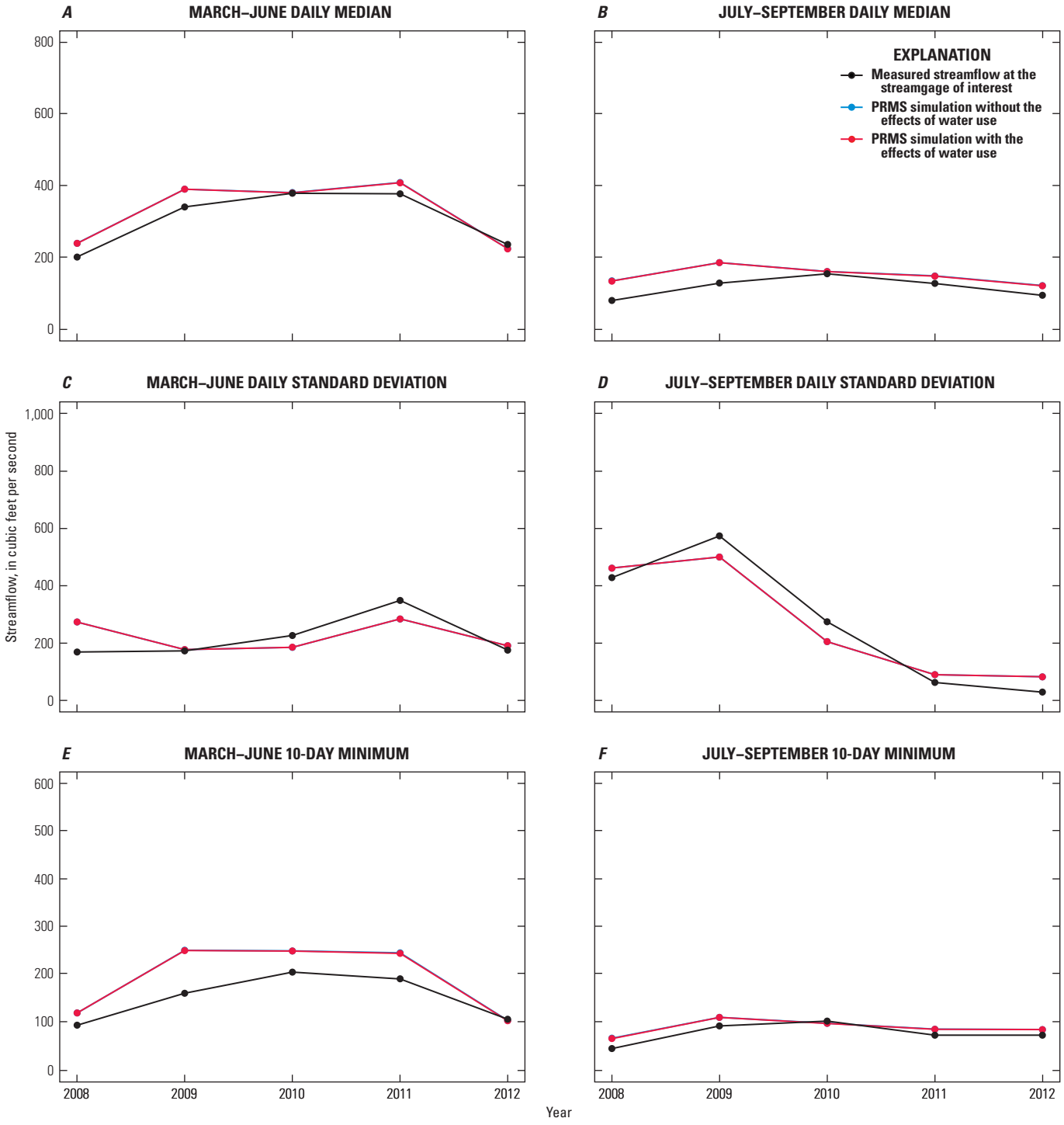

Figure 16. Plots of 10 biologically relevant hydrologic statistics for the Chestatee River subbasin for the period 2008 to 2012 at USGS streamgage 02333500 (Chestatee River near Dahlonega, GA). These plots show the variation in the statistics for the study period with and without water-use effects. The statistics shown in the plots are (*A*) March to June daily median streamflow, (*B*) July to September daily median streamflow, (*C*) March to June standard deviation of daily streamflow, (*D*) July to September standard deviation of daily streamflow, (*E*) March to June 10-day minimum moving average of daily streamflow, (*F*) July to September 10-day minimum moving average of daily streamflow, (*G*) March to June 10-day maximum moving average of daily streamflow, (*H*) July to September 10-day maximum moving average of daily streamflow, (*I*) March to June standard deviation of 10-day minimum moving average of daily streamflow, and (*J*) July to September standard deviation of 10-day minimum moving average of daily streamflow. The blue line is not visible where overlain by the red line.

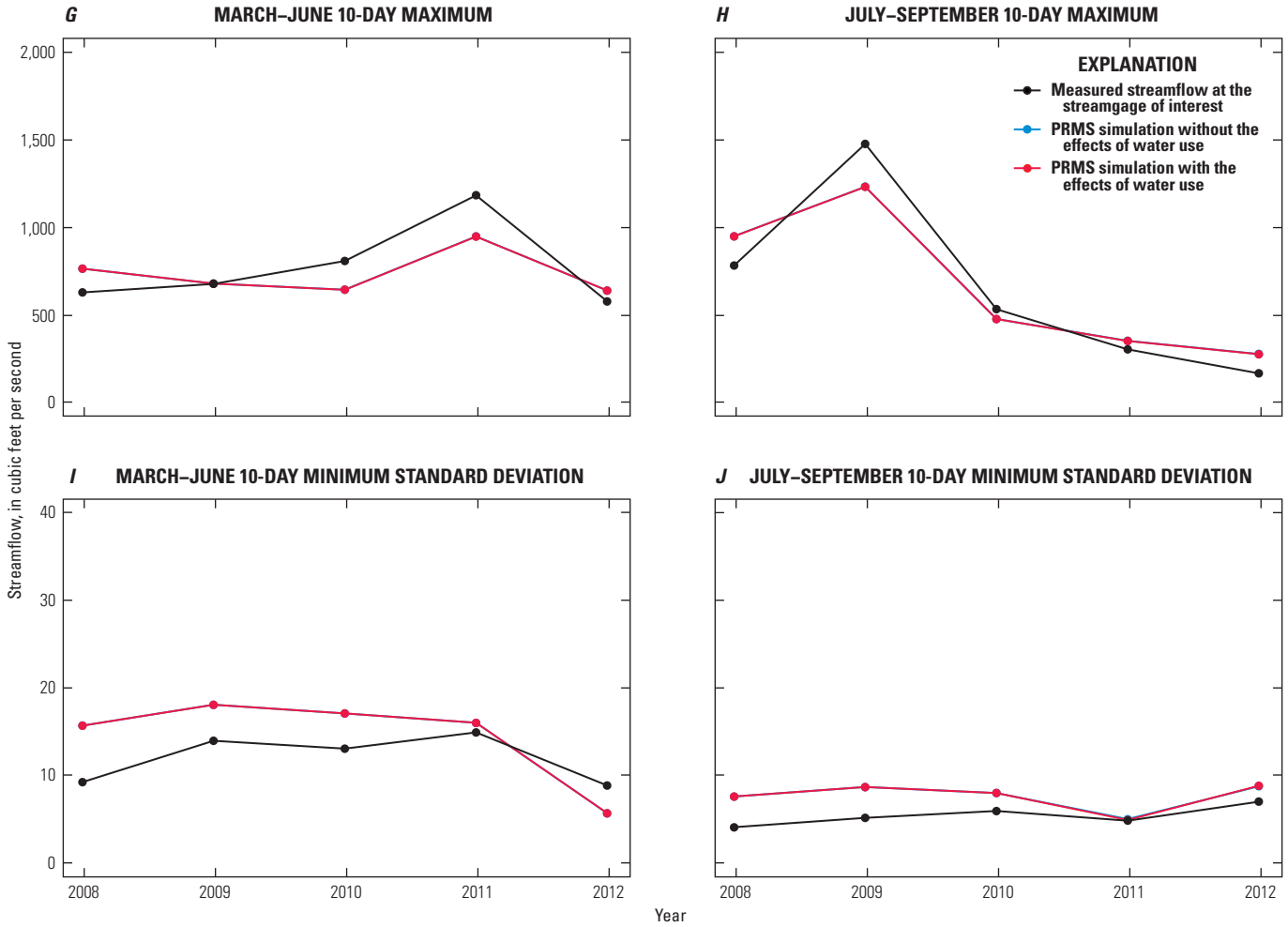

Figure 16.—Continued Plots of 10 biologically relevant hydrologic statistics for the Chestatee River subbasin for the period 2008 to 2012 at USGS streamgage 02333500 (Chestatee River near Dahlonega, GA). These plots show the variation in the statistics for the study period with and without water-use effects. The statistics shown in the plots are (*A*) March to June daily median streamflow, (*B*) July to September daily median streamflow, (*C*) March to June standard deviation of daily streamflow, (*D*) July to September standard deviation of daily streamflow, (*E*) March to June 10-day minimum moving average of daily streamflow, (*F*) July to September 10-day minimum moving average of daily streamflow, (*G*) March to June 10-day maximum moving average of daily streamflow, (*H*) July to September 10-day maximum moving average of daily streamflow, (*I*) March to June standard deviation of 10-day minimum moving average of daily streamflow, and (*J*) July to September standard deviation of 10-day minimum moving average of daily streamflow. The blue line is not visible where overlain by the red line.

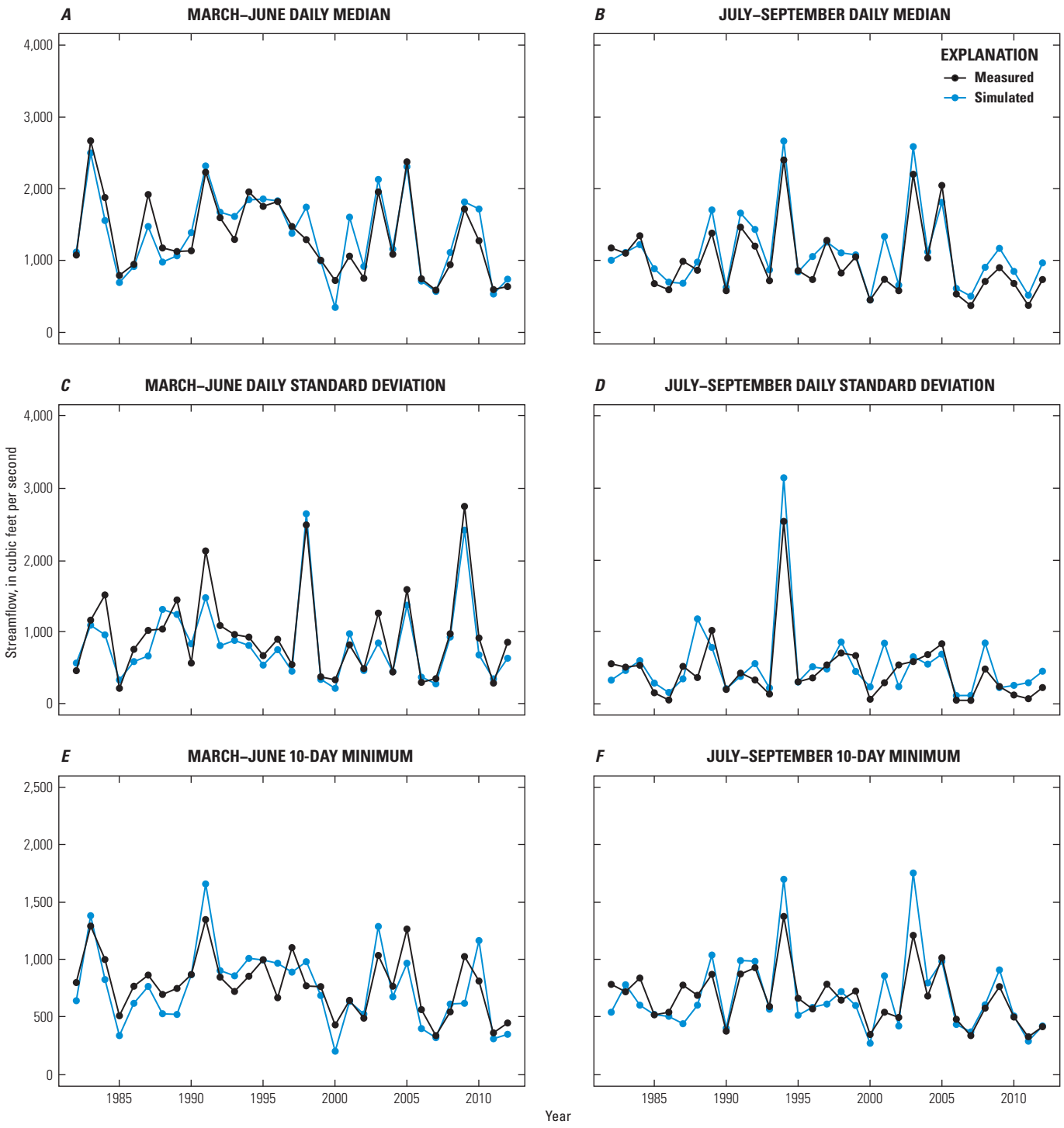

Figure 17. Plots of 10 biologically relevant hydrologic statistics for the Chipola River subbasin for the period 1982 to 2012 at USGS streamgage 02359000 (Chipola River near Altha, FL). These plots show the variation in these statistics for the recent climate period. The statistics shown in the plots are (*A*) March to June daily median streamflow, (*B*) July to September daily median streamflow, (*C*) March to June standard deviation of daily streamflow, (*D*) July to September standard deviation of daily streamflow, (*E*) March to June 10-day minimum moving average of daily streamflow, (*F*) July to September 10-day minimum moving average of daily streamflow, (*G*) March to June 10-day maximum moving average of daily streamflow, (*H*) July to September 10-day maximum moving average of daily streamflow, (*I*) March to June standard deviation of 10-day minimum moving average of daily streamflow, and (*J*) July to September standard deviation of 10-day minimum moving average of daily streamflow.

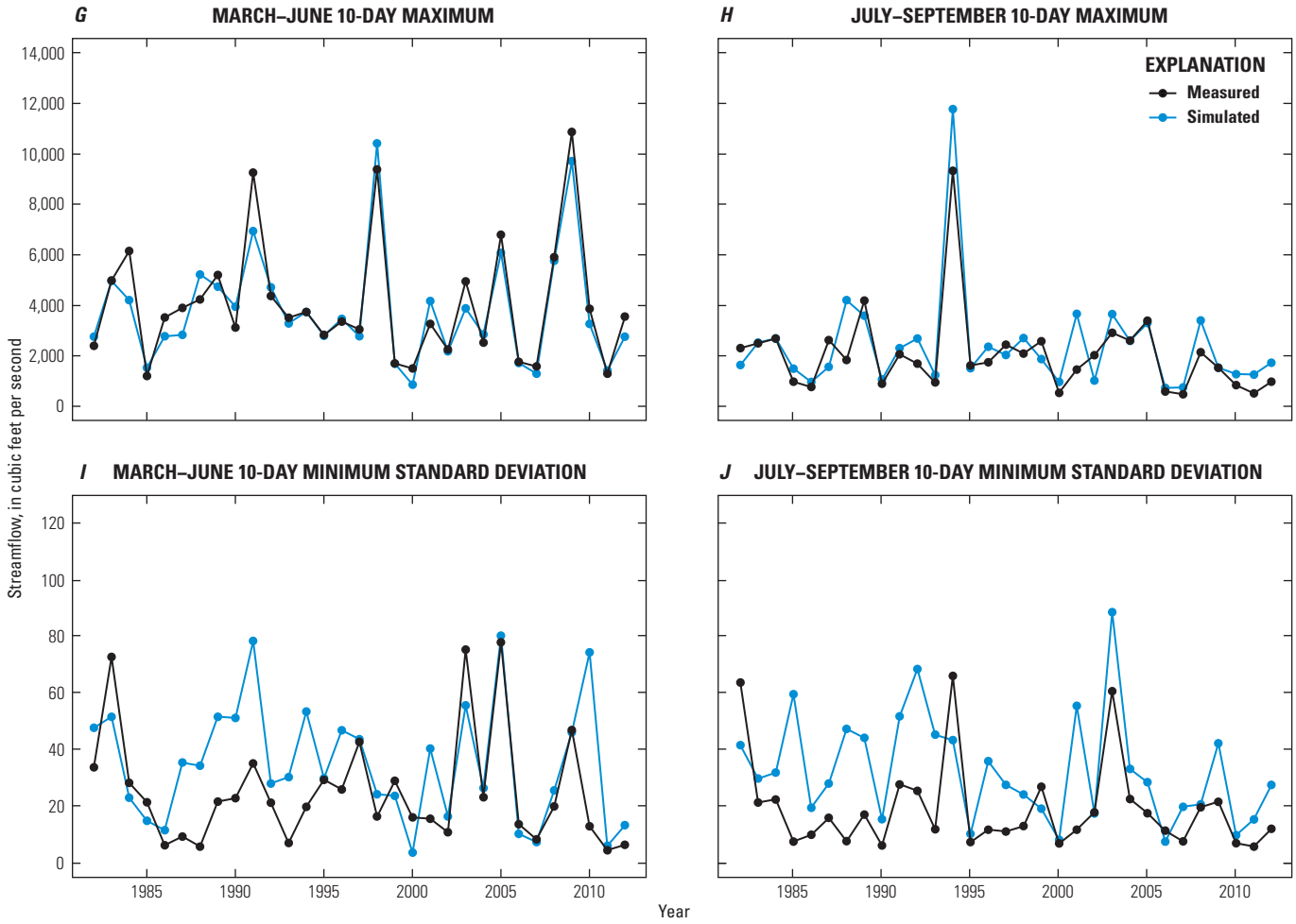

Figure 17.—Continued Plots of 10 biologically relevant hydrologic statistics for the Chipola River subbasin for the period 1982 to 2012 at USGS streamgage 02359000 (Chipola River near Altha, FL). These plots show the variation in these statistics for the recent climate period. The statistics shown in the plots are (*A*) March to June daily median streamflow, (*B*) July to September daily median streamflow, (*C*) March to June standard deviation of daily streamflow, (*D*) July to September standard deviation of daily streamflow, (*E*) March to June 10-day minimum moving average of daily streamflow, (*F*) July to September 10-day minimum moving average of daily streamflow, (*G*) March to June 10-day maximum moving average of daily streamflow, (*H*) July to September 10-day maximum moving average of daily streamflow, (*I*) March to June standard deviation of 10-day minimum moving average of daily streamflow, and (*J*) July to September standard deviation of 10-day minimum moving average of daily streamflow.

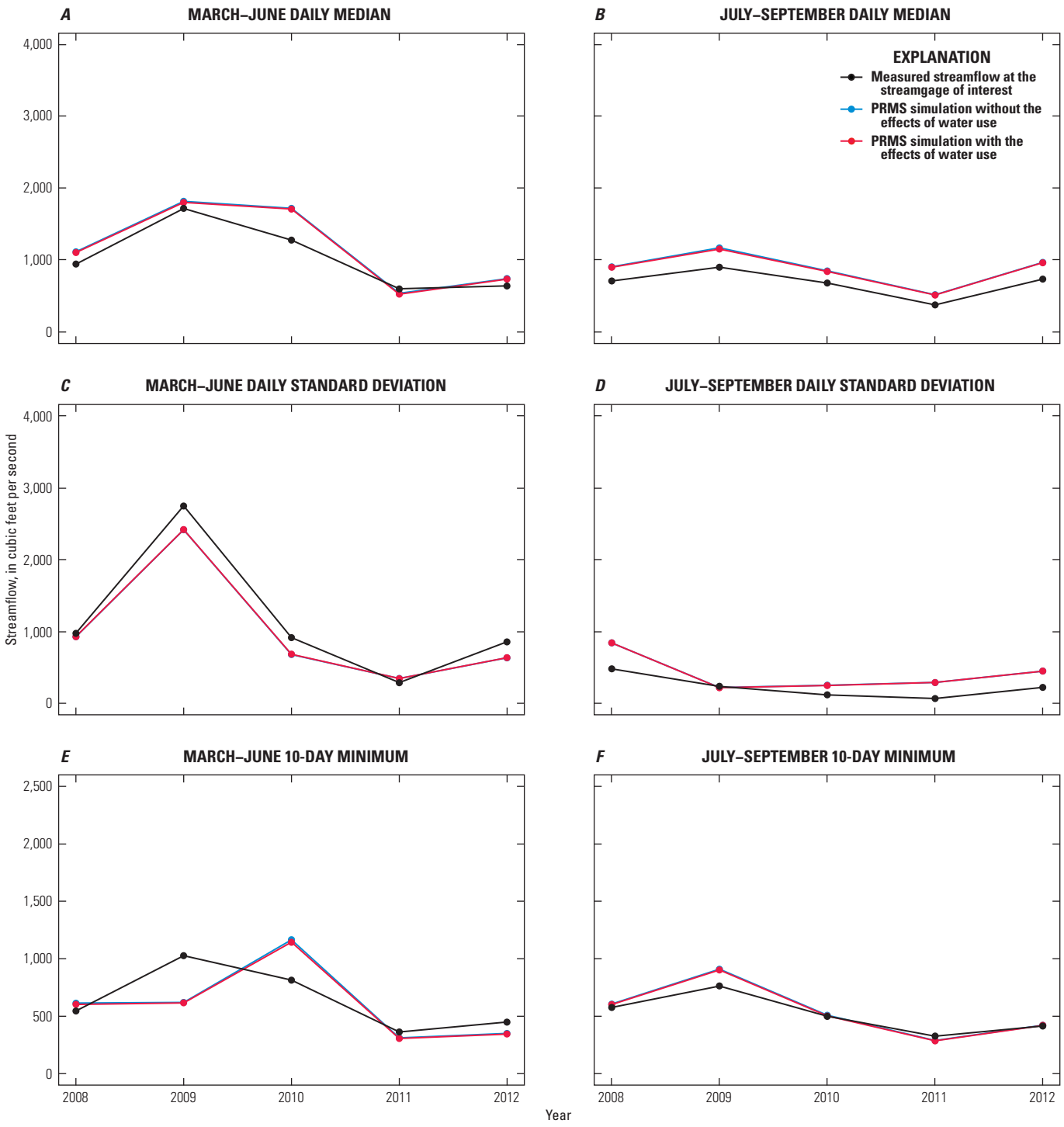

Figure 18. Plots of 10 biologically relevant hydrologic statistics for the Chipola River subbasin for the period 2008 to 2012 at USGS streamgage 02359000 (Chipola River near Altha, FL). These plots show the variation in the statistics for the study period with and without water-use effects. The statistics shown in the plots are (*A*) March to June daily median streamflow, (*B*) July to September daily median streamflow, (*C*) March to June standard deviation of daily streamflow, (*D*) July to September standard deviation of daily streamflow, (*E*) March to June 10-day minimum moving average of daily streamflow, (*F*) July to September 10-day minimum moving average of daily streamflow, (*G*) March to June 10-day maximum moving average of daily streamflow, (*H*) July to September 10-day maximum moving average of daily streamflow, (*I*) March to June standard deviation of 10-day minimum moving average of daily streamflow, and (*J*) July to September standard deviation of 10-day minimum moving average of daily streamflow. The blue line is not visible where overlain by the red line.

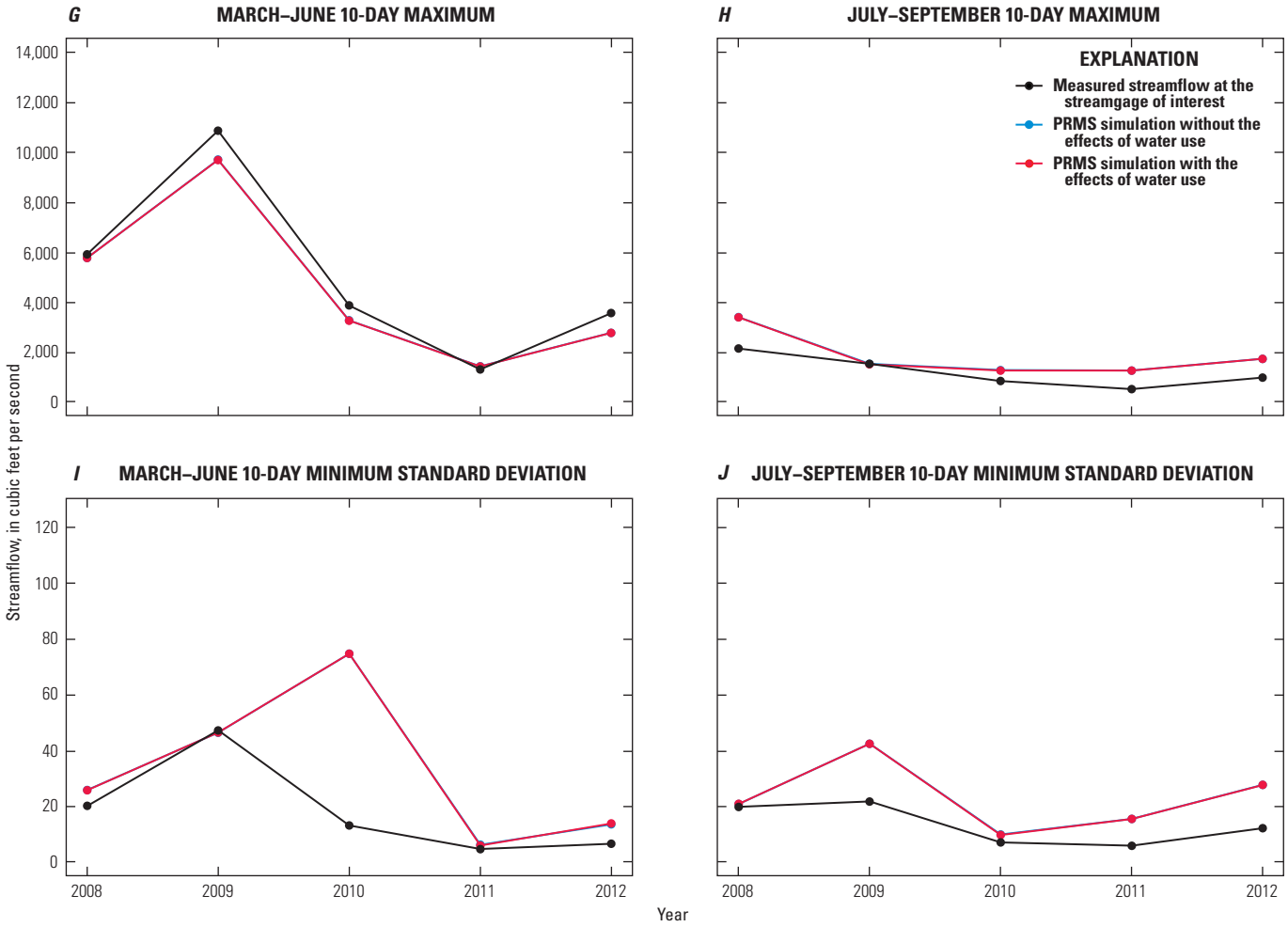

Figure 18.—Continued Plots of 10 biologically relevant hydrologic statistics for the Chipola River subbasin for the period 2008 to 2012 at USGS streamgage 02359000 (Chipola River near Altha, FL). These plots show the variation in the statistics for the study period with and without water-use effects. The statistics shown in the plots are (*A*) March to June daily median streamflow, (*B*) July to September daily median streamflow, (*C*) March to June standard deviation of daily streamflow, (*D*) July to September standard deviation of daily streamflow, (*E*) March to June 10-day minimum moving average of daily streamflow, (*F*) July to September 10-day minimum moving average of daily streamflow, (*G*) March to June 10-day maximum moving average of daily streamflow, (*H*) July to September 10-day maximum moving average of daily streamflow, (*I*) March to June standard deviation of 10-day minimum moving average of daily streamflow, and (*J*) July to September standard deviation of 10-day minimum moving average of daily streamflow. The blue line is not visible where overlain by the red line.

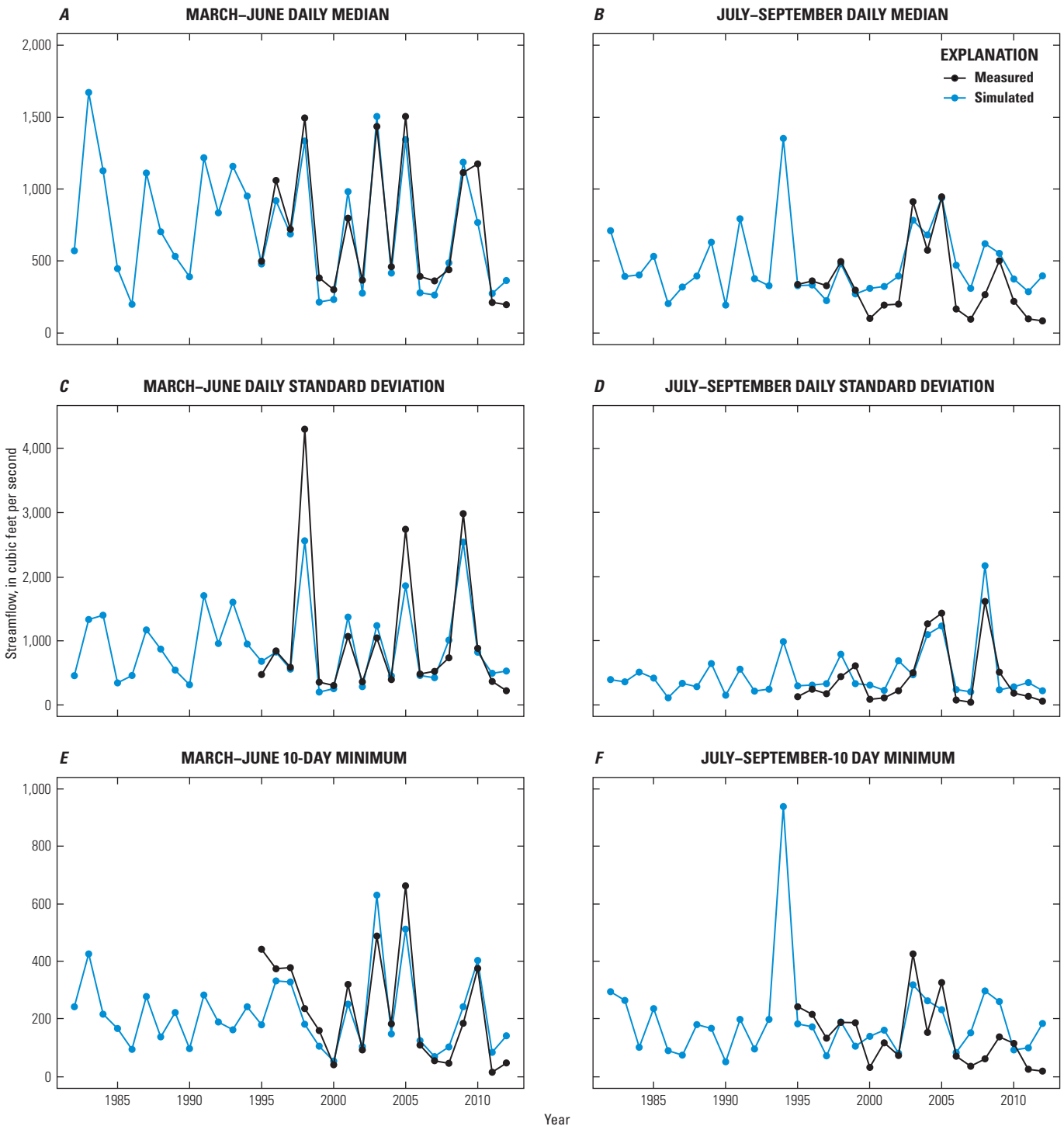

Figure 19. Plots of 10 biologically relevant hydrologic statistics for the Ichawaynochaway Creek subbasin for the period 1982 to 2012 at USGS streamgage 02354800 (Ichawaynochaway Creek near Elmodel, GA). These plots show the variation in these statistics for the recent climate period. The statistics shown in the plots are (*A*) March to June daily median streamflow, (*B*) July to September daily median streamflow, (*C*) March to June standard deviation of daily streamflow, (*D*) July to September standard deviation of daily streamflow, (*E*) March to June 10-day minimum moving average of daily streamflow, (*F*) July to September 10-day minimum moving average of daily streamflow, (*G*) March to June 10-day maximum moving average of daily streamflow, (*H*) July to September 10-day maximum moving average of daily streamflow, (*I*) March to June standard deviation of 10-day minimum moving average of daily streamflow, and (*J*) July to September standard deviation of 10-day minimum moving average of daily streamflow.

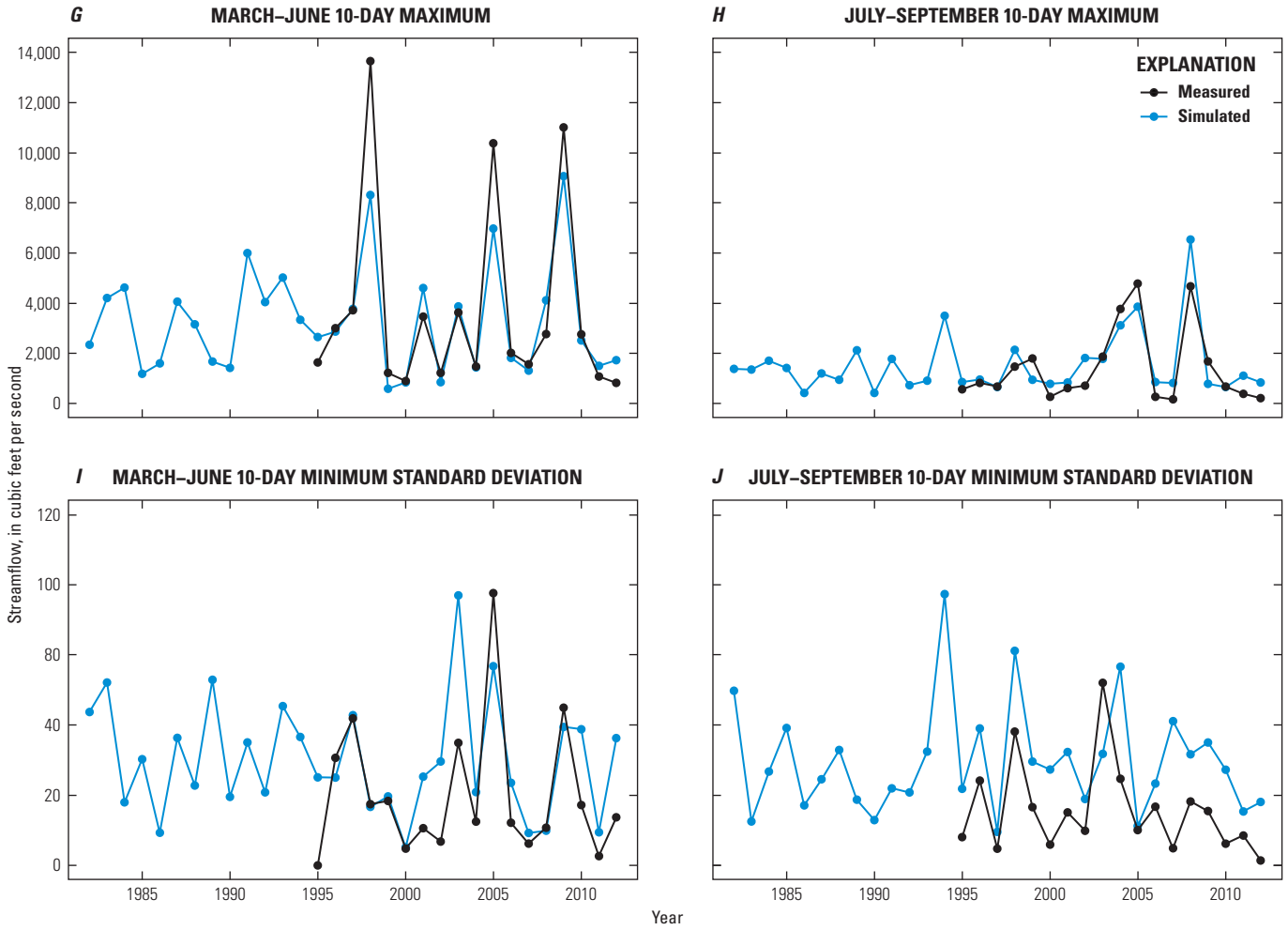

Figure 19.—Continued Plots of 10 biologically relevant hydrologic statistics for the Ichawaynochaway Creek subbasin for the period 1982 to 2012 at USGS streamgage 02354800 (Ichawaynochaway Creek near Elmodel, GA). These plots show the variation in these statistics for the recent climate period. The statistics shown in the plots are (*A*) March to June daily median streamflow, (*B*) July to September daily median streamflow, (*C*) March to June standard deviation of daily streamflow, (*D*) July to September standard deviation of daily streamflow, (*E*) March to June 10-day minimum moving average of daily streamflow, (*F*) July to September 10-day minimum moving average of daily streamflow, (*G*) March to June 10-day maximum moving average of daily streamflow, (*H*) July to September 10-day maximum moving average of daily streamflow, (*I*) March to June standard deviation of 10-day minimum moving average of daily streamflow, and (*J*) July to September standard deviation of 10-day minimum moving average of daily streamflow.

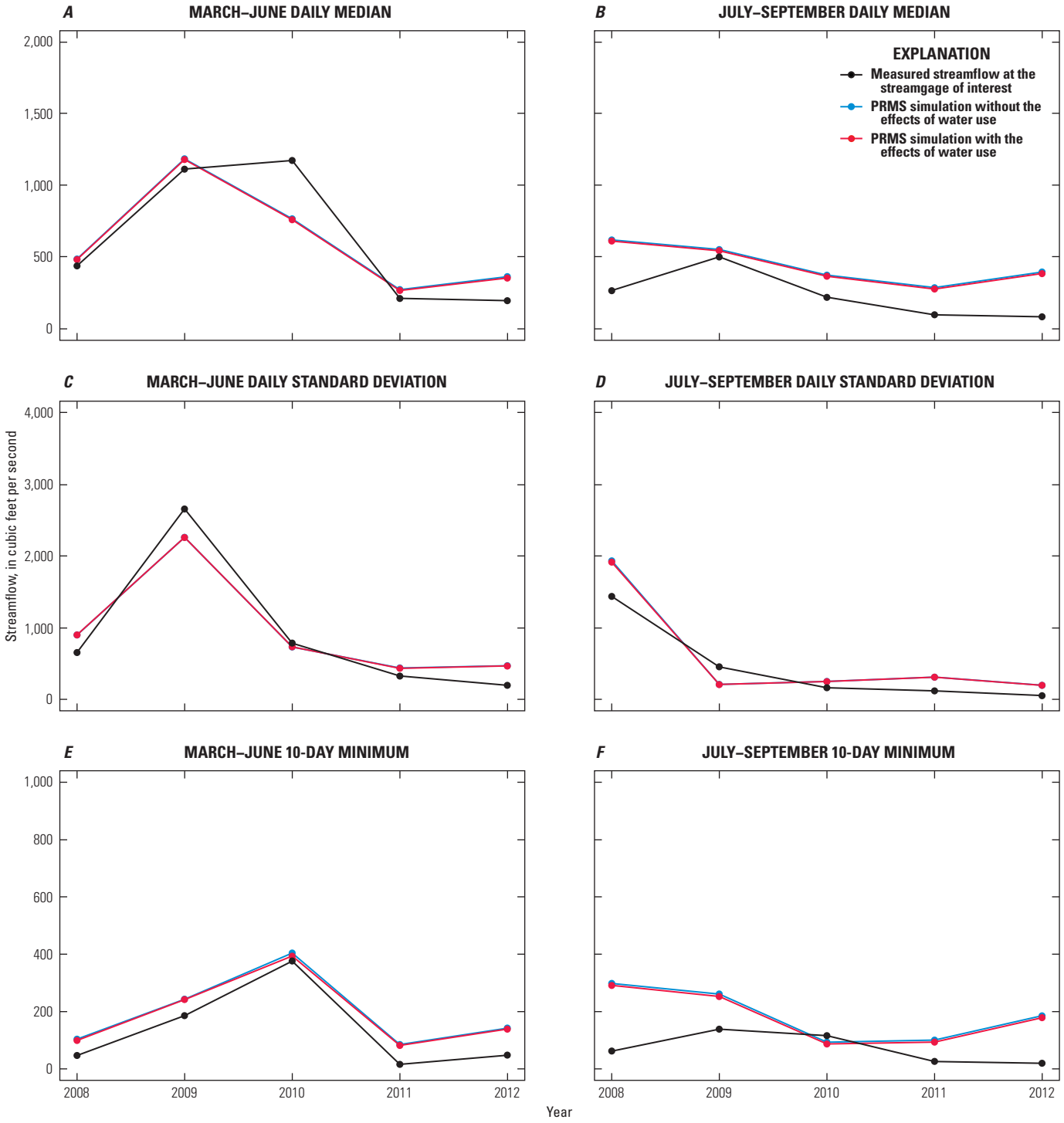

Figure 20. Plots of 10 biologically relevant hydrologic statistics for the Ichawaynochaway Creek subbasin for the period 2008 to 2012 at USGS streamgage 02354800 (Ichawaynochaway Creek near Elmodel, GA). These plots show the variation in the statistics for the study period with and without water-use effects. The statistics shown in the plots are (*A*) March to June daily median streamflow, (*B*) July to September daily median streamflow, (*C*) March to June standard deviation of daily streamflow, (*D*) July to September standard deviation of daily streamflow, (*E*) March to June 10-day minimum moving average of daily streamflow, (*F*) July to September 10-day minimum moving average of daily streamflow, (*G*) March to June 10-day maximum moving average of daily streamflow, (*H*) July to September 10-day maximum moving average of daily streamflow, (*I*) March to June standard deviation of 10-day minimum moving average of daily streamflow, and (*J*) July to September standard deviation of 10-day minimum moving average of daily streamflow. The blue line is not visible where overlain by the red line.

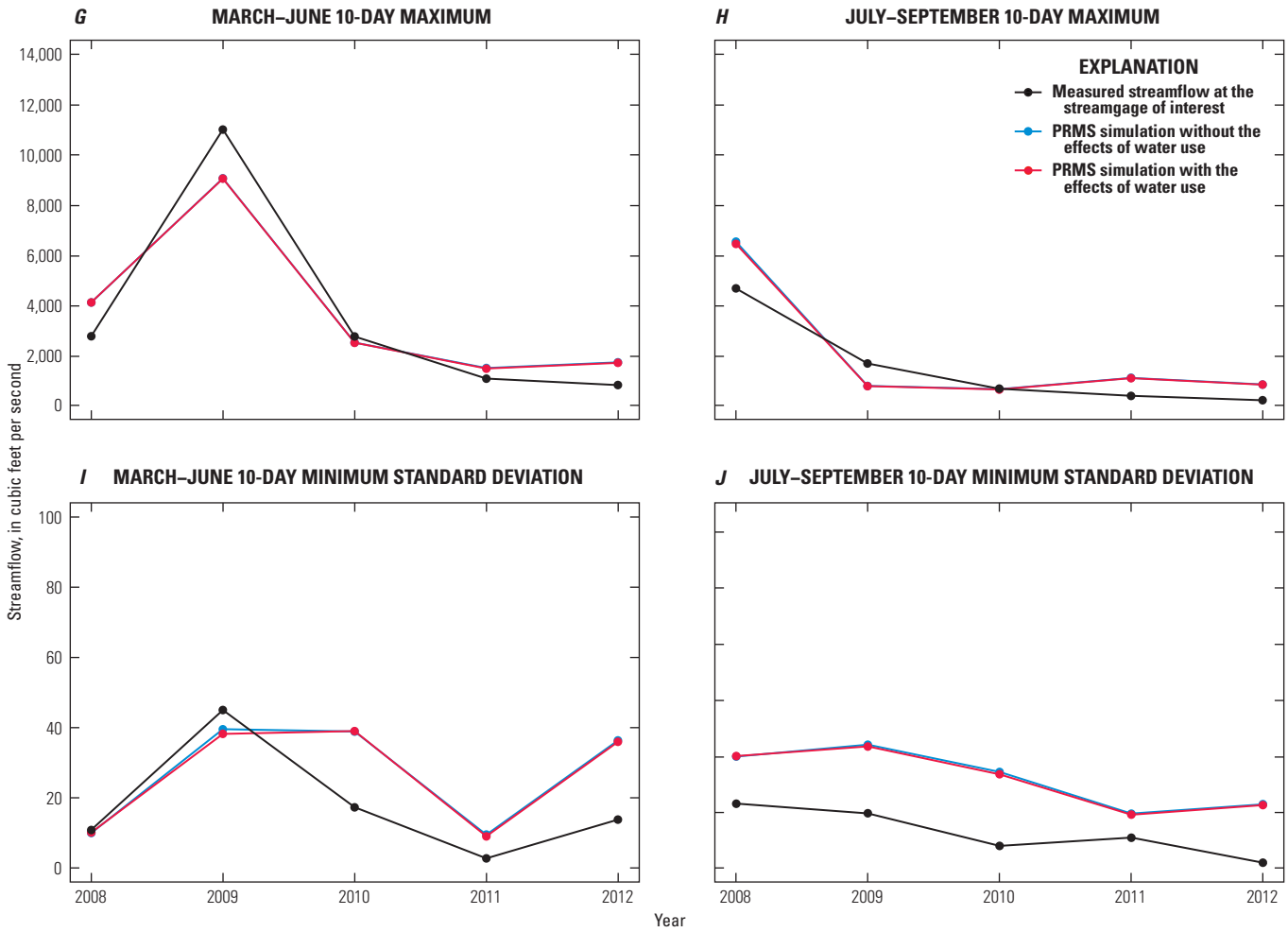

Figure 20.—Continued Plots of 10 biologically relevant hydrologic statistics for the Ichawaynochaway Creek subbasin for the period 2008 to 2012 at USGS streamgage 02354800 (Ichawaynochaway Creek near Elmodel, GA). These plots show the variation in the statistics for the study period with and without water-use effects. The statistics shown in the plots are (*A*) March to June daily median streamflow, (*B*) July to September daily median streamflow, (*C*) March to June standard deviation of daily streamflow, (*D*) July to September standard deviation of daily streamflow, (*E*) March to June 10-day minimum moving average of daily streamflow, (*F*) July to September 10-day minimum moving average of daily streamflow, (*G*) March to June 10-day maximum moving average of daily streamflow, (*H*) July to September 10-day maximum moving average of daily streamflow, (*I*) March to June standard deviation of 10-day minimum moving average of daily streamflow, and (*J*) July to September standard deviation of 10-day minimum moving average of daily streamflow. The blue line is not visible where overlain by the red line.

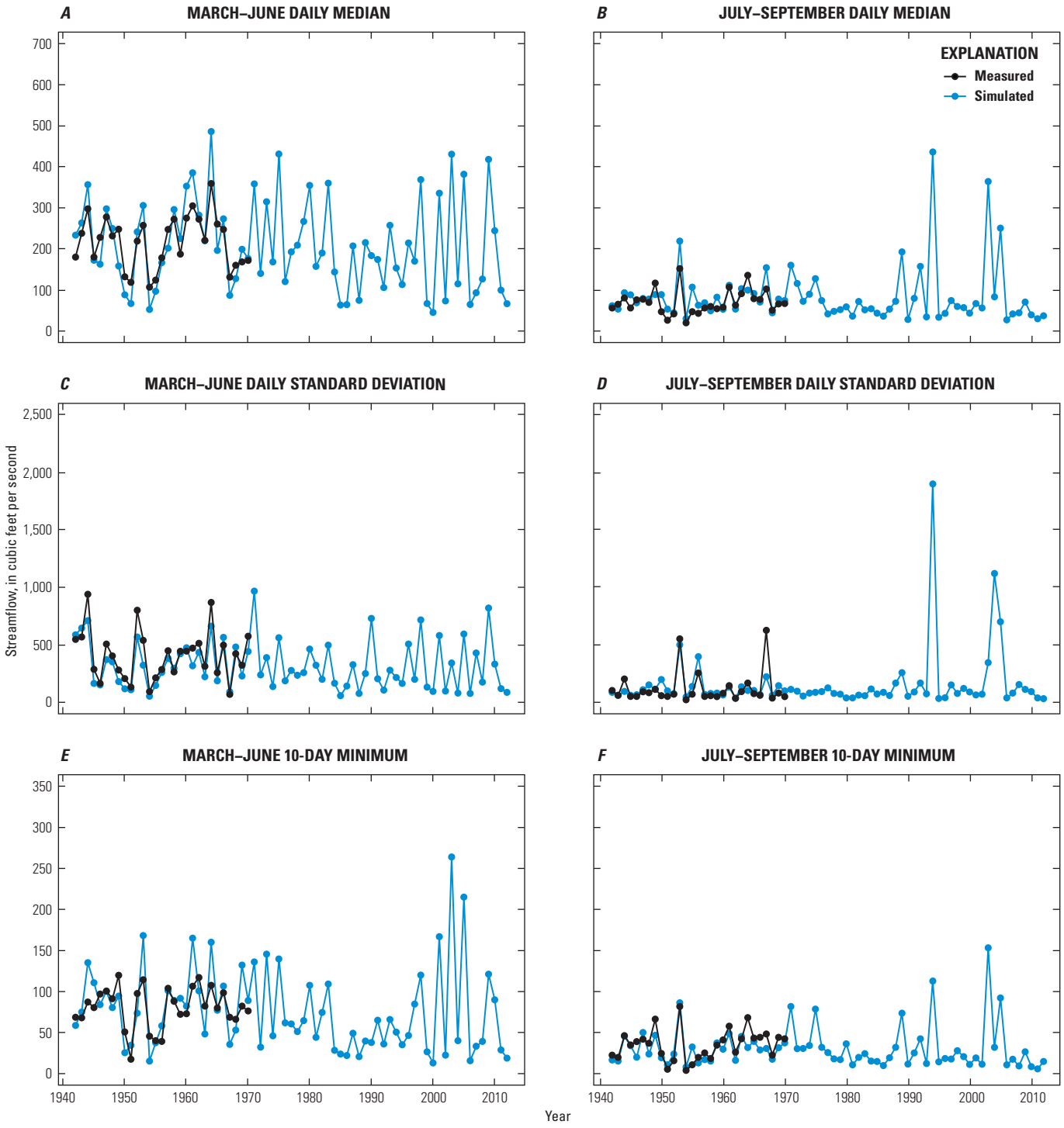

Figure 21. Plots of 10 biologically relevant hydrologic statistics for the Potato Creek subbasin for the period 1942 to 2012 at USGS streamgage 02346500 (Potato Creek near Thomaston, GA). These plots show the variation in these statistics for the recent climate period. The statistics shown in the plots are (*A*) March to June daily median streamflow, (*B*) July to September daily median streamflow, (*C*) March to June standard deviation of daily streamflow, (*D*) July to September standard deviation of daily streamflow, (*E*) March to June 10-day minimum moving average of daily streamflow, (*F*) July to September 10-day minimum moving average of daily streamflow, (*G*) March to June 10-day maximum moving average of daily streamflow, (*H*) July to September 10-day maximum moving average of daily streamflow, (*I*) March to June standard deviation of 10-day minimum moving average of daily streamflow, and (*J*) July to September standard deviation of 10-day minimum moving average of daily streamflow.

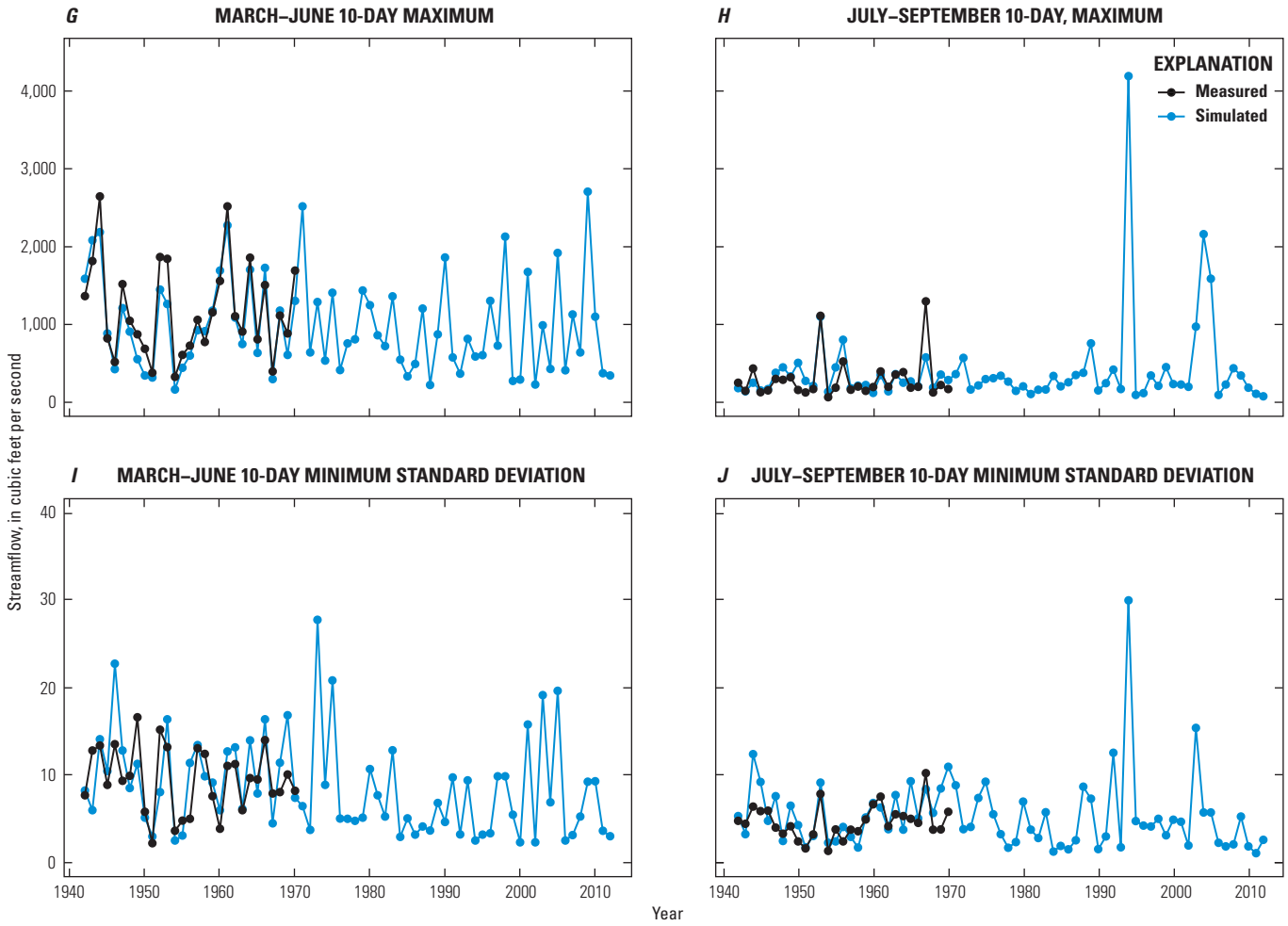

Figure 21.—Continued Plots of 10 biologically relevant hydrologic statistics for the Potato Creek subbasin for the period 1942 to 2012 at USGS streamgage 02346500 (Potato Creek near Thomaston, GA). These plots show the variation in these statistics for the recent climate period. The statistics shown in the plots are (*A*) March to June daily median streamflow, (*B*) July to September daily median streamflow, (*C*) March to June standard deviation of daily streamflow, (*D*) July to September standard deviation of daily streamflow, (*E*) March to June 10-day minimum moving average of daily streamflow, (*F*) July to September 10-day minimum moving average of daily streamflow, (*G*) March to June 10-day maximum moving average of daily streamflow, (*H*) July to September 10-day maximum moving average of daily streamflow, (*I*) March to June standard deviation of 10-day minimum moving average of daily streamflow, and (*J*) July to September standard deviation of 10-day minimum moving average of daily streamflow.

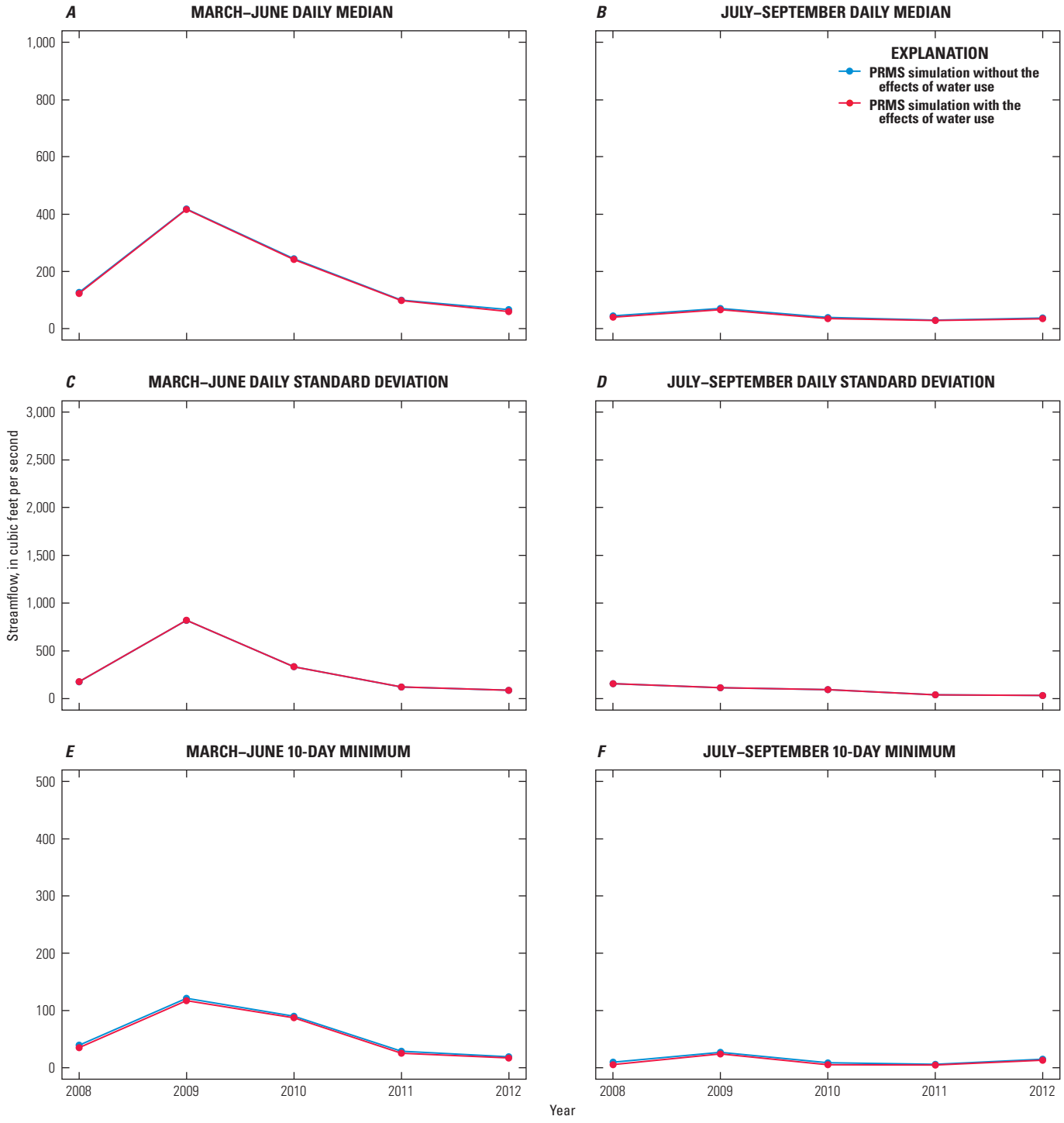

Figure 22. Plots of 10 biologically relevant hydrologic statistics for the Potato Creek subbasin for the period 2008 to 2012 at USGS streamgage 02346500 (Potato Creek near Thomaston, GA). These plots show the variation in the statistics for the study period with and without water-use effects. The statistics shown in the plots are (*A*) March to June daily median streamflow, (*B*) July to September daily median streamflow, (*C*) March to June standard deviation of daily streamflow, (*D*) July to September standard deviation of daily streamflow, (*E*) March to June 10-day minimum moving average of daily streamflow, (*F*) July to September 10-day minimum moving average of daily streamflow, (*G*) March to June 10-day maximum moving average of daily streamflow, (*H*) July to September 10-day maximum moving average of daily streamflow, (*I*) March to June standard deviation of 10-day minimum moving average of daily streamflow, and (*J*) July to September standard deviation of 10-day minimum moving average of daily streamflow. The blue line is not visible where overlain by the red line.

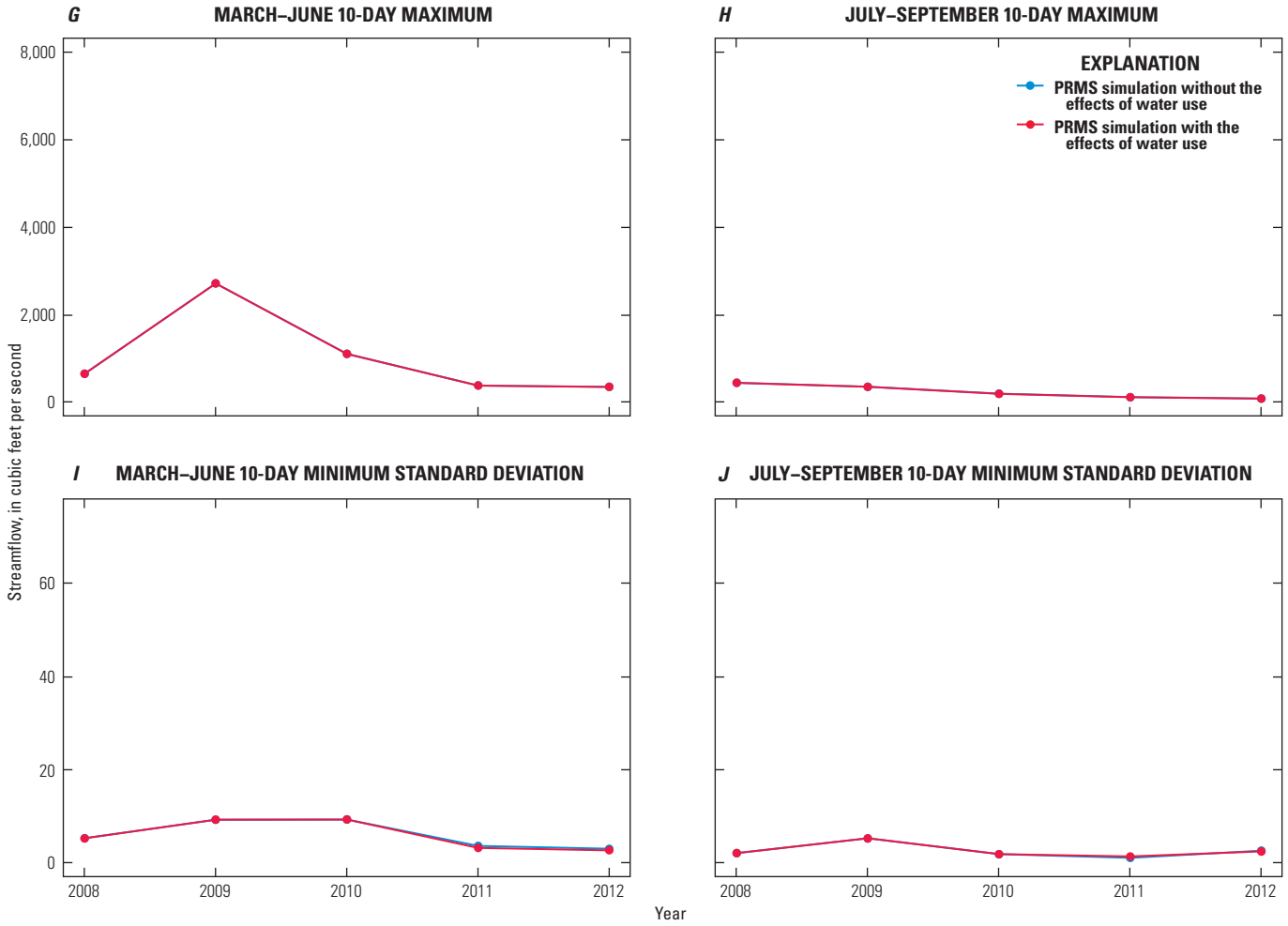

Figure 22.—Continued Plots of 10 biologically relevant hydrologic statistics for the Potato Creek subbasin for the period 2008 to 2012 at USGS streamgage 02346500 (Potato Creek near Thomaston, GA). These plots show the variation in the statistics for the study period with and without water-use effects. The statistics shown in the plots are (*A*) March to June daily median streamflow, (*B*) July to September daily median streamflow, (*C*) March to June standard deviation of daily streamflow, (*D*) July to September standard deviation of daily streamflow, (*E*) March to June 10-day minimum moving average of daily streamflow, (*F*) July to September 10-day minimum moving average of daily streamflow, (*G*) March to June 10-day maximum moving average of daily streamflow, (*H*) July to September 10-day maximum moving average of daily streamflow, (*I*) March to June standard deviation of 10-day minimum moving average of daily streamflow, and (*J*) July to September standard deviation of 10-day minimum moving average of daily streamflow. The blue line is not visible where overlain by the red line.

Streamflow Statistics for the Fine-Resolution Spring Creek Subbasin PRMS Model

Streamflow statistics described in table 2 were computed for all 345 stream segments in the Spring Creek subbasin PRMS model for the period 1952 to 2012. These statistics were computed for the 61-year historical period without water-use effects to show the variation of each statistic and with water-use effects for the period 2008–12 to compare water-use and no-water-use simulations. The statistics were also computed for measured streamflow at USGS streamgage 02357000 (Spring Creek near Iron City, GA) for available periods of record; there are some breaks in the measured streamflow record in the 1970s and early 1980s. Simulations were extended further into the historical record because this subbasin is in an area of substantial water use and it may be valuable to see if the simulations fit older periods better than more recent ones. The long-term plots (1952–2012) in figure 23 show good agreement between statistics computed for measured and simulated streamflow values for spring median flows, spring and summer standard deviations, spring 10-day maximum flows, and summer 10-day maximum flows. Measured and simulated spring 10-day minimum, and summer median and 10-day minimum flows match for the older historical period but then diverge in more recent years, in particular after the mid-1990s. Summer 10-day minimum flow standard deviations are consistently overestimated by the PRMS simulation, pointing to a limitation in the conceptualization of the groundwater flow dynamics for this subbasin (fig. 23*J*) . The study period (2008–12) plots in figure 24 show some difference between the water-use (red line) and no-water-use (blue line) simulations at streamgage 02357000, but not substantial enough to match the measurement-based statistics more than the no-water-use-based statistics. Although water use in this subbasin consists largely of groundwater withdrawals, this lack of accuracy in matching the measurement-based statistics perhaps points to the need of a more sophisticated simulation of the groundwater system at a daily time step.

Discussion

The ACFB is a heterogeneous basin with variations in climatic inputs, landscape characteristics, and hydrologic responses. Several of the hydrologic output variables, such as actual evapotranspiration, runoff, and recharge, largely correlate with precipitation inputs. The water-use evaluation period (2008–12) consisted of three of the driest years in the 31-year period (1982–2012), one of the wettest years in the 31-year period, and one near-average year. Simulations indicate that the parts of the ACFB with high precipitation accumulations generally have more actual evapotranspiration, runoff, and recharge; however, there is still local variation of those quantities between neighboring HRUs in the PRMS application. The storage change across the ACFB for the 2008–12 and 1982–2012 periods was not similar. Simulations of the long-term period showed drier conditions across most of the ACFB, but the period 2008–12 showed a mix of more storage in the northern half of the ACFB and less storage in the southern half of the ACFB. Topography, land cover, and soil datasets used to parameterize the PRMS model largely drive the hydrologic response to climatic forcings of air temperature and precipitation. The spatial variation provided by these simulations could be of use to managers and planners when determining appropriate landscape development actions.

Water-use types are not evenly distributed across the ACFB. Municipal and industrial water use in the ACFB largely occurs along the main-stem reaches of the Apalachicola, Chattahoochee, and Flint Rivers and in the northern part of the ACFB. Agricultural water use in the ACFB is distributed across the lower part of the ACFB, predominantly in the lower Flint River Basin. As a result, the effects of water use on streamflow, as shown in figure 9, are concentrated along the main stem of the Chattahoochee River in the northern part of the ACFB, with more tributaries having streamflow reductions in the lower ACFB. The more spatially distributed agricultural water use in the lower ACFB has the potential to affect tributary streamflows more readily; however, as population and demand increase in the ACFB, more tributaries may become affected by impoundments and withdrawals to keep up with demand. A previous study by LaFontaine and others (2015) considered the effects of land-cover change and potential climate change in the ACFB, but did not include water-use estimates. The models developed for the current study, combined with estimates of future water use and landscape change, could provide insight into how those future water-management scenarios could affect water availability in the basin.

The hydrologic simulations show that recharge in the ACFB is a dynamic process and that the majority of recharge in the lower ACFB occurs during the cool winter season or during wet warm season months. Recharge for warm season months with average or lower precipitation provide little, if any, recharge to the groundwater system. Evapotranspiration uses a considerable amount of water in the ACFB, generally more than half of incoming precipitation. As a result, the ACFB is dependent on winter precipitation accumulations to sustain low flows during the warmer growing season months. An unusually dry winter season could further exacerbate the effects of water use on streamflow throughout the ACFB. The sensitivity of simulated recharge to changes in climate and land cover indicate confounding effects on analyses of drought resilience in the basin.

The coupled hydrologic simulations developed as part of this study indicate that a more sophisticated representation of the groundwater system could be beneficial to simulation of climatic and water-use effects on warm season streamflows. The monthly streamflows at Ichawaynochaway Creek near Elmodel, GA (02354800), and Spring Creek near Iron City, GA (02357000; fig. 12), show a closer match between the coupled and measured streamflows than the PRMS-only simulations for the growing season months (May to September),

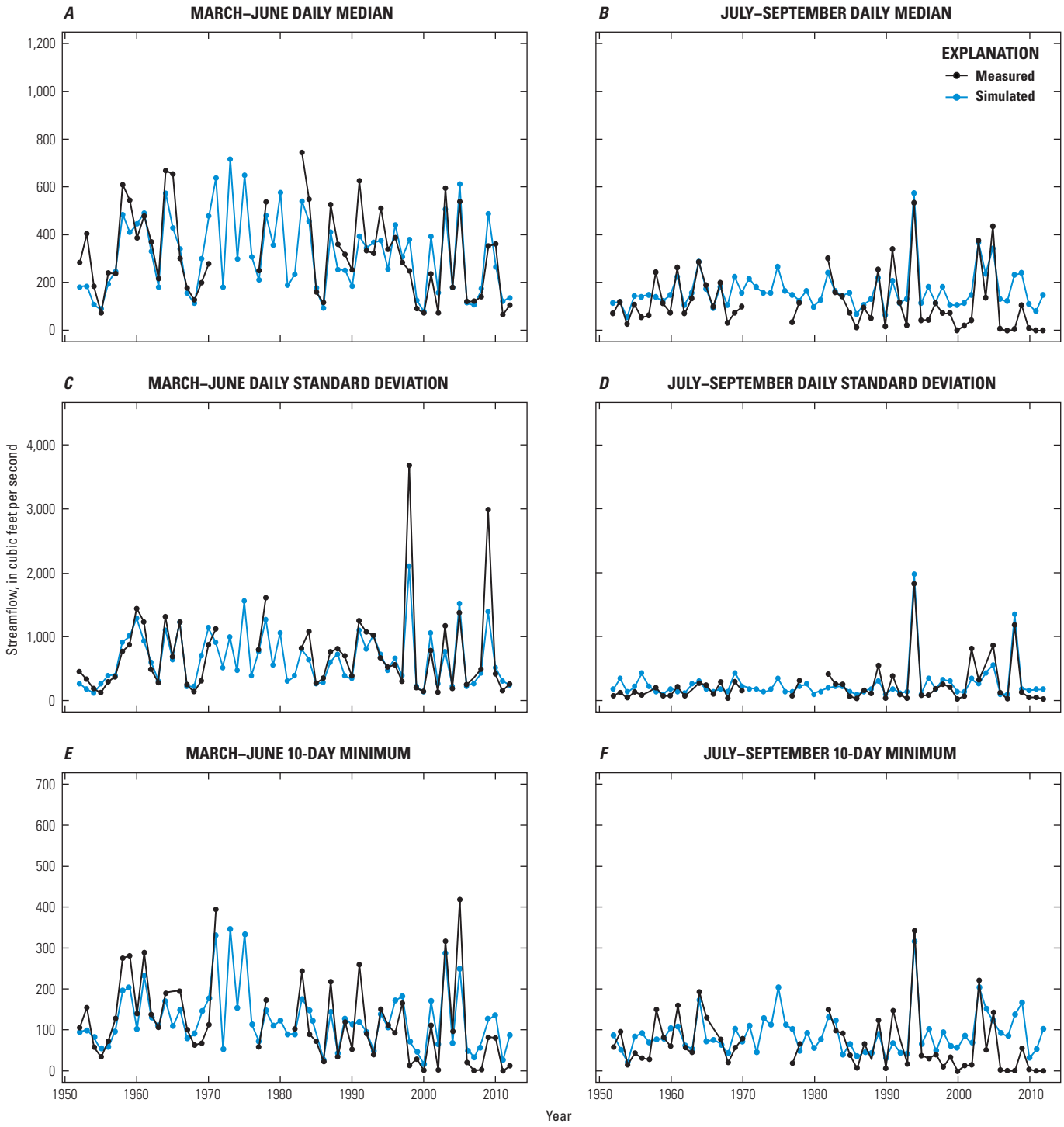

Figure 23. Plots of 10 biologically relevant hydrologic statistics for the Spring Creek subbasin for the period 1952 to 2012 at USGS streamgage 02357000 (Spring Creek near Iron City, GA). These plots show the variation in these statistics for the recent climate period. The statistics shown in the plots are (*A*) March to June daily median streamflow, (*B*) July to September daily median streamflow, (*C*) March to June standard deviation of daily streamflow, (*D*) July to September standard deviation of daily streamflow, (*E*) March to June 10-day minimum moving average of daily streamflow, (*F*) July to September 10-day minimum moving average of daily streamflow, (*G*) March to June 10-day maximum moving average of daily streamflow, (*H*) July to September 10-day maximum moving average of daily streamflow, (*I*) March to June standard deviation of 10-day minimum moving average of daily streamflow, and (*J*) July to September standard deviation of 10-day minimum moving average of daily streamflow.

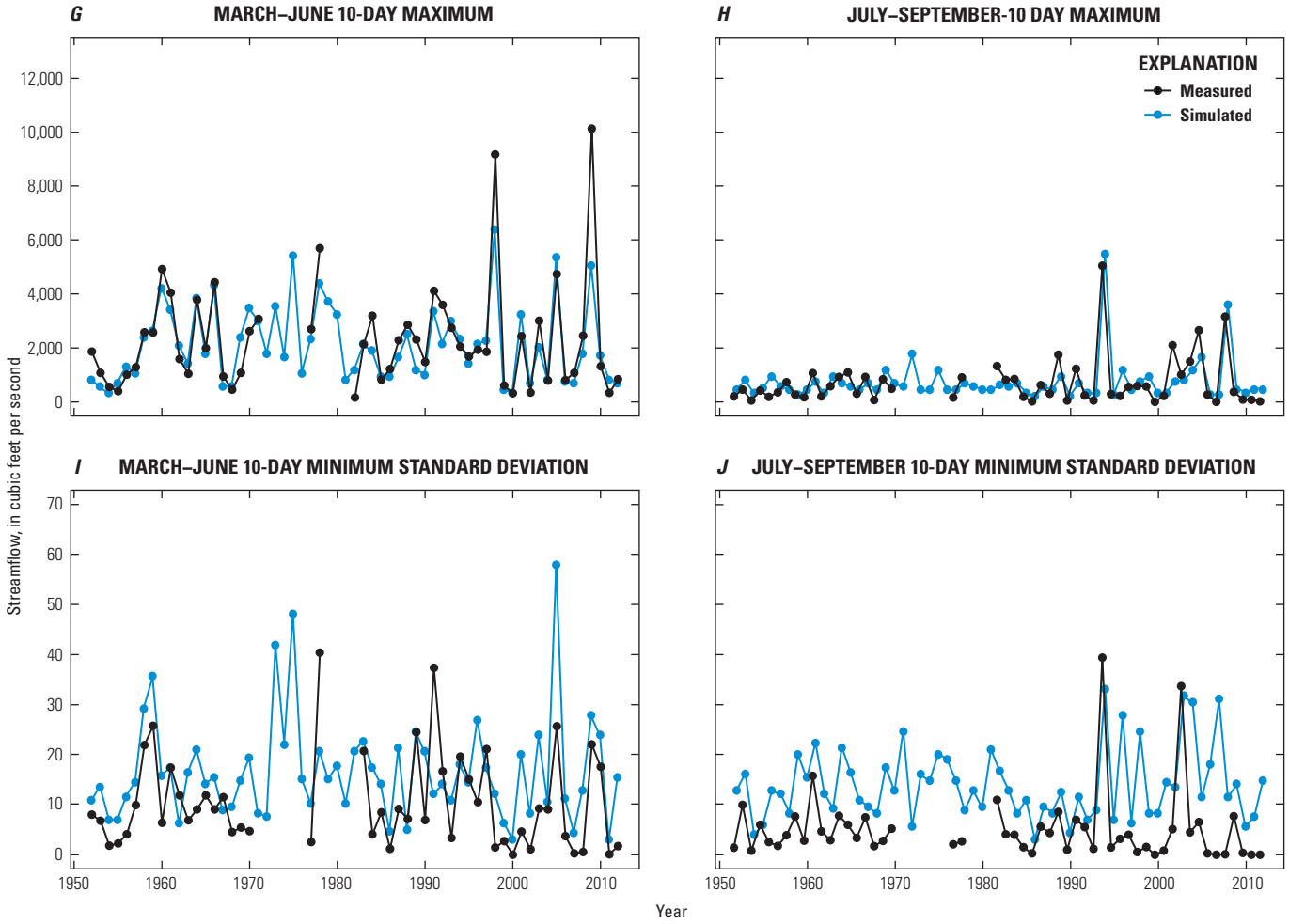

Figure 23.—Continued Plots of 10 biologically relevant hydrologic statistics for the Spring Creek subbasin for the period 1952 to 2012 at USGS streamgage 02357000 (Spring Creek near Iron City, GA). These plots show the variation in these statistics for the recent climate period. The statistics shown in the plots are (*A*) March to June daily median streamflow, (*B*) July to September daily median streamflow, (*C*) March to June standard deviation of daily streamflow, (*D*) July to September standard deviation of daily streamflow, (*E*) March to June 10-day minimum moving average of daily streamflow, (*F*) July to September 10-day minimum moving average of daily streamflow, (*G*) March to June 10-day maximum moving average of daily streamflow, (*H*) July to September 10-day maximum moving average of daily streamflow, (*I*) March to June standard deviation of 10-day minimum moving average of daily streamflow, and (*J*) July to September standard deviation of 10-day minimum moving average of daily streamflow.

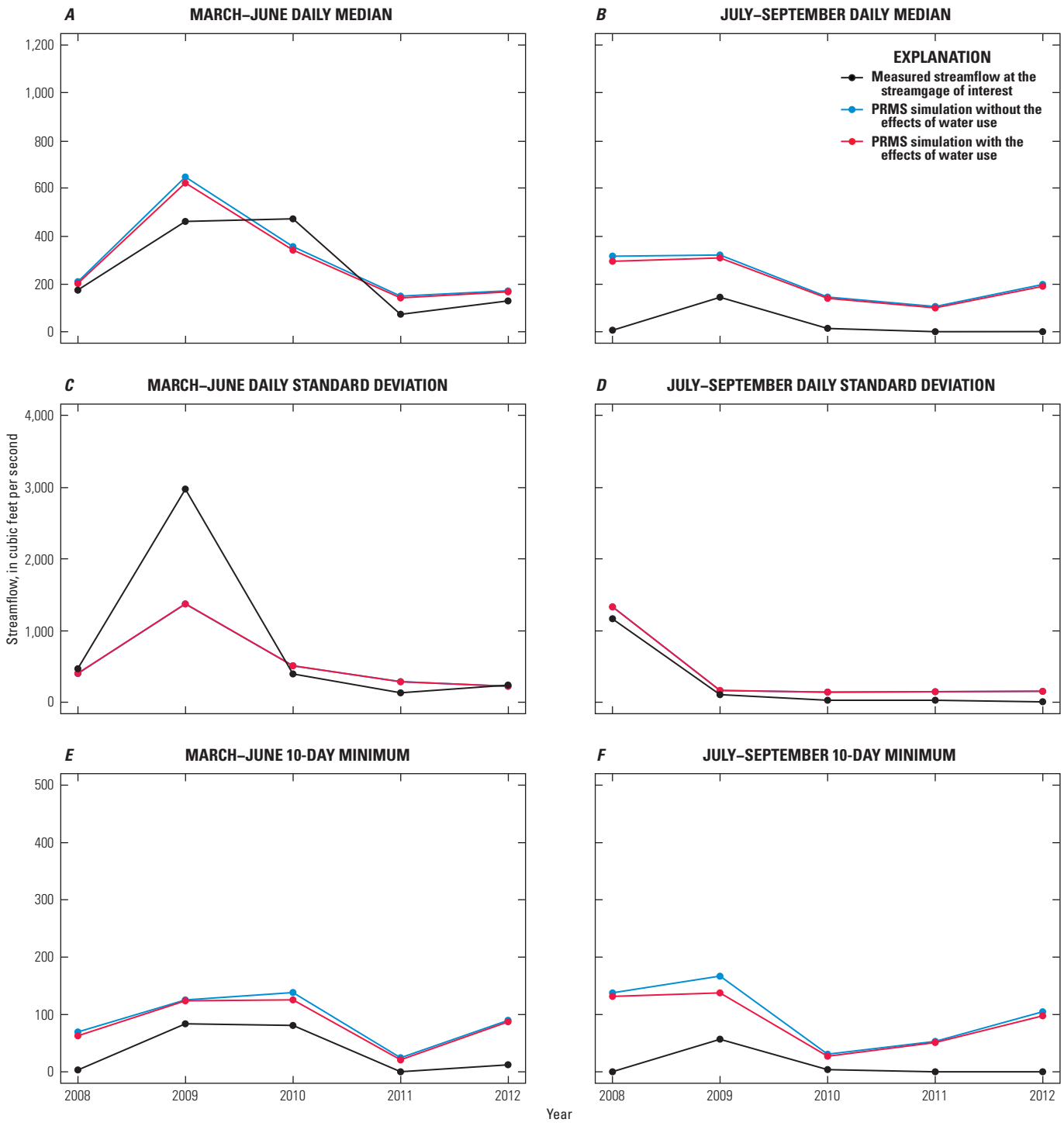

Figure 24. Plots of 10 biologically relevant hydrologic statistics for the Spring Creek subbasin for the period 2008 to 2012 at USGS streamgage 02357000 (Spring Creek near Iron City, GA). These plots show the variation in the statistics for the study period with and without water-use effects. The statistics shown in the plots are (*A*) March to June daily median streamflow, (*B*) July to September daily median streamflow, (*C*) March to June standard deviation of daily streamflow, (*D*) July to September standard deviation of daily streamflow, (*E*) March to June 10-day minimum moving average of daily streamflow, (*F*) July to September 10-day minimum moving average of daily streamflow, (*G*) March to June 10-day maximum moving average of daily streamflow, (*H*) July to September 10-day maximum moving average of daily streamflow, (*I*) March to June standard deviation of 10-day minimum moving average of daily streamflow, and (*J*) July to September standard deviation of 10-day minimum moving average of daily streamflow. The blue line is not visible where overlain by the red line.

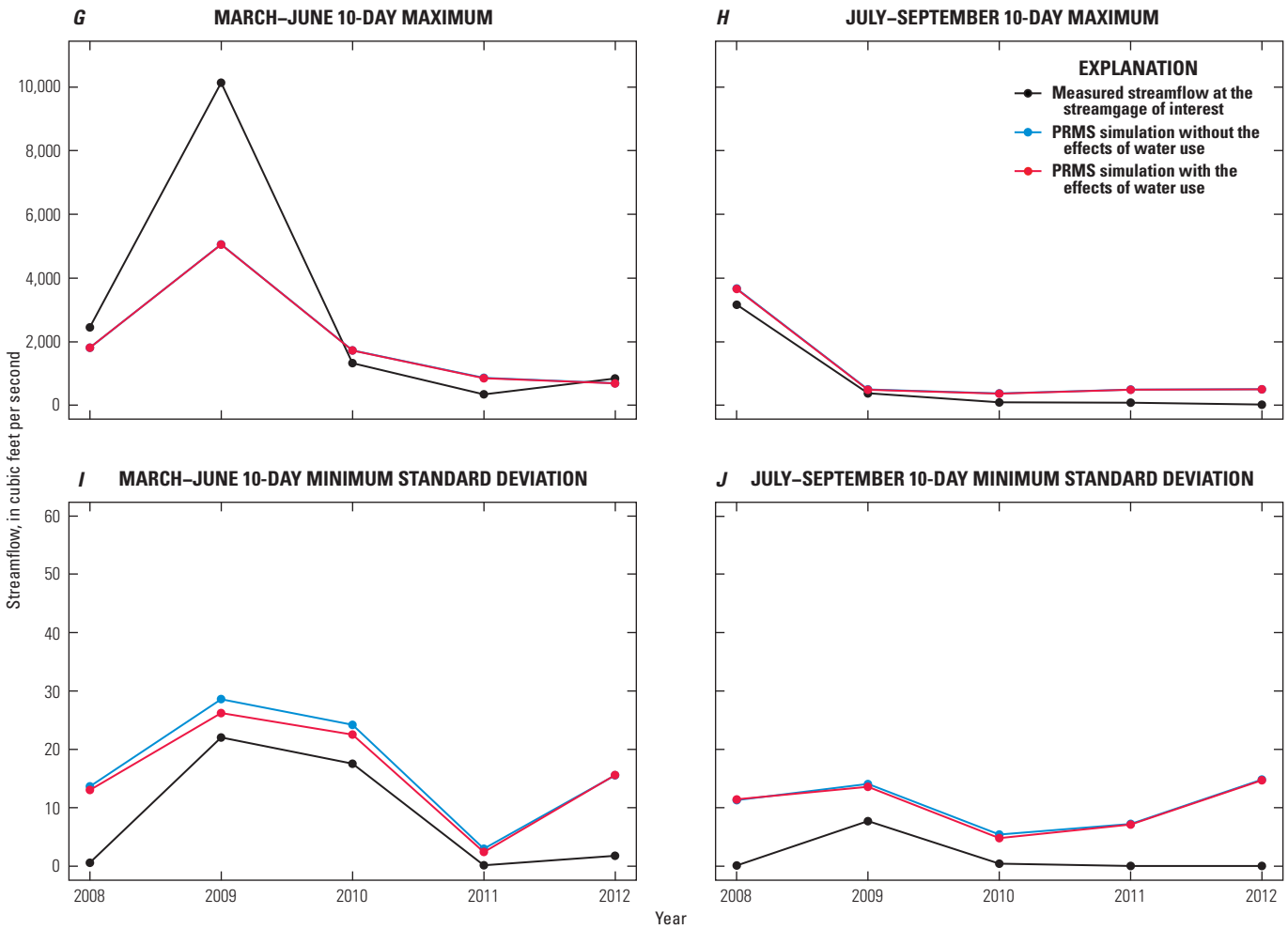

Figure 24.—Continued Plots of 10 biologically relevant hydrologic statistics for the Spring Creek subbasin for the period 2008 to 2012 at USGS streamgage 02357000 (Spring Creek near Iron City, GA). These plots show the variation in the statistics for the study period with and without water-use effects. The statistics shown in the plots are (*A*) March to June daily median streamflow, (*B*) July to September daily median streamflow, (*C*) March to June standard deviation of daily streamflow, (*D*) July to September standard deviation of daily streamflow, (*E*) March to June 10-day minimum moving average of daily streamflow, (*F*) July to September 10-day minimum moving average of daily streamflow, (*G*) March to June 10-day maximum moving average of daily streamflow, (*H*) July to September 10-day maximum moving average of daily streamflow, (*I*) March to June standard deviation of 10-day minimum moving average of daily streamflow, and (*J*) July to September standard deviation of 10-day minimum moving average of daily streamflow. The blue line is not visible where overlain by the red line.

also indicating the importance of more detailed groundwater simulation. Although these months are most critical for biologic processes, such as recruitment, reproduction, growth, persistence, migration, dispersal, and colonization, these simulations may be preferred even though they do not match the higher flows in the cool season. Moving to a fully coupled groundwater and surface-water model in the lower ACFB may also prove better for matching measured flows across all months.

The streamflow statistics generated for the six subbasin fine-resolution PRMS applications generally showed good agreement between simulation-based and measurement-based values. The less accurate simulations occurred in the Chipola River, Ichawaynochaway Creek, and Spring Creek subbasins. All three of these subbasins are located in the geologically complex karst region of the Dougherty Plain in the lower ACFB. The less optimal matches occurred for several low-flow statistics, further reinforcing a need for more sophisticated hydrologic simulation methods in the region. However, along with more sophisticated tools is a need for more types of, and more accurate, information for model development, calibration, and simulation.

Model Limitations

A suite of PRMS models was developed to provide simulations of the water budget of the ACFB and streamflow statistics of six subbasins of the ACFB. This modeling effort indicates that improvements, which are described in detail in the following sections, could be made by (1) incorporating shorter time step water-use information, (2) fully coupling the two modeling platforms used in this study (PRMS and MODFLOW) into a fully coupled GSFLOW (Markstrom and others, 2008) application to better simulate groundwater-dominated regions of the ACFB, and (3) incorporating a routing module in PRMS that allows for inclusion of lakes within the streamflow-routing module to simulate the effects of large impoundments.

Water-Use Data

Site-specific water-use data incorporated in this modeling study provided a level of accuracy that previous datasets could not provide. However, a limitation to the simulations provided in this report is that a daily time step hydrologic model was combined with monthly time step water-use information. Although this may not be as much of a concern for municipal and industrial water uses, agricultural water use can be dynamic across the time span of a month. Larger, shorter pulses of water pumping may affect highly dynamic systems like the lower ACFB beyond what could be shown in simulations that use monthly averaged information. Methods of disaggregating the existing monthly time step information to the daily time step of the PRMS hydrologic model could provide further insight into the hydrologic response to such forcings. Additionally, if methods were established to obtain measured shorter time step water-use data, the disaggregation issue could be avoided.

Model Coupling

This study loosely coupled hydrologic simulations from PRMS and MODFLOW models to provide estimates of water-use-affected streamflows in the lower ACFB. PRMS-based simulations of recharge were provided as input to the MODFLOW model. Groundwater simulations using the MODFLOW model were then merged with surface runoff flow components from the PRMS simulation. This coupling provided a more sophisticated mechanism for simulating the hydrologic response and estimating recharge in the lower ACFB than had been done previously, but there were still limitations in this methodology. By only loosely coupling the modeling applications, each model retained its own limitations. The PRMS has only a one-way flow of water in the soil zone and below. Once water infiltrates the soil zone, it can only move down through the soil to the groundwater reservoir or runoff as surface runoff or shallow subsurface flow. The movement of water is governed by factors that do not allow water to flow back up through the soil zone or move at a different rate based on changing conditions such as groundwater pumping. PRMS and MODFLOW simulated streams, rivers, and waterbodies independently. So for any interaction that occurs at that interface, uncertainty is added that the models are not considering all possible flow mechanisms. For example, PRMS does not currently consider gains or losses through the streambed, but only uses the stream network to route runoff from the HRUs downstream through a basin. In karst areas with substantial groundwater pumping like the lower ACFB, this may be an important mechanism to consider. The use of GSFLOW could potentially improve hydrologic simulations to address some of these limitations.

Reservoir Simulation

The hydrologic models developed as part of this study provide simulations of streamflow and other parts of the water budget throughout the ACFB. In their current form, these models do not account for on-channel lakes and impoundments. Recent improvements to PRMS version 4 (Regan and LaFontaine, 2017) have combined the capabilities to both simulate on-channel lakes and perform streamflow routing. A limitation to this enhancement is that the type of rule-curve operations like those used by the USACE are still not possible within PRMS. More simplistic operational schemes are available, however, and could be used with further discretized versions of the current models; the models would need to have

new HRUs representing the lakes. This method would allow for the withdrawal of water from those types of waterbodies as opposed to the current configuration of extracting water from the stream network. Currently, water withdrawals that may be from lakes are extracted from the model stream segment that would flow through that lake; the withdrawals are extracted from the stream segment storage, which is composed of upstream segment inflows and lateral inflows from directly connected HRUs. This configuration would also allow for a more accurate accounting of the water lost to evaporation from larger waterbodies, such as lakes, when accounting for the water budget of the basin.

Summary

As part of the U.S. Geological Survey's (USGS) National Water Census effort to develop new water accounting tools to assess water availability at regional and national scales, a suite of hydrologic models of the Apalachicola-Chattahoochee-Flint River Basin (ACFB) has been developed, including a coarse-resolution model of the entire ACFB and six fine-resolution subbasin models. The hydrologic models were developed using the Precipitation-Runoff Modeling System (PRMS), a deterministic, distributed-parameter, process-based system that simulates the effects of precipitation, temperature, land cover, and water use on basin hydrology. Monthly time step site-specific water-use data were used in the simulations. The coarse-resolution model was loosely coupled with a MODFLOW groundwater model in the lower ACFB to assess the effects of water use on streamflow in a complex geologic setting. The fine-resolution subbasin PRMS models were developed to provide statistics of streamflow for use in ecological response models. These statistics provide hydrologic information for the spring and summer seasons when flow conditions affect biologic processes, such as recruitment, reproduction, growth, persistence, migration, dispersal, and colonization; these processes were computed for every stream segment in the subbasin models.

The PRMS models simulated streamflow without the effects of water use at a daily time step for at least the calendar years 1982–2012. Because of the availability of measured streamflow, two of the subbasin model applications (Potato Creek and Spring Creek) simulated streamflow for the calendar years 1942–2012 and 1952–2012, respectively. Water-use-affected flows were simulated for calendar years 2008–12. The coarse-resolution model used gridded forcings of air temperature and precipitation, while the fine-resolution subbasin models used weather station data from the National Oceanic and Atmospheric Administration National Climatic Data Center. Model parameters were derived from spatial data layers of topography, land cover, soils, surficial geology, depression storage (small water bodies), and USGS streamgage data.

Outputs of recharge from the coarse-resolution model were provided as input to a MODFLOW groundwater model for the period 2008–12. Recharge was dynamic during the study period, with most recharge occurring during the winter months or during wet warm season months. Loosely coupled streamflows for the lower ACFB were simulated and aggregated at the monthly time step using flow components from the PRMS coarse-resolution model and the MODFLOW groundwater model for the period 2008–12. The loosely coupled simulations provided improved monthly streamflow estimates during the warm season months, but consistently underestimated monthly streamflow volumes during the cool season months.

A set of biologically based streamflow statistics describing spring (March to June) and summer (July to September) streamflows (daily, 10-day minimum, and 10-day maximum) were computed for the six fine-resolution subbasin models. These statistics matched the measured-flow-based statistics well for the three northern subbasins (upper Chattahoochee River, Chestatee River, and Potato Creek). The statistics had consistent overestimation of the flow statistics associated with minimum flows in the Chipola River, Ichawaynochaway Creek, and Spring Creek subbasins. This region is geologically complex with karst features and has substantial groundwater water use. Some statistics for the Spring Creek subbasin matched well in the historical period but did not match well in the more recent period.

Modeling limitations for this study include (1) using monthly time step water-use information in a daily time step hydrologic model, (2) using a loosely coupled simulation framework for the PRMS and MODFLOW models instead of a fully coupled conceptualization, and (3) not directly simulating the effects of large lakes and impoundments in the ACFB. Improvements to each of these limitations could further increase the accuracy of hydrologic simulations in the ACFB, reducing uncertainty in the estimates of water availability and the effects of climate, land cover, and water use on basin hydrology.

Acknowledgments

The authors acknowledge the Modeling of Watershed Systems (MoWS) group of the USGS National Research Program (Central Branch) for their assistance in constructing and parameterizing the initial versions of the PRMS hydrologic models and for adding the water-use enhancements to the PRMS simulation code. The study was made possible through the Water Availability and Use Science Program under the direction of Eric Evenson and Sonya Jones. The authors are grateful for the thoughtful and speedy editorial work of Kay Naugle, USGS Office of Communications and Publishing, Science Publishing Network.

References Cited

Albertson, P.N., and Torak, L.J., 2002, Simulated effects of ground-water pumpage on stream-aquifer flow in the vicinity of federally protected species of freshwater mussels in the lower Apalachicola-Chattahoochee-Flint River Basin (Subarea 4), southeastern Alabama, northwestern Florida, and southwestern Georgia: U.S. Geological Survey Water-Resources Investigations Report 02–4016, 48 p. [Also available at https://pubs.usgs.gov/wri/wri02-4016/.]

Allander, K.K., Niswonger, R.G., and Jeton, A.E., 2014, Simulation of the Lower Walker River Basin hydrologic system, west-central Nevada, Using PRMS and MODFLOW models: U.S. Geological Survey Scientific Investigations Report 2014–5190, 93 p., accessed May 4, 2015, at https://doi.org/10.3133/sir20145190.

Bauer, H.H., and Mastin, M.C., 1997, Recharge from precipitation in three small glacial-till-mantled catchments in the Puget Sound Lowland, Washington: U.S. Geological Survey Water-Resources Investigations Report 96–4219, 119 p. [Also available at https://pubs.usgs.gov/wri/1996/4219/report.pdf.]

Bruce, B.W., Clow, D.W., Maupin, M.A., Miller, M.P., Senay, G.B., Sexstone, G.A., and Susong, D.D., 2015, U.S. Geological Survey National Water Census—Colorado River Basin Geographic Focus Area Study: U.S. Geological Survey Fact Sheet 2015–3080, 4 p., accessed September 16, 2017, at https://doi.org/10.3133/fs20153080.

Caldwell, P.V., Kennen, J.G., Sun, Ge, Kiang, J.E., Butcher, J.B., Eddy, M.C., Hay, L.E., LaFontaine, J.H., Hain, E.F., Nelson, S.A.C., and McNulty, S.G., 2015, A comparison of hydrologic models for ecological flows and water availability: Ecohydrology, v. 8, no. 8, p. 1525–1546, accessed April 15, 2015, at https://doi.org/10.1002/eco.1602.

Chapman, M.J., and Peck, M.F., 1997a, Ground-water resources of the upper Chattahoochee River Basin in Georgia—Subarea 1 of the Apalachicola-Chattahoochee-Flint and Alabama-Coosa-Tallapoosa River Basins: U.S. Geological Survey Open-File Report 96–363, 43 p., accessed December 16, 2015, at https://pubs.usgs.gov/of/1996/ofr96-363/.

Chapman, M.J., and Peck, M.F., 1997b, Ground-water resources of the middle Chattahoochee River Basin in Georgia and Alabama, and upper Flint River Basin in Georgia—Subarea 2 of the Apalachicola-Chattahoochee-Flint and Alabama-Coosa-Tallapoosa River Basins: U.S. Geological Survey Open-File Report 96–492, 48 p., accessed December 16, 2015, at https://pubs.usgs.gov/of/1996/ofr96-492/.

Costa, J.E., 1975, Effects of agriculture on erosion and sedimentation in the Piedmont Province, Maryland: Geological Society of America Bulletin 86, p. 1281–1286, accessed September 27, 2016, at http://bulletin.geoscienceworld.org/content/86/9/1281.

Couch, C.A., Hopkins, E.H., and Hardy, P.S., 2010, Influences of environmental settings on aquatic ecosystems in the Apalachicola–Chattahoochee–Flint River Basin: U.S. Geological Survey Water-Resources Investigations Report 95–4278, 58 p., accessed September 27, 2016, at https://pubs.usgs.gov/wri/wrir95-4278/.

Fanning, J.L., and Trent, V.P., 2009, Water use in Georgia by county for 2005; and water-use trends, 1980–2005: U.S. Geological Survey Scientific Investigations Report 2009–5002, 186 p., accessed September 27, 2016, at https://pubs.usgs.gov/sir/2009/5002/.

Farmer, W.H., Archfield, S.A., Over, T.M., Hay, L.E., LaFontaine, J.H., and Kiang, J.E., 2015, A comparison of methods to predict historical daily streamflow time series in the Southeastern United States: U.S. Geological Survey Scientific Investigations Report 2014–5231, 34 p., accessed April 15, 2015, at http://doi.org/10.3133/sir20145231.

Freeman, M.C., Buell, G.R., Hay, L.E., Hughes, W.B., Jacobson, R.B., Jones, J.W., Jones, S.A., LaFontaine, J.H., Odom, K.R., Peterson, J.T., Riley, J.W., Schindler, J.S., Shea, C., and Weaver, J.D., 2013, Linking river management to species conservation using dynamic landscape-scale models: River Research and Applications, v. 29, no. 7, p. 906–918, accessed April 23, 2015, at https://doi.org/10.1002/rra.2575.

Fry, J., Xian, G., Jin, S., Dewitz, J., Homer, C., Yang, L., Barnes, C., Herold, N., and Wickham, J., 2011, Completion of the 2006 National Land Cover Database for the conterminous United States: Photogrammetric Engineering and Remote Sensing, v. 77, no. 9, p. 858–864, accessed September 27, 2016, at https://www.mrlc.gov/nlcd2006.php.

Golladay, S.W., Hicks, D.W., and Muenz, T.K., 2007, Streamflow changes associated with water use and climatic variation in the lower Flint River Basin, southwest Georgia: Proceedings of the 2007 Georgia Water Resources Conference, March 27–29, 2007: Athens, Ga., The University of Georgia, 4 p., accessed May 9, 2017, at http://www.gwri.gatech.edu/sites/default/files/files/docs/2007/6.6.3.pdf.

Harbaugh, A.W., 2005, MODFLOW-2005, The U.S. Geological Survey modular ground-water model—The ground-water flow process: U.S. Geological Survey Techniques and Methods, book 6, chap. A16, variously paged, accessed April 30, 2015, at https://pubs.usgs.gov/tm/2005/tm6A16/.

Hay, L.E., LaFontaine, Jacob, and Markstrom, S.L., 2014, Evaluation of statistically downscaled GCM output as input for hydrological and stream temperature simulation in the Apalachicola-Chattahoochee-Flint River Basin (1961–99): Earth Interactions, v. 18, no. 9, 32 p., accessed April 2, 2014, at https://doi.org/10.1175/2013EI000554.1.

Hay, L.E., Markstrom, S.L., Ward-Garrison, Christian, 2011, Watershed-scale response to climate change through the twenty-first century for selected basins across the United States: Earth Interactions, v. 15, no. 17, 37 p., accessed September 27, 2016, at https://doi.org/10.1175/2010EI370.1.

Homer, Collin, Dewitz, Jon, Fry, Joyce, Coan, M.J., Hossain, Nazmul, Larson, Charles, Herold, Nate, McKerrow, Alexa, VanDriel, J.N., and Wickham, J.D., 2007, Completion of the 2001 National Land Cover Database for the conterminous United States: Photogrammetric Engineering & Remote Sensing, v. 73, no. 4, p. 337–341, accessed September 15, 2016, at https://www.researchgate.net/publication/237239863.

Homer, Collin, Dewitz, Jon, Yang, Limin, Jin, Suming, Danielson, Patrick, Xian, George, Coulston, John, Herold, Nathaniel, Wickham, James, and Megown, Kevin, 2015, Completion of the 2011 National Land Cover Database for the conterminous United States—Representing a decade of land cover change information Photogrammetric Engineering & Remote Sensing, v. 81, no. 5, p. 345–354, accessed September 15, 2016, at https://www.researchgate.net/publication/282254893.

Hummel, P.R., Kittle, J.L., Duda, P.B., and Patwardhan, Avinash, 2003, Calibration of a watershed model for metropolitan Atlanta, Proceedings of the Water Environment Federation, National TMDL Science and Policy 2003: Water Environment Federation, p. 781–807, accessed September 27, 2016, at https://doi.org/10.2175/193864703784828651.

Jacobson, R.B., and D.J. Coleman, 1986, Stratigraphy and recent evolution of Maryland Piedmont flood plains: American Journal of Science, v. 286, no. 8, p. 617–637, accessed September 27, 2016, at https://doi.org/10.2475/ajs.286.8.617.

Jones, L.E., Painter, Jaime, LaFontaine, Jacob, Sepulveda, Nicasio, and Sifuentes, Dorothy, 2017, Groundwater-flow budget for the lower Apalachicola-Chattahoochee-Flint River Basin in southwestern Georgia and parts of Florida and Alabama, 2008–12: U.S. Geological Survey Scientific Investigations Report 2017–5141, 76 p., accessed December 29, 2017, at https://doi.org/10.3133/sir20175141.

Jones, L.E., and Torak, L.J., 2006, Simulated effects of seasonal ground-water pumpage for irrigation on hydrologic conditions in the lower Apalachicola-Chattahoochee-Flint River Basin, southwestern Georgia and parts of Alabama and Florida, 1999–2002: U.S. Geological Survey Scientific Investigations Report 2006–5234, 106 p., accessed December 15, 2015, at https://pubs.usgs.gov/sir/2006/5234/.

LaFontaine, J.H., Hay, L.E., Viger, R.J., Markstrom, S.L., Regan, R.S., Elliott, C.M., and Jones, J.W., 2013, Application of the Precipitation-Runoff Modeling System (PRMS) in the Apalachicola-Chattahoochee-Flint River Basin in the Southeastern United States: U.S. Geological Survey Scientific Investigations Report 2013–5162, 118 p., accessed April 30, 2015, at https://pubs.usgs.gov/sir/2013/5162/.

LaFontaine, J.H., Hay, L.E., Viger, R.J., Regan, R.S., and Markstrom, S.L., 2015, Effects of climate and land cover on hydrology in the Southeastern U.S.—Potential impacts on watershed planning: Journal of the American Water Resources Association, v. 51, no. 5, p. 1235–1261, accessed September 27, 2016, at https://doi.org/10.1111/1752-1688.12304.

LaFontaine, J.H., Jones, L.E., and Painter, J.A., 2017, Model input and output for hydrologic simulations of the Apalachicola-Chattahoochee-Flint River Basin using the Precipitation-Runoff Modeling System: U.S. Geological Survey data release, https://doi.org/10.5066/F7FJ2F1R.

Leavesley, G.H., Lichty, R.W., Troutman, B.M., and Saindon, L.G., 1983, Precipitation-runoff modeling system—User's manual: U.S. Geological Survey Water-Resources Investigations Report 83–4238, 207 p., accessed September 27, 2016, at https://pubs.usgs.gov/wri/1983/4238/report.pdf.

Lee, K.K., and Risley, J.C., 2002, Estimates of ground-water recharge, base flow, and stream reach gains and losses in the Willamette River Basin, Oregon: U.S. Geological Survey Water-Resources Investigations Report 01–4215, 52 p., accessed September 27, 2016, at https://pubs.usgs.gov/wri/2001/4215/wri01-4215.pdf.

Markewich, H.W., M.J. Pavich, and G.R. Buell, 1990, Contrasting soils and landscapes of the Piedmont and Coastal Plain, Eastern United States: Geomorphology, v. 3, no. 3–4, p. 417–447, accessed September 27, 2016, at https://doi.org/10.1016/0169-555X(90)90015-I.

Markstrom, S.L., Niswonger, R.G., Regan, R.S., Prudic, D.E., and Barlow, P.M., 2008, GSFLOW—Coupled ground-water and surface-water flow model based on the integration of the Precipitation-Runoff Modeling System (PRMS) and the Modular Ground-Water Flow Model (MODFLOW-2005): U.S. Geological Survey Techniques and Methods, book 6, chap. D1, 240 p., accessed September 27, 2016, at https://pubs.usgs.gov/tm/tm6d1/.

Markstrom, S.L., Regan, R.S., Hay, L.E., Viger, R.J., Webb, R.M.T., Payn, R.A., and LaFontaine, J.H., 2015, PRMS-IV, the Precipitation-Runoff Modeling System, version 4: U.S. Geological Survey Techniques and Methods, book 6, chap. B7, 158 p., accessed September 27, 2016, at https://doi.org/10.3133/tm6B7.

Mayer, G.C., 1997, Ground-water resources of the lower-middle Chattahoochee River Basin in Georgia and Alabama, and middle Flint River Basin in Georgia—Subarea 3 of the Apalachicola-Chattahoochee-Flint and Alabama-Coosa-Tallapoosa River Basins: U.S. Geological Survey Open-File Report 96–483, 47 p., accessed December 16, 2015, at https://pubs.usgs.gov/of/1996/ofr96-483/.

Mosner, M.S., 2002, Stream-aquifer relations and the potentiometric surface of the Upper Floridan aquifer in the Lower Apalachicola-Chattahoochee-Flint River Basin in parts of Georgia, Florida, and Alabama, 1999–2000: U.S. Geological Survey Water-Resources Investigations Report 02–4244, 45 p., accessed September 27, 2016, at https://pubs.usgs.gov/wri/wri02-4244/.

Painter, J.A., Torak, L.J., and Jones, J.W., 2015, Evaluation and comparison of methods to estimate irrigation withdrawal for the National Water Census Focus Area Study of the Apalachicola-Chattahoochee-Flint River Basin in southwestern Georgia: U.S. Geological Survey Scientific Investigations Report 2015–5118, 32 p., accessed December 16, 2015, at https://doi.org/10.3133/sir20155118.

Regan, R.S., and LaFontaine, J.H., 2017, Documentation of the dynamic parameter, water-use, stream and lake flow routing, and two summary output modules and updates to surface-depression storage simulation and initial conditions specification options with the Precipitation-Runoff Modeling System (PRMS): U.S. Geological Survey Techniques and Methods, book 6, chap. B8, 60 p., accessed October 10, 2017, at https://doi.org/10.3133/tm6B8.

Singh, Sarmistha, Srivastava, Puneet, Abebe, Ash, and Mitra, Subhasis, 2015, Baseflow response to climate variability induced droughts in the Apalachicola-Chattahoochee-Flint River Basin, U.S.A.: Journal of Hydrology, v. 528, p. 550–561, accessed May 9, 2017, at https://doi.org/10.1016/j.jhydrol.2015.06.068.

Singh, Sarmistha, Srivastava, Puneet, Mitra, Subhasis, and Abebe, Ash, 2016, Climate variability and irrigation impacts on streamflows in a Karst watershed—A systematic evaluation: Journal of Hydrology—Regional Studies, v. 8, p. 274–286, accessed May 9, 2017, at https://doi.org/10.1016/j.ejrh.2016.07.001.

Thornton, P.E., Hasenauer, Hubert, and White, M.A., 2000, Simultaneous estimation of daily solar radiation and humidity from observed temperature and precipitation—An application over complex terrain in Austria: Agricultural and Forest Meteorology, v. 104, no. 4, p. 255–271, accessed April 30, 2015, at https://doi.org/10.1016/S0168-1923(00)00170-2.

Thornton, P.E., and Running, S.W., 1999, An improved algorithm for estimating incident daily solar radiation from measurements of temperature, humidity, and precipitation: Agricultural and Forest Meteorology, v. 93, no. 4, p. 211–228, accessed April 30, 2015, at https://doi.org/10.1016/S0168-1923(98)00126-9.

Thornton, P.E., Running, S.W., and White, M.A., 1997, Generating surfaces of daily meteorological variables over large regions of complex terrain: Journal of Hydrology, v. 190, no. 3, p. 214–251, accessed accessed April 30, 2015, at https://doi.org/10.1016/S0022-1694(96)03128-9.

Torak, L.J., and McDowell, R.J., 1996, Ground-water resources of the lower Apalachicola- Chattahoochee-Flint River Basin in parts of Alabama, Florida, and Georgia—Subarea 4 of the Apalachicola-Chattahoochee-Flint and Alabama-Coosa-Tallapoosa River Basins: U.S. Geological Survey Open-File Report 95–321, 145 p., accessed December 16, 2015, at https://pubs.usgs.gov/of/1995/ofr95321/.

U.S. Army Corps of Engineers, 1997, ACT/ACF comprehensive water resources study, Surface water availability, Volume I, Unimpaired flow: U.S. Army Corps of Engineers report, 96 p. [Available upon request from the U.S. Army Corps of Engineers or the author.]

U.S. Geological Survey, 2007, Facing tomorrow's challenges—U.S. Geological Survey science in the decade 2007–2017: U.S. Geological Survey Circular 1309, 70 p. [Also available at https://pubs.usgs.gov/circ/2007/1309/.]

Viger, R.J., Hay, L.E., Jones, J.W., and Buell, G.R., 2010, Effects of including surface depressions in the application of the Precipitation-Runoff Modeling System in the Upper Flint River Basin, Georgia: U.S. Geological Survey Scientific-Investigations Report 2010–5062, 37 p., accessed September 27, 2016, at https://pubs.usgs.gov/sir/2010/5062/.

Viger, R.J., Hay, L.E., Markstrom, S.L., Jones, J.W., and Buell, G.R., 2011, Hydrologic effects of urbanization and climate change on the Flint River Basin, Georgia: Earth Interactions, v. 15, no. 20, 25 p., accessed September 27, 2016, at https://doi.org/10.1175/2010EI369.1.

Walker, J.F., Hay, L.E., Markstrom, S.L., and Dettinger, M.D., 2011, Characterizing climate-change impacts on the 1.5-yr flood flow in selected basins across the United States—A probabilistic approach: Earth Interactions, v. 15, no. 18, 16 p., accessed September 27, 2016, at https://doi.org/10.1175/2010EI379.1.

Wen, M., and Zhang, Y., 2009, Agricultural water use estimation for the Flint River Basin Regional Water Development and Conservation Plan: Proceedings of the 2009 Georgia Water Resources Conference, April 27–29, 2009, The University of Georgia, 4 p. [Digital copy, accessed May 24, 2011, is available by request from the author.]

Wen, Menghong, Zhang, Yi, and Zeng, Wei, 2007, HSPF model of the streamflow simulation for the lower Flint River watershed: Proceedings of the 2007 Georgia Water Resources Conference, March 27–29, 2007: Athens, Ga., The University of Georgia, 4 p., accessed January 19, 2011, at https://smartech.gatech.edu/handle/1853/48277.

Zeng, Wei, and Wen, Menghong, 2005, Constructing a hydrologic model of the Ichawaynochaway Creek watershed, *in* Hatcher, K.J., ed., Proceedings of 2005 Georgia Water Resources Conference, April 25–27, 2005: Athens, Ga., The University of Georgia, Institute of Ecology, 4 p., accessed May 24, 2011, at https://smartech.gatech.edu/handle/1853/47762.

Zhang, Yi, Hawkins, David, Zeng, Wei, and Wen, Menghong, 2005, The framework of GIS-based Decision Support Systems (DSS) for water resources management at the Flint River Basin, *in* Hatcher, K.J., ed., Proceedings of 2005 Georgia Water Resources Conference, April 25–27, 2005: Athens, Ga., The University of Georgia, Institute of Ecology, 4 p., accessed January 19, 2011, at https://smartech.gatech.edu/handle/1853/47767.

Zhang, Yi, and Wen, Menghong, 2005, Watershed modeling and calibration for Spring Creek subbasin in the Flint River Basin of Georgia using the EPA BASINS/HSPF Modeling Tool, *in* Hatcher, K.J., ed., Proceedings of 2005 Georgia Water Resources Conference, April 25–27, 2005: Athens, Ga., The University of Georgia, Institute of Ecology, 4 p., accessed March, 24, 2011, at https://smartech.gatech.edu/handle/1853/47763.

Appendixes 1 and 2

Appendix 1. Construction, Calibration, and Evaluation of the Apalachicola-Chattahoochee-Flint River Basin (ACFB) Coarse-Resolution Hydrologic Model

Introduction

This appendix describes the construction, calibration, and evaluation of a hydrologic model application for the entire Apalachicola-Chattahoochee-Flint River Basin (ACFB). The U.S. Geological Survey (USGS) Precipitation-Runoff Modeling System (PRMS; Leavesley and others, 1983; Markstrom and others, 2015) was used to provide hydrologic simulations of the basin. The PRMS Model Construction section describes the methodology, which comes from methods described in Viger and Bock (2014), used for developing model stream segments and hydrologic response units (HRUs). The PRMS Model Calibration section describes the general methodology used for hydrologic model parameter estimation. The ACFB PRMS-MODFLOW Model Evaluation section describes the methods used to evaluate model performance. Water-use information for the basin is also summarized in this appendix. Supporting data for the construction, calibration, and evaluation of the coarse-resolution model are available in LaFontaine and others (2017).

PRMS Model Construction

The watershed hydrology model PRMS is a deterministic, distributed-parameter, process-based model used to simulate and evaluate the effects of various combinations of precipitation, climate, and land use on basin response. Response to normal and extreme rainfall and snowmelt can be simulated to evaluate changes in water-balance relations, streamflow regimes, soil-water relations, and groundwater recharge. Each hydrologic component used for the generation of streamflow is represented within the PRMS by a process algorithm that is based on a physical law or an empirical relation with measured or calculated characteristics (figure 5 in the main body of this report). The schematic in figure 6 (in the main body of this report) provides further detail of the various processes conceptualized in the PRMS soil zone. Many internal states (storages) and fluxes (flows) are available as output from the PRMS simulations; see Markstrom and others (2015, appendix table 1–5) for more details.

Discretization

Distributed-parameter capabilities of the PRMS are provided by partitioning a basin into HRUs in which a water balance and an energy balance are computed. The PRMS uses daily climate values of measured precipitation and maximum and minimum air temperature distributed to each HRU to compute solar radiation, potential evapotranspiration, actual evapotranspiration, sublimation, snowmelt, streamflow, infiltration, and groundwater recharge in a PRMS simulation. A stream network is used in the PRMS to route HRU-based runoff flow components (surface runoff, shallow subsurface runoff, and groundwater flow) downstream to the basin outlet.

Stream Network Development

The coarse-resolution ACFB PRMS stream network was extracted from the Geospatial Fabric for National Hydrologic Modeling (Viger and Bock, 2014), an aggregation of the spatial features (catchments and flowlines) of the National Hydrography Dataset NHDPlus version 1 (http://www.horizon-systems.com/NHDPlus/NHDPlusV1_home.php, accessed April 1, 2013). Viger and Bock (2014) aggregated the flowlines into PRMS stream segments based on (1) streamgage locations, (2) inlets and outlets of large impoundments, and (3) a maximum time of travel of 24 hours (for adherence to PRMS computation assumptions). The coarse-resolution PRMS model stream network consists of 453 segments (fig. 1–1; table 1–1).

Hydrologic Response Unit Development

The coarse-resolution ACFB PRMS stream network was extracted from the Geospatial Fabric for National Hydrologic Modeling (Viger and Bock, 2014), an aggregation of the spatial features (catchments and flowlines) of the National Hydrography Dataset NHDPlus version 1 (http://www.horizon-systems.com/NHDPlus/NHDPlusV1_home.php, accessed April 1, 2013). The NHDPlus catchments were used to delineate these local contributing area units, which were formed into the HRUs. Viger and Bock (2014) divided the local contributing area of each stream segment into two areas—a unit on the left and a unit on the right of each stream segment. On the basis of stream network configuration, some stream segments may have fewer or more than two HRUs. The coarse-resolution ACFB PRMS model consists of 754 HRUs with a median size of 34.8 square kilometers (km^2) (fig. 1–1). Additional HRU statistics are provided in table 1–1.

Parameterization

PRMS is a distributed-parameter hydrologic model. Many of the model parameters vary spatially on the basis of the surface and subsurface characteristics of the model domain. The PRMS parameters describe processes such as solar radiation, potential evapotranspiration, canopy interception, snow dynamics, surface runoff, soil-zone dynamics, groundwater flow, and streamflow. For this version of PRMS, the soil-zone and groundwater reservoirs have the same spatial delineations (size and shape) as the HRUs. The base set of PRMS parameters used for this application was obtained

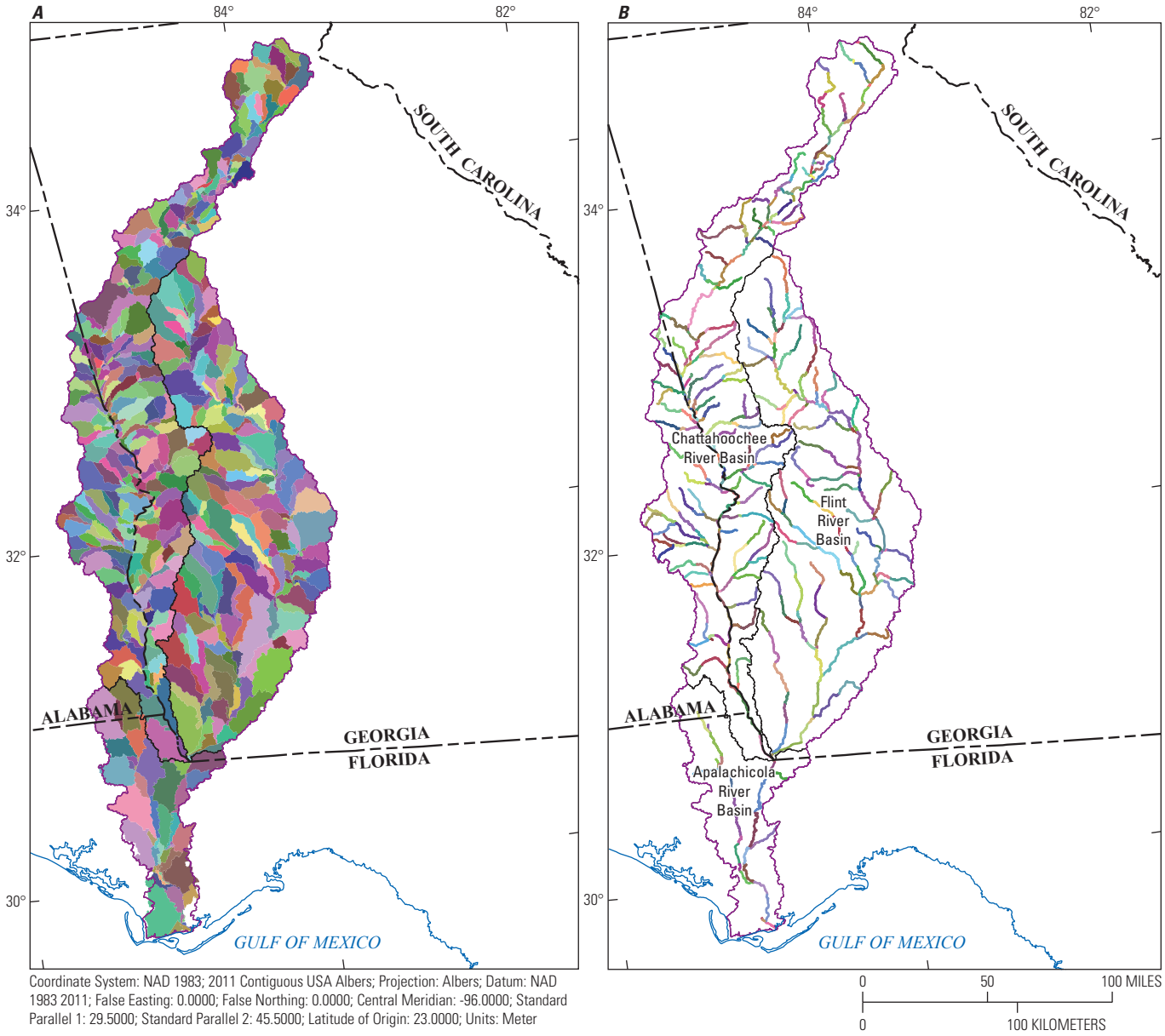

Figure 1–1. (*A*) Coarse-resolution Precipitation-Runoff Modeling System stream segments and (*B*) coarse-resolution Precipitation-Runoff Modeling System hydrologic response units. Stream segments and hydrologic response units are differentiated by color.

from the Geospatial Fabric for National Hydrologic Modeling (Viger, 2014). For the Geospatial Fabric for National Hydrologic Modeling, canopy and surface vegetation parameters were computed using the National Land Cover Dataset 2001 (NLCD; Homer and others, 2007). Soil-zone parameters were computed using the SSURGO soils database (Soil Survey Staff, Natural Resources Conservation Service, U.S. Department of Agriculture, 2012) and maps of near-surface permeability (Gleeson and others, 2011). Groundwater flow parameters were computed using a recession coefficient analysis based on hydrographs of USGS streamgages (LaFontaine and others, 2013).

Streamflow Routing Parameters

Muskingum routing was used for the coarse-resolution PRMS hydrologic model. This method is described in PRMS by two parameters, **K_coef** and **x_coef**. Viger (2014) computed values of **K_coef**, which were used to approximate the travel time, in hours, of streamflow through each stream segment of the Geospatial Fabric. These travel times were computed by summing those values from the NHDPlus version 1 dataset flowlines that composed each stream segment of the coarse-resolution model. The **x_coef** was uniformly set to an initial value of 0.2.

Table 1–1. Modeling unit information for the coarse-resolution PRMS model in the Apalachicola-Chattahoochee-Flint River Basin (ACFB).

[km^2, square kilometer; HRU, hydrologic response unit]

Model	Number of stream segments	Number of hydrologic response units	Mean HRU size (km^2)	Median HRU size (km^2)	Minimum HRU size (km^2)	Maximum HRU size (km^2)
ACFB	453	754	67.0	34.8	0.05	582

HRU Spatial Attributes and Land-Cover Parameters

Parameters describing HRU size, altitude, slope, and aspect were computed from the Digital Elevation Model (DEM) created as part of the NHDPlus version 1 dataset (Viger, 2014). Surficial features, such as percentage impervious area, vegetation density, and dominant vegetation type, were computed for each HRU using the NLCD 2001 (Homer and others, 2007). Parameters describing surface depression storage were based on the National Hydrography Dataset and associated DEM.

HRU Subsurface Reservoir Parameters

Subsurface parameters, those describing the unsaturated zone between land surface and the groundwater reservoir, were developed using the near-surface permeability maps developed by Glesson and others (2011). This parameterization follows the methods described in LaFontaine and others (2013) and provides a spatially distributed range of values that then are calibrated. This method provided the initial spatial variation that was lacking in past PRMS applications that used the same initial value for all HRUs (Viger, 2014).

HRU Groundwater Reservoir Parameters

The groundwater flow parameter, **gwflow_coef**, was derived from an analysis of the groundwater recession constants, using USGS streamflow data and methodologies similar to those described by Rutledge (1998). Annual groundwater recession constants were computed for those streamgages that had streamflow periods relatively free of anthropogenic effects. The median of the annual streamgage recession constants was used as an initial value for those HRUs surrounding each streamgage (LaFontaine and others, 2013).

PRMS to MODFLOW Mapping Parameters (**map_results** module)

The PRMS **map_results** module was used to create a PRMS output file of simulated recharge, which was then used as input to a MODFLOW model developed by Jones and others (2017). Jones and others (2017) used these inputs of recharge to simulate groundwater flow dynamics and estimates of groundwater flow to rivers and streams in the lower part of the ACFB. A geographic information system (GIS) analysis of the intersection of PRMS HRUs and MODFLOW cells was performed to construct the required PRMS parameters. MODFLOW cells outside the PRMS model domain were assigned an HRU value of 1. The required **map_results** module parameters for PRMS simulations using this mapping functionality are described in table 1–2. Recharge was output to the 118,904 MODFLOW cells in a pre-formatted, ready-to-use, MODFLOW input file for the period 1981 to 2012, using a monthly time step with a 1 year spin-up period (1980).

Climate Data and Algorithm

The PRMS requires inputs of daily maximum and minimum air temperature and daily precipitation accumulation time-series data. For the coarse-resolution ACFB model, preprocessed gridded datasets available from the USGS GeoData Portal (GDP; Blodgett and others, 2011) were used. The GDP used a GIS shapefile of the model HRUs to compute the weighted-areal-average of the maximum and minimum air temperature and precipitation for each day of the study period from the Daymet climate dataset. These daily climate inputs were distributed to the coarse-resolution PRMS model units using the **climate_hru** module.

The Daymet, version 2, gridded climate dataset was developed at Oak Ridge National Laboratory, using a collection of algorithms and computer software to interpolate and extrapolate from daily meteorological observations (Thornton and others, 1997; Thornton and Running, 1999; Thornton and others, 2000). Weather parameters generated include daily minimum and maximum air temperature, precipitation, humidity, and solar radiation produced on a 1-km^2 gridded surface over the conterminous United States, Mexico, and Southern Canada for the period 1980–2013 (Thornton and others, 2017). Input data used to construct the Daymet dataset were from the following sources: (1) weather stations as part of the Global Historical Climatology Network (GHCN) daily dataset, (2) the SNOwpack and TELemetry (SNOTEL) dataset managed and distributed by the Natural Resources Conservation Service, (3) weather station observations provided by Environment Canada, (4) weather station observations for Mexico provided by Servicio Meteorologico Nacional, and (5) a DEM. This type of gridded climate dataset is convenient for large-scale hydrologic modeling applications, but applications may be limited by the available period of record and local scale deficiencies.

Table 1–2. Precipitation-Runoff Modeling System parameters required for mapping simulated output to MODFLOW model cells.

[HRU, hydrologic response unit; nhrucell, number of unique intersections between gravity reservoirs and mapped spatial units; one, a constant]

Name	Description	Dimension	Unit	Type	Range	ACFB value
gvr_cell_id	Index of the spatial unit of target map associated with each gravity reservoir	nhrucell	none	integer	0 to number of mapped spatial units	132,924 mappings
gvr_cell_pct	Fraction of the spatial area unit of target map associated with each gravity reservoir	nhrucell	decimal fraction	real	0.0 to 1.0	132,924 mappings
gvr_hru_id	Index of the HRU associated with each gravity reservoir	nhrucell	none	integer	1 to nhrucell	132,924 mappings
mapvars_freq	Flag to specify the output frequency (0=none; 1=monthly; 2=yearly; 3=total; 4=monthly and yearly; 5=monthly, yearly, and total; 6=weekly)	one	none	integer	0 to 6	1
mapvars_units	Flag to specify the output units of mapped results (0=no units conversion; 1=converts inches/day to feet/day; 2=converts inches/day to centimeters/day; 3=converts inches/day to meters/day)	one	none	integer	0 to 3	0
ncol	Number of columns for each row of the mapped results	one	none	integer	1 to user determined	334
prms_warmup	Number of years to simulate before writing mapped results	one	years	integer	0 to user determined	1

Streamflow Data

The USGS National Water Information System (NWIS) stores published streamflow data for the USGS streamgaging network. Currently, there are more than 100 active streamgages in the ACFB (U.S. Geological Survey, 2017). Of these available streamgages, 70 were included in the development of this PRMS model (fig. 1–2); see table 1–3 for streamgage information and available streamflow data records. The 70 streamgages were selected on the basis of available period of record and inclusion in the Geospatial Fabric for National Hydrologic Modeling. The streamflow data were obtained from NWIS (U.S. Geological Survey, 2017), using the **dataRetrieval** package in the R software package (R Development Core Team, 2008).

Water-Use Inputs

Water-use inputs to the hydrologic simulations consist of monthly estimates of surface-water withdrawals and returns, and groundwater withdrawals for the ACFB for 2008 to 2012. Site-specific surface-water withdrawal and return data (primarily municipal, commercial, and industrial) were compiled for Alabama (2008 to 2011), Florida (2008 to 2010), and Georgia (2008 to 2012) and cataloged in the USGS Site-Specific Water Use Data System (SWUDS), which is part of the USGS NWIS (U.S. Geological Survey, 2017). In Georgia, agricultural water-use data collected at several thousand meters (a combination of annual, monthly, and daily telemetered sites) as part of a cooperative program with the State of Georgia Soil and Water Conservation Commission were synthesized by Painter and others (2015) to provide estimates of agricultural surface-water and groundwater withdrawals for the lower ACFB. Methods for interpolating these meter data to produce spatial and temporal distributions of agricultural-irrigation pumping were developed and documented by Torak and Painter (2011). Agricultural withdrawal data were available only for 2010 for Alabama and Florida. The stand-alone PRMS application incorporates both surface-water and groundwater withdrawals from agricultural use. The coupled PRMS application incorporates only the surface-water withdrawal fraction of agricultural water use because the groundwater flow model developed by Jones and others (2017) incorporated the groundwater withdrawal fraction. A study to determine the effects of septic tank return flows on streamflow in the ACFB near Metropolitan Atlanta was conducted as part of the USGS National Water Census (Clarke and Painter, 2014). The primary findings of that study indicate that the septic tank contribution to streamflow was not clearly detected, and so those flow estimates were not included in the PRMS hydrologic simulations.

Irrigation Withdrawals

Water-use regulations, monitoring, and reporting for agriculture vary among Florida, Alabama, and Georgia, so several methods were used to estimate irrigation groundwater withdrawal for the model. The Northwest Florida Water Management District provided site-specific reported irrigation water withdrawals for the parts of the basin in Florida, which

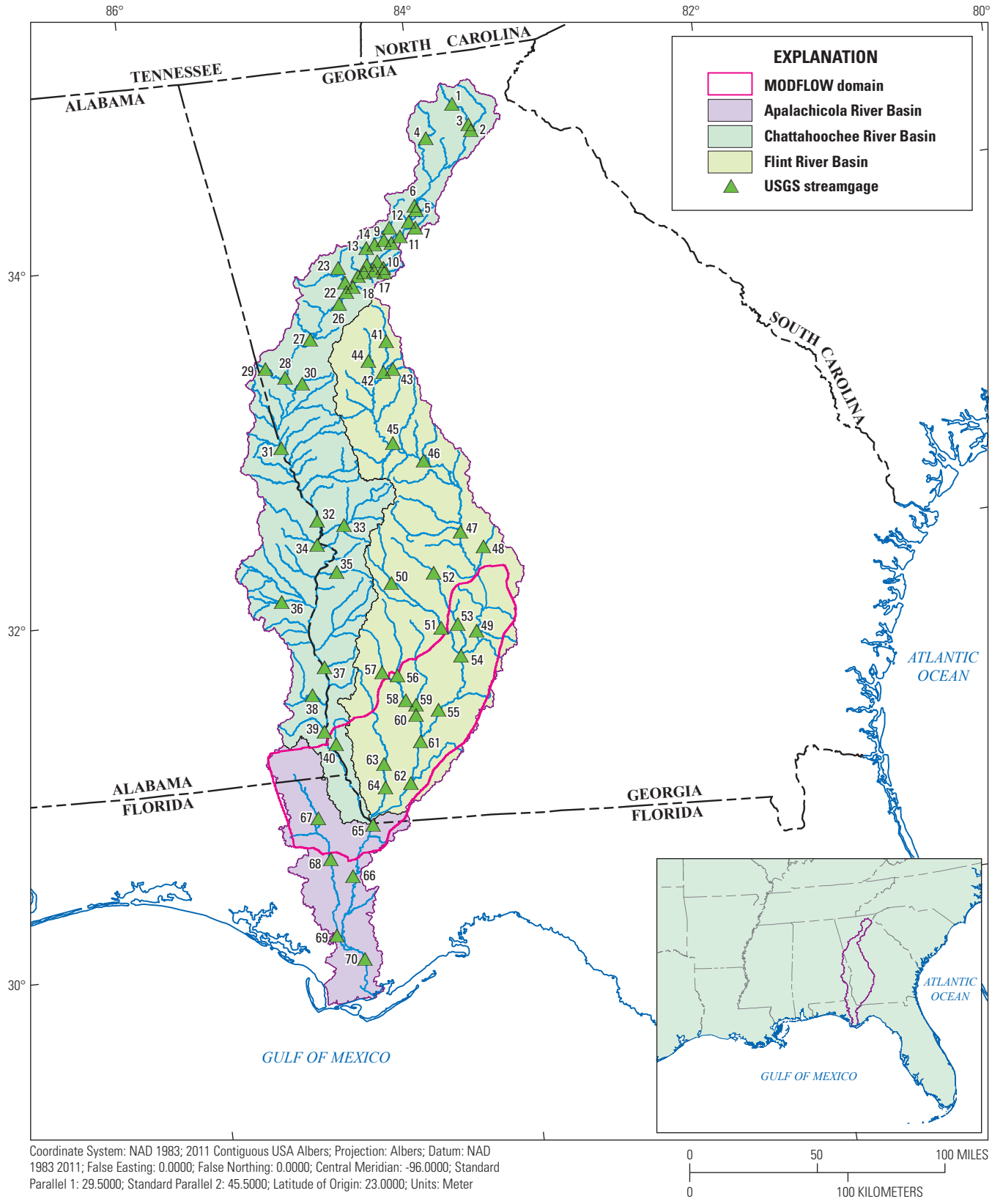

Figure 1–2. U.S. Geological Survey (USGS) streamgages included for the coarse-resolution Precipitation-Runoff Modeling System model.

Table 1–3. U.S. Geological Survey streamflow gages used in Apalachicola-Chattahoochee-Flint River Basin model construction.

[PRMS output variable for simulated flow is *seg_outflow*. km², square kilometer; USGS, U.S. Geological Survey; GF, Geospatial Fabric; Point of interest type: C, calibration; E, evaluation; FS, flow substitution. USACE, U.S. Army Corps of Engineers]

Map ID	Station number	Short name	Station name	USGS drainage area (km²)	GF drainage area (km²)	Drainage area difference (GF minus USGS)	Coarse stream segment	Point of interest type	Period of discharge record
Chatahoochee River Basin									
1	02330450	cha01	Chattahoochee River at Helen, GA	116	119	3.0	2	E	1981–current
2	02331000	cha02	Chattahoochee River near Leaf, GA	388	393	1.2	6	E	1940–71; 2009–current
3	02331600	cha03	Chattahoochee River near Cornelia, GA	815	824	1.0	10	C	1957–current
4	02333500	che01	Chestatee River near Dahlonega, GA	396	391	–1.2	9	C	1929–current
5	02334430	cha04	Chattahoochee River at Buford Dam, near Buford, GA	2,690	2,680	–0.3	35	FS	1942–current
6	02334480	rch01	Richland Creek at Suwanee Dam Road, near Buford, GA	24.2	24.4	0.8	20	E	2001–current
7	02334620	dik01	Dick Creek at Old Atlanta Rd, near Suwanee, GA	17.9	18.0	0.4	23	E	2004–current
8	02334885	suw01	Suwanee Creek at Suwanee, GA	122	122	0.0	25	C	1984–current
9	02335000	cha06	Chattahoochee River near Norcross, GA	3,030	3,030	0.1	50	E	1903–46; 1956–current
10	02335350	crk01	Crooked Creek near Norcross, GA	23.0	23.9	4.0	49	E	2001–current
11	02335450	cha07	Chattahoochee River above Roswell, GA	3,160	3,150	–0.2	51	E	1941–60; 1976–current (1941–60 at station 02335500)
12	02335700	big01	Big Creek near Alpharetta, GA	186	191	2.9	24	C	1960–current
13	02335815	cha08	Chattahoochee River below Morgan Falls Dam, GA	3,550	3,530	–0.7	54	E	2001–current
14	02335870	sop01	Sope Creek near Marietta, GA	75.6	86.3	14	40	E	1984–current
15	02336000	cha09	Chattahoochee River at Atlanta, GA	3,750	3,760	0.3	55	E	1928–current
16	02336120	pea02	N.F. Peachtree Creek, Buford Hwy, near Atlanta, GA	90.1	91.9	2.0	44	E	2003–current
17	02336240	pea03	S.F. Peachtree Creek Johnson Rd, near Atlanta, GA	71.5	77.5	8.4	48	E	2003–current
18	02336300	pea04	Peachtree Creek at Atlanta, GA	225	227	1.1	46	E	1958–current
19	02336360	nan01	Nancy Creek at Rickenbacker Drive, at Atlanta, GA	68.9	72.8	5.7	42	E	2003–current

Table 1–3. U.S. Geological Survey streamflow gages used in Apalachicola-Chattahoochee-Flint River Basin model construction.—Continued

[PRMS output variable for simulated flow is *seg_outflow*, km², square kilometer; USGS, U.S. Geological Survey; GF, Geospatial Fabric; Point of interest type: C, calibration; E, evaluation; FS, flow substitution. USACE, U.S. Army Corps of Engineers]

Map ID	Station number	Short name	Station name	USGS drainage area (km²)	GF drainage area (km²)	Drainage area difference (GF minus USGS)	Coarse stream segment	Point of interest type	Period of discharge record
20	02336490	cha10	Chattahoochee River at GA 280, near Atlanta, GA	4,120	4,140	0.5	127	E	1981–current
21	02336635	nik01	Nickajack Creek at US 78/278, near Mableton, GA	81.5	81.5	0.0	117	E	1995–current
22	02336728	uto01	Utoy Creek at Great Southwest Pkwy nr Atlanta, GA	87.8	90.4	2.9	120	E	1994–96; 2003–current
23	02336968	nos01	Noses Creek at Powder Springs Rd, Powder Springs, GA	115	125	8.6	115	E	1998–current
24	02337000	swt01	Sweetwater Creek near Austell, GA	637	628	–1.4	123	C	1937–current
25	02337040	swt02	Sweetwater Creek below Austell, GA	679	684	0.7	121	E	
26	02337170	cha11	Chattahoochee River near Fairburn, GA	5,330	5,320	–0.1	133	E	1965–current
27	02338000	cha12	Chattahoochee River near Whitesburg, GA	6,290	6,250	–0.6	144	E	1938–54; 1965–current
28	02338500	cha13	Chattahoochee River at GA 100, at Franklin, GA	6,940	6,920	–0.3	149	E	1928–31; 1939; 1958–59; 2004–current
29	02338523	hil01	Hillabahatchee Creek at Thaxton Rd, nr Franklin, GA	43.5	44.6	2.4	145	E	2001–current
30	02338660	new01	New River at GA 100, near Corinth, GA	329	326	–0.9	137	C	1978–current
31	02339500	cha14	Chattahoochee River at West Point, GA	9,190	9,170	–0.2	200	FS	1896–current
32	02341505	cha15	Chattahoochee River at US 280, near Columbus, GA	12,100	12,100	–0.2	253	E	1929–current (1929–2002 at 02341500)
33	02341800	upt01	Upatoi Creek near Columbus, GA	885	884	–0.2	244	C	1968–current
34	02342500	uch01	Uchee Creek near Fort Mitchell, AL	834	837	0.4	266	C	1946–current
35	02342850	han01	Hannahatchee Creek at Union Road, at Union, GA	313	313	–0.1	249	E	1964–65; 2008–current
36	02342933	cow01	South Fork Cowikee Creek near Batesville, AL	290	290	0.0	280	E	1963–71; 1974–2011
37	023432415	cha16	Chattahoochee R .36 mi ds WFG Dam nr Ft Gaines, GA	19,300	19,300	0.2	93	E	1964–current (1964–2009 from USACE)
38	02343300	abb01	Abbie Creek near Haleburg, AL	378	379	0.2	104	C	1958–71; 1974–92

Table 1–3. U.S. Geological Survey streamflow gages used in Apalachicola-Chattahoochee-Flint River Basin model construction.—Continued

[PRMS output variable for simulated flow is *seg_outflow*, km², square kilometer; USGS, U.S. Geological Survey; GF, Geospatial Fabric; Point of interest type: C, calibration; E, evaluation; FS, flow substitution. USACE, U.S. Army Corps of Engineers]

Map ID	Station number	Short name	Station name	USGS drainage area (km²)	GF drainage area (km²)	Drainage area difference (GF minus USGS)	Coarse stream segment	Point of interest type	Period of discharge record
39	02343801	cha17	Chattahoochee River near Columbia, AL	21,300	21,200	–0.3	109	E	1975–current
40	02343940	saw01	Sawhatchee Creek at Cedar Springs, GA	166	168	1.5	103	C	2002–current
			Flint River Basin						
41	02344350	fln01	Flint River near Lovejoy, GA	337	331	–1.6	347	E	1985–current
42	02344478	sho01	Shoal Creek at Shoal Creek Road, near Griffin, GA	33.4	34.8	4.2	334	E	2004–current
43	02344500	fln02	Flint River near Griffin, GA	704	698	–0.8	350	C	1937–current
44	02344700	lin01	Line Creek near Senoia, GA	261	265	1.5	348	E	1964–current
45	02346180	fln03	Flint River near Thomaston, GA	3160	3,150	–0.3	365	E	1966–92
46	02347500	fln04	Flint River at US 19, near Carsonville, GA	4,790	4,800	0.1	386	C	1911–23; 1928–31; 1937–current
47	02349605	fln05	Flint River at GA 26, near Montezuma, GA	7,560	7,580	0.2	401	C	1904–12; 1930–current
48	02349900	tur01	Turkey Creek at Byromville, GA	116	124	7.1	388	C	1958–current
49	02350512	fln06	Flint River at GA 32, near Oakfield, GA	10,000	10,200	2.0	411	E	1929–58; 1987–current
50	02350600	kin01	Kinchafoonee Creek at Preston, GA	510	512	0.3	424	E	1951–77; 1987–2002; 2009–current
51	02350900	kin02	Kinchafoonee Creek at Pinewood Road, near Dawson, GA	1,360	1,370	0.4	430	C	1985–current
52	02351500	muc01	Muckalee Creek near Americus, GA	363	364	0.3	423	E	2001–current
53	02351890	muc02	Muckalee Creek at GA 195, near Leesburg, GA	937	945	0.8	429	C	1979–current
54	02352500	fln07	Flint River at Albany, GA	13,700	13,800	0.7	221	FS	1901–21; 1929–current
55	02353000	fln08	Flint River at Newton, GA	14,900	15,100	1.6	226	E	1938–50; 1956–current
56	02353265	ich01	Ichawaynochaway Creek at GA 37, near Morgan, GA	780	774	–0.7	452	C	2001–current
57	02353400	pac01	Pachitla Creek near Edison, GA	487	476	–2.2	440	C	1959–71; 1988–current
58	02353500	ich02	Ichawaynochaway Creek at Milford, GA	1,600	1,610	0.8	448	C	1939–current
59	02354500	chk01	Chickasawhatchee Creek at Elmodel, GA	828	825	–0.4	447	C	1939–49; 1995–current
60	02354800	ich03	Ichawaynochaway Creek near Elmodel, GA	2,590	2,690	3.7	445*	C	1995–current
61	02355662	fln09	Flint river at River-view Plantation, nr Hopeful, GA	17,900	18,000	0.8	227	E	2002–current
62	02356000	fln10	Flint River at Bainbridge, GA	19,600	19,500	–0.4	233	E	1907–13; 1928–71; 2001–current

Table 1–3. U.S. Geological Survey streamflow gages used in Apalachicola-Chattahoochee-Flint River Basin model construction.—Continued

[PRMS output variable for simulated flow is *seg_outflow*, km², square kilometer; USGS, U.S. Geological Survey; GF, Geospatial Fabric; Point of interest type: C, calibration; E, evaluation; FS, flow substitution. USACE, U.S. Army Corps of Engineers]

Map ID	Station number	Short name	Station name	USGS drainage area (km²)	GF drainage area (km²)	Drainage area difference (GF minus USGS)	Coarse stream segment	Point of interest type	Period of discharge record
63	02357000	spr02	Spring Creek near Iron City, GA	1,270	1,250	–1.6	325	C	1937–71; 1982–current
64	02357150	spr03	Spring Creek near Reynoldsville, GA	1,610	1,500	–6.6	327	E	1998–current
			Apalachicola River Basin						
65	02358000	apa01	Apalachicola River at Chattahoochee, FL	44,500	44,400	–0.1	75	FS	1928–current
66	02358700	apa02	Apalachicola River near Blountstown, FL	45,600	45,400	–0.4	79	E	1957–current
67	02358789	chp01	Chipola River at Marianna, FL	1,200	1,350	12	64	C	1999–current
68	02359000	chp02	Chipola River near Altha, FL	2,020	2,190	8.6	63	C	1921–27; 1929–31; 1943–current
69	02359051	chp03	Chipola River at Cockran Landing, FL	3,120	3,240	4.0	73	E	1991–95; 1998–current
70	02359170	apa04	Apalachicola River near Sumatra, FL	49,700	49,700	0.0	86	E	1977–current

*, PRMS variable for simulated flow is *seg_upstream_inflow*.

included Calhoun, Gadsden, and Jackson Counties (Tony Countryman, Northwest Florida Water Management District, written commun., July 1, 2013). The State of Alabama does not require reporting of irrigation withdrawals; therefore, estimation methods employing a combination of spatial analyses and field reconnaissance were used to provide irrigation groundwater withdrawal estimates for the southern part of Houston County, Alabama.

A preliminary inventory of irrigated cropland in Houston County, exclusive of the northwestern part of the county, during 2014 provided the spatial distribution of approximate irrigation withdrawal locations (Marella and Dixon, 2015). An assumption that Houston County crop distribution and irrigation practices were similar to those in Calhoun and Jackson Counties in Florida guided the assignment of withdrawals in Houston County. The preliminary cropland inventory showed that for the part of Houston County in the model, irrigated cropland area was 27.5 percent of the sum of irrigated cropland areas in Calhoun and Jackson Counties in Florida, for the same growing season. Therefore, 27.5 percent of the sum of irrigation withdrawals from Calhoun and Jackson Counties for each month was estimated as the total Houston County irrigation withdrawals. Within Houston County, the total estimated irrigation withdrawal was distributed to each identified site as a ratio of the area represented by each site to the total irrigated area in Houston County. Subsequent to incorporation of these preliminary data, estimates of irrigated cropland for Calhoun, Gadsden, and Jackson Counties in Florida, and for Houston County, exclusive of the northwest part of the county, in Alabama, were published by Marella and Dixon (2015). The final analysis of those data indicated a slightly different ratio of irrigated cropland in Houston County relative to the irrigated cropland in Calhoun and Jackson Counties, Florida. However, the discrepancy resulted in a small enough difference in groundwater pumping rates and distribution, relative to total groundwater pumping in the model, as well as other potential sources of model error, that no attempt was made to revise the model with updated information.

The Georgia Agricultural Water Conservation and Metering Program provided monthly and annually reported groundwater irrigation withdrawal volumes for selected irrigation withdrawal sites in Georgia for the simulation period as part of a cooperative program between the USGS and the Georgia Soil and Water Conservation Commission, the managing agency for the Georgia Agricultural Water Conservation and Metering Program. To estimate irrigation withdrawals for the model area, geostatistical techniques involving structural analysis, variogram development, interpolation (kriging), and conditional simulation (Painter and others, 2015) were used to create monthly irrigation-depth

distributions (irrigation volume divided by corresponding acres). The resulting irrigation-depth patterns were applied to the distribution of irrigated acres in the model area to obtain irrigation withdrawal rates for model input. The estimates of irrigated acres were provided by the Georgia Department of Natural Resources (Danna Betts, Georgia Department of Natural Resources, written commun., May 2010), by growing season, to eliminate inadvertent assignment of irrigation depths to non-irrigated land.

Monthly irrigation rates for withdrawal sites in Georgia for the 2009 growing season (March–October) and the first 3 months (March–May) of the 2010 growing season were estimated from precipitation data because meter data were not available. Irrigation rates for the period of missing meter data were developed by comparing monthly irrigation rates and precipitation patterns for 2012 with comparable months during 2009 and 2010. The precipitation data were obtained from 33 Georgia Automated Environmental Monitoring Network stations in the model area (University of Georgia, 2017). For each set of precipitation and meter data, monthly proportions of precipitation were developed that normalized the precipitation during 2012 to the precipitation reported for the missing months during 2009 and 2010. Precipitation during 2012 bracketed the precipitation corresponding to the missing months, which allowed for the computation of required irrigation based on precipitation shortfalls. For example, if the precipitation for a given month during 2012 was twice that in a corresponding month during 2009, then a multiplier of two was applied to the 2012 monthly rates to obtain the pumping rates used as model inputs for that month during 2009, the premise being that half the precipitation during 2009 would require twice the irrigation as in 2012.

Public-Supply Water Withdrawals

Monthly estimates of public-supplied water usage amounts for 2008 to 2012 were obtained from Alabama, Florida, and Georgia for inclusion in the USGS SWUDS. Public-supplied water use includes water withdrawn, treated, and delivered to domestic, commercial, and industrial customers (Lawrence, 2016). Alabama public-supply usage estimates were obtained from the Alabama Water Use Reporting Program (Amy Gill, USGS, written commun., 2014). Florida public-supply usage estimates were obtained from (1) consumptive water-use permit compliance files or annual reports provided by the Northwest Florida Water Management District (NWFWMD), (2) monthly operating reports supplied to the Florida Department of Environmental Protection (FDEP) Drinking Water Program, and (3) directly from individual public water suppliers (Marella, 2014; NWFWMD, 2014; Lawrence, 2016). Georgia public-supply usage estimates were based on data reported to the Georgia Environmental Protection Division (GaEPD) under the Nonfarm Water Withdrawal Permit Program (Lawrence, 2016). Water users of less than 100,000 gallons per day were not specifically included in the data used in this report.

Surface-Water Return Flows

Monthly estimates of surface-water returns for 2008 to 2012 were obtained from Alabama, Florida, and Georgia for inclusion in the USGS SWUDS. Surface-water returns generally include the discharge of treated wastewater from public and private wastewater-treatment plants, commercial and industrial sources, and raw and treated water from mining activities, as well as discharges from those thermoelectric-power facilities in the ACFB that use a once-through cooling process. Alabama surface-water return estimates were obtained from the Alabama Department of Environmental Management Electronic Discharge Monitoring Reporting (eDMR) System database (Amy Gill, USGS, written communication, 2014; Lawrence, 2016). Florida surface-water return estimates were obtained from the annual Florida Reuse Inventory published by the FDEP (Florida Department of Environmental Protection, 2011; Marella, 2014; Lawrence, 2016). Georgia surface-water return estimates were obtained from GaEPD for those water users permitted under the U.S. Environmental Protection Agency National Pollutant Discharge Elimination System and the Georgia Power Company (Lawrence, 2016).

Mapping to Hydrologic Modeling Units

Water-use estimates of irrigation withdrawals, public-supplied water, and surface-water returns were mapped to the PRMS model units (HRUs and stream segments) through a GIS overlay analysis with the water-use locations. Surface-water-based withdrawals and returns were mapped to stream segments, and groundwater-based withdrawals were mapped to HRUs. For the PRMS-only simulation, groundwater-based withdrawals were extracted from the PRMS conceptual groundwater reservoir using the PRMS water-use module (Regan and LaFontaine, 2017; figure 5 in the main body of this report). These groundwater withdrawals have no effect on the outputs of recharge to the MODFLOW model by Jones and others (2017) because recharge is conceptualized as water moving vertically downward from the soil zone to the groundwater reservoir. To simulate water use in PRMS, the water-use estimates were formatted into PRMS-specific water-use input files as specified in Regan and LaFontaine (2017). Separate water-use input files were created for (1) water withdrawn from streams, (2) water returned to streams, and (3) water withdrawn from the groundwater reservoir.

ACFB Water-Use Summary

Water use in the ACFB coarse-resolution model domain consisted of surface-water withdrawals and returns, and groundwater withdrawals. Mean monthly surface-water withdrawals ranged from 1,150 to 1,540 cubic feet per second (ft^3/s), mean monthly surface-water returns ranged from 720 to 937 ft^3/s, and mean monthly groundwater withdrawals ranged from 40.9 to 1,030 ft^3/s (table 1–4). Mean monthly

Table 1–4. Summary of mean monthly water withdrawals for the ACFB, by type, for the period 2008–12.

[GW, groundwater; SW, surface water; W, withdrawal; R, return]

Water-use source	Water-use type	Mean monthly water withdrawals for 2008–12, in cubic feet per second											
		Jan.	Feb.	Mar.	April	May	June	July	Aug.	Sept.	Oct.	Nov.	Dec.
SW	W	1,320	1,250	1,200	1,230	1,320	1,500	1,540	1,520	1,390	1,260	1,150	1,200
SW	R	937	880	893	745	782	833	905	919	769	742	720	873
GW	W	40.9	55.0	172	269	422	1,030	736	522	366	192	60.7	47.2
SW return ratio		0.71	0.70	0.74	0.61	0.59	0.56	0.59	0.60	0.55	0.59	0.63	0.73

surface-water and groundwater withdrawals were largest in the summer months of June, July, and August. For 2008 to 2012, monthly surface-water withdrawals ranged from 1,040 to 1,710 ft^3/s, monthly surface-water returns ranged from 598 to 1,120 ft^3/s, and groundwater withdrawals ranged from 0 to 1,380 ft^3/s (fig. 1–3). Groundwater withdrawals had the largest seasonal variation due to agricultural uses, with surface-water withdrawals having a smaller seasonal variation.

MODFLOW Groundwater Flux Inputs

To better assess the effects of groundwater use on streamflows in the lower ACFB, PRMS surface hydrology simulations were coupled with MODFLOW groundwater flow simulations. The PRMS simulates three flow components for each HRU: surface runoff, shallow subsurface flow, and groundwater flow. Surface runoff and shallow subsurface flow are conceptualized in PRMS as that fraction of precipitation that runs off the landscape as overland flow and shallow subsurface flow. The groundwater flow component is conceptualized as that fraction of streamflow generated from the saturated zone (base flow). For this study, the PRMS groundwater flow component is assumed to be conceptually equivalent to the flows generated by the MODFLOW river and drain features. Estimates of recharge, the water that infiltrates through the soil profile and contributes water to the saturated zone, were simulated using the PRMS model and provided as input to the MODFLOW groundwater model. The MODFLOW model then simulated groundwater flows (using rivers and drains) to the stream network of the lower ACFB. Finally, the simulated flow components for surface runoff (PRMS), shallow subsurface flow (PRMS), and groundwater flow (MODFLOW), and stream-based water use, were aggregated on a monthly time step to simulate streamflow in the lower ACFB.

A spatial overlay of the PRMS HRUs and MODFLOW zones was completed to provide integrated groundwater flows at streamgage locations in the lower ACFB (fig. 1–4). The spatial overlay was necessary for those areas where the MODFLOW domain contained only a fraction of some PRMS HRUs or only part of a watershed. For those HRUs and watersheds not completely in the groundwater model domain, the area-weighted fractions of upstream PRMS groundwater flow and MODFLOW groundwater flow were computed and then added to the PRMS surface runoff and shallow subsurface flow components, and stream-based water use estimates, to estimate water use-affected streamflow at a monthly time step.

PRMS Model Sensitivity

Model parameter sensitivity analysis can be used to determine the link between dominant processes and model parameters across varying landscape and hydroclimatic conditions. The sensitivity analysis performed by Markstrom and others (2016) at the contiguous United States (CONUS) scale, using PRMS and the Fourier Amplitude Sensitivity Test (FAST; Cukier and others, 1973; Schaibly and Shuler, 1973; Cukier and others, 1975; Saltelli and others, 2006), was used to formulate the automated calibration strategy used in this study; the five most sensitive PRMS parameters for eight hydrologic processes and three objective functions for the HRUs in the ACFB are listed in table 1–5. The sensitivity analysis by Markstrom and others (2016) showed that evapotranspiration, and runoff (for a relatively small part of the basin), were the most dominant hydrologic processes across the ACFB; snowmelt, base flow, and infiltration were the least dominant hydrologic processes across the ACFB.

PRMS Model Calibration

The PRMS parameters selected for calibration were assigned to one of six calibration steps in two phases (table 1–6). In the first phase, two steps were used to calibrate parameters associated with simulation of solar radiation and potential evapotranspiration. In the second phase, two steps were used to calibrate parameters associated with the overall water balance and streamflow timing. The automated calibration tool, Luca (Hay and others, 2006; Hay and Umemoto, 2006), was used to optimize the parameters identified by the FAST analysis by Markstrom and others (2016). Luca is a graphical user interface that applies the Shuffled Complex Evolution method developed by Duan and others (1992, 1994) for parameter optimization. The automated calibration was supplemented by manual adjustment to improve simulations of low-flow days. A geographically nested procedure similar to that used by LaFontaine and others (2013) was then used to apply the calibration method downstream through the basin.

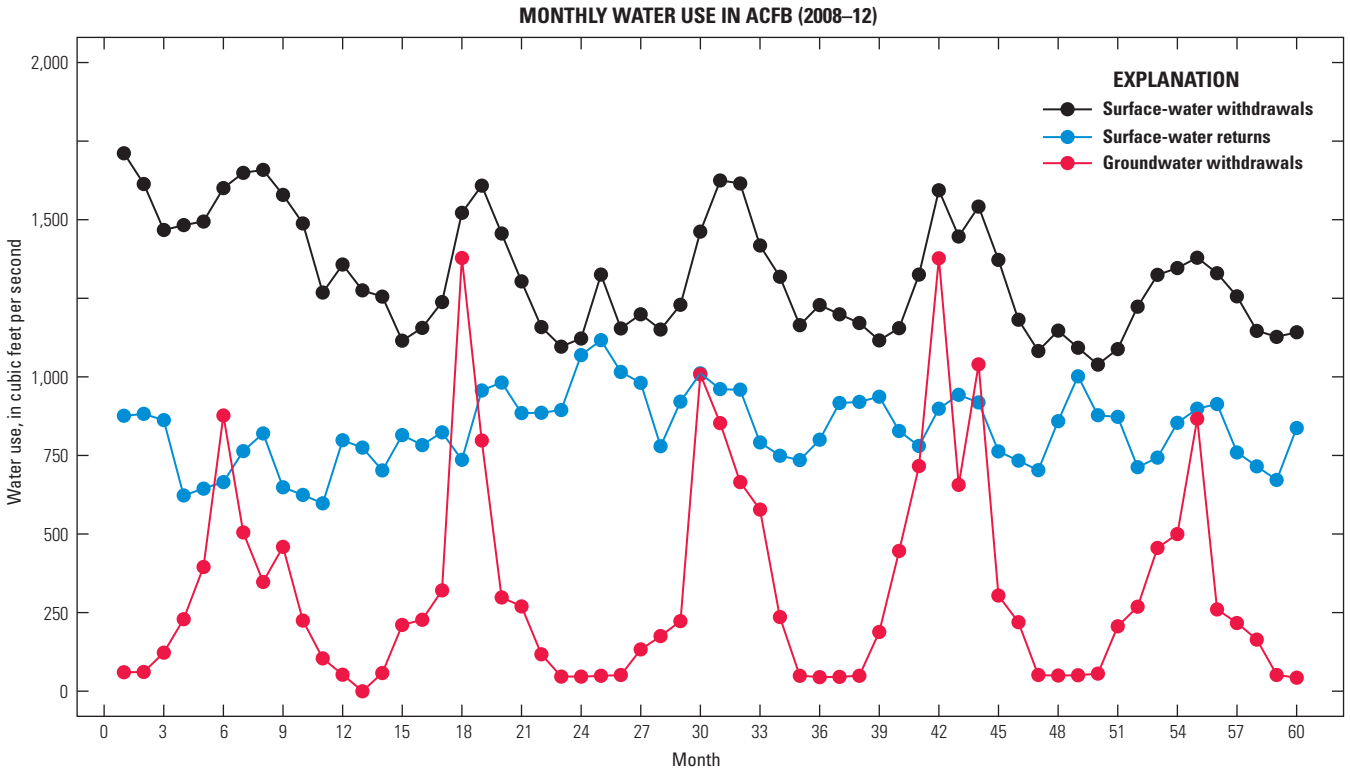

Figure 1–3. Plot of monthly surface-water withdrawals and returns, and groundwater withdrawals for the ACFB for the period 2008 to 2012.

Phase 1: Calibration of Solar Radiation and Potential Evapotranspiration

In the first phase, model parameters were calibrated to optimize the simulation of solar radiation and potential evapotranspiration (table 1–6). A surrogate for measured solar radiation calibration data consisted of mean monthly values developed by the National Renewable Energy Laboratory (http://www.nrel.gov/gis/data_solar.html, accessed August 7, 2014). Surrogate measured potential evapotranspiration data consisted of mean monthly values developed by Farnsworth and Thompson (1982). The parameter calibration objective functions targeted minimization of the absolute difference between simulated and measured solar radiation and potential evapotranspiration on a mean monthly time step (eq. 1–1). Once calibrated, the new parameter values for these nine subregions were merged into the basinwide PRMS parameter file.

$$AbsDiff = \sum_{m=1}^{12} abs\left(SIM_m - MSD_m\right), \tag{1–1}$$

where

$AbsDiff$ is the absolute difference objective function,
m is the month,
MSD_m are the mean monthly measured values of either SR or PET, and
SIM_m are the mean monthly simulated values of either SR or PET.

Phase 2: Calibration of Streamflow Volume and Timing

In the first phase, model parameters were calibrated to optimize the simulation of streamflow volume and timing to measured USGS streamflow data (table 1–6). During this phase, parameters adjusted to match measured streamflow volume were optimized for (1) annual, (2) monthly, and (3) mean monthly time steps. Parameters adjusted to match streamflow timing for high, low, and all flows were optimized at the daily time step. The objective functions for this phase of calibration minimized the

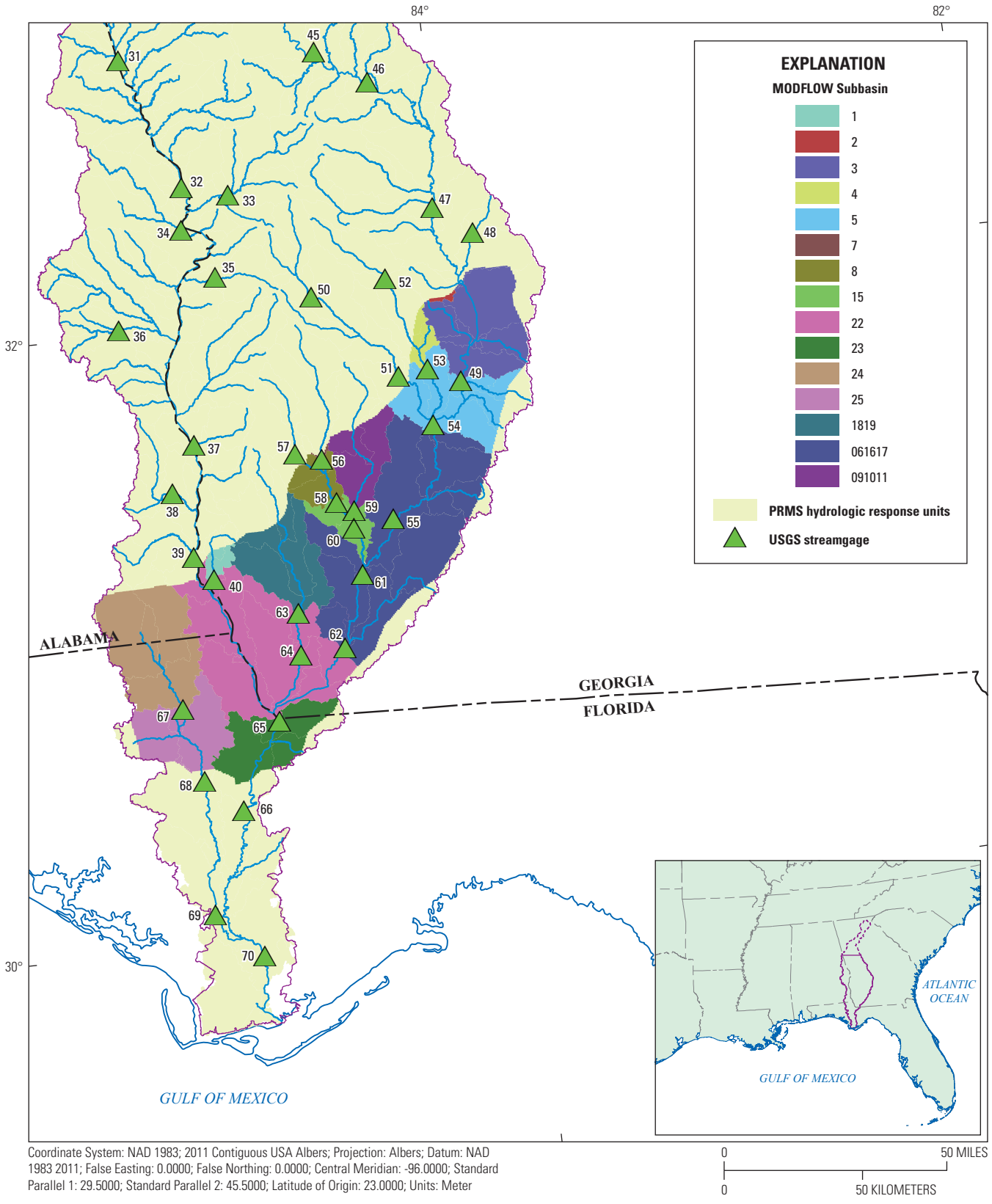

Figure 1–4. Spatial overlay of PRMS HRUs and MODFLOW zone budgets.

Table 1–5. The five most sensitive PRMS model parameters, and fraction of total sensitivity, for eight hydrologic processes and three objective functions for the Apalachicola-Chattahoochee-Flint River Basin.

[From Markstrom and others, 2016. The fraction of total sensitivity is the percentage of the total sensitivity that the five most sensitive parameters, for all hydrologic response units in the ACFB, represent. See Markstrom and others, 2015, for a full description of the PRMS parameters. CV, coefficient of variation; AR1, autoregressive lag 1 correlation coefficient; —, not computed]

Process	Performance statistic		
	Mean	CV	AR1
Evapotranspiration	jh_coef	jh_coef	jh_coef
	soil_moist_max	radmax	radmax
	radmax	soil_moist_max	dday_intcp
	dday_intcp	dday_intcp	dday_slope
	dday_slope	dday_slope	soil_moist_max
fraction of total sensitivity	0.89	0.97	0.94
Runoff	jh_coef	gwflow_coef	slowcoef_sq
	soil_moist_max	soil_moist_max	soil_moist_max
	radmax	fastcoef_lin	carea_max
	dday_intcp	pref_flow_den	gwflow_coef
	dday_slope	jh_coef	soil2gw_max
fraction of total sensitivity	0.89	0.96	0.94
Soil moisture	soil_moist_max	jh_coef	soil_moist_max
	jh_coef	soil_moist_max	jh_coef
	radmax	radmax	dday_intcp
	dday_intcp	dday_intcp	radmax
	dday_slope	dday_slope	jh_coef_hru
fraction of total sensitivity	0.95	0.90	0.96
Infiltration	srain_intcp	srain_intcp	srain_intcp
	carea_max	carea_max	carea_max
	soil_moist_max	smidx_exp	smidx_exp
	smidx_coef	jh_coef	soil_moist_max
	smidx_exp	smidx_coef	jh_coef
fraction of total sensitivity	0.89	0.92	0.96
Surface runoff	jh_coef	carea_max	soil_moist_max
	carea_max	srain_intcp	carea_max
	soil_moist_max	jh_coef	srain_intcp
	smidx_exp	smidx_exp	smidx_exp
	smidx_coef	smidx_coef	jh_coef
fraction of total sensitivity	0.86	0.94	0.96
Baseflow	jh_coef	gwflow_coef	gwflow_coef
	soil_moist_max	soil_moist_max	soil_moist_max
	radmax	smidx_coef	carea_max
	dday_intcp	soil2gw_max	soil2gw_max
	soil2gw_max	srain_intcp	smidx_exp
fraction of total sensitivity	0.82	0.87	0.85
Interflow	soil_moist_max	fastcoef_lin	soil_moist_max
	jh_coef	soil_moist_max	carea_max
	pref_flow_den	carea_max	fastcoef_lin
	soil2gw_max	pref_flow_den	slowcoef_sq
	carea_max	jh_coef	smidx_exp
fraction of total sensitivity	0.86	0.77	0.88
Snowmelt	tmax_allsnow	—	—
	tmax_allrain	—	—
	ssr2gw_rate	—	—
	srain_intcp	—	—
	adjmix_rain	—	—
fraction of total sensitivity	0.98	—	—

Table 1–6. Calibration procedure using the Luca software.

[Hay and others, 2006; Hay and Umemoto, 2006]

Calibration dataset (model state)	Objective function(s)	Parameters used to calibrate model state	Parameter range		Parameter description
		Phase 1			
		Step 1 - Solar radiation			
Basin mean monthly solar radiation (SR)	Absolute difference	dday_intcp	–60	10	Intercept in temperature degree-day relation
		dday_slope	0.2	0.9	Slope in temperature degree-day relation
		tmax_index	50	90	Index temperature used to determine precipitation adjustments to solar radiation, units specified by tmax_index parameter
		Step 2 - Potential evapotranspiration			
Basin mean monthly potential evapotranspiration (PET)	Absolute difference	jh_coef	0.005	0.09	Coefficient used in Jensen-Haise PET computations
		Phase 2			
		Step 1 - Annual and monthly water balance			
Water balance	Normalized root mean square error: 1. Annual mean 2. Monthly mean 3. Mean monthly	adjust_rain	–0.4	0.4	Precipitation adjustment factor for rain days (adjust_rain is for use with the xyz_dist module and rain_cbh_adj is for use with the climate_hru module)
		rain_cbh_adj	0.6	1.4	
		soil_moist_max	4	15	Maximum available water holding capacity of soil profile, inches
		soil2gw_max	0.0001	5	Maximum rate of soil water excess moving to groundwater, inches
		soil_rechr_max_frac	0.0001	1	Maximum available water holding capacity for soil recharge zone, fraction
		Step 2 - Daily timing high flows			
Daily streamflow timing	Normalized root mean square error: 1. Daily time step	carea_max	0.01	0.8	Maximum area contributing to surface runoff, as fraction of HRU area
		fastcoef_lin	0.0001	0.4	Linear preferential-flow routing coefficient
		pref_flow_den	0	0.2	Preferential flow pore density
		smidx_coef	0.0001	0.2	Coefficient in nonlinear surface runoff contribution area algorithm
		smidx_exp	0.2	0.8	Exponent in nonlinear surface runoff contribution area algorithm
		slowcoef_sq	0.05	0.3	Coefficient to route gravity-flow storage down slope
		Step 3 - Daily timing low flows			
Daily streamflow timing	Normalized root mean square error: 1. Daily time step	gwflow_coef	0.004	0.08	Groundwater routing coefficient
		ssr2gw_exp	0.2	3	Coefficient in equation used to route water from the subsurface reservoirs to the groundwater reservoirs
		Step 4 - Daily timing all flows			
Daily streamflow timing	Normalized root mean square error: 1. Daily time step	K_coef	0.01	23.9	Muskingum storage coefficient
		x_coef	0.05	0.25	Muskingum routing weighting factor

ratio of the root mean square error to the standard deviation of the measured streamflow (*RSR*; Moriasi and others, 2007) between measured and simulated streamflow as follows:

$$RSR = \frac{\sqrt{\sum_{n=1}^{nstep}\left(SIM_n - MSD_n\right)^2}}{\sqrt{\sum_{n=1}^{nstep}\left(MSD_n - MN\right)^2}}, \qquad (1–2)$$

where

n is the time step,
$nstep$ is the total number of time steps,
MSD_n are the measured streamflow values,
SIM_n are the simulated streamflow values, and
MN is the mean of all measured streamflow values for the objective function time period.

For regions of the ACFB where the main-stem streamflow is affected by flow regulation, at dams in particular, parameters for model HRUs and stream segments were adjusted according to the calibration of adjacent tributary streamgages. This methodology resulted in parameterizations that are representative of local tributary processes contributing runoff to main-stem streams, as opposed to the method used by LaFontaine and others (2013) to adjust parameterizations to simulate regulated main-stem streamflows.

Additional statistics were used to assess the accuracy of the hydrologic simulations for volume and timing: the Nash-Sutcliffe Index (*NSE*; Nash and Sutcliffe, 1970; eq. 1–3) and percent bias (P_{bias}; eq. 1–4) of total volume. The *NS*E metric was calculated using the following equation:

$$NSE = 1.0 - \left[\frac{\sum_{n=1}^{nstep}\left(SIM_n - MSD_n\right)^2}{\sum_{n=1}^{nstep}\left(MSD_n - MN\right)^2}\right]. \qquad (1–3)$$

An *NSE* value of 1.0 indicated a perfect fit between the simulated and measured values, an *NSE* value of zero indicated the simulated values represented the hydrologic response as well as the mean of the measured values, and a negative *NSE* value indicated that the mean of the measured values provided a better fit than the simulated values.

The P_{bias} metric was calculated as follows:

$$P_{bias} = \frac{\left(SIM_n - MSD_n\right)}{MSD_n} * 100 . \qquad (1–4)$$

A negative or positive P_{bias} value indicated an underestimation or overestimation of streamflow, respectively.

ACFB PRMS Model Calibration and Evaluation (Phase 1)

As the solar radiation and potential evapotranspiration modules of PRMS both depend on air temperature inputs, which vary across the ACFB with latitude and altitude, nine subregions of the ACFB were individually calibrated (fig. 1–5). Each subregion consisted of a group of HRUs that had similar air temperature averages. Subregions were smaller in the mountainous northern part of the ACFB to account for more rapid changes in air temperature compared to the regions in the southern part of the ACFB, where the altitude changes are more gradual. Calibration results for the simulated solar radiation and potential evapotranspiration are shown in figures 1–6 and 1–7, respectively. These plots show good agreement between observed and simulated solar radiation and potential evapotranspiration for each calibration subregion and the entire ACFB for the period 1981 to 2012.

ACFB PRMS Model Calibration and Evaluation (Phase 2)

Twenty-four streamgages were used to calibrate the ACFB coarse-resolution PRMS model (table 1–3). Each of the 24 streamgages was used to calibrate a subbasin of the ACFB (fig. 1–8). Adjustments were made, using Luca software, to the model parameters in each subbasin relative to the adjustment made to the HRUs and stream segments in the calibration streamgage's catchment. So, the relative distribution of the model parameters in each subbasin was preserved as the Luca software was used to optimize the model parameters to match the measured streamflow at each calibration streamgage. The comparison within the Luca software to optimize the model parameters was between USGS measured streamflow and the PRMS variable *seg_outflow* for the PRMS model stream segment associated with the calibration streamgage. Because there were a total of 70 streamgages used for model construction, the use of only 24 streamgages for calibration left many streamgages for model evaluation. A split-period calibration strategy was used with the 24 calibration streamgages, with a subset of the available measured streamflow for the period 1981 to 2012 used for calibration and the remaining part of the record used for evaluation; see table 1–7 for a summary of the calibration and evaluation periods. The period 1997 to 2012 was used for most of the calibration streamgages because that provided a sufficient record length to keep the hydrologic model generalized and also included the period of interest for this study (2008 to 2012), a very wet year (1998), and a substantial drought period (1999–2001). Performance metrics of *NSE*, *RSR*, and P_{bias} for each calibration and evaluation streamgage are summarized in table 1–7. An *NSE* value

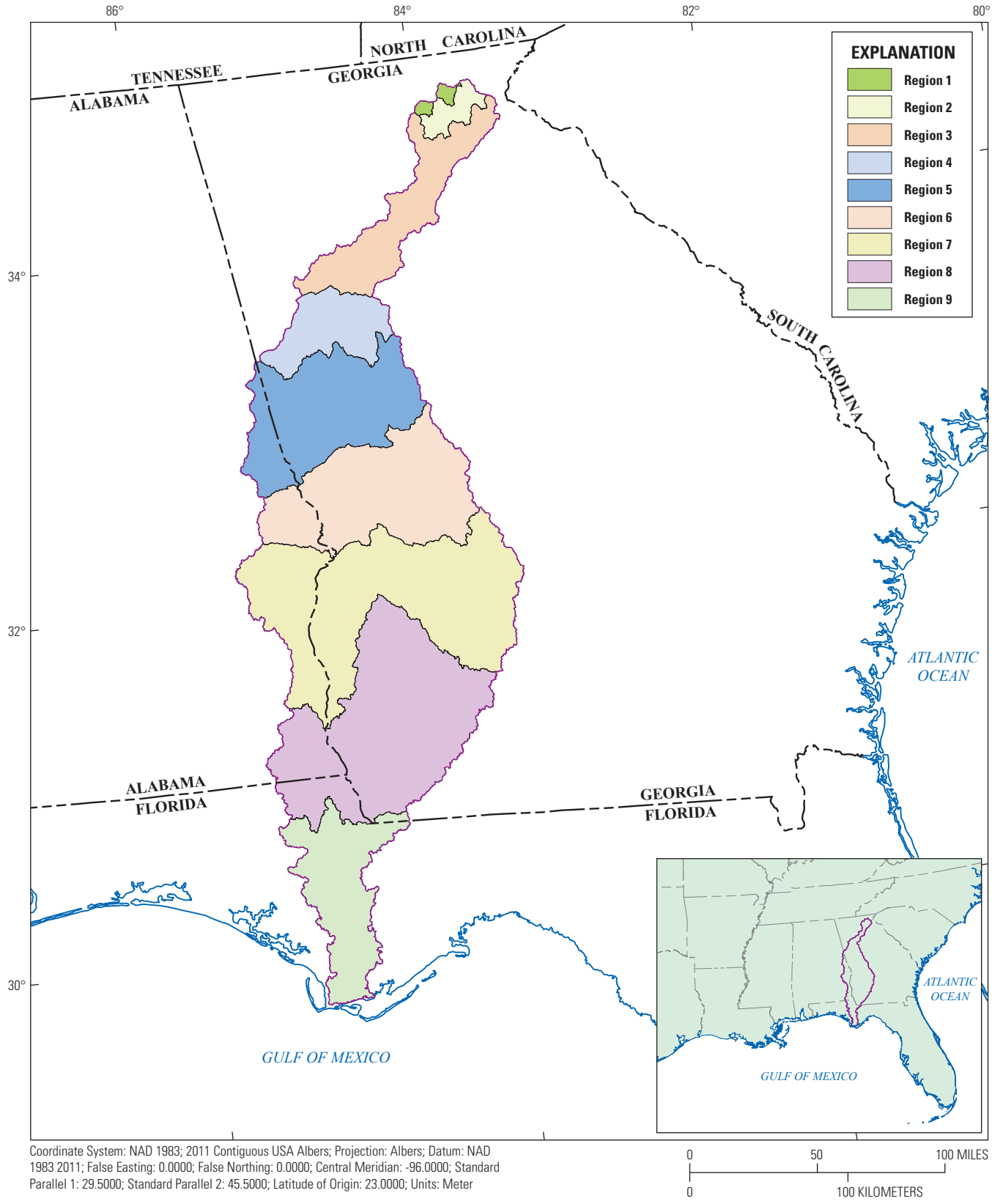

Figure 1–5. Solar radiation and potential evapotranspiration calibration regions in the ACFB.

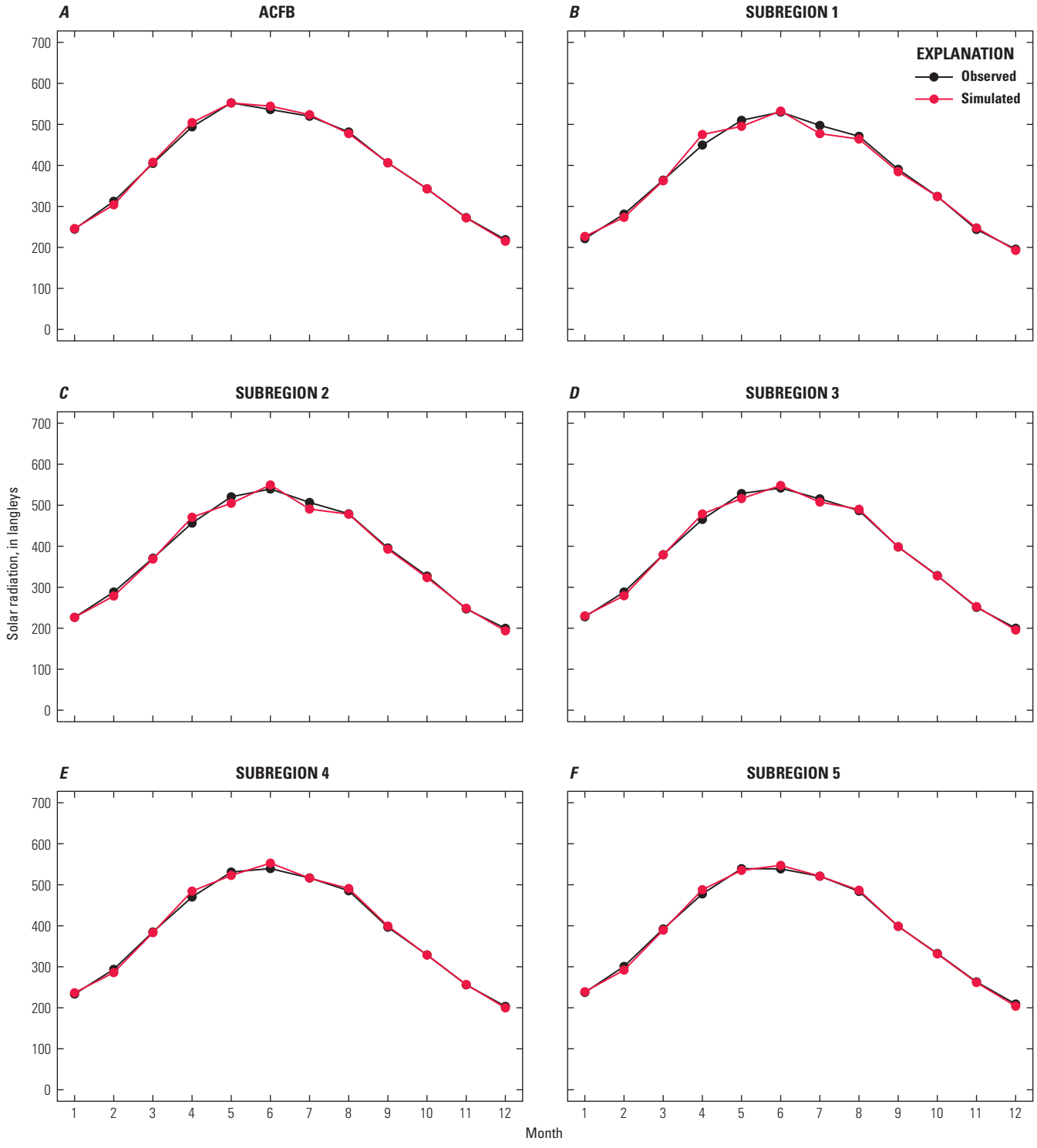

Figure 1–6. Solar radiation calibration results for the nine subregions and the ACFB.

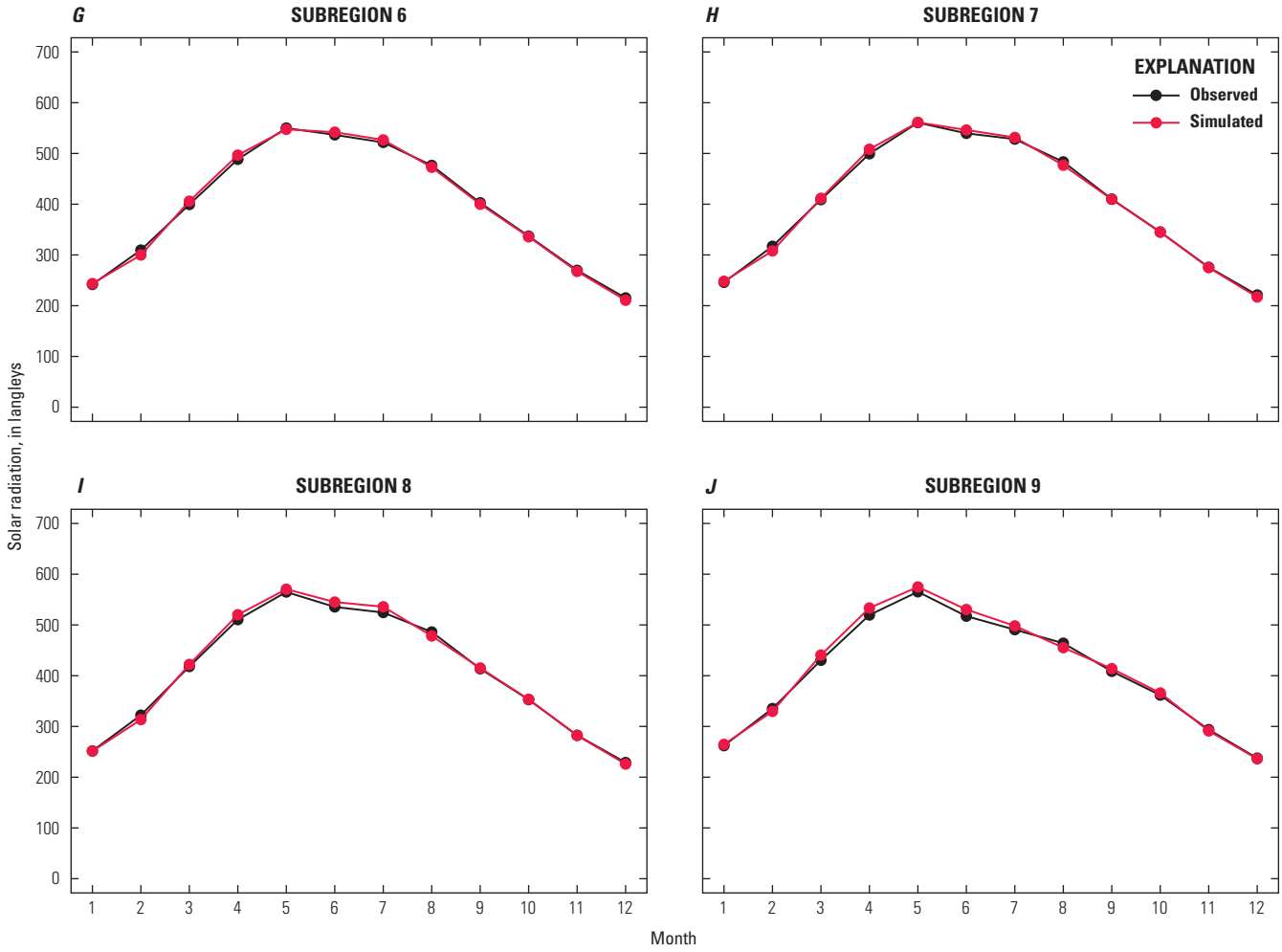

Figure 1–6.—Continued Solar radiation calibration results for the nine subregions and the ACFB.

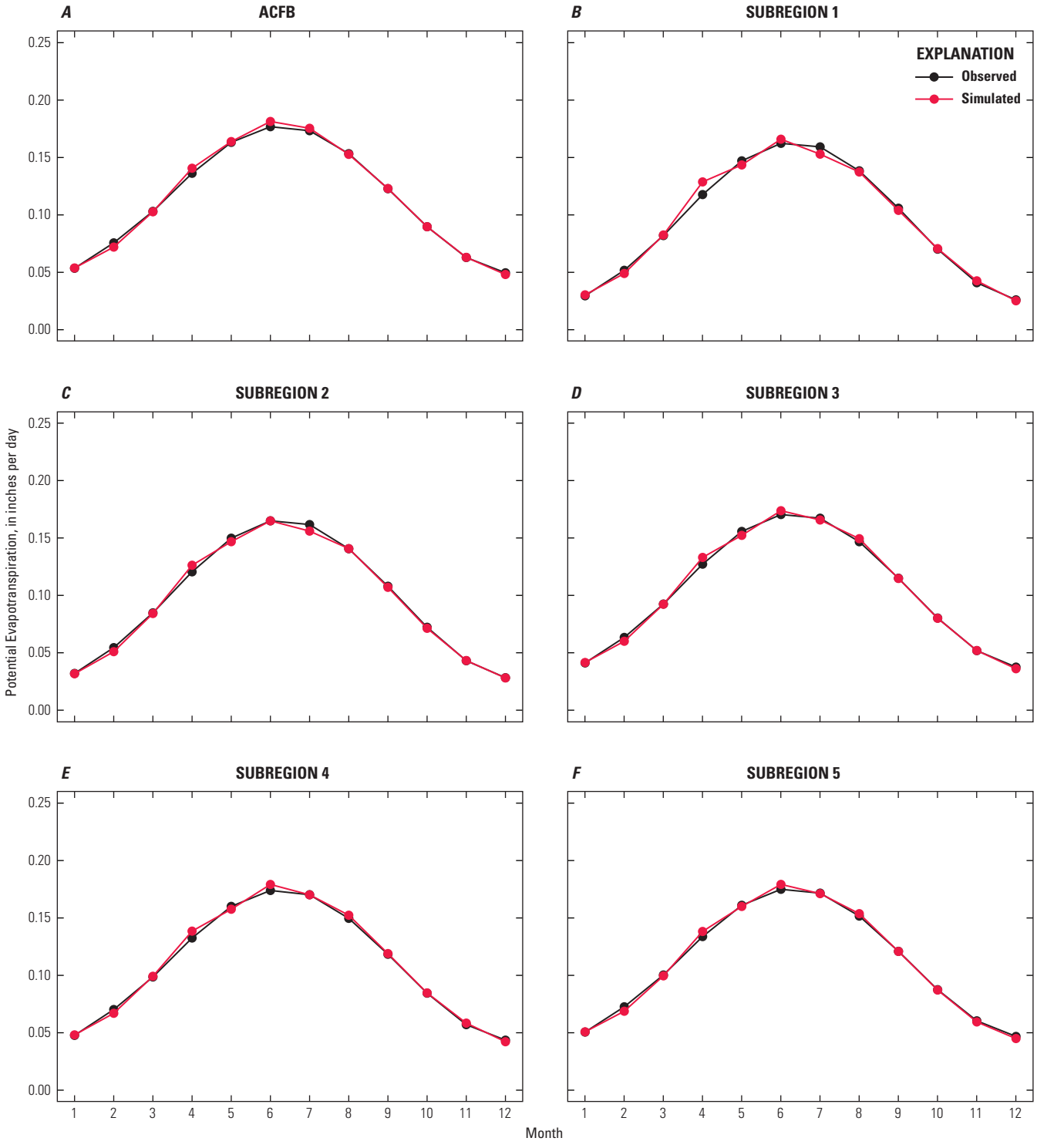

Figure 1–7. Potential evapotranspiration calibration results for the nine subregions and the ACFB.

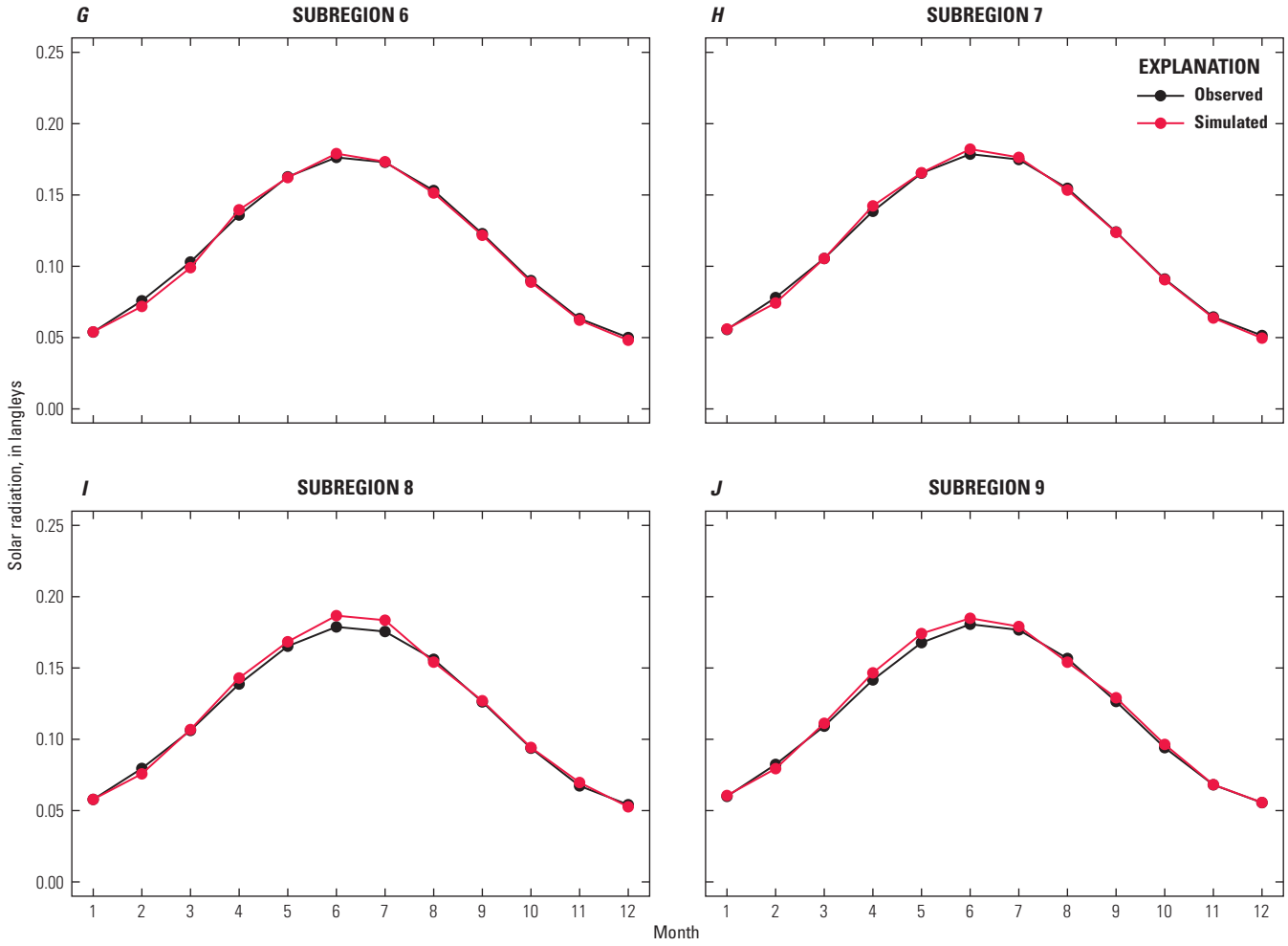

Figure 1–7.—Continued Potential evapotranspiration calibration results for the nine subregions and the ACFB.

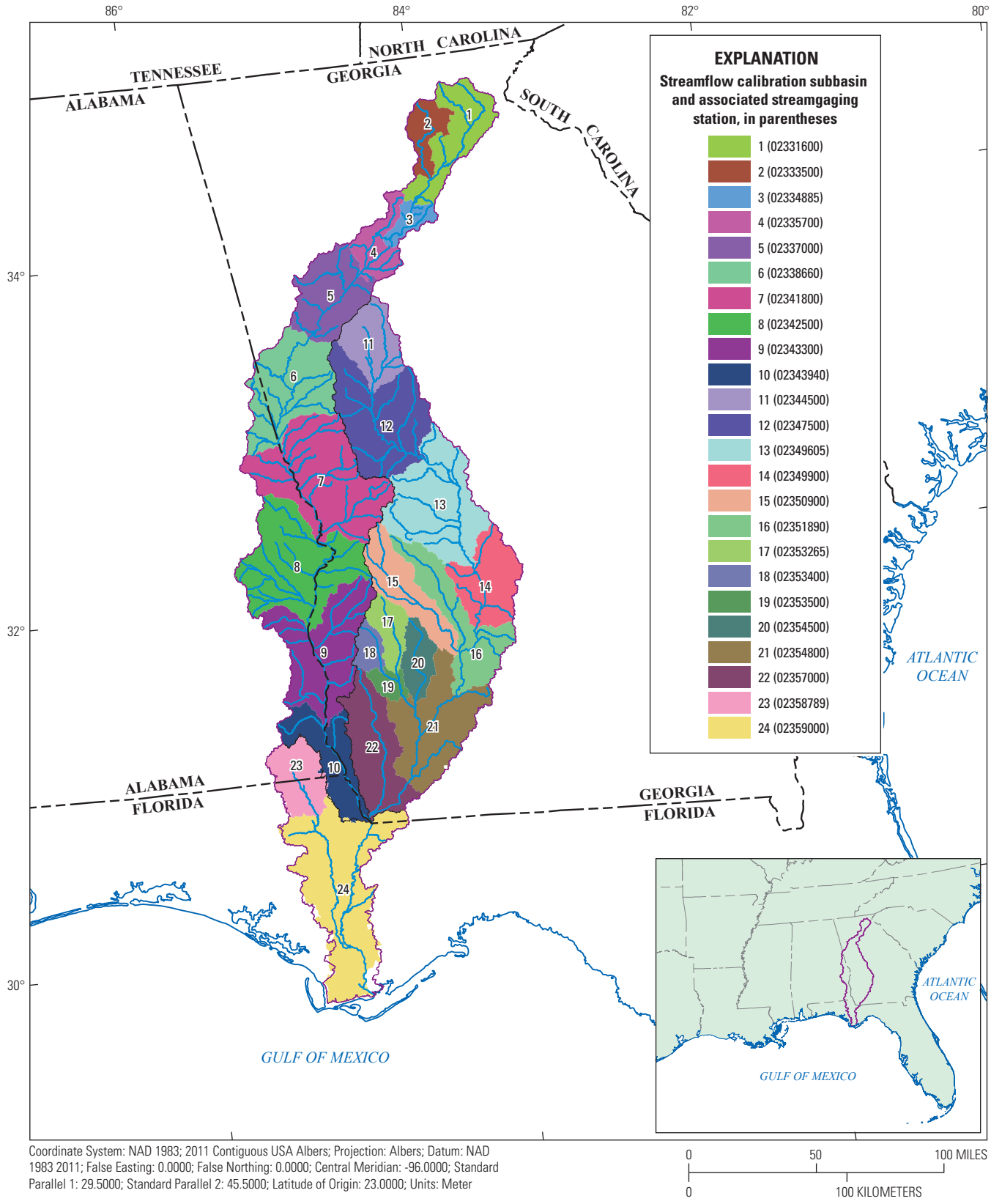

Figure 1–8. The 24 streamflow calibration regions used for the coarse-resolution ACFB model.

Table 1–7. Performance statistics of daily time step streamflow simulations for the PRMS-only Apalachicola-Chattahoochee-Flint River Basin model.

[For the Station number column: green boxes indicate "good" model performance, yellow boxes indicate "fair" model performance, orange boxes indicate "poor" model performance. For the NSE, RSR, and P_{bias} columns under the Calibration and Evaluation headings: green boxes indicate the performance metric value passed the established criteria, and orange boxes indicate that the performance metric value did not pass the established criteria. NSE, Nash-Sutcliffe model efficiency index (Nash and Sutcliffe, 1970); RSR, root-mean square error normalized to standard deviation; P_{bias}, percent bias; —, not computed; * , model drainage area substantially different from streamgage drainage area; **, streamgage affected by backwater from impoundments and diverted flows; ***, streamgage used for reservoir outflow replacement]

Count	Station number	Calibration					Evaluation				
		Start year	End year	NSE	RSR	P_{bias}	Start year	End year	NSE	RSR	P_{bias}
1	02330450	—	—	—	—	—	1982	2012	0.66	0.58	–16
2	02331000	—	—	—	—	—	2010	2012	0.79	0.46	–11
3	02331600	1997	2012	0.79	0.46	–1.5	1981	1996	0.77	0.48	–7.3
4	02333500	1997	2012	0.77	0.48	–0.4	1981	1996	0.79	0.46	–4.4
5***	02334430	—	—	—	—	—	1981	2012	1.00	0.00	0.0
6	02334480	—	—	—	—	—	2002	2012	0.27	0.86	–14
7	02334620	—	—	—	—	—	2005	2012	0.44	0.75	–2.0
8	02334885	1997	2012	0.70	0.55	–0.2	1985	1996	0.69	0.55	6.6
9	02335000	—	—	—	—	—	1981	2012	0.90	0.31	–0.8
10	02335350	—	—	—	—	—	2002	2012	0.52	0.69	11
11	02335450	—	—	—	—	—	1981	2012	0.84	0.41	3.6
12	02335700	1997	2012	0.78	0.47	0.3	1981	1996	0.72	0.53	8.7
13	02335815	—	—	—	—	—	2002	2012	0.83	0.41	3.6
14	02335870	—	—	—	—	—	1985	2012	0.45	0.74	11
15	02336000	—	—	—	—	—	1981	2012	0.84	0.40	4.4
16	02336120	—	—	—	—	—	2004	2012	0.54	0.68	17
17	02336240	—	—	—	—	—	2004	2012	0.36	0.80	24
18	02336300	—	—	—	—	—	1981	2012	0.53	0.69	28
19	02336360	—	—	—	—	—	2004	2012	0.50	0.71	17
20	02336490	—	—	—	—	—	1982	2012	0.82	0.42	1.9
21	02336635	—	—	—	—	—	1996	2012	0.43	0.76	0.3
22	02336728	—	—	—	—	—	2004	2012	0.02	0.99	53
23	02336968	—	—	—	—	—	1999	2012	0.59	0.64	22
24	02337000	1997	2012	0.70	0.55	1.8	1981	1996	0.76	0.49	–1.9
25*	02337040	—	—	—	—	—	2004	2007	0.48	0.72	–0.7
26	02337170	—	—	—	—	—	1981	2012	0.86	0.38	3.4
27	02338000	—	—	—	—	—	1981	2012	0.83	0.42	1.6
28	02338500	—	—	—	—	—	2005	2012	0.79	0.46	–1.9
29	02338523	—	—	—	—	—	2002	2012	–0.10	1.05	22
30	02338660	1997	2012	0.66	0.58	2.5	1981	1996	0.76	0.49	–17
31	02339500	—	—	—	—	—	1981	2012	0.50	0.71	–0.5
32	02341505	—	—	—	—	—	1981	2012	0.68	0.57	–0.7
33	02341800	1997	2012	0.77	0.49	–2.4	1981	1996	0.71	0.54	–20
34	02342500	1997	2012	0.80	0.45	–4.9	1981	1996	0.73	0.52	–21
35	02342850	—	—	—	—	—	2009	2012	0.38	0.79	6.1
36	02342933	—	—	—	—	—	1981	2010	0.67	0.58	22
37	023432415	—	—	—	—	—	2010	2012	0.60	0.64	12
38	02343300	1982	1992	0.53	0.69	0.2	—	—	—	—	—
39	02343801	—	—	—	—	—	1981	2012	0.64	0.60	7.8

Table 1–7. Performance statistics of daily time step streamflow simulations for the PRMS-only Apalachicola-Chattahoochee-Flint River Basin model.—Continued

[For the Station number column: green boxes indicate "good" model performance, yellow boxes indicate "fair" model performance, orange boxes indicate "poor" model performance. For the NSE, RSR, and P_{bias} columns under the Calibration and Evaluation headings: green boxes indicate the performance metric value passed the established criteria, and orange boxes indicate that the performance metric value did not pass the established criteria. NSE, Nash-Sutcliffe model efficiency index (Nash and Sutcliffe, 1970); RSR, root-mean square error normalized to standard deviation; P_{bias}, percent bias; —, not computed; * , model drainage area substantially different from streamgage drainage area; **, streamgage affected by backwater from impoundments and diverted flows; ***, streamgage used for reservoir outflow replacement]

Count	Station number	Calibration					Evaluation				
		Start year	End year	NSE	RSR	P_{bias}	Start year	End year	NSE	RSR	P_{bias}
40	02343940	2003	2012	0.58	0.65	7.0	—	—	—	—	—
41	02344350	—	—	—	—	—	1986	2012	0.75	0.50	–3.7
42	02344478	—	—	—	—	—	2005	2012	0.27	0.86	47
43	02344500	1997	2012	0.81	0.44	13.7	1981	1996	0.75	0.50	–4.6
44	02344700	—	—	—	—	—	1981	2012	0.59	0.64	–15
45	02346180	—	—	—	—	—	1981	1991	0.85	0.39	–14
46	02347500	1997	2012	0.78	0.47	0.7	1981	1996	0.78	0.47	–17
47	02349605	1997	2012	0.77	0.48	–3.2	1981	1996	0.74	0.51	–18
48	02349900	1997	2012	0.75	0.50	11.9	1981	1996	0.67	0.58	–3.5
49	02350512	—	—	—	—	—	1988	2012	0.77	0.48	–12
50	02350600	—	—	—	—	—	1988	2001	0.60	0.63	–3.7
51	02350900	1997	2012	0.82	0.42	3.2	1986	1996	0.75	0.50	–1.3
52	02351500	—	—	—	—	—	2002	2012	0.56	0.67	–2.0
53	02351890	1997	2012	0.82	0.43	2.5	1981	1996	0.50	0.71	–7.0
54	02352500	—	—	—	—	—	1981	2012	0.84	0.41	–5.1
55	02353000	—	—	—	—	—	1981	2012	0.82	0.43	–6.7
56	02353265	2003	2012	0.78	0.47	3.2	—	—	—	—	—
57	02353400	1997	2012	0.69	0.56	5.7	1989	1996	0.79	0.46	–12
58	02353500	1997	2012	0.77	0.48	15.8	1981	1996	0.74	0.51	0.9
59	02354500	1997	2012	0.67	0.57	–12.7	—	—	—	—	—
60	02354800	1997	2012	0.79	0.45	12.2	—	—	—	—	—
61	02355662	—	—	—	—	—	2003	2012	0.82	0.42	0.4
62	02356000	—	—	—	—	—	2002	2012	0.74	0.51	0.8
63	02357000	1997	2012	0.62	0.62	30.1	1983	1996	0.69	0.55	18
64**	02357150	—	—	—	—	—	1999	2012	–1.40	1.55	48
65	02358000	—	—	—	—	—	1981	2012	0.73	0.52	–2.7
66	02358700	—	—	—	—	—	1981	2012	0.64	0.60	-0.8
67	02358789	2001	2012	0.68	0.56	–3.4	—	—	—	—	—
68	02359000	1997	2012	0.74	0.51	–8.8	1981	1996	0.74	0.51	–14
69**	02359051	—	—	—	—	—	1999	2008	–1.50	1.58	–71
70	02359170	—	—	—	—	—	1981	2012	0.61	0.63	–3.9

of 0.5 or greater was defined as the passing performance threshold. The passing performance thresholds for the *RSR* and P_{bias} metrics were less than 0.7 and between plus or minus 10.0, respectively.

Simulations at each streamgage location were evaluated on the basis of how many performance metrics were within the acceptable criteria. A calibration streamgage location that had both a calibration and evaluation period was rated "good" if five or six of the criteria (*NSE*, *RSR*, and P_{bias}, for both periods) were passing or acceptable, "fair" if three or four of the criteria were acceptable, and "poor" if less than three of the criteria were acceptable. An evaluation-only streamgage location was rated "good" if all three of the criteria (*NSE, RSR*, and P_{bias}) were acceptable, "fair" if only two of the criteria were acceptable, and "poor" if less than two of the criteria were acceptable. A summary of simulation performance for all streamgage locations, calibration locations, and evaluation locations is shown in table 1–8. The evaluation results show that 21 of the 24 calibration locations were rated "good" while only 21 of the 46 evaluation locations were rated "good."

Table 1–8. Summary of daily time step performance statistics for the PRMS-only simulations.

Rating	All	Calibration	Evaluation
Total	70	24	46
Good	42	21	21
Fair	15	3	12
Poor	13	0	13

ACFB PRMS-MODFLOW Model Evaluation

Monthly time step hydrologic simulations of water-use-affected flows were developed for both a PRMS-only case and a coupled PRMS-MODFLOW case for the period 2008–12. The PRMS-only case incorporated both monthly time step surface-water withdrawals and returns, and groundwater withdrawals in the ACFB PRMS model. The coupled PRMS-MODFLOW simulation incorporated monthly surface-water withdrawals and returns, daily PRMS surface runoff and shallow subsurface runoff, and monthly MODFLOW groundwater flows. The groundwater withdrawals were excluded from the coupled simulation because they were already included in the MODFLOW simulation. The two simulations were evaluated using the *NSE*, *RSR*, and P_{bias} metrics for the 60-month simulation period; a minimum of 24 monthly values were required for evaluation.

The PRMS-only simulations were evaluated at 67 of the 70 streamgage locations (23 calibration locations, and 44 evaluation locations); the three remaining locations did not have measured streamflow for the period 2008–12. The results for these simulations are shown in table 1–9. The same ranking criteria were used for these evaluations as for the initial PRMS calibration; a "good" rating for streamgages that had acceptable values of all three metrics, a "fair" rating for streamgages that had two acceptable metric values, and a "poor" rating for streamgages that had one or zero acceptable metric values. For the 67 streamgage locations evaluated, 16 were rated "good," 39 were rated "fair," and 12 were rated "poor." This evaluation is a substantial decrease from the full time period (1981–2012) evaluations that showed a total of 42 streamgage locations were rated "good" (table 1–8). This result is not surprising because the model was calibrated for a much longer time period to capture the natural variability in climatic forcings so that the hydrologic model would be generalizable. The tradeoff is that any short time period within the simulation may not perform as well as the entire simulation period.

The coupled PRMS-MODFLOW simulations were evaluated at 18 of the 19 streamgage locations that had at least some overlap with the MODFLOW domain (9 calibration locations, and 9 evaluation locations; table 1–9). One evaluation location was excluded because that streamgage location did not have measured streamflow for the period 2008–12. The evaluation criteria resulted in six locations rated "good," eleven locations rated "fair," and one location rated "poor" (table 1–10). The measures of *NSE* and *RSR* metrics for the coupled simulations compared to the PRMS-only simulations were improved for eight and seven streamgage locations, respectively, were worse for seven locations, and remained the same for three and four locations, respectively. Measures of P_{bias} at the 18 locations were improved with the coupled simulations for 13 of the locations and were worse for 4 locations, and were the same at one location. The streamgage location rated "poor" is on the lower reach of Spring Creek (USGS station 02357150) and is affected by backwater from Lake Seminole. The P_{bias} for this location, however, still decreased from +54 percent for the PRMS-only simulation to +24 percent for the coupled simulation. In general, these results suggest that the coupled methodology may provide more accurate simulations at the monthly time step for much of this geologically complex, groundwater-dominated region of the ACFB.

Table 1–9. Performance statistics of the monthly time step streamflow simulations of the PRMS-only and coupled PRMS-MODFLOW Apalachicola-Chattahoochee-Flint River Basin models for the period 2008–12.

[For the NSE, RSR, and P_{bias} columns under the PRMS-only and PRMS-MODFLOW coupled headings: green boxes indicate the performance metric value passed the established criteria, and orange boxes indicate that the performance metric value did not pass the established criteria. NSE, Nash-Sutcliffe model efficiency index (Nash and Sutcliffe, 1970); RSR, Normalized root mean square error; P_{bias}, percent bias; PRMS, Precipitation-Runoff Modeling System; Months, number of months of data available for period 2008–12; —, not computed; * , model drainage area substantially different from streamgage drainage area; **, streamgage affected by backwater from impoundments and diverted flows; ***, streamgage affected by reservoir management; ****, streamgage does not have at least 2 years of observed streamflow for period 2008–12; C, Calibration streamgage; E, Evaluation streamgage]

Count	Station number	Point of interest type	Months	PRMS-only			PRMS-MODFLOW coupled		
				NSE	RSR	P_{bias}	NSE	RSR	P_{bias}
1	02330450	E	60	0.82	0.43	–14.4	—	—	—
2	02331000	E	51	0.90	0.31	–9.3	—	—	—
3	02331600	C	60	0.94	0.24	3.0	—	—	—
4	02333500	C	60	0.92	0.28	2.9	—	—	—
5***	02334430	E	60	–0.34	1.16	32.9	—	—	—
6	02334480	E	60	0.68	0.57	–0.8	—	—	—
7	02334620	E	60	0.84	0.40	1.1	—	—	—
8	02334885	C	60	0.91	0.30	2.1	—	—	—
9***	02335000	E	60	–0.20	1.10	29.8	—	—	—
10	02335350	E	60	0.74	0.51	12.7	—	—	—
11***	02335450	E	60	0.10	0.95	25.4	—	—	—
12	02335700	C	60	0.90	0.31	8.8	—	—	—
13***	02335815	E	60	–0.12	1.06	29.5	—	—	—
14	02335870	E	60	0.82	0.43	26.5	—	—	—
15***	02336000	E	60	0.30	0.84	19.4	—	—	—
16	02336120	E	60	0.75	0.50	23.0	—	—	—
17	02336240	E	60	0.61	0.62	35.4	—	—	—
18	02336300	E	60	0.37	0.79	53.8	—	—	—
19	02336360	E	60	0.74	0.51	37.8	—	—	—
20***	02336490	E	60	0.39	0.78	18.7	—	—	—
21	02336635	E	60	0.88	0.34	7.7	—	—	—
22	02336728	E	60	–1.09	1.45	73.0	—	—	—
23	02336968	E	60	0.78	0.47	29.9	—	—	—
24	02337000	C	60	0.82	0.42	10.3	—	—	—
25*	02337040	E	47	–0.44	1.20	82.3	—	—	—
26	02337170	E	60	0.48	0.72	24.2	—	—	—
27***	02338000	E	60	0.61	0.63	19.9	—	—	—
28	02338500	E	60	0.73	0.52	13.5	—	—	—
29	02338523	E	60	0.72	0.53	23.4	—	—	—
30	02338660	C	60	0.78	0.47	32.1	—	—	—
31***	02339500	E	60	0.69	0.56	18.1	—	—	—
32***	02341505	E	60	0.70	0.55	24.6	—	—	—
33	02341800	C	60	0.89	0.33	14.0	—	—	—
34	02342500	C	60	0.89	0.33	–5.9	—	—	—
35	02342850	E	55	0.84	0.40	–0.3	—	—	—
36	02342933	E	45	0.85	0.39	3.4	—	—	—
37***	023432415	E	42	0.88	0.34	14.8	—	—	—
38***	02343300	C	0	—	—	—	—	—	—

Table 1–9. Performance statistics of the monthly time step streamflow simulations of the PRMS-only and coupled PRMS-MODFLOW Apalachicola-Chattahoochee-Flint River Basin models for the period 2008–12.—Continued

[For the NSE, RSR, and P_{bias} columns under the PRMS-only and PRMS-MODFLOW coupled headings: green boxes indicate the performance metric value passed the established criteria, and orange boxes indicate that the performance metric value did not pass the established criteria. NSE, Nash-Sutcliffe model efficiency index (Nash and Sutcliffe, 1970); RSR, Normalized root mean square error; P_{bias}, percent bias; PRMS, Precipitation-Runoff Modeling System; Months, number of months of data available for period 2008–12; —, not computed; * , model drainage area substantially different from streamgage drainage area; **, streamgage affected by backwater from impoundments and diverted flows; ***, streamgage affected by reservoir management; ****, streamgage does not have at least 2 years of observed streamflow for period 2008–12; C, Calibration streamgage; E, Evaluation streamgage]

Count	Station number	Point of interest type	Months	PRMS-only			PRMS-MODFLOW coupled		
				NSE	RSR	P_{bias}	NSE	RSR	P_{bias}
39***	02343801	E	60	0.83	0.42	25.2	—	—	—
40	02343940	C	60	0.75	0.50	13.0	0.69	0.56	–16.8
41	02344350	E	60	0.88	0.35	15.7	—	—	—
42	02344478	E	60	0.24	0.87	62.4	—	—	—
43	02344500	C	60	0.84	0.40	23.6	—	—	—
44	02344700	E	60	0.79	0.46	18.0	—	—	—
45****	02346180	E	0	-	-	-	—	—	—
46	02347500	C	60	0.89	0.33	18.1	—	—	—
47	02349605	C	60	0.90	0.31	9.7	—	—	—
48	02349900	C	60	0.81	0.44	33.7	—	—	—
49	02350512	E	60	0.92	0.28	8.2	0.92	0.28	6.9
50	02350600	E	39	0.88	0.35	14.8	—	—	—
51	02350900	C	60	0.91	0.30	10.6	—	—	—
52	02351500	E	60	0.78	0.47	7.2	—	—	—
53	02351890	C	60	0.91	0.30	15.1	0.92	0.29	13.1
54	02352500	E	60	0.90	0.31	16.8	0.91	0.31	15.9
55	02353000	E	60	0.89	0.33	12.9	0.89	0.33	11.8
56	02353265	C	60	0.91	0.31	7.1	0.91	0.31	7.1
57	02353400	C	60	0.83	0.42	11.9	—	—	—
58	02353500	C	60	0.84	0.40	21.7	0.86	0.37	16.9
59	02354500	C	60	0.78	0.47	–4.9	0.69	0.56	–22.4
60	02354800	C	60	0.86	0.37	15.7	0.84	0.40	5.8
61	02355662	E	60	0.90	0.32	9.9	0.89	0.33	7.3
62	02356000	E	60	0.87	0.36	10.7	0.88	0.35	6.7
63	02357000	C	60	0.68	0.57	40.1	0.64	0.60	12.5
64**	02357150	E	54	–3.01	2.00	53.9	–1.49	1.58	23.7
65***	02358000	E	60	0.88	0.34	15.6	0.89	0.33	11.8
66***	02358700	E	60	0.85	0.38	17.7	0.87	0.37	13.6
67	02358789	C	60	0.80	0.45	–4.6	0.72	0.53	–14.4
68	02359000	C	60	0.82	0.43	–2.3	0.71	0.53	–3.4
69**,****	02359051	E	21	—	—	—	—	—	—
70***	02359170	E	60	0.71	0.53	23.0	0.73	0.52	19.1

Table 1–10. Summary of monthly time step performance statistics for the PRMS-only and coupled PRMS-MODFLOW simulations for the period 2008–12.

	PRMS-only (entire ACFB)			PRMS-only (MODFLOW domain)			PRMS-MODFLOW coupled		
	All	Calibration	Evaluation	All	Calibration	Evaluation	All	Calibration	Evaluation
Total	70	24	46	19	9	10	19	9	10
Good	16	9	7	6	4	2	6	3	3
Fair	39	14	25	11	5	6	11	6	5
Poor	12	0	12	1	0	1	1	0	1
Not evaluated	3	1	2	1	0	1	1	0	1

References Cited

Blodgett, D.L., Booth, N.L., Kunicki, T.C., Walker, J.I., and Viger, R.J., 2011, Description and testing of the Geo Data Portal—A data integration framework and web processing services for environmental science collaboration: U.S. Geological Survey Open-File Report 2011–1157, 9 p., accessed March 2, 2017, at https://pubs.usgs.gov/of/2011/1157.

Clarke, J.S., and Painter, J.A., 2014, Influence of septic systems on stream base flow in the Apalachicola-Chattahoochee-Flint River Basin near Metropolitan Atlanta, Georgia, 2012: U.S. Geological Survey Scientific Investigations Report 2014–5144, 68 p., accessed December 16, 2015, at https://doi.org/10.3133/sir20145144.

Couch, C.A., Hopkins, E.H., and Hardy, S.P., 2010, Influences of environmental settings on aquatic ecosystems in the Apalachicola-Chattahoochee-Flint River Basin: U.S. Geological Survey Water-Resources Investigations Report 95–4278, 58 p., accessed September 27, 2016, at https://pubs.usgs.gov/wri/wrir95-4278/.

Cukier, R.I., Fortuin, C.M., and Shuler, K.E., 1973, Study of the sensitivity of coupled reaction systems to uncertainties in rate coefficients, I. Theory: The Journal of Chemical Physics, v. 59, no. 8, p. 3873–3878, accessed March 8, 2017, at https://doi.org/10.1063/1.1680571.

Cukier, R.I., Schaibly, J.H., and Shuler, K.E., 1975, Study of the sensitivity of coupled reaction systems to uncertainties in rate coefficients, III. Analysis of the approximations: The Journal of Chemical Physics, v. 63, no. 3, p. 1140–1149, accessed March 8, 2017, at https://doi.org/10.1063/1.431440.

Duan, Qingyun, Sorooshian, Soroosh, and Gupta, Vijai, 1992, Effective and efficient global optimization for conceptual rainfall-runoff models: Water Resources Research, v. 28, no. 4, p. 1015–1031, accessed September 2, 2009, at https://doi.org/10.1029/91WR02985.

Duan, Qingyun, Sorooshian, Soroosh, and Gupta, V.K., 1994, Optimal use of the SCE-UA global optimization method for calibrating watershed models: Journal of Hydrology, v. 158, p. 265–284, accessed September 2, 2009, at http://doi.org/10.1016/0022-1694(94)90057-4.

Farnsworth, R.K., and Thompson, E.S., 1982, Mean monthly, seasonal, and annual pan evaporation for the United States: National Oceanic and Atmospheric Administration Technical Report, NWS 34, 82 p.

Florida Department of Environmental Protection, 2011, Florida reuse inventory database and annual report: Florida Department of Environmental Protection, accessed January 20, 2015, at http://www.dep.state.fl.us/water/reuse/inventory.htm.

Gleeson, T., Smith, L., Moosdorf, N., Hartmann, J., Durr, H.H., Manning, A.H., van Beek, L.P.H., and Jellinek, A.M., 2011, Mapping permeability over the surface of the Earth: Geophysical Research Letters, v. 38, L. 02401, 6 p.

Hay, L.E., Leavesley, G.H., Clark, M.P., Markstrom, S.L., Viger, R.J., and Umemoto, M., 2006, Step wise, multiple objective calibration of a hydrologic model for a snowmelt dominated basin: Journal of the American Water Resources Association, v. 42, no. 4, p. 877–890.

Hay, L.E., and Umemoto, M., 2006, Multiple-objective stepwise calibration using Luca: U.S. Geological Survey Open-File Report 2006–1323, 28 p.

Homer, C., Dewitz, J., Fry, J., Coan, M., Hossain, N., Larson, C., Herold, N., McKerrow, A., VanDriel, J.N., and Wickham, J., 2007, Completion of the 2001 National Land Cover Database for the conterminous United States: Photogrammetric Engineering & Remote Sensing, v. 73, no. 4, p. 337–341.

Jones, L.E., Painter, Jaime, LaFontaine, Jacob, Sepulveda, Nicasio, and Sifuentes, Dorothy, 2017, Groundwater-flow budget for the lower Apalachicola-Chattahoochee-Flint River Basin in southwestern Georgia and parts of Florida and Alabama, 2008–12: U.S. Geological Survey Scientific Investigations Report 2017–5141, 76 p., accessed December 29, 2017, at https://doi.org/10.3133/sir20175141.

LaFontaine, J.H., Hay, L.E., Viger, R.J., Markstrom, S.L., Regan, R.S., Elliott, C.M., and Jones, J.W., 2013, Application of the Precipitation-Runoff Modeling System (PRMS) in the Apalachicola-Chattahoochee-Flint River Basin in the Southeastern United States: U.S. Geological Survey Scientific Investigations Report 2013–5162, 118 p., accessed September 27, 2016, at https://pubs.usgs.gov/sir/2013/5162/.

LaFontaine, J.H., Jones, L.E., and Painter, J.A., 2017, Model input and output for hydrologic simulations of the Apalachicola-Chattahoochee-Flint River Basin using the Precipitation-Runoff Modeling System: U.S. Geological Survey data release, https://doi.org/10.5066/F7FJ2F1R.

Lawrence, S.J., 2016, Water use in the Apalachicola-Chattahoochee-Flint River Basin, Alabama, Florida, and Georgia, 2010, and water-use trends, 1985–2010: U.S. Geological Survey Scientific Investigations Report 2016–5007, 72 p., accessed October 19, 2016, at https://doi.org/10.3133/sir20165007.

Leavesley, G.H., Lichty, R.W., Troutman, B.M., and Saindon, L.G., 1983, Precipitation-runoff modeling system—User's manual: U.S. Geological Survey Water-Resources Investigations Report 83–4238, 207 p., accessed April 26, 2017, at https://pubs.usgs.gov/wri/1983/4238/report.pdf.

Marella, R.L., 2014, Water withdrawals, use, and trends in Florida, 2010: U.S. Geological Survey Scientific Investigations Report 2014–5088, 59 p., accessed February 16, 2017, at https://doi.org/10.3133/sir20145088.

Marella, R.L., and Dixon, J.F., 2015, Agricultural irrigated land-use inventory for Jackson, Calhoun, and Gadsden Counties in Florida, and Houston County in Alabama, 2014: U.S. Geological Survey Open-File Report 2015–1170, 14 p., accessed February 16, 2017, at https://doi.org/10.3133/ofr20151170.

Markstrom, S.L., Hay, L.E., and Clark, M.P., 2016, Towards simplification of hydrologic modeling—Identification of dominant processes: Hydrology and Earth System Sciences, v. 20, no. 11, p. 4655–4671, accessed March 8, 2017, at https://doi.org/10.5194/hess-20-4655-2016.

Markstrom, S.L., Regan, R.S., Hay, L.E., Viger, R.J., Webb, R.M.T., Payn, R.A., and LaFontaine, J.H., 2015, PRMS-IV, the Precipitation-Runoff Modeling System, version 4: U.S. Geological Survey Techniques and Methods, book 6, chap. B7, 158 p., accessed February 13, 2017, at https://doi.org/10.3133/tm6B7.

Moriasi, D.N., Arnold, J.G., Van Liew, M.W., Bingner, R.L., Harmel, R.D., and Veith, T.L., 2007, Model evaluation guidelines for systematic quantification of accuracy in watershed simulations: Transactions of the American Society of Agricultural and Biological Engineers, v. 50, no. 3, p. 885–900, accessed January 5, 2017, at http://ssl.tamu.edu/media/1312/MoriasiModelEval.pdf.

Nash, J.E., and Sutcliffe, J.V., 1970, River flow forecasting through conceptual models part I—A discussion of principles: Journal of Hydrology, v. 10, no. 3, p. 282–290, accessed September 2, 2009, at https://doi.org/10.1016/0022-1694(70)90255-6.

Northwest Florida Water Management District [NWFWMD], 2014, 2013 water supply assessment update: Havana, Fla., Northwest Florida Water Management District, Water Resources Assessment 14–01, 185 p., accessed February 27, 2015, at http://www.nwfwmd.state.fl.us/water-resources/wsp/.

Painter, J.A., Torak, L.J., and Jones, J.W., 2015, Evaluation and comparison of methods to estimate irrigation withdrawal for the National Water Census Focus Area Study of the Apalachicola-Chattahoochee-Flint River Basin in southwestern Georgia: U.S. Geological Survey Scientific Investigations Report 2015–5118, 32 p., accessed December 16, 2016, at https://doi.org/10.3133/sir20155118.

R Development Core Team, 2008, R—A language and environment for statistical computing: The R Foundation for Statistical Computing website, accessed May 16, 2017, at http://www.R-project.org.

Regan, R.S., and LaFontaine, J.H., 2017, Documentation of the dynamic parameter, water-use, stream and lake flow routing, and two summary output modules and updates to surface-depression storage simulation and initial conditions specification options with the Precipitation-Runoff Modeling System (PRMS): U.S. Geological Survey Techniques and Methods, book 6, chap. B8, 60 p., accessed October 10, 2017, at https://doi.org/10.3133/tm6B8.

Rutledge, A.T., 1998, Computer programs for describing the recession of ground-water discharge and for estimating mean ground-water recharge and discharge from streamflow records—Update: U.S. Geological Survey Water-Resources Investigations Report 98–4148, 43 p., accessed December 26, 2015, at https://pubs.usgs.gov/wri/wri984148/.

Saltelli, Andrea, Ratto, Marco, and Tarantola, Stefano, 2006, Sensitivity analysis practices—Strategies for model-based inference: Reliability Engineering and System Safety, v. 91, no. 10–11, p. 1109–1125, accessed March 8, 2017, at https://doi.org/10.1016/j.ress.2005.11.014.

Schaibly, J.H., and Shuler, K.E., 1973, Study of the sensitivity of coupled reaction systems to uncertainties in rate coefficients, II. Applications: The Journal of Chemical Physics, v. 59, no. 8, p. 3879–3888, accessed March 8, 2017, at https://doi.org/10.1063/1.1680572.

Soil Survey Staff, Natural Resources Conservation Service, U.S. Department of Agriculture, 2012, Soil Survey Geographic (SSURGO) Database: Natural Resources Conservation Service website, accessed July 10, 2013, at https://sdmdataaccess.sc.egov.usda.gov.

Thornton, P.E., Hasenauer, Hubert, and White, M.A., 2000, Simultaneous estimation of daily solar radiation and humidity from observed temperature and precipitation—An application over complex terrain in Austria: Agricultural and Forest Meteorology, v. 104, no. 4, p. 255–271, accessed March 30, 2015, at https://doi.org/10.1016/S0168-1923(00)00170-2.

Thornton, P.E., and Running, S.W., 1999, An improved algorithm for estimating incident daily solar radiation from measurements of temperature, humidity, and precipitation: Agricultural and Forest Meteorology, v. 93, no. 4, p. 211–228, accessed March 30, 2015, at https://doi.org/10.1016/S0168-1923(98)00126-9.

Thornton, P.E., Running, S.W., and White, M.A., 1997, Generating surfaces of daily meteorological variables over large regions of complex terrain: Journal of Hydrology, v. 190, no. 3, p. 214–251, accessed March 30, 2015, at https://doi.org/10.1016/S0022-1694(96)03128-9.

Thornton, P.E., Thornton, M.M., Mayer, B.W., Wei, Y., Devarakonda, R., Vose, R.S., and Cook, R.B., 2017, Daymet—Daily surface weather data on a 1-km grid for North America, Version 3: ORNL DAAC website, accessed March 8, 2017, at https://doi.org/10.3334/ORNLDAAC/1328. [Time period: 1980–01–01 to 2012–12–31. Spatial Range: N=35, S=29.5, E=–83, W=–86.]

Torak, L.J., and Painter, J.A., 2011, Summary of the Georgia Agricultural Water Conservation and Metering Program and evaluation of methods used to collect and analyze irrigation data in the middle and lower Chattahoochee and Flint River Basins, 2004–2010: U.S. Geological Survey Scientific Investigations Report 2011–5126, 25 p., accessed April 30, 2015, at https://pubs.usgs.gov/sir/2011/5126/.

University of Georgia, 2017, Georgia Automated Environmental Monitoring Network: University of Georgia, College of Agricultural & Environmental Sciences web page, accessed February 15, 2017, at http://www.georgiaweather.net/.

U.S. Geological Survey, 2017, USGS water data for the Nation: U.S. Geological Survey National Water Information System database, accessed March 2, 2017, at https://doi.org/10.5066/F7P55KJN.

Viger, R.J., 2014, Preliminary spatial parameters for PRMS based on the Geospatial Fabric, NLCD2001 and SSURGO: U.S. Geological Survey metadata, accessed April 30, 2015, at https://doi.org/10.5066/F7WM1BF7.

Viger, R.J., and Bock, Andrew, 2014, GIS Features of the Geospatial Fabric for National Hydrologic Modeling: U.S. Geological Survey metadata, accessed April 30, 2015, at https://doi.org/10.5066/F7542KMD.

Appendix 2. Construction, Calibration, and Evaluation of Fine-Resolution Hydrologic Models of Six Subbasins of the Apalachicola-Chattahoochee-Flint River Basin (ACFB)

Introduction

This appendix describes the construction, calibration, and evaluation of hydrologic models for six subbasins of the Apalachicola-Chattahoochee-Flint River Basin (ACFB): (1) upper Chattahoochee River, (2) Chestatee River, (3) Chipola River, (4) Ichawaynochaway Creek, (5) Potato Creek, and (6) Spring Creek (see figure 2 in the main body of this report). These fine-resolution subbasin Precipitation-Runoff Modeling System (PRMS) models were developed by the U.S. Geological Survey (USGS) to provide various statistics of streamflow for use in ecological response models. The statistics are for the spring and summer seasons when flow conditions affect biologic processes, such as recruitment, reproduction, growth, persistence, migration, dispersal, and colonization (Freeman and others, 2013). These statistics are computed for every stream segment in the subbasin models. The PRMS was used to provide hydrologic simulations for each subbasin (Leavesley and others, 1983; Markstrom and others, 2015; Regan and LaFontaine, 2017). The PRMS Model Construction section describes the methodology for model construction, which comes primarily from methods described in LaFontaine and others (2013). Methods for incorporating water-use data in the hydrologic models are the same as those documented in appendix 1 of this report. Mean monthly water-use information for 2008 to 2012 for the six subbasins is presented in appendix 2. Methods for calibrating and evaluating this set of hydrologic models are the same as those documented in appendix 1 of this report. Supporting data for these model developments are available in LaFontaine and others (2017).

Precipitation Runoff Modeling System (PRMS) Model Construction

The watershed hydrology model PRMS (Leavesley and others, 1983; Markstrom and others, 2015) is a deterministic, distributed-parameter, process-based model used to simulate and evaluate the effects of various combinations of precipitation, climate, and land use on basin response. Response to normal and extreme rainfall and snowmelt can be simulated to evaluate changes in water-balance relations, streamflow regimes, soil-water relations, and groundwater recharge. Each hydrologic component used for the generation of streamflow is represented within PRMS by a process algorithm that is based on a physical law or an empirical relation with measured or calculated characteristics (figure 5 in the main body of this report). The schematic in figure 6 in the main body of this report provides further detail of the various processes conceptualized in the PRMS soil zone. Many internal states (storages) and fluxes (flows) are available as output from PRMS simulations; see Markstrom and others (2015, appendix table 1–5) for further details. Methods for incorporating water-use data in the hydrologic models are the same as those documented in appendix 1 of this report.

Discretization

Distributed-parameter capabilities of the PRMS are provided by partitioning a basin into hydrologic response units (HRUs) in which a water balance and an energy balance are computed. The PRMS uses measured values of daily precipitation and maximum and minimum air temperature distributed to each HRU to compute solar radiation, potential evapotranspiration, actual evapotranspiration, sublimation, snowmelt, streamflow, infiltration, and groundwater recharge in a PRMS simulation. A stream network is used in the PRMS to route runoff flow components (surface runoff, shallow subsurface runoff, and groundwater flow) computed for the HRUs downstream from the basin outlet.

Stream Network Development

The model stream networks were derived from a digital elevation model (DEM) analysis by Elliott and others (2014). This dataset was developed using a 30-meter scale DEM and standard topographic analysis of flow accumulation. For this study, algorithms were used to discretize the flow accumulation grid into a stream network that had a resolution, drainage density, and structure similar to the 1:100,000-scale National Hydrography Dataset; the same scale as NHDPlus version 1 (http://www.horizon-systems.com/NHDPlus/NHDPlusV1_home.php, accessed April 1, 2013). The dataset developed by Elliott and others (2014) had a comparable stream network density to the National Hydrography Dataset in the northern part of the ACFB, but generally was denser in the southern part of the ACFB. The new stream networks for all six subbasins, however, were more detailed than existing stream networks available in the Geospatial Fabric for National Hydrologic Modeling (Viger and Bock, 2014). Table 2–1 lists the number of stream segments for each subbasin shown in figures 2–1 through 2–6.

Hydrologic Response Unit Development

The derived stream networks were used to create the HRUs for the model applications. Generally, the HRUs were created by dividing the local contributing area of each stream segment into two areas, a unit on the left and a unit on the

Table 2–1. Modeling unit information for each fine-resolution Precipitation-Runoff Modeling System model in the Apalachicola-Chattahoochee-Flint River Basin.

[km², square kilometer; HRU, hydrologic response unit]

Model	Number of stream segments	Number of hydrologic response units	Mean HRU size (km²)	Median HRU size (km²)	Minimum HRU size (km²)	Maximum HRU size (km²)
Upper Chattahoochee River	328	600	1.4	1.0	0.10	8.1
Chestatee River	168	312	1.3	1.0	0.10	5.8
Chipola River	778	1,472	1.5	1.1	0.09	7.9
Ichawaynochaway Creek	824	1,542	1.8	1.3	0.10	15.2
Potato Creek	221	427	1.4	1.2	0.10	6.4
Spring Creek	345	674	2.0	1.4	0.09	17.4

right of each stream segment. On the basis of stream network configuration, some stream segments may have fewer or more than two HRUs. The model HRUs were developed using the geographic information system (GIS) Weasel software developed by Viger and Leavesley (2007). Table 2–1 lists the number and general sizes of HRUs for each subbasin shown in figures 2–1 through 2–6.

Parameterization of Stream Segments and HRUs

PRMS is a distributed-parameter hydrologic model. Many of the model parameters vary spatially on the basis of surface and subsurface characteristics of the model domain. The PRMS parameters are used to characterize processes such as solar radiation, potential evapotranspiration, canopy interception, snow dynamics, surface runoff, soil-zone dynamics, groundwater flow, and streamflow. For this version of PRMS, the soil-zone and groundwater reservoirs have the same spatial delineations (size and shape) as the HRUs.

Stream Network Parameterization

Muskingum routing was used for all subbasin PRMS hydrologic models. This method is described in PRMS by two parameters, **K_coef** and **x_coef**. Initial values of **K_coef**, which approximates the travel time, in hours, of streamflow through each stream segment, were computed using the procedure documented in LaFontaine and others (2013). That method uses the length of each stream segment and the average velocity as computed using the Manning equation (Gray, 1973). The parameter **x_coef** was given an initial value of 0.2 and was then calibrated.

Hydrologic Response Unit Parameterization

Parameters describing HRU size, altitude, slope, and aspect were computed from the same DEM used to delineate the subbasins. Canopy and surface vegetation parameters were computed using the National Land Cover Database (NLCD; Homer and others, 2007). Surficial features such as percentage impervious area, vegetation density, and dominant vegetation type were computed for each HRU using the NLCD 2001 (Homer and others, 2007). The PRMS surface depression storage parameters were computed using satellite imagery as described in LaFontaine and others (2013). The surface depression storage dataset was derived for the ACFB as part of the USGS Southeast Regional Assessment Project (Dalton and Jones, 2010) and used Landsat 5 Thematic Mapper imagery from April 2010 (a relatively wet period) to assign a maximum possible extent of surface depression storage for the ACFB.

Soil-zone parameters were computed using the SSURGO soils database (U.S. Department of Agriculture, https://www.nrcs.usda.gov/wps/portal/nrcs/detail/soils/survey/?cid=nrcs142p2_053627, accessed on January 25, 2016). Subsurface parameters, those describing the unsaturated zone between land surface and the groundwater reservoir, were developed using the near-surface permeability maps developed by Glesson and others (2011). This parameterization follows the methods described in LaFontaine and others (2013) and provides a spatially distributed range of values that were then calibrated. This method provided the initial spatial variation lacking in past PRMS applications that used the same initial value for all HRUs.

The groundwater flow parameter, **gwflow_coef**, was derived from an analysis of the groundwater recession constant for streamgages in the ACFB as described in appendix 1 of this report. Annual groundwater recession constants were computed for those streamgages that had recorded periods deemed relatively free of anthropogenic effects. The median of the annual streamgage recession constants was used as an initial value for those HRUs proximal to each analyzed streamgage.

Climate Data, Distribution Algorithms, and Regional Parameterization

The PRMS requires inputs of daily maximum and minimum air temperature and daily precipitation accumulation time-series data. Weather station data from the National

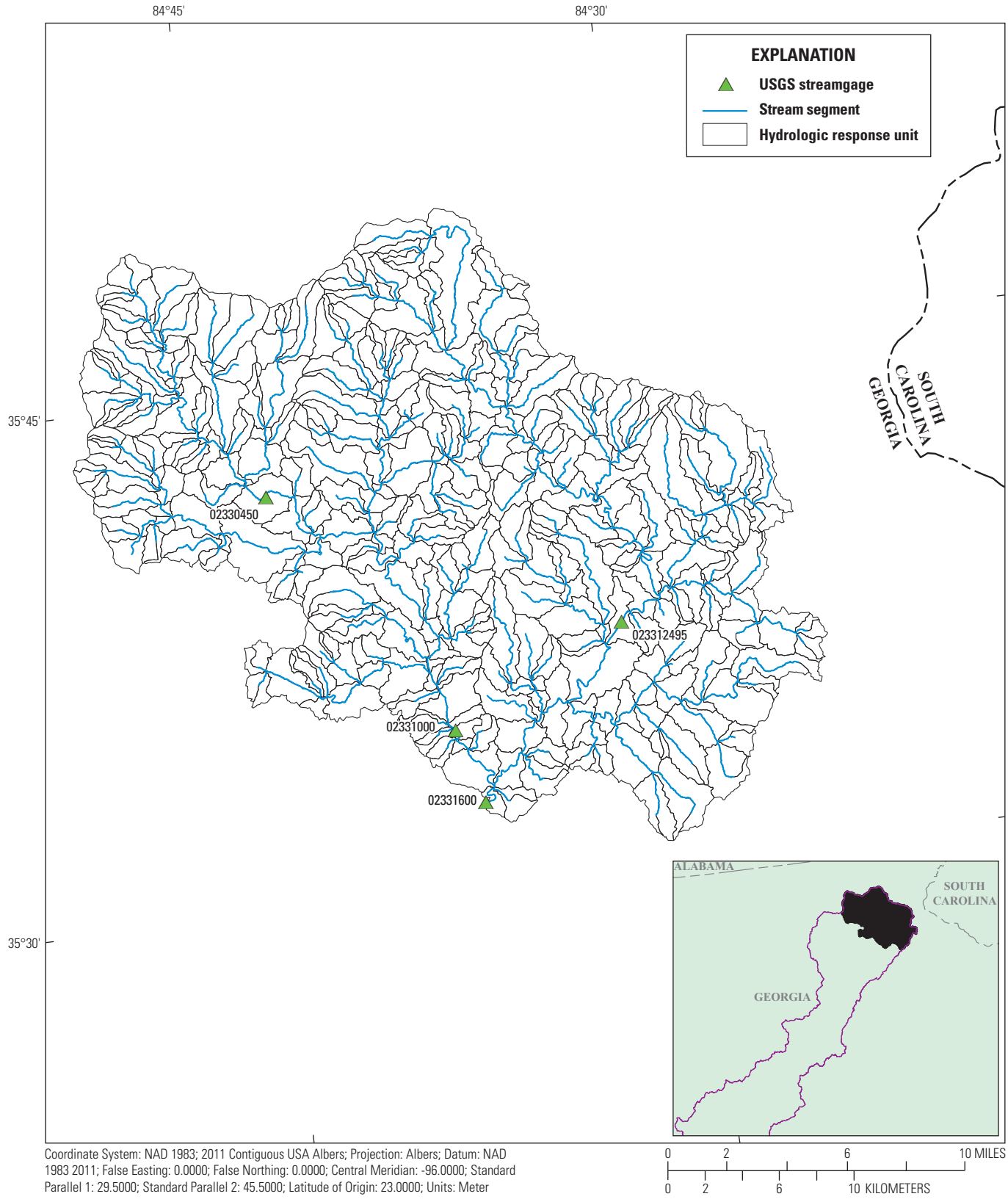

Figure 2–1. Precipitation-Runoff Modeling System hydrologic response units and stream network, as well as U.S. Geological Survey streamgages for the upper Chattahoochee River subbasin.

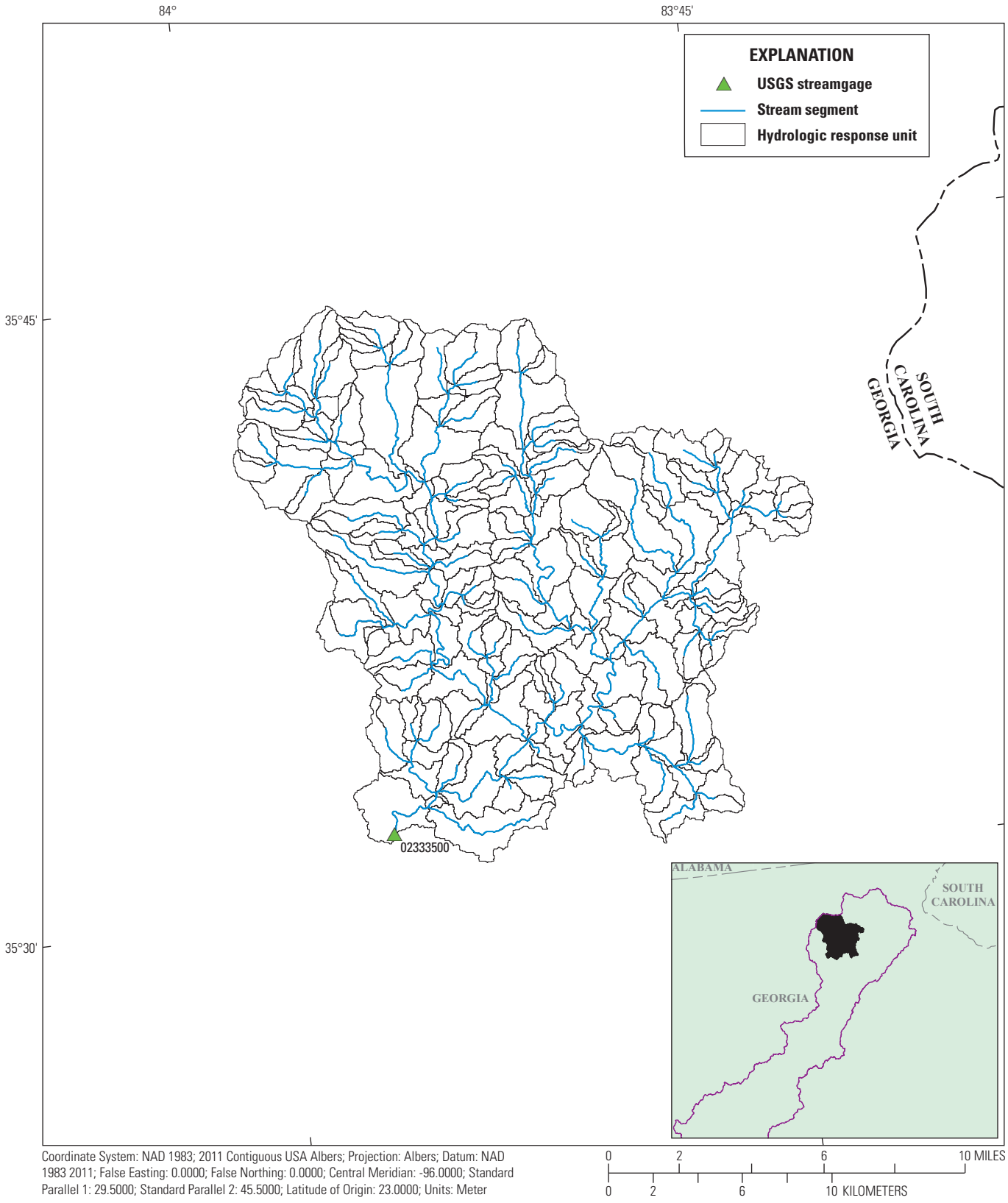

Figure 2–2. Precipitation-Runoff Modeling System hydrologic response units and stream network, as well as U.S. Geological Survey streamgages for the Chestatee River subbasin.

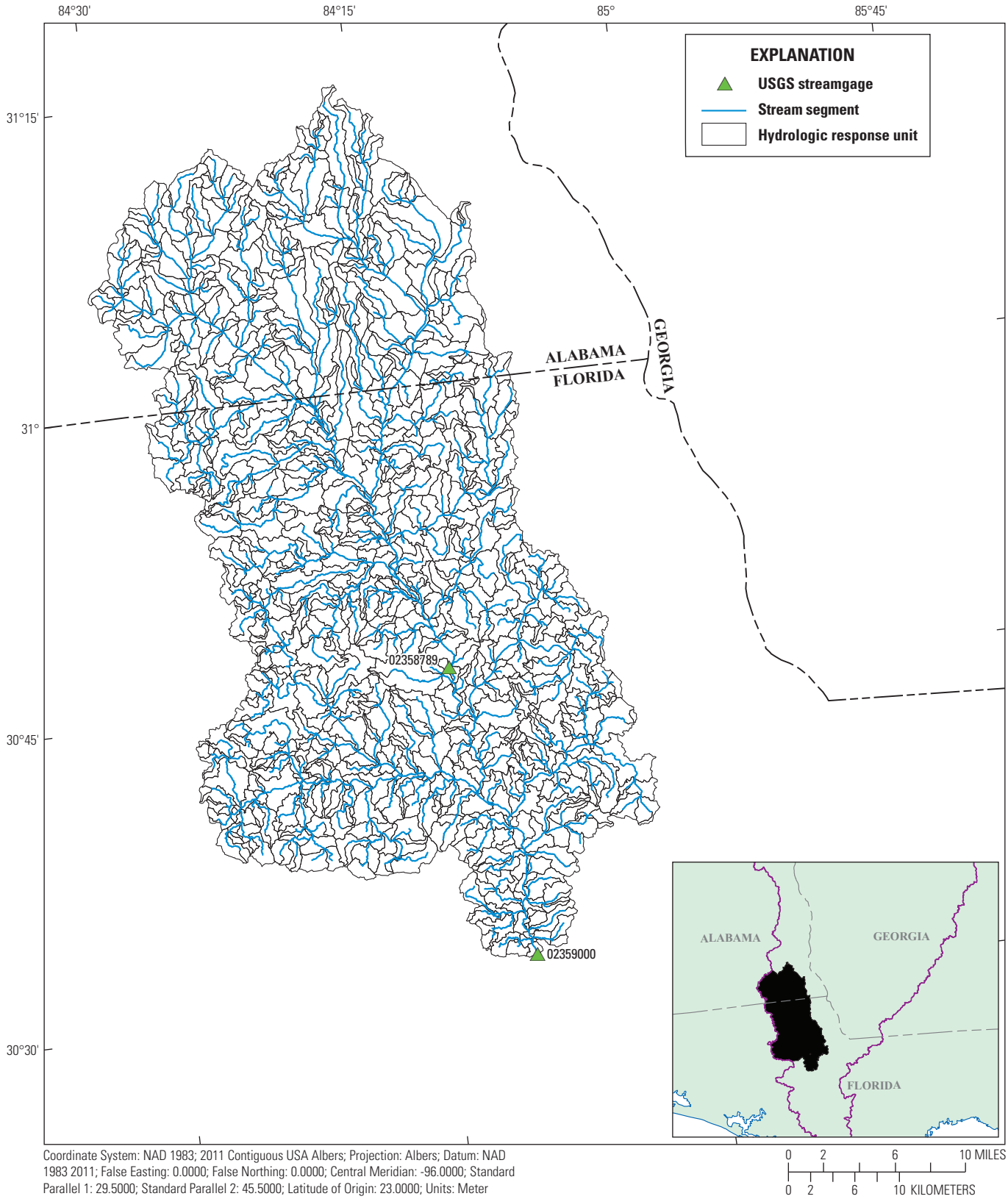

Figure 2–3. Precipitation-Runoff Modeling System hydrologic response units and stream network, as well as U.S. Geological Survey streamgages for the Chipola River subbasin.

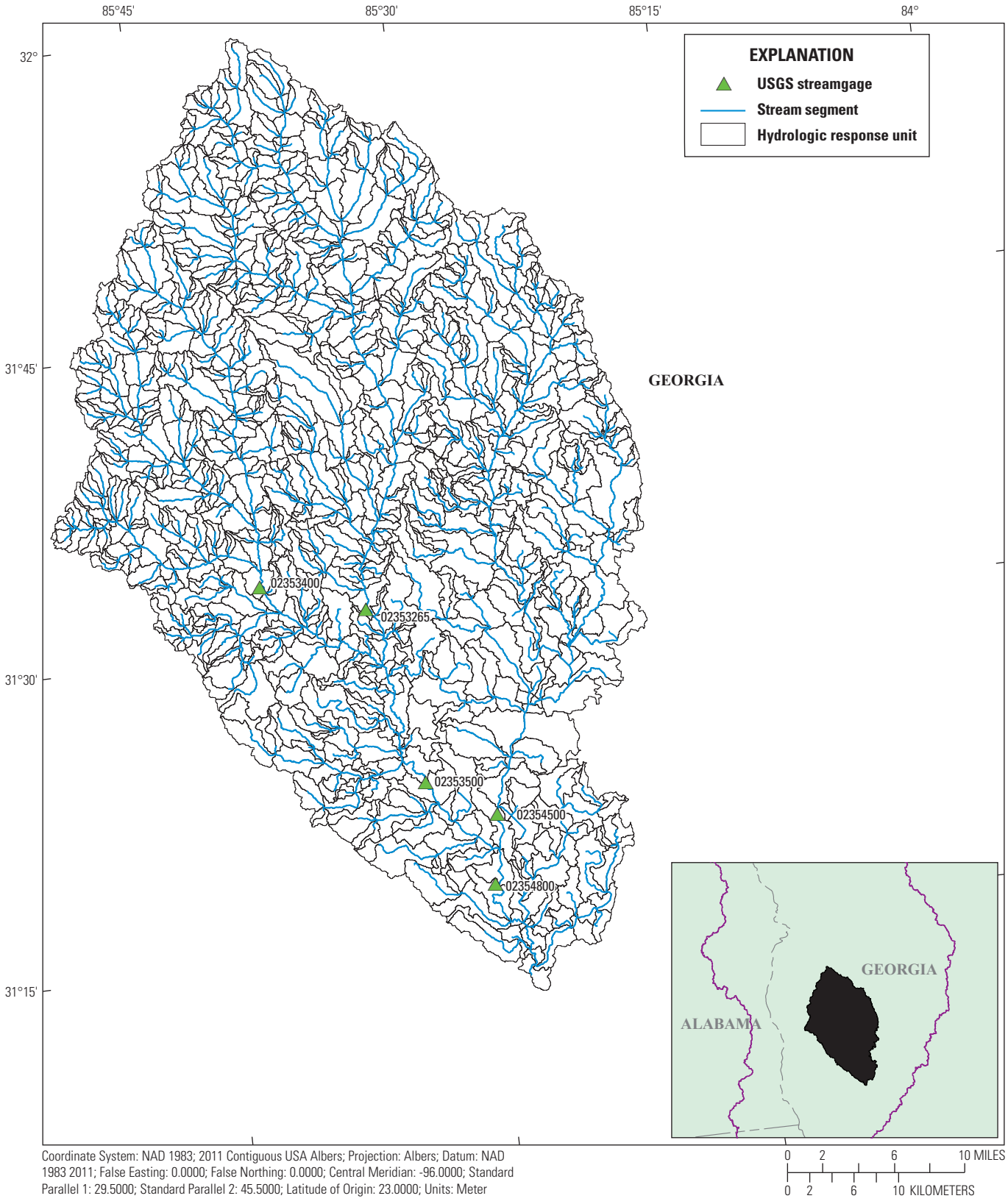

Figure 2–4. Precipitation-Runoff Modeling System hydrologic response units and stream network, as well as U.S. Geological Survey streamgages for the Ichawaynochaway Creek subbasin.

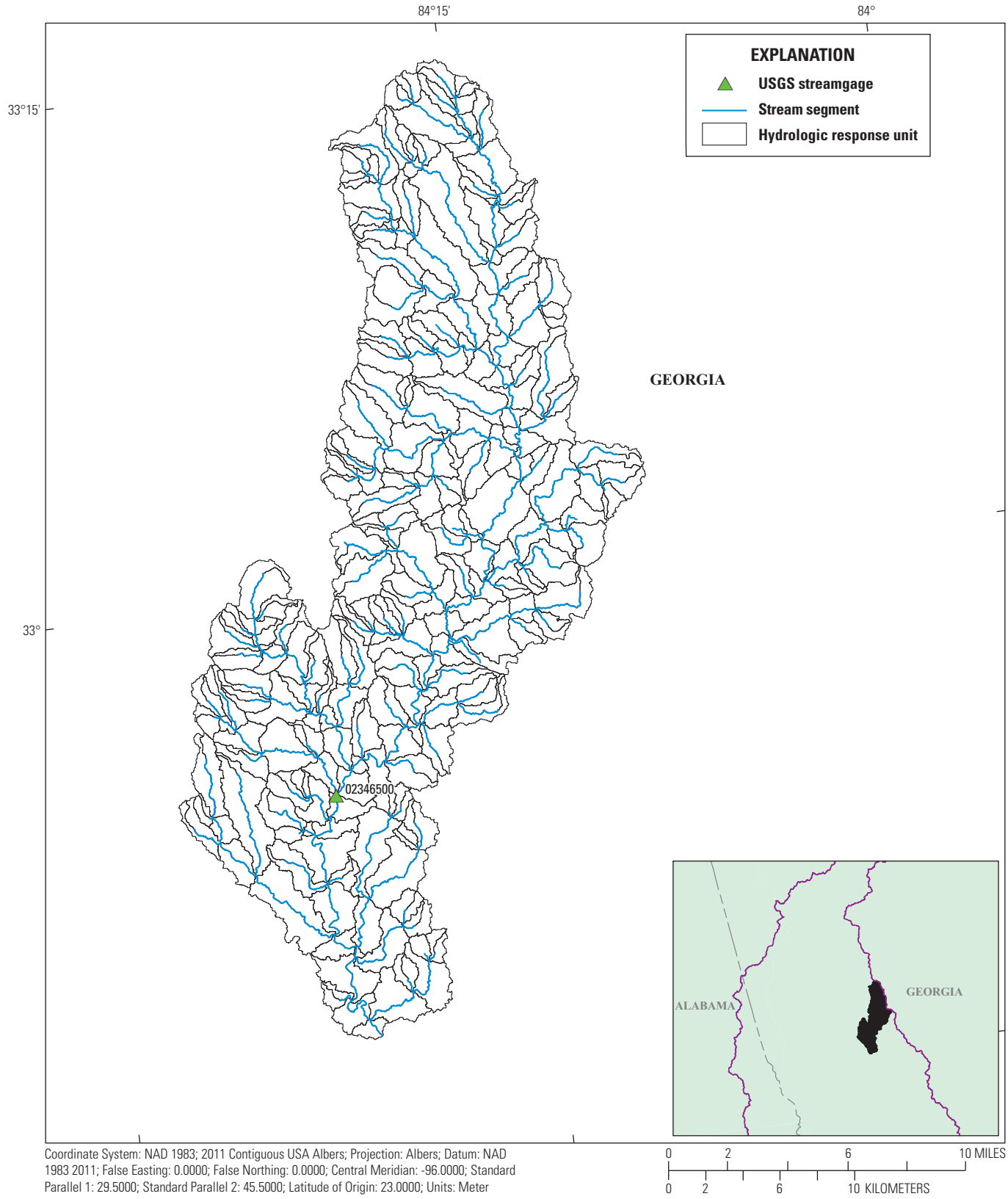

Figure 2–5. Precipitation-Runoff Modeling System hydrologic response units and stream network, as well as U.S. Geological Survey streamgages for the Potato Creek subbasin.

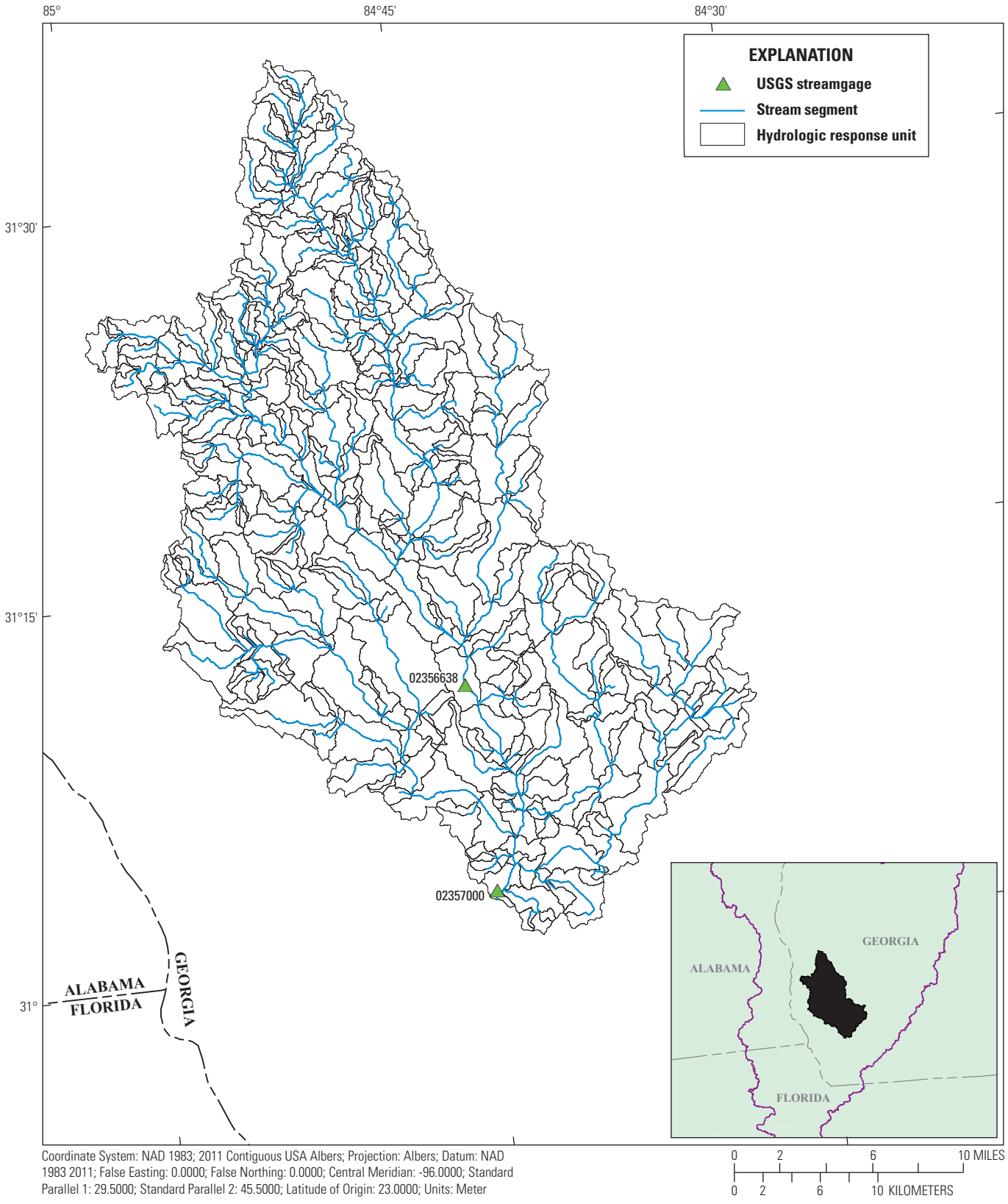

Figure 2–6. Precipitation-Runoff Modeling System hydrologic response units and stream network, as well as U.S. Geological Survey streamgages for the Spring Creek subbasin.

Weather Service National Climatic Data Center (NCDC) network were used for climate forcings for the subbasin models (https://www.ncdc.noaa.gov/). The NCDC station-based dataset allows access to climate inputs as far back as the early 1900s and as late as the previous day before access. A drawback to using the NCDC station dataset is that substantial quality control must be performed prior to using the data, and stations may have discontinuous records. The NCDC weather station data were distributed to the modeling units using the **xyz_dist** module in PRMS, a regression-based distribution process that occurs during a PRMS simulation as described in Markstrom and others (2015, p. 84–85).

To use the **xyz_dist** algorithm, the weather station data were analyzed to determine monthly PRMS parameters (**ppt_lapse, max_lapse, min_lapse**). These parameters are derived from regional regressions, using weather station latitude, longitude, and altitude as independent variables. An iterative process, using various combinations of available NCDC stations, was used for each subbasin. This process included analyzing groups of at least 10 NCDC stations that covered the distribution of latitude, longitude, and altitude for each subbasin. The iteration ended when a sufficient level of performance was attained for all months ($r^2 > 0.9$ for temperature, and $r^2 > 0.7$ for precipitation). The selected subset of the weather stations for each subbasin was used to describe regional climate relations, and a potentially different subset of weather stations was used for model forcings. Different subsets of stations were used for each process because local precipitation information is critical to accurately simulate local streamflow, whereas a broader spatial range of locations may be needed to characterize regional climate setting. Therefore, weather stations that were within or in close proximity to each subbasin were chosen to compute model forcings, and weather stations farther away from each subbasin may have been chosen to compute the regional climate regressions. The PRMS parameters **psta_nuse** and **tsta_nuse** were used to select the final set of weather stations (from within the set used in the regional regressions) for model forcings. The weather stations used for these hydrologic simulations for the entire ACFB study area are shown in figure 2–7.

Water-Use Inputs

The water-use datasets and application methods described in appendix 1 of this report were used in the six fine-resolution subbasin simulations. Water-use inputs consist of monthly estimates of surface-water withdrawals and returns, and groundwater withdrawals for the period 2008 to 2012. The water-use locations were applied to the PRMS model units (HRUs and stream segments) through a GIS overlay analysis. To simulate water use in PRMS, separate PRMS input files were created for three types of water use: withdrawals from streams, returns to streams, and withdrawals from groundwater (Regan and LaFontaine, 2017). Mean monthly values of water use by subbasin and type are listed in table 2–2.

Water use in the Upper Chattahoochee River, Chestatee River, and Potato Creek subbasins included surface-water withdrawals and returns. Water use in these three subbasins had little seasonal variation because the data are primarily from municipal and industrial use types. Water use in the Ichawaynochaway Creek and Spring Creek subbasins consisted of a mix of surface-water withdrawals and returns, and groundwater withdrawals. The Chipola River subbasin had only groundwater withdrawals. Surface-water withdrawals in the Ichawaynochaway Creek and Spring Creek subbasins were for agricultural use, and surface-water returns were from municipal and industrial use. The groundwater withdrawals in the southern three subbasins varied seasonally on the basis of agricultural irrigation use, with the Spring Creek subbasin having the largest quantity of groundwater withdrawals for the period (annual average of 40.9 cubic feet per second [ft^3/s] per month), followed by the Ichawaynochaway Creek subbasin (annual average of 18.0 ft^3/s per month) and the Chipola River subbasin (annual average of 14.8 ft^3/s per month). Groundwater withdrawals for agricultural use peaked in June for all three subbasins with that type of water use.

Upper Chattahoochee River Subbasin PRMS Model

The upper Chattahoochee River subbasin consists of the area upstream from the USGS streamgage 02331600 (Chattahoochee River near Cornelia, Georgia). This subbasin encompasses 815 square kilometers (km^2) and is located in the northernmost region of the ACFB (figure 2 in main body of this report). The average altitude of the subbasin is 539 meters above the North American Vertical Datum of 1988 (NAVD 88), ranging from 344 to 1,340 meters. The land cover is dominated by forest (more than 70 percent), with developed area increasing from 8.6 percent (2001) to 10.0 percent (2011) (table 2–3). The subbasin is located in both the Blue Ridge and Piedmont physiographic provinces and is underlain by crystalline rock (figure 2 in main body of this report).

Climate Inputs

Twenty-two NCDC weather stations were used to develop regional climate regressions and model forcings of precipitation and air temperature (table 2–4). Various combinations of the weather stations were used, depending on regional regression analysis, proximity to the basin, and data availability. From the 22 weather stations used for this subbasin, 15 were used for the maximum temperature regressions, 15 were used for the minimum temperature regressions (but only 13 weather stations were used for both maximum and minimum temperature regressions), and 18 stations were used for the precipitation regressions (table 2–4). All 15 weather stations used for either maximum or minimum temperature regressions and all 18 weather stations used for the

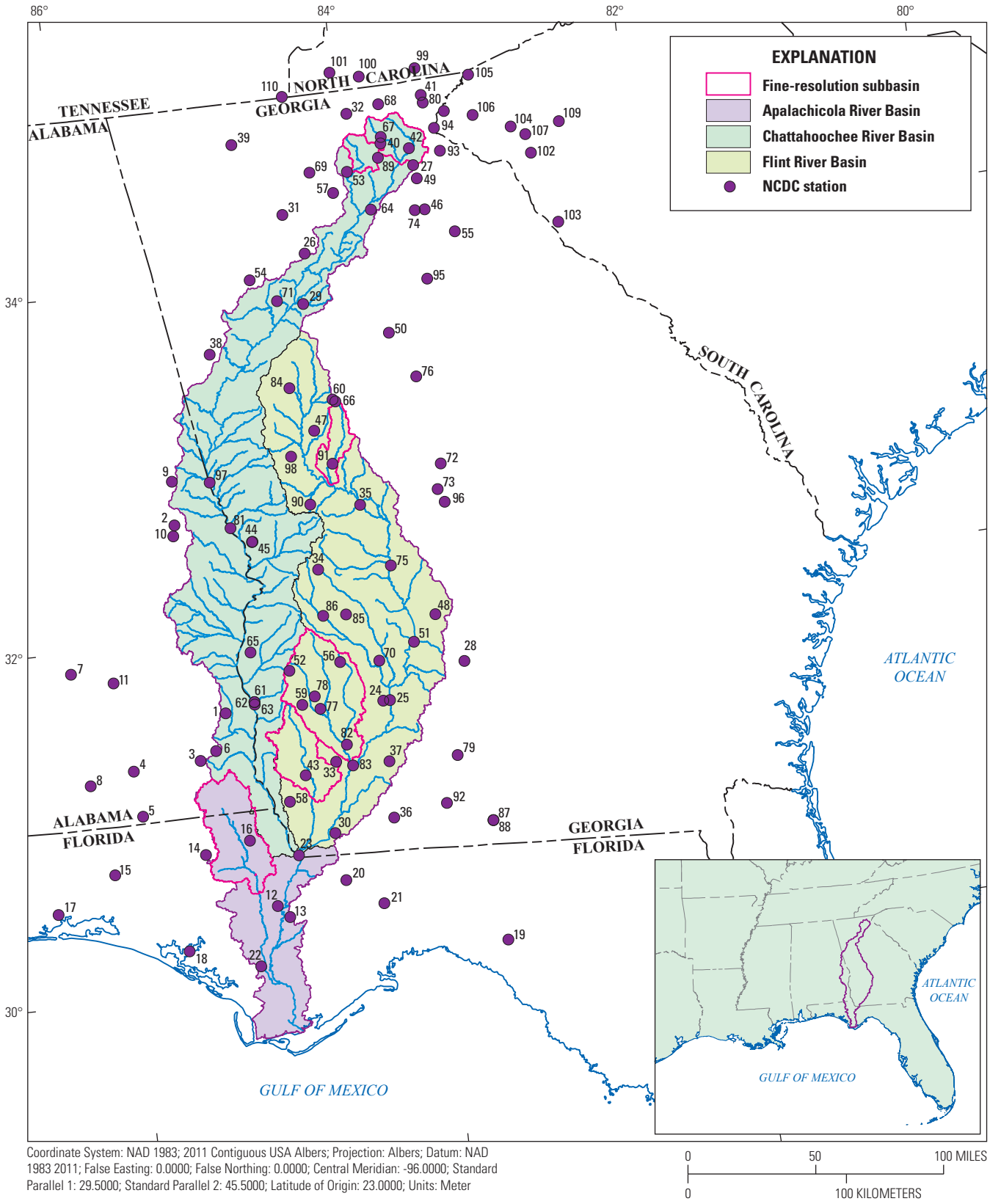

Figure 2–7. National Climatic Data Center (NCDC) weather stations used to develop precipitation and air temperature inputs to the fine-resolution PRMS models.

Table 2–2. Summary of water use, by type and source, for the six fine-resolution subbasins.

[Water use is presented as mean monthly values for years 2008 to 2012, in cubic feet per second. GW, groundwater; SW, surface water; W, withdrawal; R, return; —, no data]

Basin	Water-use source	Water-use type	Mean monthly water withdrawals for 2008–12, in cubic feet per second											
			Jan.	Feb.	Mar.	Apr.	May	June	July	Aug.	Sept.	Oct.	Nov.	Dec.
Upper Chattahoochee River	SW	W	3.51	3.42	3.31	3.47	3.64	3.95	4.00	4.04	3.90	3.67	3.53	3.52
	SW	R	1.16	1.10	0.89	1.06	1.14	1.15	0.92	1.30	1.29	0.84	0.76	0.94
	GW	W	—	—	—	—	—	—	—	—	—	—	—	—
Chestatee River	SW	W	0.82	0.73	0.68	0.77	0.86	1.00	0.99	0.97	0.83	0.82	0.80	0.78
	SW	R	0.44	0.45	0.51	0.46	0.39	0.48	0.35	0.45	0.54	0.27	0.32	0.42
	GW	W	—	—	—	—	—	—	—	—	—	—	—	—
Chipola River	SW	W	—	—	—	—	—	—	—	—	—	—	—	—
	SW	R	—	—	—	—	—	—	—	—	—	—	—	—
	GW	W	3.82	6.44	12.2	24.2	29.2	32.1	27.8	18.4	8.45	5.79	4.82	4.49
Ichawaynochaway Creek	SW	W	0	0	0.12	0.12	0.14	1.35	1.21	0.21	0.11	0.09	0	0
	SW	R	2.18	2.46	2.10	2.17	1.65	1.52	1.61	1.83	1.79	1.61	1.51	2.22
	GW	W	0.02	0.03	7.94	11.5	16.7	59.0	47.2	43.7	18.3	11.7	0.39	0.02
Potato Creek	SW	W	6.22	4.89	5.18	5.19	5.41	4.82	5.00	5.00	4.53	5.24	5.69	5.77
	SW	R	5.97	6.34	6.45	6.07	5.38	4.93	4.81	5.05	4.69	5.02	5.11	5.77
	GW	W	—	—	—	—	—	—	—	—	—	—	—	—
Spring Creek	SW	W	0	0	0.12	0.12	0.24	0.96	1.22	0.19	0.05	0.01	0	0
	SW	R	1.58	2.00	1.95	1.62	1.17	0.94	0.85	1.04	0.91	0.83	0.78	1.44
	GW	W	0.65	0.79	13.7	32.5	41.9	176	100	59.1	45.7	18.1	1.19	0.77

Table 2–3. Land-cover percentages of the fine-resolution model subbasins in the Apalachicola-Chattahoochee-Flint River Basin.

[km², square kilometer; NLCD, National Land Cover Database]

Land-cover type	Land-cover percentage					
	Upper Chattahoochee River[1]	Chestatee River[2]	Chipola River[3]	Ichawaynochaway Creek[4]	Potato Creek[5]	Spring Creek[6]
2001 NLCD						
Developed	8.6	7.3	6.6	3.5	10.5	4.6
Forest	72.6	77.8	28.3	37.9	55.5	25.4
Cultivated crops	0.0	0.0	21.9	27.4	0.1	40.1
Hay/Pasture	12.7	9.6	10.1	6.5	21.1	6.3
Water	0.5	0.4	0.5	0.4	1.3	0.2
Barren	0.3	0.5	0.1	0.1	0.5	0.1
Shrub/Scrub/Herb	5.2	4.4	16.2	8.7	6.3	7.0
Wetlands	0.1	0.1	16.3	15.5	4.8	16.3
2006 NLCD						
Developed	8.8	7.4	6.7	3.5	10.9	4.7
Forest	72.0	77.3	28.5	38.3	54.9	27.4
Cultivated crops	0.0	0.0	21.7	27.2	0.1	39.7
Hay/Pasture	12.6	9.5	9.6	6.5	20.3	6.0
Water	0.5	0.4	0.7	0.5	1.3	0.3
Barren	0.3	0.3	0.0	0.1	0.2	0.1
Shrub/Scrub/Herb	5.6	5.0	16.5	8.5	7.3	6.1
Wetlands	0.1	0.1	16.2	15.4	4.8	15.8
2011 NLCD						
Developed	10.0	8.5	6.8	3.6	11.3	4.7
Forest	71.3	76.9	28.4	38.3	52.2	27.6
Cultivated crops	0.0	0.0	21.2	26.8	0.1	39.5
Hay/Pasture	12.1	9.0	9.4	6.2	20.0	5.9
Water	0.5	0.4	0.7	0.5	1.4	0.3
Barren	0.3	0.3	0.1	0.1	0.2	0.1
Shrub/Scrub/Herb	5.7	4.8	18.6	9.1	10.1	5.9
Wetlands	0.1	0.1	14.9	15.5	4.8	16.0

[1]Drainage area = 815 km².

[2]Drainage area = 396 km².

[3]Drainage area = 2,020 km².

[4]Drainage area = 2,690 km².

[5]Drainage area = 482 km².

[6]Drainage area = 1,260 km².

Table 2–4. National Climatic Data Center weather stations in the upper Chattahoochee River subbasin for regional climate regressions and for daily precipitation and air temperature forcings.

[Prcp, daily precipitation accumulation; Tmax, maximum daily temperature; Tmin, minimum daily temperature; —, means were not used]

ID	Station ID	Latitude	Longitude	Altitude (meters)	Regressions			Forcings		
					Tmax	Tmin	Prcp	Tmax	Tmin	Prcp
27	090236	34.44	–83.52	280	x	x	x	x	x	x
32	090969	34.85	–83.94	594	x	—	—	x	x	—
41	091982	34.86	–83.41	584	x	x	—	x	x	—
42	092006	34.59	–83.77	478	x	x	x	x	x	x
46	092180	34.26	–83.49	250	x	x	x	x	x	x
49	092283	34.52	–83.53	448	x	x	x	x	x	x
53	092475	34.53	–83.99	475	x	x	x	x	x	x
57	092578	34.42	–84.10	409	—	—	x	—	—	x
64	093621	34.30	–83.86	357	—	x	x	x	x	x
67	094230	34.70	–83.73	455	—	x	x	x	x	x
68	094281	34.88	–83.72	671	—	—	x	—	—	x
74	095633	34.26	–83.56	277	—	—	x	—	—	x
80	096093	34.90	–83.41	1,056	—	—	x	—	—	x
89	097827	34.66	–83.73	485	x	x	x	x	x	x
99	312102	35.06	–83.43	685	x	x	x	x	x	x
100	313921	35.05	–83.83	579	—	—	x	—	—	x
101	316001	35.10	–84.02	480	x	x	—	x	x	—
102	380170	34.50	–82.71	232	x	x	x	x	x	x
103	381277	34.09	–82.59	162	x	—	x	x	x	x
104	381770	34.66	–82.82	251	x	x	—	x	x	—
107	387687	34.61	–82.73	250	x	x	x	x	x	x
109	389122	34.65	–82.49	263	x	x	x	x	x	x

precipitation regressions were used for the model forcings. This was done to provide consistency and adequate temporal and spatial coverage in the model forcings for the simulations. On the basis of the NCDC weather stations used for model forcings for the period 1980 to 2013, the subbasin receives an annual average precipitation of 1,680 millimeters (66.1 inches) and has mean monthly air temperatures that range from 3.7 degrees Celsius (°C; 38.7 degrees Fahrenheit [°F]) to 23.7 °C (74.7 °F).

PRMS Model Calibration and Evaluation

An automated calibration, as described in appendix 1 of this report, was completed for the NCDC station-driven PRMS model. Simulations of solar radiation and potential evapotranspiration match the measured data well for the upper Chattahoochee River subbasin for both the calibration and evaluation periods (fig. 2–8). One streamgage was used to calibrate and evaluate the upper Chattahoochee River subbasin PRMS models, and two additional streamgages were used only for evaluation (table 2–5). A split-period strategy was used to calibrate and evaluate the model at the streamgages. The period 1997 to 2012 was used to calibrate the model at the 02331600 streamgage, with the evaluation periods varying on the basis of available measured streamflow data. Streamflow performance metrics of Nash-Sutcliffe model efficiency index (NSE; 0.64 to 0.81), normalized root mean square error (RSR; 0.43 to 0.60), and percent bias (P_{bias}; –8.2 to 8.2) were within the established criteria for the three streamgages for both calibration and evaluation for the NCDC station-driven simulations (table 2–6). An NSE value of 0.5 or greater was defined as the passing performance threshold. The passing performance thresholds for the RSR and P_{bias} metrics were less than 0.7 and between plus or minus 10.0, respectively.

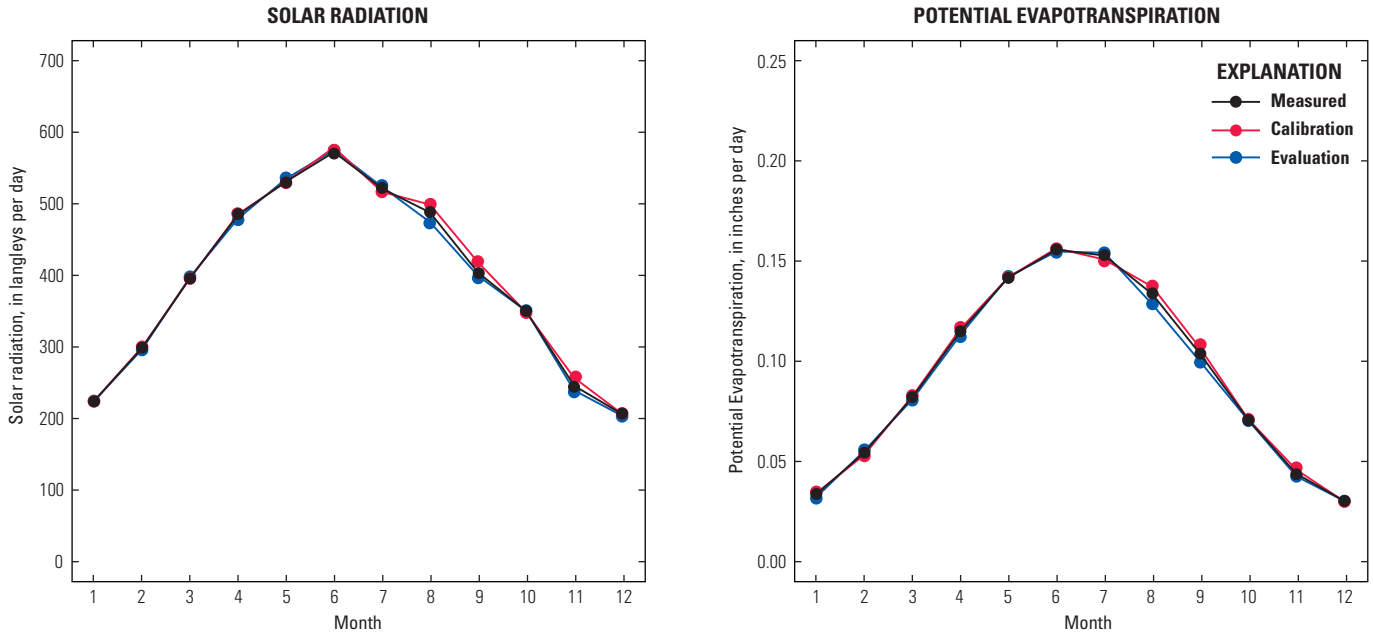

Figure 2–8. Solar radiation and potential evapotranspiration calibration and evaluation results for the upper Chattahoochee River subbasin for the calibration period (1997–2012) and evaluation period (1981–96).

Table 2–5. Streamgages used for model calibration for each of the six fine-resolution model subbasins of the Apalachicola-Chattahoochee-Flint River Basin.

[PRMS output variable for simulated flow is *seg_outflow*. km², square kilometer; Point of interest type: C, calibration; E, evaluation]

Count	Station number	Station name	USGS drainage area (km²)	Point of interest type	Stream segment	Period of streamflow record
			Upper Chattahoochee River subbasin			
1	02330450	Chattahoochee River at Helen, GA	116	E	297	1981–current
2	023312495	Soque River at GA 197, near Clarkesville, GA	243	E	307	2007–current
3	02331600	Chattahoochee River near Cornelia, GA	815	C/E	328	1957–current
			Chestatee River subbasin			
4	02333500	Chestatee River near Dahlonega, GA	396	C/E	168	1929–current
			Chipola River subbasin			
5	02358789	Chipola River at Marianna, FL	1,200	E	753	1999–current
6	02359000	Chipola River near Altha, FL	2,020	C/E	778	1921–27; 1929–31; 1943–current
			Ichawaynochaway Creek subbasin			
7	02353265	Ichawaynochaway Creek at GA 37, near Morgan, GA	780	E	802	2001–current
8	02353400	Pachitla Creek near Edison, GA	487	E	777	1959–71; 1988–current
9	02353500	Ichawaynochaway Creek at Milford, GA	1,600	E	812	1939–current
10	02354500	Chickasawhatchee Creek at Elmodel, GA	828	E	782*	1939–49; 1995–current
11	02354800	Ichawaynochaway Creek near Elmodel, GA	2,590	C/E	818	1995–current
			Potato Creek subbasin			
12	02346500	Potato Creek near Thomaston, GA	482	C/E	212*	1937–71
			Spring Creek subbasin			
13	02357000	Spring Creek near Iron City, GA	1,260	C/E	344	1937–71; 1982–current

*, PRMS variable for simulated flow is *seg_inflow*.

Table 2–6. Streamflow performance metrics for the Upper Chattahoochee River subbasin PRMS model.

[NSE, Nash-Sutcliffe model efficiency index (Nash and Sutcliffe, 1970); RSR, normalized root mean square error; P_{bias}, percent bias]

Station number	Period type	Start year	End year	NSE	RSR	P_{bias}
National Climatic Data Center station-driven						
02330450	Evaluation	1982	1996	0.64	0.60	–8.2
02330450	Evaluation	1997	2012	0.68	0.57	–3.8
023312495	Evaluation	2008	2012	0.64	0.60	8.2
02331600	Evaluation	1981	1996	0.81	0.43	–3.5
02331600	Calibration	1997	2012	0.81	0.44	1.6

Chestatee River Subbasin PRMS Model

The Chestatee River subbasin consists of the area upstream from the USGS streamgage 02333500 (Chestatee River near Dahlonega, Georgia). This subbasin encompasses 396 km^2 and is located in the northernmost region of the ACFB (figure 2 in the main body of this report). The average altitude of the subbasin is 554 meters, ranging from 345 to 1,340 meters above NAVD 88. The land cover is dominated by forest (more than 75 percent) with stable levels of developed land cover (table 2–3). The subbasin is located in both the Blue Ridge and Piedmont physiographic provinces, underlain by crystalline rock (figure 2 in the main body of this report).

Climate Inputs

Nineteen NCDC weather stations were used to develop regional climate regressions and model forcings of precipitation and air temperature (table 2–7). Various combinations of the weather stations were used depending on regional regression analysis, proximity to the basin, and data availability. On the basis of weather stations used for model forcings for the period 1980 to 2013, the subbasin receives an annual average precipitation of 1,660 millimeters (65.5 inches) and has mean monthly air temperatures that range from 3.5 °C (38.3 °F) to 23.6 °C (74.5 °F).

PRMS Model Calibration and Evaluation

An automated calibration, as described in appendix 1 of this report, was completed for the NCDC station-driven PRMS model. Simulations of solar radiation and potential evapotranspiration match the measured data well for the Chestatee River subbasin for both the calibration and evaluation periods (fig. 2–9). One streamgage was used to calibrated and evaluate the Chestatee River subbasin PRMS model (table 2–5). A split-period strategy was used to calibrate and evaluate the model at the streamgage. The period 1997 to 2012 was used for calibration, and the period 1961 to 1996 was used for evaluation of the NCDC-driven simulation. Streamflow performance metrics of NSE (0.77 to 0.82), RSR (0.42 to 0.48), and P_{bias} (–1.6 to 5.0) were all within the acceptable range of the established criteria for the NCDC station-driven simulation for the calibration and evaluation periods (table 2–8).

Table 2–7. National Climatic Data Center weather stations used in the Chestatee River subbasin for regional climate regressions and for daily precipitation and air temperature forcings.

[Prcp, daily precipitation accumulation; Tmax, maximum daily temperature; Tmin, minimum daily temperature; —, means were not used]

ID	Station ID	Latitude	Longitude	Altitude (meters)	Regressions			Forcings		
					Tmax	Tmin	Prcp	Tmax	Tmin	Prcp
26	090219	34.10	–84.35	347	—	x	—	x	x	—
31	090603	34.33	–84.47	387	x	—	—	x	x	—
32	090969	34.85	–83.94	594	x	—	—	x	x	—
39	091863	34.76	–84.76	216	x	x	x	x	x	—
40	091965	34.62	–83.54	424	x	x	—	x	x	—
41	091982	34.86	–83.41	584	x	—	—	x	x	—
42	092006	34.59	–83.77	478	x	x	x	x	x	x
46	092180	34.26	–83.49	229	—	x	—	x	x	—
53	092475	34.53	–83.99	475	—	—	x	—	—	x
55	092517	34.12	–83.30	238	—	x	—	x	x	—
64	093621	34.30	–83.86	357	x	—	—	x	x	—
69	094688	34.55	–84.25	399	x	x	—	x	x	—
89	097827	34.66	–83.73	485	—	—	x	—	—	x
93	098740	34.58	–83.33	308	—	—	x	—	—	—
94	098842	34.71	–83.35	233	—	—	x	—	—	—
105	384581	34.98	–83.07	762	x	x	x	x	x	—
106	385278	34.80	–83.27	503	x	x	x	x	x	—
108	388887	34.75	–83.08	299	—	—	x	—	—	—
110	402024	34.99	–84.38	442	x	x	x	x	x	—

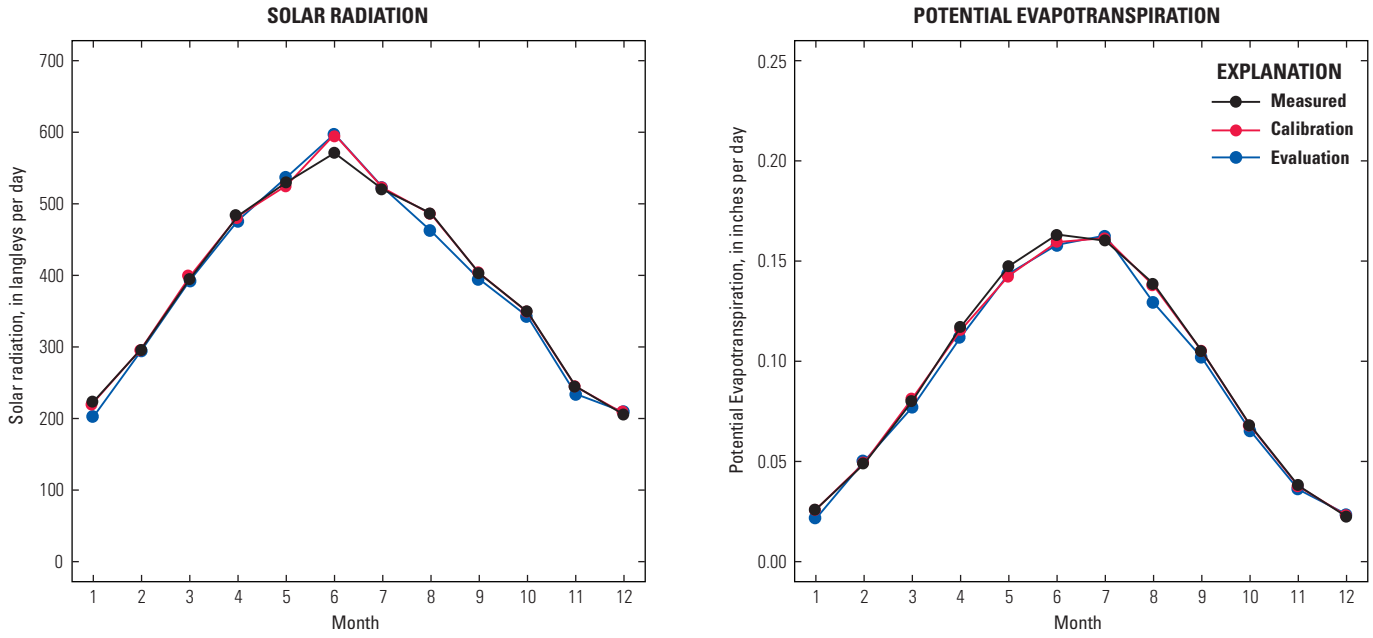

Figure 2–9. Solar radiation and potential evapotranspiration calibration and evaluation results for the Chestatee River subbasin for the calibration period (1997–2012) and evaluation period (1981–96).

Table 2–8. Streamflow performance metrics for the Chestatee River subbasin PRMS model.

[NSE, Nash-Sutcliffe model efficiency index (Nash and Sutcliffe, 1970); RSR, normalized root mean square error; P_{bias}, percent bias]

Station number	Period type	Start year	End year	NSE	RSR	P_{bias}
National Climatic Data Center station-driven						
02333500	Evaluation	1961	1980	0.77	0.48	–1.6
02333500	Evaluation	1981	1996	0.82	0.42	–2.8
02333500	Calibration	1997	2012	0.77	0.48	5.0

Chipola River Subbasin PRMS Model

The Chipola River subbasin consists of the area upstream from the USGS streamgage 02359000 (Chipola River near Altha, Florida). This subbasin encompasses 2,020 km^2 and is located in the southwestern part of the ACFB (figure 2 in the main body of this report). The average altitude of the watershed is 45 meters, ranging from 8 to 108 meters above NAVD 88. The largest land-cover type in the watershed is forest (about 28 percent) followed by cultivated crops (about 21 percent) (table 2–3). The watershed also has a considerable amount of wetlands (about 15 percent) and is located almost entirely within the karst environment of the Dougherty Plain. The watershed is located in the Coastal Plain physiographic province, which is underlain by sedimentary rock (figure 2 in the main body of this report).

Climate Inputs

Thirty-three NCDC weather stations were used to develop regional climate regressions and model forcings of precipitation and air temperature (table 2–9). Various combinations of the weather stations were used, depending on regional regression analysis, proximity to the basin, and data availability. On the basis of weather stations used for model forcings for the period 1980 to 2013, the subbasin receives an annual average precipitation of 1,480 millimeters (58.2 inches) and has mean monthly air temperatures that range from 10.0 °C (50.0 °F) to 27.5 °C (81.5 °F).

PRMS Model Calibration and Evaluation

An automated calibration, as described in appendix 1 of this report, was completed for the NCDC station-driven PRMS models. Simulations of solar radiation and potential evapotranspiration match the measured data well for the Chipola River subbasin for both the calibration and evaluation periods (fig. 2–10). One streamgage was used to calibrate and evaluate the Chipola River subbasin PRMS models, and one additional streamgage was used only for evaluation (table 2–5). A split-period strategy was used to calibrate and evaluate the model at the streamgages. The period 1997 to 2012 was used to calibrate the model at the 02359000 streamgage, with the evaluation periods varying on the basis of available measured streamflow data. Streamflow performance metrics of NSE (0.70 to 0.81), RSR (0.44 to 0.55), and P_{bias} (–4.0 to 6.4) were within the established criteria for the two streamgages for both calibration and evaluation for the NCDC station-driven simulations (table 2–10).

Table 2–9. National Climatic Data Center weather stations used in the Chipola River subbasin for regional climate regressions and for daily precipitation and air temperature forcings.

[Prcp, daily precipitation accumulation; Tmax, maximum daily temperature; Tmin, minimum daily temperature; —, means were not used]

ID	Station ID	Latitude	Longitude	Altitude (meters)	Regressions			Forcings		
					Tmax	Tmin	Prcp	Tmax	Tmin	Prcp
3	012372	31.32	–85.45	114	—	—	—	x	x	x
4	012675	31.30	–85.90	103	—	—	—	x	x	—
5	013251	31.04	–85.87	44	x	x	—	x	x	x
6	013761	31.36	–85.34	113	—	—	—	x	x	x
7	013816	31.88	–86.25	132	—	x	—	—	—	—
8	014431	31.24	–86.19	82	—	—	—	—	—	x
11	018323	31.81	–85.97	165	x	—	—	—	—	—
12	080804	30.45	–85.05	18	x	x	x	—	—	—
13	081022	30.38	–84.98	44	—	—	—	—	—	x
14	081544	30.78	–85.48	40	—	—	x	x	x	x
15	082220	30.72	–86.09	75	—	—	—	x	x	—
16	085367	30.84	–85.18	34	x	—	—	x	x	x
17	086240	30.53	–86.49	18	—	—	x	—	—	—
18	086842	30.25	–85.66	2	—	—	—	x	x	—
19	087025	30.10	–83.57	14	x	—	—	—	—	—
21	088758	30.39	–84.35	17	x	x	—	—	—	—
22	089566	30.12	–85.20	13	—	—	x	x	x	x
23	089795	30.72	–84.87	33	—	—	—	—	—	x
24	090140	31.53	–84.15	55	—	x	—	—	—	—
25	090145	31.54	–84.19	58	x	—	x	—	—	—
34	091372	32.32	–84.52	197	—	—	x	—	—	—
37	091500	31.19	–84.20	53	—	x	—	—	—	—
43	092153	31.17	–84.77	47	—	—	—	x	x	—
48	092266	31.99	–83.77	94	x	—	—	—	—	—
51	092361	31.85	–83.94	75	—	x	—	—	—	—
52	092450	31.77	–84.79	141	x	—	—	—	—	—
56	092570	31.78	–84.45	108	—	—	x	—	—	—
78	096043	31.61	–84.65	83	—	—	x	—	—	—
82	096362	31.31	–84.47	54	—	x	—	—	—	—
83	096364	31.19	–84.45	48	x	x	—	—	—	—
85	097087	32.05	–84.37	152	—	x	—	—	—	—
87	097276	30.78	–83.57	56	—	—	x	—	—	—
92	098666	30.91	–83.86	73	—	—	x	—	—	—

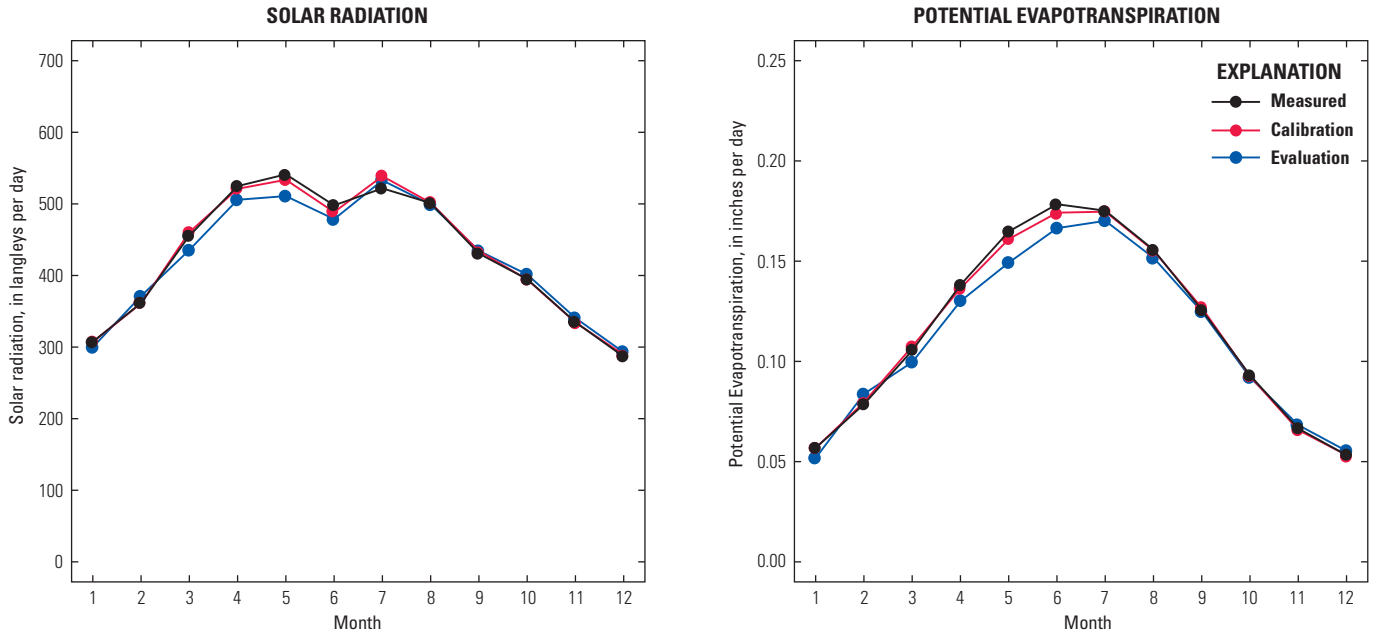

Figure 2–10. Solar radiation and potential evapotranspiration calibration and evaluation results for the Chipola River subbasin for the calibration period (1997–2012) and evaluation period (1981–96).

Table 2–10. Streamflow performance metrics for the Chipola River subbasin PRMS model.

[NSE, Nash-Sutcliffe model efficiency index (Nash and Sutcliffe, 1970); RSR, normalized root mean square error; P_{bias}, percent bias]

Station number	Period type	Start year	End year	NSE	RSR	P_{bias}
National Climatic Data Center station-driven						
02358789	Evaluation	2001	2012	0.77	0.48	6.4
02359000	Evaluation	1951	1980	0.73	0.52	–4.0
02359000	Evaluation	1981	1996	0.70	0.55	1.5
02359000	Calibration	1997	2012	0.81	0.44	5.2

Ichawaynochaway Creek Subbasin PRMS Model

The Ichawaynochaway Creek subbasin consists of the area upstream from the USGS streamgage 02355350 (Ichawaynochaway Creek below Newton, Georgia). This subbasin encompasses 2,690 km^2 and is located in the lower Flint River Basin (figure 2 in the main body of this report). The average altitude of the subbasin is 89 meters, ranging from 31 to 178 meters above NAVD 88. The largest land-cover type in the subbasin is forest (about 38 percent) followed by cultivated crops (about 27 percent) (table 2–3). The subbasin also has a considerable amount of wetlands (about 15 percent) and is partly located within the karst environment of the Dougherty Plain. The subbasin is located in the Coastal Plain physiographic province, which is underlain by sedimentary rock (figure 2 in the main body of this report).

Climate Inputs

Thirty-five NCDC weather stations were used to develop regional climate regressions and model forcings of precipitation and air temperature (table 2–11). Various combinations of the weather stations were used, depending on regional regression analysis, proximity to the basin, and data availability. On the basis of weather stations used for model forcings for the period 1980 to 2013, the subbasin receives an annual average precipitation of 1,310 millimeters (51.7 inches) and has mean monthly air temperatures that range from 9.1 °C (48.5 °F) to 27.5 °C (81.4 °F).

PRMS Model Calibration and Evaluation

An automated calibration, as described in appendix 1 of this report, was completed for the NCDC station-driven PRMS models. Simulations of solar radiation and potential evapotranspiration match the measured data well for both versions of the Ichawaynochaway Creek subbasin for the calibration and evaluation periods (fig. 2–11). One streamgage was used to calibrate and evaluate the Ichawaynochaway Creek subbasin PRMS models, and four additional streamgages were used only for evaluation (table 2–5). A split-period strategy was used to calibrate and evaluate the model at the streamgages. The period 1997 to 2012 was used to calibrate the model at the 02354800 streamgage, with the evaluation periods varying

Table 2–11. National Climatic Data Center weather stations used in the Ichawaynochaway Creek subbasin for regional climate regressions and for daily precipitation and air temperature forcings.

[Prcp, daily precipitation accumulation; Tmax, maximum daily temperature; Tmin, minimum daily temperature; —, means were not used]

ID	Station ID	Latitude	Longitude	Altitude (meters)	Regressions			Forcings		
					Tmax	Tmin	Prcp	Tmax	Tmin	Prcp
1	010008	31.57	–85.25	139	—	—	x	—	—	—
2	010425	32.60	–85.47	166	x	—	—	—	—	—
3	012372	31.32	–85.45	114	x	—	—	—	—	—
6	013761	31.36	–85.34	113	x	—	—	—	—	—
9	014502	32.91	–85.43	226	—	x	x	—	—	—
10	016129	32.66	–85.45	195	x	x	x	—	—	—
16	085367	30.84	–85.18	34	—	x	—	—	—	—
20	087429	30.55	–84.58	75	—	—	x	—	—	—
24	090140	31.53	–84.15	55	—	—	—	x	x	x
25	090145	31.54	–84.19	58	x	x	—	x	x	—
33	090979	31.22	–84.56	82	—	—	—	x	x	x
37	091500	31.19	–84.20	53	—	—	—	x	x	x
45	092166	32.52	–84.94	119	x	—	—	—	—	—
48	092266	31.99	–83.77	94	—	x	—	—	—	—
51	092361	31.85	–83.94	75	—	x	—	—	—	—
52	092450	31.77	–84.79	141	x	x	—	—	—	—
59	093028	31.57	–84.73	90	—	—	—	—	—	x
61	093516	31.60	–85.05	104	—	—	—	x	x	—
62	093578	31.62	–85.05	64	—	—	—	x	x	—
65	093658	31.90	–85.04	149	—	—	—	x	x	—
70	095061	31.76	–84.19	79	—	—	—	x	x	—
72	095440	32.83	–83.61	84	—	—	x	—	—	—
73	095443	32.68	–83.65	105	—	x	x	—	—	—
75	095979	32.29	–84.03	100	—	—	x	—	—	—
77	096038	31.53	–84.62	82	—	—	—	x	x	—
78	096043	31.61	–84.65	83	—	—	—	—	—	x
79	096087	31.18	–83.75	104	x	x	—	—	—	—
82	096362	31.31	–84.47	54	—	—	—	x	x	—
83	096364	31.19	–84.45	48	—	—	—	x	x	—
85	097087	32.05	–84.37	152	—	—	—	x	x	x
88	097276	30.78	–83.57	56	—	—	x	—	—	—
90	098535	32.69	–84.52	195	x	x	—	—	—	—
91	098661	32.90	–84.34	230	—	—	x	—	—	—
96	099124	32.61	–83.62	128	—	x	—	—	—	—
97	099291	32.88	–85.18	175	x	x	x	—	—	—

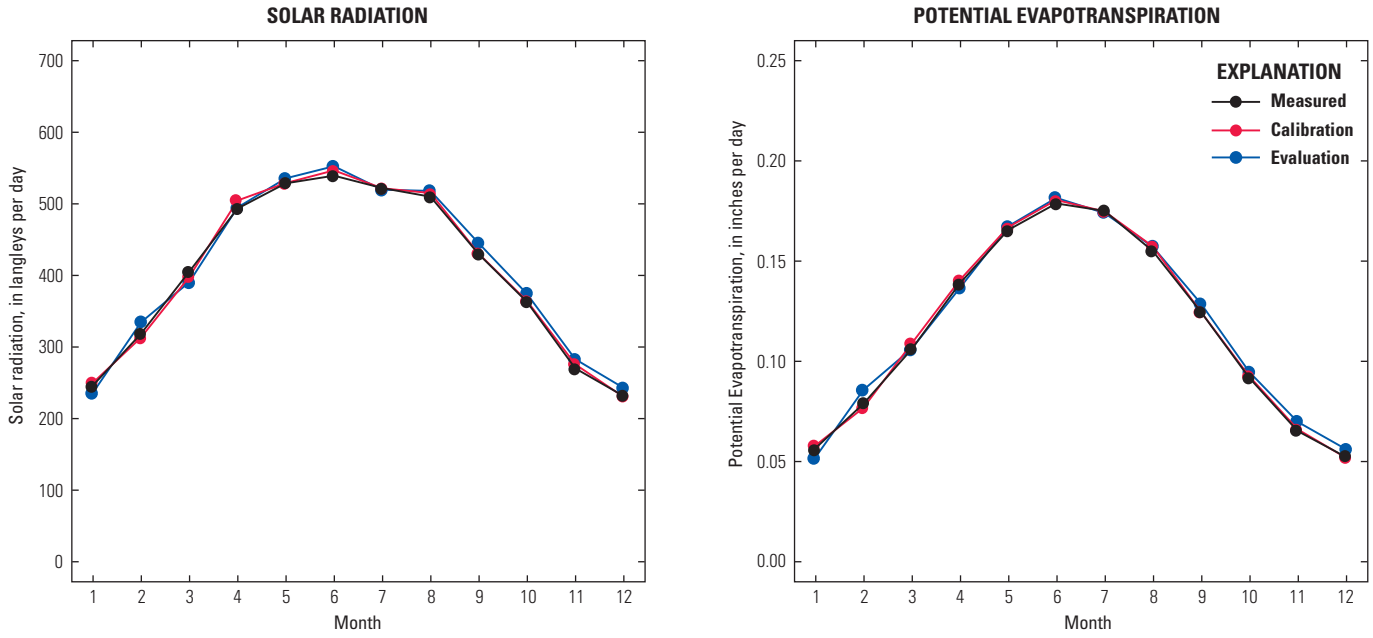

Figure 2–11. Solar radiation and potential evapotranspiration calibration and evaluation results for the Ichawaynochaway Creek subbasin for the calibration period (1997–2012) and evaluation period (1981–96).

on the basis of available measured streamflow data. The 02355350 streamgage was not used for calibration or evaluation because the streamflow record is affected by backwater from the Flint River during periods of high flow. Streamflow performance metrics of NSE (0.34 to 0.81) and RSR (0.44 to 0.81) were mostly within the established criteria for the five streamgages for both calibration and evaluation for the NCDC station-driven simulations except for streamgage 02353400 (table 2–12) for which the period 1989–96 (NCDC station driven) was outside the acceptable limits. The P_{bias} streamflow metric was within the allowable 10 percent threshold for 4 of the 10 periods evaluated. The calibration streamgage (02354800) was within the acceptable limits for all criteria for both simulations. Flow volumes that were outside the allowable 10 percent mostly had a negative bias, meaning the simulated flows were lower than the measured streamflow. Compensation for anthropogenic factors (for example, water use) during model calibration for the 1997–2012 period may have resulted in the larger negative flow volume bias seen in the earlier historical periods. The tradeoff between using a longer or earlier period of record for model calibration to keep the model temporally generalizable and using only the period for which water-use data are available (2008–12) results in compensating for altered streamflows in model parameterizations. An earlier calibration period could have been used for model parameterization, but the added uncertainty of how applicable the model would be for the more recent climate period was considered problematic and so a current climate period was used instead.

Table 2–12. Streamflow performance metrics for the Ichawaynochaway Creek subbasin PRMS model.

[NSE, Nash-Sutcliffe model efficiency index (Nash and Sutcliffe, 1970); RSR, normalized root mean square error; P_{bias}, percent bias]

Station number	Period type	Start year	End year	NSE	RSR	P_{bias}
National Climatic Data Center station-driven						
02353265	Evaluation	2002	2012	0.54	0.68	10.5
02353400	Evaluation	1960	1970	0.53	0.68	–23.3
02353400	Evaluation	1989	1996	0.34	0.81	–27.6
02353400	Evaluation	1997	2012	0.61	0.63	–3.7
02353500	Evaluation	1941	1980	0.67	0.58	–17.2
02353500	Evaluation	1981	1996	0.54	0.68	–9.0
02353500	Evaluation	1997	2012	0.68	0.57	9.9
02354500	Evaluation	1941	1949	0.72	0.53	–35.1
02354500	Evaluation	1997	2012	0.78	0.47	–18.0
02354800	Calibration	1997	2012	0.81	0.44	1.2

Potato Creek Subbasin PRMS Model

The Potato Creek subbasin consists of the area upstream from the USGS streamgage 02346500 (Potato Creek near Thomaston, Georgia). This subbasin encompasses 482 km^2 and is located in the upper Flint River Basin (figure 2 in the main body of this report). The average altitude of the subbasin is 234 meters, ranging from 119 to 390 meters above NAVD 88. The largest land-cover type in the subbasin is forest (about 52 percent in 2011) followed by hay/pasture

(about 20 percent) (table 2–3). Developed land percentage has increased from 10.5 percent (2001) to 11.3 percent (2011) (table 2–3). The subbasin is located entirely within the Piedmont physiographic province, which is underlain by crystalline rock (figure 2 in the main body of this report).

Climate Inputs

Twenty-five NCDC weather stations were used to develop regional climate regressions and model forcings of precipitation and air temperature (table 2–13). Various combinations of the weather stations were used, depending on regional regression analysis, proximity to the basin, and data availability. On the basis of weather stations used for model forcings for the period 1980 to 2013, the subbasin receives an annual average precipitation of 1,280 millimeters (50.4 inches) and has mean monthly air temperatures that range from 6.9 °C (44.5 °F) to 26.5 °C (79.8 °F).

PRMS Model Calibration and Evaluation

An automated calibration, as described in appendix 1 of this report, was completed for the NCDC station-driven PRMS model. Simulations of solar radiation and potential evapotranspiration match the measured data well for the Potato Creek subbasin for both the calibration and evaluation periods (fig. 2–12). One streamgage was used to calibrate and evaluate the Potato Creek subbasin PRMS model (table 2–5). A split-period strategy was used to calibrate and evaluate the model at the streamgage. The period 1955 to 1970 was used to calibrate the model at the 02346500 streamgage, with the evaluation period being 1941 to 1954. This streamgage was discontinued in 1971 so a more contemporary calibration period was not available. Streamflow performance metrics of NSE (0.83 to 0.84), RSR (0.40 to 0.42), and P_{bias} (–4.3 to 0.8) were within the established criteria for the streamgage for both calibration and evaluation for the NCDC station-driven simulation (table 2–14).

Table 2–13. National Climatic Data Center weather stations used in the Potato Creek subbasin for regional climate regressions and for daily precipitation and air temperature forcings.

[Prcp, daily precipitation accumulation; Tmax, maximum daily temperature; Tmin, minimum daily temperature; —, means were not used]

ID	Station ID	Latitude	Longitude	Altitude (meters)	Regressions			Forcings		
					Tmax	Tmin	Prcp	Tmax	Tmin	Prcp
2	010425	32.60	–85.47	166	x	x	x	—	—	—
9	014502	32.91	–85.43	226	—	x	x	—	—	—
10	016129	32.66	–85.45	195	x	x	x	—	—	—
29	090463	33.82	–84.40	253	—	—	x	—	—	—
35	091425	32.65	–84.19	136	—	—	—	x	x	x
38	091640	33.60	–85.08	303	x	—	x	—	—	—
44	092159	32.52	–84.94	133	x	x	—	—	—	—
45	092166	32.52	–84.94	119	x	x	x	—	—	—
47	092198	33.10	–84.43	253	—	—	—	x	x	x
50	092318	33.60	–83.84	234	x	—	—	—	—	—
54	092485	33.99	–84.75	335	—	x	x	—	—	—
60	093271	33.26	–84.28	285	—	—	—	x	x	x
66	093936	33.25	–84.27	299	—	—	—	x	x	x
71	095404	33.85	–84.58	299	—	x	—	—	—	—
72	095440	32.83	–83.61	84	—	—	x	—	—	—
73	095443	32.68	–83.65	105	x	x	x	—	—	—
76	095988	33.33	–83.70	158	—	—	—	x	x	—
81	096148	32.61	–85.08	153	—	x	—	—	—	—
84	096848	33.36	–84.57	243	x	x	—	x	x	—
85	097087	32.05	–84.37	152	—	—	x	—	—	—
90	098535	32.69	–84.52	195	—	—	—	x	x	x
91	098661	32.90	–84.34	230	—	—	—	x	x	x
95	098950	33.87	–83.54	256	x	x	—	—	—	—
97	099291	32.88	–85.18	175	x	—	—	—	—	—
98	099506	32.97	–84.61	223	—	—	—	x	x	x

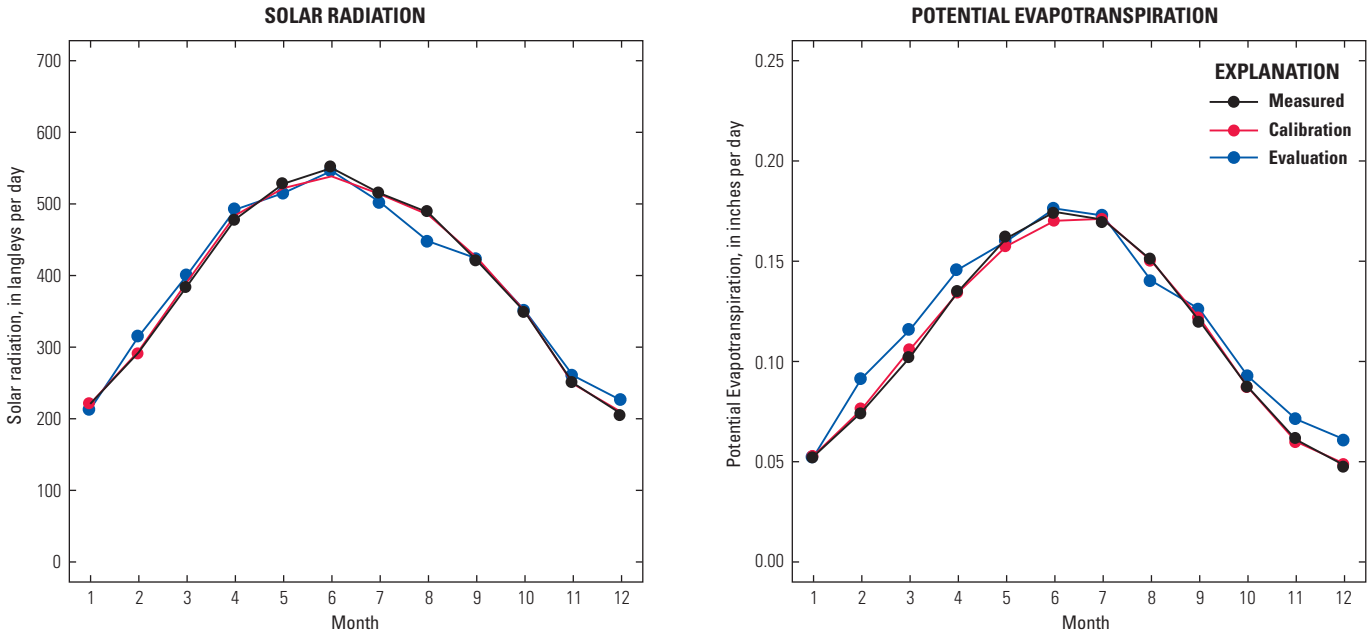

Figure 2–12. Solar radiation and potential evapotranspiration calibration and evaluation results for the Potato Creek subbasin for the calibration period (1997–2012) and evaluation period (1981–96).

Table 2–14. Streamflow performance metrics for the Potato Creek subbasin PRMS model.

[NSE, Nash-Sutcliffe model efficiency index (Nash and Sutcliffe, 1970); RSR, normalized root mean square error; P_{bias}, percent bias]

Station number	Period type	Start year	End year	NSE	RSR	P_{bias}
National Climatic Data Center station-driven						
02346500	Evaluation	1941	1954	0.84	0.40	–4.3
02346500	Calibration	1955	1970	0.83	0.42	0.8

Spring Creek Subbasin PRMS Model

The Spring Creek subbasin consists of the area upstream from the USGS streamgage 02357000 (Spring Creek near Iron City, Georgia). This subbasin encompasses 1,270 km^2 and is located in the lower Flint River Basin (figure 2 in the main body of this report). The average altitude of the basin is 59 meters, ranging from 30 to 125 meters above NAVD 88. The largest land-cover type in the subbasin is cultivated crops (about 40 percent in 2011) followed by forest (about 28 percent in 2011) (table 2–3). The subbasin also has a considerable amount of wetlands (about 16 percent) and is mostly located within the karst environment of the Dougherty Plain. The subbasin is located entirely within the Coastal Plain physiographic province, which is underlain by sedimentary rock (figure 2 in the main body of this report).

Climate Inputs

Thirty NCDC weather stations were used to develop regional climate regressions and model forcings of precipitation and air temperature (table 2–15). Various combinations of the weather stations were used, depending on regional regression analysis, proximity to the basin, and data availability. On the basis of weather stations used for model forcings for the period 1980 to 2013, the subbasin receives an annual average precipitation of 1,350 millimeters (53.0 inches) and has mean monthly air temperatures that range from 9.6 °C (49.4 °F) to 27.6 °C (81.7 °F).

PRMS Model Calibration and Evaluation

An automated calibration, as described in appendix 1 of this report, was completed for the NCDC station-driven PRMS model. Simulations of solar radiation and potential evapotranspiration match the measured data well for both versions of the Spring Creek subbasin for the calibration and evaluation periods (fig. 2–13). One streamgage was used to calibrate and evaluate the Spring Creek subbasin PRMS model (table 2–5). A split-period strategy was used to calibrate and evaluate the model at the streamgage. The period 1997 to 2012 was used to calibrate the model at the 02357000 streamgage, with two evaluation periods (1951–70 and 1983–96). This streamgage was inactive for most of the period 1971–82. Streamflow performance metrics of NSE (0.65 to 0.72), RSR (0.53 to 0.59) were within the established criteria for the calibration period and two evaluation periods for streamgage 02357000. The P_{bias} performance metric (–11.8 to 8.1) was within the 10 percent criteria for all periods except the evaluation period of 1983–96 (table 2–16).

Table 2–15. National Climatic Data Center weather stations used in the Spring Creek subbasin for regional climate regressions and for daily precipitation and air temperature forcings.

[Prcp, daily precipitation accumulation; Tmax, maximum daily temperature; Tmin, minimum daily temperature; —, means were not used]

ID	Station ID	Latitude	Longitude	Altitude (meters)	Regressions			Forcings		
					Tmax	Tmin	Prcp	Tmax	Tmin	Prcp
6	013761	31.36	–85.34	113	—	—	—	x	x	—
14	081544	30.78	–85.48	40	—	x	—	—	—	—
16	085367	30.84	–85.18	34	x	x	—	—	—	—
19	087025	30.10	–83.57	14	x	x	—	—	—	—
20	087429	30.55	–84.58	75	—	—	x	—	—	—
21	088758	30.39	–84.35	17	x	x	x	—	—	—
22	089566	30.12	–85.20	13	—	x	—	—	—	—
24	090140	31.53	–84.15	55	x	—	x	—	—	—
25	090145	31.54	–84.19	58	—	x	x	x	x	—
28	090406	31.70	–83.62	133	x	—	—	—	—	—
30	090586	30.82	–84.62	58	—	—	—	x	x	—
33	090979	31.22	–84.56	82	x	x	—	x	x	x
34	091372	32.32	–84.52	197	—	—	x	—	—	—
36	091463	30.87	–84.22	61	x	x	—	—	—	—
37	091500	31.19	–84.20	53	—	—	—	x	x	—
43	092153	31.17	–84.77	47	—	—	—	x	x	x
48	092266	31.99	–83.77	94	—	x	—	—	—	—
51	092361	31.85	–83.94	75	x	—	—	—	—	—
52	092450	31.77	–84.79	141	x	—	—	—	—	x
56	092570	31.78	–84.45	108	—	—	x	—	—	—
58	092738	31.03	–84.89	46	—	—	—	x	x	—
63	093578	31.62	–85.05	64	—	—	x	x	x	—
65	093658	31.90	–85.04	149	—	—	x	—	—	—
78	096043	31.61	–84.65	83	—	—	—	—	—	x
79	096087	31.18	–83.75	104	—	—	x	—	—	—
82	096362	31.31	–84.47	54	—	—	—	x	x	—
83	096364	31.19	–84.45	48	—	—	—	x	x	—
85	097087	32.05	–84.37	152	x	x	—	—	—	—
86	097201	32.05	–84.52	123	—	—	x	—	—	—
88	097276	30.78	–83.57	56	—	—	x	—	—	—

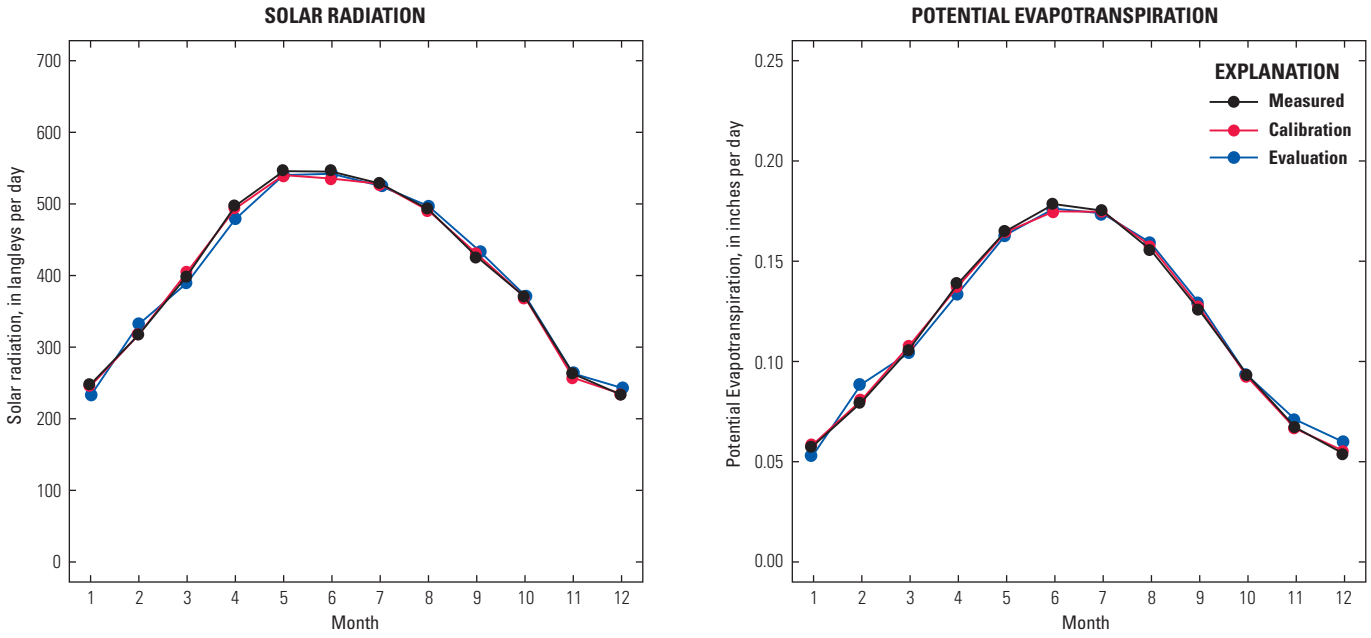

Figure 2–13. Solar radiation and potential evapotranspiration calibration and evaluation results for the Spring Creek subbasin for the calibration period (1997–2012) and evaluation period (1981–96).

Table 2–16. Streamflow performance metrics for the Spring Creek subbasin PRMS model.

[NSE, Nash-Sutcliffe model efficiency index (Nash and Sutcliffe, 1970); RSR, normalized root mean square error; P_{bias}, percent bias]

Station number	Period type	Start year	End year	NSE	RSR	P_{bias}
National Climatic Data Center station-driven						
02357000	Evaluation	1951	1970	0.65	0.59	–2.9
02357000	Evaluation	1983	1996	0.72	0.53	–11.8
02357000	Calibration	1997	2012	0.69	0.56	8.1

References Cited

Dalton, M.S., and Jones, S.A., comps., 2010, Southeast Regional Assessment Project for the National Climate Change and Wildlife Science Center, U.S. Geological Survey: U.S. Geological Survey Open-File Report 2010–1213, 38 p., accessed September 27, 2016, at https://pubs.usgs.gov/of/2010/1213/.

Elliott, C.M., Jacobson, R.B., and Freeman, M.C., 2014, Stream classification of the Apalachicola-Chattahoochee-Flint River System to support modeling of aquatic habitat response to climate change: U.S. Geological Survey Scientific Investigations Report 2014–5080, 79 p., accessed September 27, 2016, at https://doi.org/10.3133/sir20145080.

Freeman, M.C., Buell, G.R., Hay, L.E., Hughes, W.B., Jacobson, R.B., Jones, J.W., Jones, S.A., LaFontaine, J.H., Odom, K.R., Peterson, J.T., Riley, J.W., Schindler, J.S., Shea, C., and Weaver, J.D., 2013, Linking river management to species conservation using dynamic landscape-scale models: River Research and Applications, v. 29, no. 7, p. 906–918, accessed April 23, 2015, at https://doi.org/10.1002/rra.2575.

Gleeson, T., Smith, L., Moosdorf, N., Hartmann, J., Durr, H.H., Manning, A.H., van Beek, L.P.H., and Jellinek, A.M., 2011, Mapping permeability over the surface of the Earth: Geophysical Research Letters, v. 38, L. 02401, 6 p.

Gray, D.M., 1973, Handbook on the principles of hydrology: Water Information Center, Inc., 591 p.

Homer, C., Dewitz, J., Fry, J., Coan, M., Hossain, N., Larson, C., Herold, N., McKerrow, A., VanDriel, J.N., and Wickham, J., 2007, Completion of the 2001 National Land Cover Database for the conterminous United States: Photogrammetric Engineering & Remote Sensing, v. 73, no. 4, p. 337–341.

LaFontaine, J.H., Hay, L.E., Viger, R.J., Markstrom, S.L., Regan, R.S., Elliott, C.M., and Jones, J.W., 2013, Application of the Precipitation-Runoff Modeling System (PRMS) in the Apalachicola-Chattahoochee-Flint River Basin in the Southeastern United States: U.S. Geological Survey Scientific Investigations Report 2013–5162, 118 p., accessed September 27, 2016, at https://pubs.usgs.gov/sir/2013/5162/.

LaFontaine, J.H., Jones, L.E., and Painter, J.A., 2017, Model input and output for hydrologic simulations of the Apalachicola-Chattahoochee-Flint River Basin using the Precipitation-Runoff Modeling System: U.S. Geological Survey data release, https://doi.org/10.5066/F7FJ2F1R.

Leavesley, G.H., Lichty, R.W., Troutman, B.M., and Saindon, L.G., 1983, Precipitation-runoff modeling system—User's manual: U.S. Geological Survey Water-Resources Investigations Report 83–4238, 207 p., accessed September 27, 2016, at https://pubs.er.usgs.gov/publication/wri834238.

Markstrom, S.L., Regan, R.S., Hay, L.E., Viger, R.J., Webb, R.M.T., Payn, R.A., and LaFontaine, J.H., 2015, PRMS-IV, the Precipitation-Runoff Modeling System, version 4: U.S. Geological Survey Techniques and Methods, book 6, chap. B7, 158 p., accessed September 27, 2016, at https://doi.org/10.3133/tm6B7.

Nash, J.E., and Sutcliffe, J.V., 1970, River flow forecasting through conceptual models part I—A discussion of principles: Journal of Hydrology, v. 10, no. 3, p. 282–290, accessed September 27, 2016, at https://doi.org/10.1016/0022-1694(70)90255-6.

Regan, R.S., and LaFontaine, J.H., 2017, Documentation of the dynamic parameter, water-use, stream and lake flow routing, and two summary output modules and updates to surface-depression storage simulation and initial conditions specification options with the Precipitation-Runoff Modeling System (PRMS): U.S. Geological Survey Techniques and Methods, book 6, chap. B8, 60 p., accessed October 10, 2017, at https://doi.org/10.3133/tm6B8.

Viger, R.J., and Bock, Andrew, 2014, GIS Features of the Geospatial Fabric for National Hydrologic Modeling: U.S. Geological Survey metadata, accessed September 27, 2016, at https://doi.org/10.5066/F7542KMD.

Viger, R.J., and Leavesley, G.H., 2007, The GIS Weasel user's manual: U.S. Geological Survey Techniques and Methods, book 6, chap. B4, 201 p., accessed October 1, 2016, at https://pubs.usgs.gov/tm/2007/06B04/.

Manuscript was approved on November 2, 2017.

For additional information, contact
Director, South Atlantic Water Science Center
U.S. Geological Survey
720 Gracern Road
Stephenson Center, Suite 129
Columbia, SC 29210
(803) 750-6100

Or visit the South Atlantic Water Science Center website at
https://www.usgs.gov/water/southatlantic/

Publishing support provided by the USGS Science Publishing Network,
Reston Publishing Service Center

ISSN 2328-0328 (online)
https://doi.org/10.3133/